The Dissertation Committee for Robert Scott Evans
certifies that this is the approved version of the following dissertation:

Indirect Rapid Manufacturing of Silicon Carbide Composites

Committee:

_____
Matthew I. Campbell, Supervisor

_____
David L. Bourell

_____
Joseph J. Beaman

_____
Ofodike A. Ezekoye

_____
Joseph H. Koo

Indirect Rapid Manufacturing of Silicon Carbide Composites

by
Robert Scott Evans, B.S., M.S.

Dissertation

Presented to the Faculty of the Graduate School of
the University of Texas at Austin
in Partial Fulfillment
of the Requirements
for the Degree of

Doctor of Philosophy

The University of Texas at Austin
May, 2005

"Engineers uphold and advance the integrity, honor and dignity of the engineering profession by… using their knowledge and skill for the enhancement of human welfare…"

-From the ASME CODE OF ETHICS OF ENGINEERS

Acknowledgements

This section might also be correctly called "Cast of Characters." My name appears on the cover page, but there are many people who made the completion of this document possible.

I watched my mother, Linda Carpenter, complete her dissertation in the evenings and on weekends while I was in High School (emptying the refrigerator daily, with the assistance of my brother). It is one of many examples of her strength, determination and high standards that have influenced and continue to shape my own decisions. If I were going to dedicate this work to one person, it would most certainly be her.

My wife, Kelsey, secretly wants me to include the following sentence somewhere in the text. I dragged her across the country six days after our wedding to begin my graduate studies at Georgia Tech. More seriously, she is the love of my life and a great source of strength and perspective. I cannot overstate the influence of her unflagging support during my graduate studies.

I had the fortune (or perhaps, misfortune) to work on three different projects during my time at UT. Dr. Matt Campbell has worked with me on all of them: through work with optics, MEMS design and finally the materials science, technology transfer, and manufacturing project that fills the following pages. He has always helped to keep forward progress going during all three, and has always contributed an insightful perspective while allowing me to own the progress in the projects. More importantly, I have watched him develop his program of research from his first days as a professor. I see it as a good example to follow. I think of his experience as I consider an academic career going forward.

I have taken graduate level courses in a wide variety of areas, but not materials science. For this project, I have had to pick it up. Fortunately Dr. David Bourell helped to make sure that I treated the materials issues studied in the project at an appropriate level of understanding. He also provided valuable perspective both in planning the research and in analyzing the sometimes complex results. In Chapter 2 some of the challenges of being a student while at the same time being heavily involved in company formation and commercialization activities are outlined. Without Dr. Bourell's efforts to help make the elephant (UT) dance with the new company (ALM, LLC) this project might not have generated Ph.D. research.

It is a little dangerous when Dr. "DK" Ezekoye and I start talking. There are too many ideas to pursue, and just enough rebelliousness on the team to consider chasing them. During some of those idea filled discussions he provided excellent perspective on the technical depth and other aspects of an appropriate dissertation. I have enjoyed helping with Dr. Ezekoye's project to develop an undergraduate workshop and semester course both covering entrepreneurial issues for future engineers. For any graduate students who may be reading this, whether you need to take heat transfer or not, take Dr. Ezekoye's class. Even if the subject matter is not your favorite it will be valuable to watch him work in the classroom.

My first foray into the realm of technology transfer was in the spring of 2002 when I took Dr. Steve Nichols' course called Enterprise of Technology. I see this as the most important course of my graduate career. It changed the way I think about engineering and engineering education and began my work with entrepreneurship. This led to involvement in the Technology Entrepreneurship Society, to competitions and ultimately to the completion of this project. Dr. Nichols is really the sixth committee member. His efforts to help facilitate the

license agreement, sponsored research agreement and visiting scientist agreements that were negotiated before research actually began were absolutely instrumental. I am concluding my work at the university by helping to teach the same Enterprise of Technology course – in other words - if you really want to learn something teach it to someone. I have told people of Dr. Nichols that it helps to get that morning coffee working before talking with him, he is always on. What I mean is that like many other greats, he elevates the play of those around him.

In a way there were two committees for this dissertation. Bruce Thornton is the chairman of the other committee. His heartfelt interest in helping the university, passion for starting and running new companies and patience teaching others how to do it supported half of what I have learned completing this project. At the same time that I was working within the walls of the university to become a scholar of engineering, Mr. Thornton was helping to make sure that I was also becoming an entrepreneur.

This list would be incomplete without properly recognizing my partner-in-crime throughout the project. Donnie Vanelli and I started working on the business plan included in the appendices in January of 2003. We both saw opportunity in it, but never realized at the time where it would go. If I have been the lead in making the technical side of this project go, then Donnie has certainly been the driver on the commercial side. As he has learned to run a company (again with not a little influence from Mr. Thornton), I have watched to see how it is supposed to be done.

To these and other teachers, friends and role models I owe many thanks.

Indirect Rapid Manufacturing of Silicon Carbide Composites

Publication No._____

Robert Scott Evans, Ph.D.
The University of Texas at Austin, 2005

Supervisor: Matthew I. Campbell

Rapid manufacturing has been a goal since the development of rapid prototyping in the mid to late 1980's. The term refers to using Rapid Prototyping techniques, capable of rendering objects directly from CAD files, to produce fully functional parts. Yet, significant barriers to realizing rapid manufacturing still exist in terms of the range and capability of materials that can be processed. Selective laser sintering (SLS) is an additive fabrication technique regarded as having the broadest set of materials. The SLS process allows parts to be built from a series of thin layers of fused powder. Still, there are only five prototyping materials commercially available for SLS. The powdered materials that have been demonstrated include single component polymers and multiple component systems where the polymers act as binders adhering particles of an inert material together to form porous parts.

For many types of composite materials, manufacturing methods have not been established that promote their widespread use in finished goods. Despite advantages in material stiffness, strength and abrasion resistance, forming parts from particulate reinforced composite materials remains very challenging.

In this dissertation a new binder for SLS processing is developed along with strategies for machining, polymer infiltration and metal infiltration of the porous preforms. Where material properties are established after SLS processing the overall process is called, "indirect." Examined together these processes form a fabrication method that improves the material set available for rapid manufacturing and also provides a means of forming parts from particulate reinforced composites.

As with many other technologies developed within universities, there is a significant work required to transform a technology that is established in a laboratory into one that is used in manufacturing practice. The concurrent development of a company and funding from a Texas Technology Development and Transfer Grant made the technology transfer an inherent part of this project in addition to providing thermoset materials and indirect fabrication methods for SLS. Matching funds and significant in-kind donations were provided by Advanced Laser Composites, LLC. An NCIIA E-team grant supported market research and also the ultimate creation of the company. The project served as a test case for collaborative research where academic merit and commercial viability were pursued simultaneously.

Table of Contents

List of Figures

Chapter 1 Introduction

The concept of Rapid Manufacturing has been considered for as long as Rapid Prototyping techniques have been explored. Rapid Prototyping refers to a family of fabrication methods where 3D objects are created directly from CAD data while Rapid Manufacturing refers to using the same capability to produce fully functional finished parts. The ability to create parts directly from a CAD file without part specific tooling and procedures would have a massive impact on the way products are produced. Current Rapid Prototyping methods are limited in terms of material properties, speed and reliability. These technical hurdles indicate that pulling completed parts out of some type three dimensional printing machine will take many years. However, with post processing these hurdles may be cleared, at least partially, much sooner.

The current project advances a manufacturing process based on the Selective Laser Sintering (SLS) Rapid Prototyping technology coupled with a variety of post processing operations. SLS is described in detail in Chapter 3. In this way the shape is still prepared directly from a CAD file, but parts can be made from a wider variety of useful materials. More precisely, the current project advances a fabrication process that builds parts from combinations of three materials; a base, a binder and an infiltrant. The first two are formed into a porous, three dimensional solid directly from a CAD file via SLS. The base, which can be a hard, strong, functional material, is inert during this process while the binder is active and serves to maintain the desired part shape. This porous solid is then filled with a liquid material that solidifies or crosslinks to create a solid, non-porous object. For certain infiltrants there are also chemical reactions that form other desirable materials during the process. Basically, from the work in this project,

parts can be made that are a composite of three different materials, but the key is to examine the value of this in terms of more traditional manufacturing methods.

There are three different perspectives that can be used to establish the merit of the current project. The first is in terms of material science. For many types of particulate-reinforced composites, forming useful parts is difficult and costly. Highly functional combinations, such as tungsten carbide reinforced iron easily become heterogeneous during melt processing because of the relative densities of the two materials. This type of material is also very difficult to machine, due to the inclusion of hard, abrasive particles. Similar problems are found in particulate reinforced polymers. In the current project the binder material helps to maintain homogeneity throughout the fabrication process while also establishing the capability to form near-net shapes. Near-net shapes are those that require limited additional machining or other processing to achieve the final, desired part shape. The second perspective is that of the SLS industry. The SLS process is capable of making complex shapes directly from CAD files (without tooling), but both the function and variety of materials available are both very limited. Further, almost all parts require some amount of post processing to create the desired part properties. The current work establishes a new set of materials that may be processed in the SLS machine. With post processing similar to current industry practice, the variety and functionality of materials can be expanded significantly. The third perspective of interest stems from the challenge of actually getting the technology transferred from the university laboratory to commercial product development and product manufacturing activities. The first two perspectives establish the technical prowess of the work while this last involves societal impact. The transfer of university based technology and the role of engineers in terms of technology transfer are also important elements of the current project.

Many types of composites have been researched and commercialized and indirect methods are prevalent in the SLS industry today. The current work provides a test case for combining the two in a systematic way. Instead of an *ad hoc* combination for a particular material the current work instead seeks a method capable of being used for many different combinations of materials. The project was coupled to an effort to commercialize the technology, which is outlined in Chapter 2. This helped to bring a deeper understanding of current SLS industry practice and also many key elements of actual manufacturing into the project. While no parts were sold during the research, additional development is planned to continue outside the university.

1.1 Silicon Carbide (SiC) and Metal Matrix Composites

Silicon Carbide is a semiconducting ceramic with a high thermal conductivity, a high strength, and a hardness near that of diamond. Some of the many current industrial applications of SiC are listed in Table 1. However, the abrasion resistance, heat resistance and chemical resistance that make SiC a very desirable engineering material also makes manufacturing SiC products very challenging. SiC can cost \$400/in^3 (\$3450/lb) for pure, monolithic raw material. The most prevalent manufacturing methods (with example companies) for SiC include; Chemical Vapor Deposition (Rohm and Haas), Chemical Vapor Infiltration (Poco Graphite), Sintering (Saint-Gobain) and Hot Pressing (Dynacer). These methods produce finished parts with a variety of material properties and costs. CVD requires 50 hours to deposit an inch of material and parts must be machined from the resulting stock. CVI requires porous parts and tends to leave weaker, graphite-rich regions in the final material. Sintering and hot pressing require high-purity SiC and costly molds and/or significant machining to achieve final part

shapes. All of these methods require very high temperatures (>2000°C) during lengthy furnace processes (10-30+hours).

Table 1 Silicon Carbide Applications

Ballistic Armor	Automotive	Ball valve parts
Furnace Batts	Furnace Beams	Bearings
Metal working equipment	Wear & Corrosion Resistant Components	DC Magnetron Sputtering
Faucet Washers	Foundry equipment	Heat Exchanger Tubing
Heat exchangers	High Temperature Components	Hydrocyclones
Kiln furniture	Kiln Systems	Mechanical Seal Faces
Brakes	Posts and Rollers	Pulp and Paper
Semiconductor	Thermocouple Tubes/Prices	Turbine components
Valve & Valve Trim	Burner Nozzles	Wear plates

Powdered SiC is formed directly into a particulate form using the Acheson process. In contrast to bulk material, it is cheap and readily available. 280 grit powder, as an example, can be purchased for about $1.20 per pound (Industrial Supply Company, aaa-industrialsupply.com, 2004). This price is significantly lower than other prominent engineering ceramics available as powdered materials as may be seen in Table 2 . High purity or special crystal forms of SiC powder tend to have prices similar to that listed for alumina. Still, the availability, and low cost of powdered SiC underlines the interest in using SiC as a reinforcing material for Metal Matrix Composites (MMCs).

Table 2 Cost Comparison for 30-70μ Powdered Materials

(from various suppliers, for comparison only)

30-70 micron Powder	Vol. Cost per in^3	Price per lb.	Density g/cm^3
Graphite	$ 0.04	$ 1.00	1.20
Silicon Carbide	$ 0.14	$ 1.20	3.22
Silicon	$ 1.12	$ 13.36	2.33
Alumina	$ 1.91	$ 13.34	3.97
Zirconia	$ 3.01	$ 14.14	5.89
Titanium Carbide	$ 5.15	$ 28.90	4.93
Boron Carbide	$ 5.63	$ 61.82	2.52
Aluminum Nitride	$ 7.21	$ 61.25	3.26
Titanium Diboride	$ 9.31	$ 57.27	4.50
Tungsten Carbide	$ 22.45	$ 39.76	15.63

Reaction bonded silicon carbide (RBSiC) is a composite that has properties similar to monolithic SiC. Silicon infiltration into a carbon and silicon carbide preform forms reaction-bonded or siliconized silicon carbide a process common to several established and commercial processes. Since Si remains within the material it does have a lower strength and maximum use temperature. It requires lower temperatures (1450-1600°C) and short processing times (5minutes - 4 hours) relative to the pure SiC fabrication processes. Other advantages of this "liquid phase," "reactive" sintering include near net-shape capability and the ability to make non-porous parts (Clyne, 2001, Corman, 1997). Rajesh and Bhagat (1999), and Suyama et al. (2003), both claim reaction bonding to be the most commercially viable SiC fabrication method. SiC particulates, fibers and whiskers have been used for highly functional MMC's with Al, Mg, and Ti matrices. The main properties of interest demonstrated from these composites are higher stiffness, greater strength, better high-temperature performance and to a lesser extent, improved thermal or electrical conductivity. Mortensen (2001) lists Al, Fe and Ti as the most widely used matrices with alumina, SiC, TiC and C (fiber) as the top

reinforcing materials. The same review also indicates that infiltration processes are used for 47% of all MMC material formation, with shaping processes being divided chiefly among casting, extrusion and machining, which are more difficult when working with MMC's. Metal matrix composites have found application in heat sinks for electronics packaging, brake rotors, engines, friction components and other demanding applications. Finally, with the proper selection of materials, infiltration based synthesis of MMC's can be done without external pressure allowing an SLS preform to be used. In this way, the shape of the part would be retained during final material formation. The main challenges of fabricating MMC's are associated with material synthesis and part shaping through molding or machining.

The appeal of silicon carbide and metal matrix composites is clear from the properties the materials offer, but the technical challenges of creating products has inhibited their use in mainstream engineering practice.

1.2 SLS Technology

Hausholder (US Patent #4247508) envisioned a technology where a 3D part could be "molded" by building with layers of fused powder. Later, Deckard, in his research at the University of Texas, realized a practical embodiment by scanning layers of powdered wax and polymeric materials with an IR laser (US Patent#4,863,538). Shortly thereafter, the concept of processing "a plurality of materials" was also patented (US Patent #4,944,817). In 1992, two years after the first of several multiple-materials SLS patents was granted, DTM Corporation (now a part of 3D Systems, Inc.) offered the first commercial SLS machine. Today, aside from a few closely related low-volume offerings, the materials available to a service bureau manufacturing SLS parts are; nylon-12, Somos elastomer, polystyrene casting resin, glass filled nylon and steel powders with binders. The

Somos material is infiltrated with polyurethane, the polystyrene with casting wax and the steel powders with molten bronze. These are "indirect" processes since the final material properties are created after the shape of the article is formed in the SLS process. Compared to other approaches such as 3 Dimensional Printing, Laminated Object Manufacturing, Fused Deposition Modeling and Stereolithography, SLS is touted as having a very broad material offering (Pham and Wang, 2000, Wohlers, 2004). In addition SLS has slight advantages in speed and part accuracy compared to other RP technologies. Yet, the industry-wide desire to produce more functional parts and pursue Rapid Manufacturing applications is largely inhibited by the available materials (Hague et al., 2003, Pham and Dimov, 2003, Wohlers, 2004).

> Rapid prototyping is in the early stages of becoming a manufacturing tool…Limitations in speed, materials and accuracy create barriers to the success of RM (Wohlers, 2004, p.33)

In terms of metal matrix composites, more specifically, Vaucher et al., (2002), state, "a global search in the main databases in the field allows one to conclude that at present no European company or academic institution is able to process complex near-net shaped MMC's meeting the… requirements for industrial upscaling."

University and industry researchers have examined a variety of direct polymeric (ABS, PMMA, nano-composite nylon, etc.) and indirect SLS techniques. The main body of patents covering materials for the SLS process may be found listed in the References and Additional Reading section. There are several examples of indirect methods from previous SLS research projects. Deckard and Claar, (1993), described a process for creating SiC/ Al_2O_3 CMC and SiC/Al MMC parts using a Poly-methyl-methyl-methacrylate (PMMA) binder. The main

shortcomings to their process were significant lateral growth in the parts and low reinforcement density. A detailed description of the SLS of PMMA-coated SiC was described by Nelson, et al., (1995). Their work was used as a benchmark for the current study. Using a similar binder system, Wohlert and Bourell (1996), successfully infiltrated Mg into SiC preforms. Their preforms became very weak during post processing since the PMMA binder burned out completely. The preform was held together by the formation of SiO_2 during a furnace burnout prior to infiltration. In addition, reactions between the Mg and the SiO_2 were relatively complex and difficult to control. Each of these examples used binders and ultimately entire processes that could not be generalized to a variety of materials. The most recent work at the University of Texas at Austin established a basic method for forming reaction bonded silicon carbide and provided some technical foundation for the current project (Wang, 1999). Moon et al. (2001), describe an alternate rapid prototyping route to RBSiC by infiltrating porous graphite preforms. The preforms were made with liquid binder and graphite powder using the ink-jet/ powder technology called 3-Dimensional Printing, originally developed at MIT.

1.3 Previous Indirect SLS Research at UT

The previous research at UT established an indirect SLS method for making RBSiC components (Wang, 1999). A wafer boat from that project is shown in Figure 1.

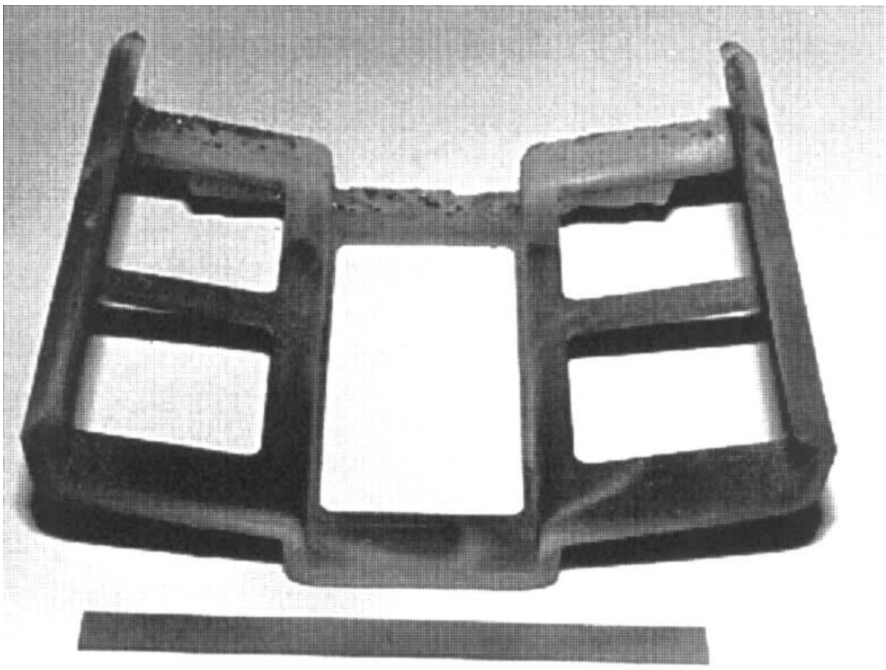

Figure 1 Wafer Boat Model From Previous Research (with 6" scale)

The wafer boat was made in three basic steps. The first involved the formation of a preform part with Selective Laser Sintering (SLS) and using a three-component binder containing phenolic, wax and nylon. The second step was carbonizing the binder materials under an inert, vacuum atmosphere to make a brown part (held together by residual carbon). The final step was infiltration of molten silicon metal into the brown part. A graphite vacuum furnace at the University of Rhode Island was used to infiltrate the preforms. One of the features of the process is that silicon reacts with the carbon to create more SiC and also creates a fully dense RBSiC composite part.

The binder formula used for the processing of RBSiC during the previous research at UT was a mixture of Nylon-12, Stearamide Wax (a lubricant for powder metallurgy processes) and GP-5546 rapid-cure phenolic (a novolac resin system) in a 50, 10, 40% mixture respectively. This formula was an early metal powder binder system from DTM Corporation adopted because of the expected

retention of mechanical properties by the phenolic throughout the processing temperatures for silicon infiltration. The current project examined a phenolic-only binder for greater residual carbon since the nylon and wax both vaporize during furnace processing. Higher intermediate part strength and additional SiC were expected.

1.4 Project Setup and Support

The project has been supported by a Texas Technology Development and Transfer grant. Advanced Laser Composites, L.L.C., a company formed for the purpose of commercializing the technology has supplied matching funds. The goal of actual application has helped bring to the current research a very significant study of current industry practice, especially in the SLS industry and related intellectual property. What really makes the current technology special is the ability to form parts in the SLS machine that can be post processed into highly functional finished parts. The most important aspect of the entire process is the binder which facilitates both SLS processing and all of the post processing operations as well. For this reason the binder and the SLS process has been studied in greater detail during this project. Polymer infiltration represents the quickest path to commercial parts since no vacuum furnace is required. This has emphasized the examination of commercial applications for polymer infiltrated parts during the project. The high-temperature furnace infiltration, in contrast, has been approached in terms of supporting additional academic research while the commercial feasibility of the current process has been analyzed.

1.5 Thesis

Indirect Selective Laser Sintering with thermosetting binders is a platform for commercially driven rapid manufacturing of polymer and metal matrix composites.

This platform is supported by the development of two base ceramics (glass and SiC) and includes research of thermoset binder chemistries and several infiltrants. The commercial viability is established via basic economic analysis, market application research and analysis of test parts by potential customers.

The dissertation is divided into three main chapters. Chapter 2 reviews the development of the new company and discusses the issues related to university research when coupled with technology transfer activities. This includes a new model of coupled transfer and university research activities including educational implications. Chapter 3 is focused on the development of a new type of binder material for the SLS process. In addition the development of the binder has been used to establish a more general materials development process. Chapter 4 covers the post processing of parts to create more functional materials, including machining, polymer infiltration, and metal infiltration. The final chapter is a review of several key elements of rapid manufacturing and the manufacturing process formed by connecting the processes examined in Chapter3 and Chapter 4.

The final chapter is a review of the platform for creating parts from base, binder and infiltrant materials. The second section of the final chapter is a more general discussion about rapid manufacturing. The contributions of this project and promising future work are integrated into these sections.

Chapter 2 Commercialization and the Education of Engineers

Technology commercialization predated and influenced the research. The efforts to transfer the technology from the university laboratory to the commercial sector also provide a test case for sponsored research and engineering education. The roots of the discussion stem from a long-running debate about the role of universities in terms of supporting profitable enterprise. On one side of the argument, "to commercialize a university is to engage in practices widely regarded in the academy as suspect, if not downright disreputable (Bok, 2003, p.18)." On the other is a realization that the missions of the university are not necessarily at odds with reaping financial benefit from the transfer of knowledge and technology to society at large. While the following discussion tends toward the latter, it is not intended to be a comprehensive treatment university commercialization. Instead some of the main issues raised within the current project are discussed while a more comprehensive treatment is left to future work.

2.1 An Example of Technology Commercialization

The commercialization analyses performed in graduate courses, for competitions and in support of the development of a new company all preceded the research effort for this project. Further, the commercialization process, including a license agreement, was connected to the support of additional research. It is typical for the commercial potential of a technology to be assessed well after research has begun if not after it has been completed altogether. In this research, graduate students have been heavily involved in all stages of the commercialization analysis and in the actual entrepreneurial effort to form a company and license the technology from the University of Texas. This allowed

the research effort and ultimately the technology to be evolved into an area of greater potential impact, instead of just trying to determine the best fit at the conclusion of the research.

In November of 2000 a patent was filed to cover the knowledge created during previous research. The following year, a $200,000 Texas Technology Development and Transfer (TDT) grant was awarded to the University of Texas in support of previous work to make semiconductor manufacturing fixtures using the SLS process, and furnace infiltration. More information about the funding source for the transfer grant program may be found on the internet at (www.arpatp.org). This grant required matching funding and in-kind support from a company interested in commercializing the technology. At the beginning of 2003, the initial company slated to provide this support was unable to participate. Dr. David Bourell, the lead researcher on the project was interested in having a commercialization analysis prepared in hopes of attracting another company interested in supporting the research (and allowing the grant funds to be used). Initially this was done by students participating in cross-disciplinary graduate courses during the Spring semester of 2003. A new application in metal casting dies was discovered and analyzed by those students. The in-class analysis was leveraged with significant additional work by the author and Donnie Vanelli (another engineering graduate student) for the Idea to Product competition in April of 2003. During that competition an entrepreneur-in-residence for the University of Texas, Bruce Thornton, expressed interest in the commercial potential of the technology and especially the application and market identified. More information about the entrepreneur-in-residence program may be found at (http://www.engr.utexas.edu/cofe/eir.cfm). During the second quarter of 2003, Mr. Thornton lead a team consisting of angel investors, the author and Mr. Vanelli

to start a new company, called Advanced Laser Composites. This new company was able to negotiate the first royalty-free, equity-only license with the University of Texas, become the supporting company for the TDT grant and help guide the research. A sponsored research agreement covering the work funded by the TDT and visiting scientist agreements for Mr. Vanelli and the author were also established. Research began in September of 2003.

An NCIIA E-team grant was awarded to the effort during the summer of 2003. The author and Donnie Vanelli prepared a business plan with the assistance of Chris Schaefer, an undergraduate engineering student, for the University of North Texas, Shirley Murphy Center Business Plan Competition which was held in November. The writeup of the plan is not included while, the presentation is in Appendix 5. They took first place with an all engineering team. Mr. Vanelli and the author also competed in the first International Idea to Product Competition (http://www.ideatoproduct.org), taking second place. That presentation may be found inAppendix 4. During the first two quarters of 2004, research continued while a second company was created to pursue broad materials development opportunities for the SLS industry. The analysis of the market and connections created in support of ALC allowed the broader materials development opportunities within the SLS industry to be seen. This second company was able to hire two employees and establish office space in Belton, Texas. These two companies were merged during the Fall of 2004 into Advanced Laser Materials, L.L.C. Commercial application of high-temperature infiltrated parts will require further research and development. Nearer term SLS materials products and new research grants are expected to support this additional work and several other technical avenues identified during the current research project.

An intriguing conclusion to the current project is that university research has resulted in the creation of jobs and an organization capable of generating greater societal impact. Further, students provided leadership. It also provides an example indicating that technology transfer coupled with research addresses several critical problems within the university and in terms of the education of engineers.

2.2 Commercialization of University Technology

Technology-based industry grows primarily in clusters where universities, communities and culture provide an appropriate environment. Examples of these regions include Silicon Valley, the Route 128 corridor, Raleigh-Durham and Austin. The role of the university in these value creating regions is enormous. 29 of the top 30 technology industry clusters in the country feature a large research university. More telling is that nearly half of the annual income in the Silicon Valley economy can be attributed to Stanford University faculty and graduates. This massive impact in Silicon Valley and elsewhere is the result of technology transfer. Dollars are an easy measure of the effect of technology transfer, but this process is not strictly related to business development, and not limited to those filling the traditional guise of 'entrepreneur' - it is very simply the creative synthesis involved in transforming ideas and knowledge to usable goods and services.

The three missions of the University of Texas are research (the creation of new knowledge), education (creating new knowledge creators), and public service (applying knowledge and knowledge creators to societal needs). The functions of the university may be simplistically represented in terms of inputs, transformations and outputs, as shown in Figure 2.

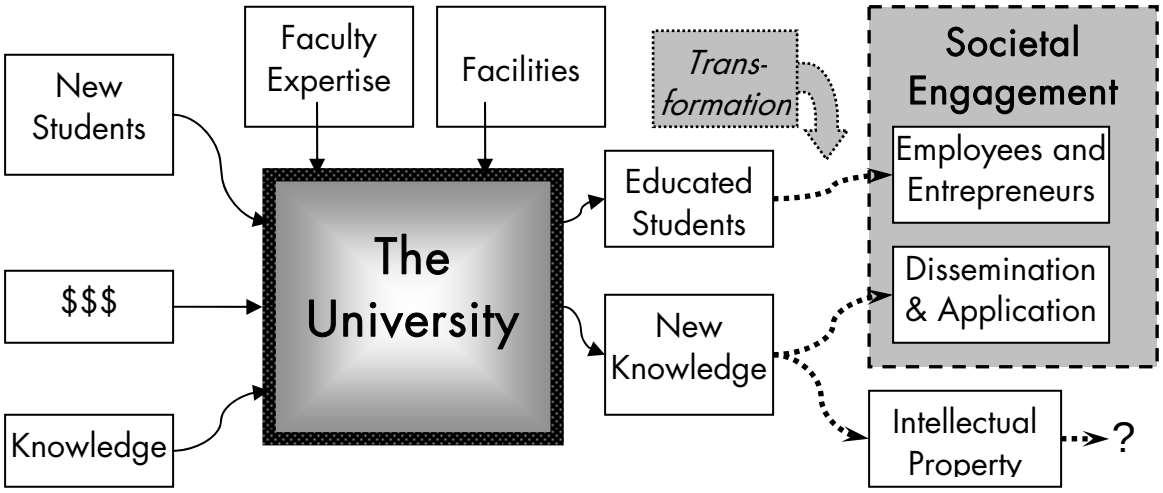

Figure 2 University Functional Diagram

Faculty expertise and effort, the work of students and facilities all participate in the research mission of the university. This obviously creates new knowledge and hopefully, coupled with course work, educated students. These students must be transformed into active employees, educators and entrepreneurs for value to be realized within the public. The new knowledge that is transferred to the public can also play a role in educating those outside of the university which is a portion of public service. This transfer of knowledge is not useful without a certain amount of transformation as well. As an example, knowledge that cola inhibits plant growth could be transformed into a discussion about the merits of pouring cola on certain types of weeds and published in an appropriate place. Only then could it be applied to the creation of societal value.

Intellectual property, protected rather than disseminated information, is similar. It does not inherently fulfill the missions of the university, though students may have been educated in the course of creating it. Instead, another organization must be enlisted to actually engage societal needs, symbolized by the question mark in the lower right corner of Figure 2. On the side of the university there is intellectual property which is often represented by a patent. A

commercial organization (a new or established company) has the capacity for and purpose of commercial enterprise – societal impact (in the form of jobs, more efficient processes, the creation of value, and the transfer of licensing monies back to the university). The traditional bridge for this gap is a license agreement permitting the company to leverage the IP for, among other things, assailing the marketplace. The university participates in this activity (for its direct benefit) in the form of a combination of equity in the company, royalties tied to the companies operations and one-time licensing fees from the company. The purpose of this is to support additional commercialization from the university, reward inventors and reinvest in new research activities. Before this license can be struck each side needs something from the other. Naturally, the company must understand the potential value of the IP to its operations. The university must recognize the capability of the company to risk the potential future value of the IP in the company's charge. The challenge for the university is to prepare a preliminary assessment of the technology that will allow potential licensees to recognize its potential. This process traditionally favors deals with larger companies and incremental technical advances. The potential of incremental technology is more easily understood and a large established company has domain expertise and infrastructure for creating products, supporting additional research and funding a license agreement which is also easily understood. With more disruptive or entirely new technologies the risks to potential licensees are initially greater and the potential benefits are farther into the future, though they are also larger. This pertains to a significant portion of the technology the universities have ripe for transfer: technology that is not just an incremental advance, technology that does not have a clear market, technology that is not tied to an existing application.

Transfer of this type of technology requires new companies that can innovate rapidly, change direction rapidly and focus on evolving the technology for a high-value application. Smaller companies or those formed specifically around particular technologies present greater risks to the university in terms of longevity and profit potential. The more novel the technology the more difficult it is for potential licensees to see potential applications (and actual value). It is also challenging for the university to understand the capability of early stage licensees, creating a problem for both sides (Vanelli, 2004). For a new company to establish funding the potential of the technology and the opportunity for licensing must be understood; for the university to negotiate a license deal there must be capable company. In the current project the license agreement was supported from both sides by leveraging existing university assets, including students. In particular it was student teams in courses and in preparation for the Idea to Product Competition that established the statement of value for the technology. The relationship between university technology, student analysis and the support of a license agreement which was outlined in Section 2.1 is shown in general form in Figure 3, below.

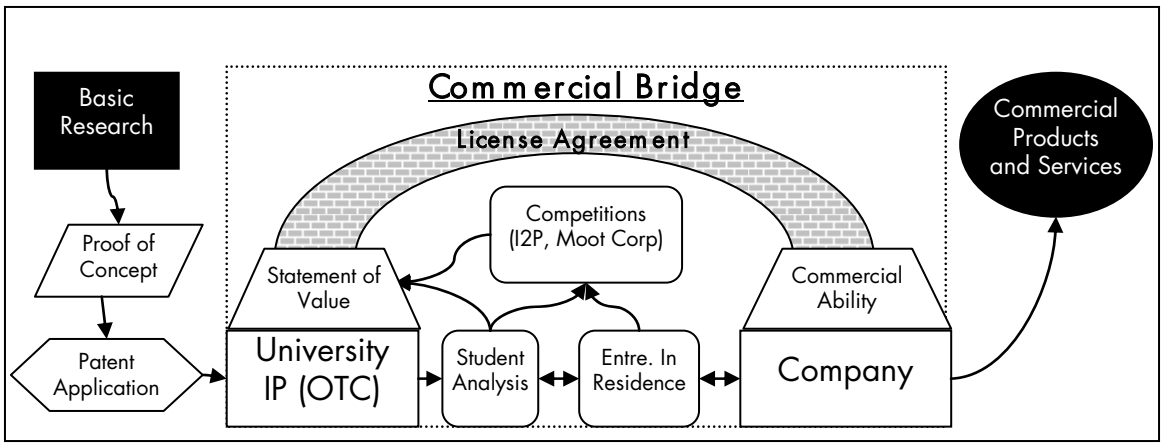

Figure 3 Technology Transfer with UT Resources (adapted from Vanelli, 2004)

Yet, this diagram of the people and organizations involved does not tell the complete story. Since many technologies do not have immediate commercial value, there is additional development that must be done. The same challenges that exist in terms of characterizing the potential of new technologies also exists in terms of understanding the additional research necessary to develop the technology into a form directly supporting goods and services. The actual status of the technology is difficult to determine. As an example, it was assumed that the siliconized silicon carbide technology patented after previous research was developed to the point where parts could be made reliably. Instead, challenges with the binder and infiltration process are still significant. Details of these challenges are discussed in the following chapters. The developmental risk in terms of the maturity and reliability of the technology must be considered in addition to risk associated with potential matches of the technology to applications. The development status of the technology may be a proof of concept, alpha-stage product test or simply implied by closely related work. In any case there is a technical gap between the status of the technology within the university and that which will actually allow the production of viable goods and services. This technology risk decreases the potential investment of new companies and is amplified by the lack of research infrastructure new companies have to advance technology.

In the current project this was addressed via sponsored research and a TDT grant. By examining the role of this sponsored research another perspective of commercialization may be seen. In Figure 4, below the sponsored research is depicted as another complimentary vehicle for transferring and transforming the technology from the university to the commercial sector. Essentially the license agreement sets forth transference of rights to the company and appropriate

monetary benefits back to the university. The sponsored research adds a means of transferring the technical expertise and also converting knowledge into capability. In the end, the level of development required to facilitate a patent application and the level required for actual goods and services are fundamentally different. In addition, the patent itself does not contain the expertise of the researcher.

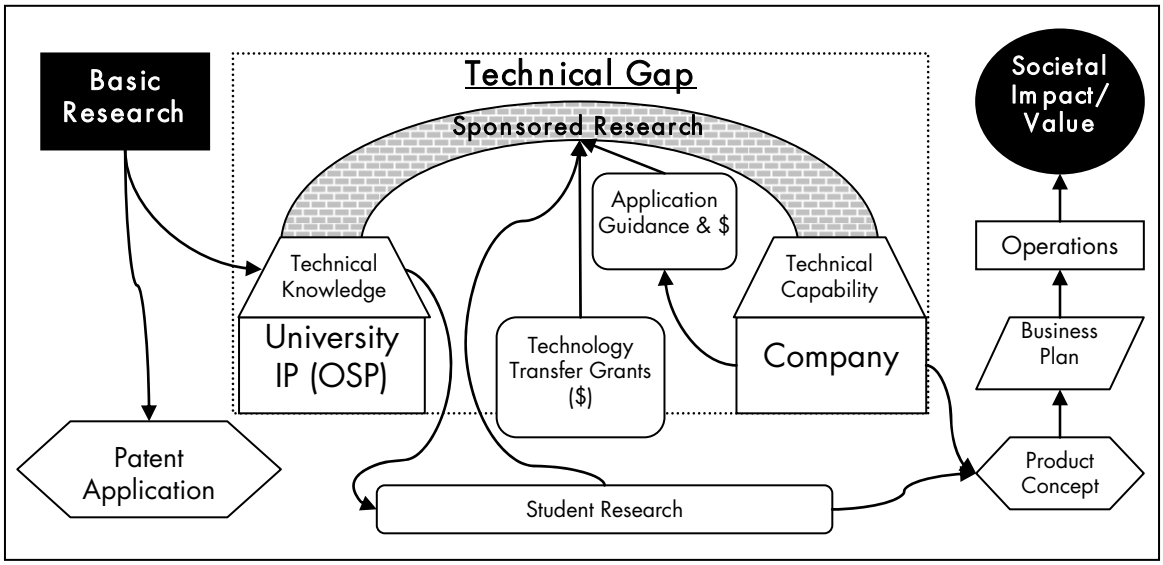

Figure 4 The Technical Gap

This additional risk of the technical gap could be assuaged prior to actual technology transfer with a greater understanding of the development status of the technology coupled with an understanding of its potential applications. Understanding the potential of a technology in a particular application requires a reasonable understanding of the technology, the application and the key questions about the effect of the technology on the market containing that application. The depth of understanding needed in terms of potential applications and mapping the effect of a new technology into those applications is greater than that required of the technology itself. On the other hand, assessing the actual status of the technology is far more heavily dependent upon domain expertise. Researchers may be the ones most capable of doing it, but this requires consideration of a far-

reaching culture of commercialization which is beyond the scope of present discussion.

It is important to consider the objectives of a new company in terms of sponsored research and the technical gap. Realizing a return on investment is a harsh taskmaster. The principles of a new company are interested in rapid, focused targeting of products and services that generate cash. Setting up and operating a company costs money and even if expenditures are kept to a bare minimum, the time value of money with respect to other investment opportunities is still keeping the pressure on. This has been amplified during the project by the need for the company to provide matching funds. The push to get some type of product to market quickly is different from the goals of research within a university which include education and establishing the potential for further research. On one hand the goal is to establish an academically viable understanding. On the other the goal is the most rapid creation of a commercially viable product. Sponsored research coupled with commercialization certainly supports education and also technology transfer, but not without conflicts of interest. In the following section this conflict is addressed in terms of student involvement in the current project.

2.3 Technology Transfer and Engineering Education

An engineer's expertise spans scientific knowledge, a capacity for the identification and analysis of problems, and the ability to synthesize solutions to those problems. There is a common element to various codes of ethics for engineers and engineer's creed (from the American Society of Professional Engineers) it is possible to add a context for this expertise. It is one of placing the public welfare above all other concerns. One way of interpreting the role of engineers is in terms of taking technology and using it to solve relevant societal

problems; engineers are then agents of technology transfer. They operate at the intersection of four primary concerns, as seen in Figure 5.

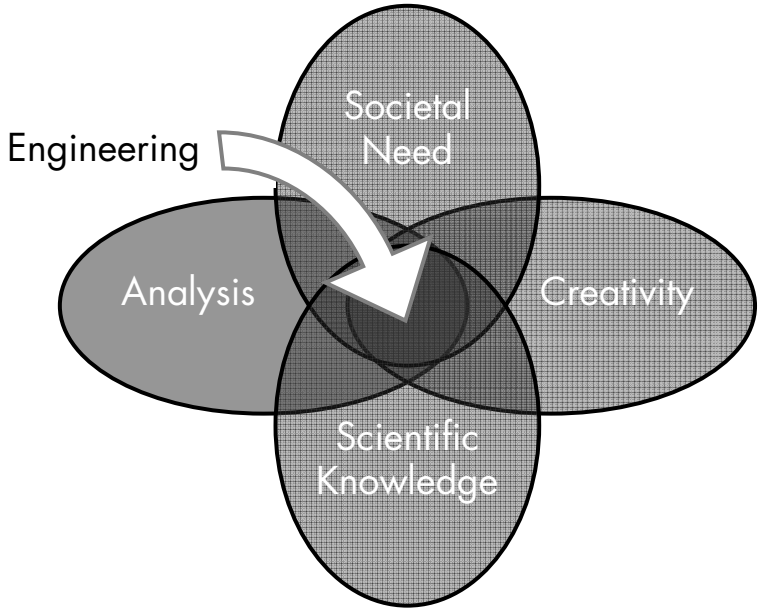

Figure 5 The Role of Engineering (adapted from Nichols, 2004)

The education of engineers, then, should address each of these four areas. Each university creates its own objectives and guidelines for the education of engineers (albeit often reinterpreting ABET accreditation). The mechanical engineering department at the University of Texas at Austin has published the following objectives.

ME EDUCATIONAL OBJECTIVES

The Mechanical Engineering Department at the University of Texas at Austin is dedicated to **graduating mechanical engineers** who:

1. Practice mechanical engineering in the general stems of thermal/fluid systems, mechanical systems and design, and materials and manufacturing in industry and government settings.
2. Are prepared for advanced education, research and development, and other creative efforts in science and technology.
3. Conduct themselves in a responsible, professional, and ethical manner.
4. Participate as leaders in activities that support service to and economic development of the region, state, and nation.

Bypassing questions about the definitions of "practice" in objective 1 and "other efforts" in objective 2, it is objective 4 from the list above that is the most intriguing for the present discussion. It is this objective that clearly addresses cultivating the element of engaging societal need in engineering education. Preparing engineers to be leaders in service and economic development takes this takes it an appropriate step further. Graduate students conduct research (analysis) based upon their scientific knowledge and propose new experiments and solutions (synthesis). Three of the four regions from Figure 5 are inherently part of the process, but the fourth is not. At the undergraduate level, there is clearly a greater burden in establishing an appropriate level of scientific understanding (including supporting continuing education). Still there is analysis, and in terms of the capstone design course, there is certainly synthesis and even a regard for service and economic development, though in the form of existing customer needs. There is a critical element of engineering that involves realizing, assessing and addressing societal need. Finally from the above list, there is also some dedication among educators to create engineers as leaders in terms of that engagement.

Commercialization, strictly defined, is the selling of work for a profit (Bok, 2003, p.6). Technology transfer is variously defined as going from lab to market, transforming idea to impact and building a union between a technology and a societal need. This last one is most appropriate here. The work of engineers and especially those who are leaders in service and economic development should be an embodiment of engaging societal need with technology. The current project, as outlined in Section 2.1, provides a test case for coursework, competitions and other technology transfer activities in terms of the effect on the education of engineering graduate students. For the sake of discussion, these may be organized into four levels. These levels are organized around key activities and student's responsibilities in the actual commercialization of the technology. At one level, students analyze the commercialization potential of technologies and even prepare hypothetical business plans for its deployment. On another, graduate students are co-founders of angel-backed companies and participate as officers and board members. These levels and their main issues are briefly discussed below.

2.3.1 Level 1: Analysis of Technology Potential

Figure 3, above, illustrates that coursework and entries into competitions served as a vehicle for creating a "statement of value." One realization of this is called a "quicklook analysis" which is a document that contains a discussion of the main features of a particular technology and those of a particular needy market. The list below is a brief outline of the main features of a Quicklook document.

1. Technology Description
2. Potential Applications
3. Development Status of Technology
4. IP Status of Technology
5. Competing Technologies and Competitors

6. Potential Markets
7. Barriers to Market Entry
8. Recommendations

More importantly, this document also contains a creative matching of the technology with a promising market and an assessment of the effect of this match. The quicklook provides an answer to whether the commercialization of a technology should be pursued further. The Idea to Product Competition features student teams presenting what is essentially a quicklook analysis.

Level 1 addresses both the need at the university to assess the commercial potential of its technology (and create a "statement of value") and the need for engineering students to cultivate an ability to engage societal needs with the development of new technology. There are courses and competitions that support this level of student involvement in the transfer of university technology. Still, additional courses especially at the undergraduate level could support this idea further. More widespread student involvement would better address the need for universities to understand the potential value of the technology and for engineers to become leaders in the application of technology for the benefit of society at large.

2.3.2 Level 2: Assessment of the Technology Development Status

With clear hindsight, a more complete assessment of the status of the previous SiC technology would have been very beneficial to the current research. Instead, the amount of work that remained in order to realize a robust metal matrix composite forming technology was not well understood. The patent application and dissertation prepared from the previous work were examined in conjunction with various discussions with the inventing professors. Yet, the actual development status of the technology was not understood. On the side of the company it was expected that silicon carbide composite parts could be reliably built (once a

furnace was installed). However, significant work still remained to establish that capability. At the close of the research, there is still not a transferable manufacturing process capable of producing commercial parts. As will be discussed in subsequent chapters this is in part due to; 1) the realization that other materials present a much larger opportunity (both academically and commercially), and 2) to the discovery of additional technical challenges. Still one of the key outcomes of the current project is a clear and comprehensive understanding of the work necessary to realize a commercially viable manufacturing method.

Considering again more disruptive technologies, Level 2 can be a greater challenge than establishing a valuable market match. While a new software technology may only require testing in a commercial beta test, a manufacturing technology might also require appropriate application in a value chain, high reliability and a reduction to practice. The activities contained in Level 1 are clearly within the missions of the university and within the educational objectives for engineers. It is a well defined process. Establishing the developmental status of a technology, in contrast, requires substantial technical understanding, and likely the participation of the researchers. Further, the technical and commercial domain expertise for software is different from biological sciences which are different from manufacturing technologies. While programs can be created to assist in this process, Level 2 requires a more fundamental, cultural change in terms of what researchers (including graduate students) do and the breadth of knowledge they create. Although the process can be more clearly defined it is unlikely that competitions can be created in support of it.

2.3.3 Level 3: Coupled Research and Commercialization

Another aspect of this project was that additional university research was pursued in conjunction with commercialization activities. Research money came from a new company and from a technology transfer grant for the purpose of building upon the proof of concept established in previous work. The research was guided toward greater potential impact and at the same time toward a more commercial status. In terms of the research there were conflicting perspectives, which can be illustrated by the different questions that were asked regarding the work done on a new binder formula (and discussed in Chapter 3). The question from the company was, "Why are we examining a new binder formula when there was one already prepared during previous research?" Within the university the question was, "Why aren't we looking at a wider variety of binder materials and trying to establish a more general understanding of binders?"

While levels 1 and 2 above are focused on the creation of new understanding about an existing technology, Level 3 covers the process of making the technology more commercially viable. Guidelines of what research is or should be regarded as coupled with commercialization activities is left to subsequent work along with defining the appropriate roles of the university, students and commercializing entity. The merits of involving students in the previous levels are fairly clear, as is the relationship of the activities with regard to the missions of the university and to the education of engineers. At this third level some form of advising or participation in the management of the research seems possible for students. Level 3, can be defined as having students involved as researchers who are also involved in assessing the application, technology status and ultimately the evolution of the research itself. Ironing this out in practice is

more challenging than for Level 1 or Level 2 and is ultimately also beyond the scope of this document.

The experience of the author and Mr. Vanelli was heavily influenced by the commercialization effort. Their roles were unusual because they were involved in the leadership of the commercial venture, which is discussed in the following section. They were also exposed to technology transfer issues in coursework. This allowed the author, especially, to be involved in the evolution of the research as outlined above. In contrast, three other graduate students who worked with the project were influenced very little. In other words they were primarily traditional researchers even though the funding came partly from a commercializing entity. Similar to Level 2, there is great opportunity for developing the role of students in sponsored research. What is clear is that with the background of existing coursework and by leveraging existing programs at the university it is possible for graduate students to have a significant and positive role in the commercialization of technology. For these students, there is not only education about technology, technical development, and the assessment of value, but also about the work required to actually create value from it. In addition, there can be great insight created in terms of the actual form and level of development of the technology required to support the creation of value. Thinking in this way, real world examples can be coupled with academic education. Real value has been created during this project, but not without conflicts between educational and commercial goals. There seem to be some interesting educational opportunities that could be developed. Yet, as Bok suggests, "a university must have a clear sense of the values needed to pursue its goals with a high degree of quality and integrity (Bok, 2003, p.6), " to keep commercialization within reasonable bounds. Based on this

set of values the appropriate student roles and the support structure for those roles should be considered.

2.3.4 Level 4: Student Lead Entrepreneurship

The author and Mr. Vanelli were involved with the creation of two startup companies, held board seats and served as officers. These activities were pursued in addition to research and preparation for Ph.D. degrees. The conflicts of interest, of expectations and of appropriate time commitment are relatively straight forward. The angel investors on the side of the companies put forth a good effort to engage and work with the university. The professors were similarly open to supporting this project. Still, the actual value to the company of association with the university including education, technical development and future grant proposals was difficult to characterize in terms of the issues facing a startup company – namely rapid deployment of cash creating operations. For engineering students involved in the creation of a new venture, what is the academic value of their involvement? There could be some criteria established for offering some type of credit to student entrepreneurs, but startup companies will obviously operate in their best interest. With only the present project as an example, it is difficult to make far-reaching statements about startup companies engaged in sponsored research. What is clear is that conflicts of priorities between the two types of organizations will persist and this provides some guidance for student involvement in new ventures. It is simply a matter of managing (and avoiding) the situations where the needs of the company and the tasks required to complete a degree are at odds. The student involvement and responsibility in a new venture can be set at a level where ample progress toward the degree is still feasible, or the degree program can be suspended in favor of taking a greater role in the company. If student researcher involvement in new

ventures becomes more commonplace, some type of student advocacy program will probably need to be established. This could help negotiate appropriate roles for students in new ventures while helping them maintain progress toward their degree. This program could also help seasoned entrepreneurs establish appropriate expectations of university research, and of student researchers. In this project two different solutions to the conflict were pursued. Mr. Vanelli chose to put his research (on technology commercialization) on hold to become president of the second company, which was started in January of 2004. The author resigned his position as president of the first company in November of 2004 to pursue the completion of his dissertation. At the request of the board of the merged company he also sold a majority of his ownership stake thereafter.

2.4 Toward a Culture of Technology Transfer

There is more to realizing societal benefit from technology (an arbitrary unit of scientific knowledge) than simply creating and defining it. It is within the mission of the university to have some involvement in actually transferring technology to entities capable of addressing societal needs. The value of being involved extends to the experience of students in technical fields as their careers will involve some level of technology transfer in the form of technical papers, products and services and even research grant proposals. In the case of engineers, societal engagement is inherently part of what defines their field, even though some of those who were educated as engineers choose to take on more of the traditional role of a scientist.

The current project has addressed a variety of issues in terms of technology commercialization and in particular student involvement in that process. It not only validated the current programming in graduate coursework and the I2P competition, but also sheds light on many remaining challenges. The evolution of

technology commercialization will see developments in a variety of areas simultaneously. These areas can be organized into a hierarchy which is used to organize the following discussion of future work. The underlying philosophy or set of principles is the most fundamental. Then appropriate university infrastructure can be addressed in terms of those principles. Finally, the student role in and educational merit of commercializing university technology can be put into appropriate context.

2.4.1 The Principles of University Technology Transfer

> To keep profit-seeking within reasonable bounds, a university must have a clear sense of the values needed to pursue its goals with a high degree of quality and integrity. – Bok, 2003, p.6

The lingering question about determining the development status of a technology leads to others. When is university research over and when does commercial research begin? What role should universities play? What knowledge should be protected for generating financial benefit and what should be disseminated for societal benefit? To what degree should researchers consider applications? How much should commercialization be considered during research and within university laboratories? How can better information about the developmental status of a technology be created? What things should the university do (that may be outside its direct charge or explicit mission) to facilitate the next steps in technology transfer? Commercialization has generated significant and well publicized financial benefits for universities in recent years. This has been a source of additional income for faculty researchers and for perennially cash-starved higher education institutions. It is important to place commercialization in proper scale. Large research universities have licensing

revenues of perhaps several million dollars per year while their annual operating budget may exceed one billion. Still, the compromise of academic ideals (including pedagogical influences) associated with this, if any, is difficult to define.

Going forward there is significant work to be done to clarify an appropriate influence of commercial interests in academic research. This will be a case of not only setting general guidelines, but also one of universities maintaining an appropriate balance of academic ideals in their portfolio of technical inquiry. In other words, some research projects will appropriately be highly commercially oriented. At the same time the academy should retain significant research activity that is unencumbered by the constraints of immediate or foreseeable societal impact. Historically and paradoxically there have been immense longer-term social benefits that, "depended on a vigorous program of basic research that only universities could provide (Bok, 2003, p.59)."

2.4.2 University Infrastructure

While the underlying principles will need to be ironed out, universities will continue to commercialize technologies developed within their walls. And, that process should be made as effective as possible for the interests of the university licensing and for the licensees as well. Some of the challenges faced during this project highlight opportunities for further development of programs spanning university offices, programs and procedures with regard to the transfer of technology. There is potential not only in the facilitation of transfer, but also in greater support of the commercial success (scope of societal impact) of the technology.

The license agreement was achieved in principle in only two weeks, but actual execution of a license agreement took over 4 months largely due to unclear legal issues regarding the previous research. Negotiating with the Office of

Technology Commercialization (for the license) and the Office of Sponsored Projects (to participate in this research project) was an additional challenge. The management of the research was carried out mostly within the university. But, with the university taking an equity position in the company and with the inventors sharing in any funds coming into the university, there was an interest in including the company in the progress of the research. In other words, the research was still mostly controlled within the university and therefore in accord with its missions.

The formation of the company, license agreement and ultimate execution of new research would not have occurred without the source of additional funds. The grant money helped to offset the uncertainty of university research. While it would have been costly to carry out research entirely outside the university, the prospect of overhead charges and not having well defined control over the research and its timing did not make the university a viable option either. In addition the university role in sponsored research was not adequately specified. It was difficult to predict the involvement of professors prior to the research project. There were no set deliverables, timelines or clear responsibilities established prior to the beginning of the research. The expectations of student researchers were also not specified. Finally the role of the company in participating in the guidance of the research was not set forth. All parties acted in good faith, but without a clear *a priori* match of company expectations with appropriate deliverables of university research. This led to a persistent perception of lacking progress and performance within the company.

This project would also probably not have occurred if the difficulties (and associated costs) that were encountered in establishing a license agreement and a sponsored research agreement had been known in advance. Each document required a separate negotiation with a separate office within the university. In

each case it was very difficult to make changes to the standard boiler-plate versions of the documents without requiring a time consuming review process by UT System legal counsel. These documents were created to protect the interests of the university and did not seem to contain a means of facilitating licensing deals, promoting collaborative research efforts or helping extend the impact of university technology.

Aside from establishing appropriate practices within the university, the problem is one of education. It is about educating those within the academy about the academically appropriate aspects of commercialization, the evolving infrastructure supporting it, and finally the potential of including commercialization in the educational experiences of university students. Faculty members will choose their own commitment to technology transfer, but should consider what is appropriate and should also know who to call with questions.

2.4.3 Engineering Education

One of the most compelling elements of the Enterprise of Technology course (ME 397, Management 385, etc.) briefly described above is that it features real technology transfer analysis. For the university, real assessment of commercial potential is invaluable to determining which technologies should be promoted and which should only inhabit university file cabinets. Incorporating students into technology transfer serves to promote a vital element in the activities of a research university. It leverages its own assets for the creation of societal impact from its technology.

Again the prospects for going forward may be illustrated by several questions that remain unanswered. Chief among these is; what is the appropriate incorporation of issues pertaining to societal engagement within engineering education? When should this be done and with what programs or revisions to the

existing curriculum? Along with the question about where university technology ends is a similar question about where student inquiry ends. But, what should engineering students, who may later assume roles as different as basic research and the management of investments, regard as a part of their education? More analysis of the potential impact of technology and more integration of that analysis into the expectation of engineering students seems valuable. Some of the answers to questions about education and student involvement will rely on the development of the "sense of values" suggested by Bok and on the infrastructure developed at the university level. Included in this will be the development of expectations on students to provide a better assessment of technology status. There may also be greater potential for collaboration between colleges integrating legal and traditional business perspectives into technical research.

Chapter 3 Thermoset Binders

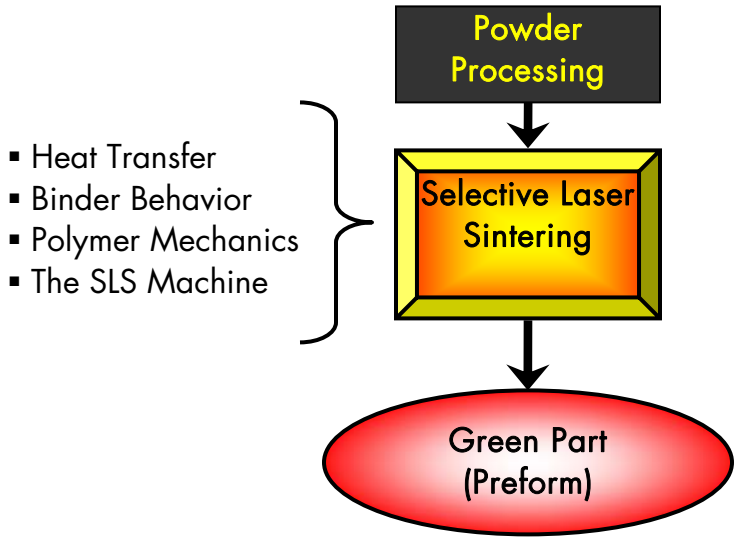

Figure 6 Subject of Chapter 3

In this chapter the issues related to the formation of a green part (or preform) using the SLS process are discussed. In particular, this involves getting a binder to adhere base material particles together into a desired shape. What is perhaps the most critical element of the indirect SLS manufacturing platform introduced in Chapter 1 is the binder. Although thermoset polymers have been used as components of binder systems little SLS research has been done to date on the behavior of thermosets in the SLS machine. The high adhesion, strength and temperature resistance generally associated with this type of polymer makes a compelling case for a new class of SLS binders. There is an additional advantage of some thermoset polymers in terms of their decomposition which is reviewed in Chapter 4. In this chapter, the main characteristics of the SLS process are reviewed. This is supported by a review of the heat transfer associated with laser scanning, curing characteristics of thermosets (especially phenolic) and also an examination of the behavior of powdered materials. This technical background provides a basis for the experimentation and analysis presented in the Method

and Results sections of the chapter. During the course of the SLS research there was significant work completed to examine the state of the art for the industry. This included a review of the materials patents covering previous SLS materials, interaction with industry leaders in SLS machine operation and concurrent involvement with thermoplastic SLS materials development work at Advanced Laser Materials. This contextual effort is reflected in the SLS process background, the analysis and discussion section of the chapter.

An additional goal of the work with thermoset binders is to prepare a systematic method for assessing the SLS processing potential of powdered materials in general. By combining the main technical issues related to SLS processing with the results of the research such a method has been assembled in an initial form and is presented at the end of the chapter.

There are two hypotheses addressed in this chapter:

1) Thermosetting polymers can be used as effective binders for SLS processing and can be crosslinked under the laser, representing a significant advantage over the use of thermoplastic resins that simply solidify.

2) By combining the basic principles of powder mechanics, SLS heat transfer, and polymer rheology, a systematic material screening method can be prepared for assessing new SLS materials.

3.1 Background

3.1.1 The Selective Laser Sintering Process

Although modifications to the machine itself would be advantageous, the current project leverages the standard SLS process to prepare parts using thermosetting polymers. Recommended machine modifications will be discussed in the discussion section at the end of this chapter. The basic physical elements of the

SLS machine include; two "feed beds" where the supply of powder is held, a "part bed" where the parts are actually made, a roller for spreading the powder from the feed beds across the part bed and a laser which is scanned across the surface of the powder. There is also a chamber enclosing the powder bed which can be purged with nitrogen. Figure 7 is a cross sectional diagram of the SLS machine. The build process begins with a first thin layer of powder being spread across the build chamber. A portion of the powder is fused by scanning the beam of a CO_2 laser (10,600 nanometer wavelength) on selected regions of the powder. The beam is scanned by the movement of two mirrors. These regions are the first cross-section of the part, or parts, to be built. The powder within the build chamber is then lowered by the thickness of the next part layer. The feed chamber is raised to deliver an appropriate amount of powder which is then spread by the roller across the build chamber. A second cross-section of the part is fused together in this second powder layer and also fused to the initial layer. The remaining cross-sections of the part are built in this fashion until the entire part has been created from layers of powder. More information on this process including diagrams and video may be found at the 3D Systems company website.

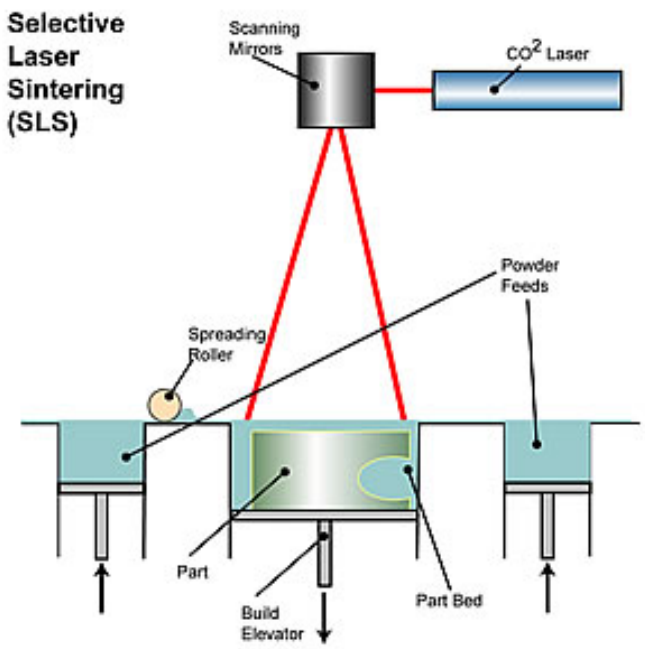

Figure 7 The SLS Machine (www.padtinc.com)

Modeling the process of fusing powder with a scanned laser is immensely complicated as it involves several different coupled physical processes. These include, laser/ powder interaction, very rapid heat transfer, rheology, adhesion and powder mechanics. Fortunately several simplified models exist. Kolossov et al., 2004, advanced a model for laser sintering based on continuous media theory where a "sintering potential," $\phi(\mathbf{x},t)$ can have values from 0, relating to loose powder and can tend to 1, which corresponds to fully sintered, 100% dense material. As seen in Equation (1), the sintering rate, $\zeta(T)$, is defined as a ratio of the surface tension, $\gamma(T)$ to the viscosity of the molten material, $\mu(T)$.

$$(1)\quad \zeta(T) = \frac{\gamma(T)}{\mu(T)}$$

The sintering potential is modeled as an asymptotic exponential as seen in Equation (2). Simple cases such as sintering at a constant temperature are easily evaluated, yet integrating changing surface tensions and viscosities, especially during the rapid heating cycles characteristics of laser processing are more

complex. It is also important to consider that the micro-scale details of actual softening, particle coalescence, flow and adhesion, particularly with rapid heating, are not expressly represented in the model. The heat transfer behavior describing the evolution of temperature during the SLS process is examined in greater detail in Section 3.1.4

$$(2)\quad \phi(\vec{x},t) = 1 - \exp\left(-\int_0^t \zeta\left(T\left(\vec{x},s\right)\right) ds \right)$$

The behavior of γ(T) and μ(T) are based upon polymer chemistry and rheological effects which are still being actively researched and characterized. Diagrams of these functions for various thermosetting powder-coating polymers, shown in Figure 8 and Figure 9, however, do shed light on sintering during the SLS process. In these diagrams the top data line is for an epoxy resin while the remaining lines show data for various polyester blends. Within the temperature range shown the surface tension decreases by about 30% while the viscosity is decreased more than six orders of magnitude (the material is melting and then thinning with increased temperature). The melt temperature for the polymers is about 90°C which corresponds to the fall in viscosity. With the lower viscosity there is a relatively large value for the sintering rate, ζ(T).

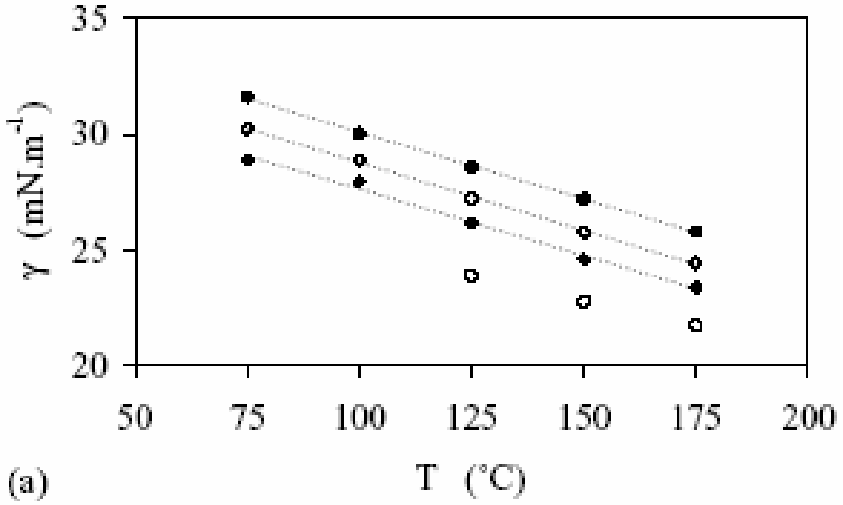

Figure 8 Surface Tension for Various Coating Resins (Wouters, et al. 2003)

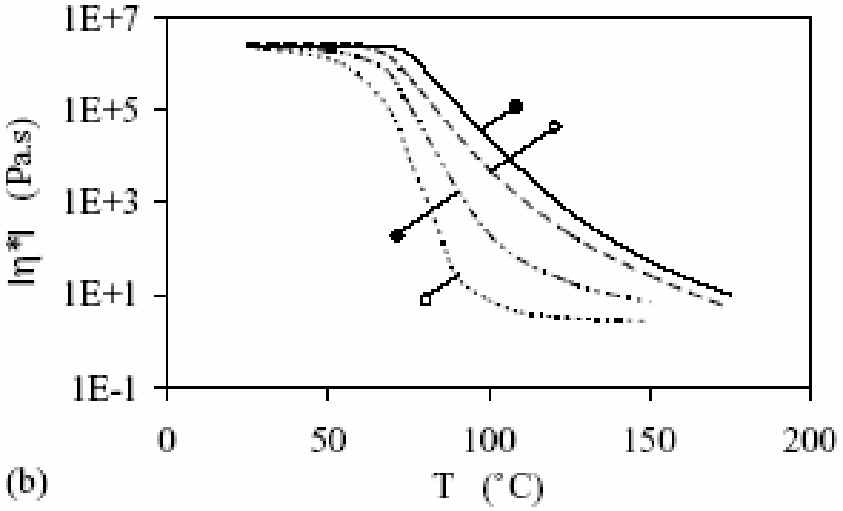

Figure 9 Viscosity for Various Coating Resins (Wouters, et al. 2003)

Building from the information in Figure 8 and Figure 9, Equation (2) can be simplified by substituting a linear function for $\gamma(T)$ and a two-value function for $\mu(T)$. This assumes that the sintering process occurs at temperatures where the viscosity can be assumed constant: away from the melt temperature and within a reasonable temperature range.

$$\gamma(T) = C_\gamma T + \gamma_0 \qquad C_\gamma = d\gamma / dT = const. \tag{3}$$

$$(4)\quad \begin{aligned} \mu(T) &= \infty \quad \forall T \le T_m \\ \mu(T) &= \mu_{liq} \quad \forall T > T_m \end{aligned}$$

The integral in Equation (2) , then, extends only during the time (from t_i to t_f) where the temperature has exceeded the melt temperature, T_m. The substitution of the temperature field, $T(\vec{x},t)$, into the function for sintering potential, $\phi(\vec{x},t)$ becomes more clear than in Equation (2). It is reduced to an integration of the temperature field rather than the sintering rate, as seen in the following equation.

$$(5)\quad \phi(\vec{x},t) = 1 - \exp\left({}^{-1}\!/_{\mu_{liq}} \int_{t_i}^{t_f} C_\gamma T(\vec{x},s) + \gamma_0 \, ds \right)$$

Still, C_γ, γ_0 and μ_{liq} must be determined for each polymer and the temperature field within the SLS machine is a challenging subject as is discussed in Section 3.1.4.

Building from the melting and recrystallization behavior of 3D Systems Duraform (a nylon-based material), the key parameters of SLS processing and Differential Scanning Calorimetry (DSC) may be introduced. The values discussed below are for Duraform and do not apply exactly to other materials. However, the basic elements of the following do apply whether a blend of polymers or polymers mixed with inert elements are considered. As introduced above, powder is supplied from the feed beds which are monitored by thermocouples within the powder and near the top surface. The part bed is monitored by an IR sensor. (In newer machines the part bed temperatures are also monitored via IR sensing) For each of these areas IR heaters are controlled via a feedback loop to maintain a desired upper surface temperature. Though these sensors are not rigorously calibrated, a standard temperature for the top of the part bed is 170°C while the top layers of the feed chambers are set in the range of 120 to 140°C. Some SLS machines have a part bed heater to maintain a constant temperature within the

depth of the part bed. More often this is either not used or not installed so the temperature decreases with distance from the top of the bed. As seen in the Differential Scanning Calorimeter (DSC) plot in Figure 10, 170°C is between the melt temperature (187°C) and the lower recrystallization temperature (146.5°C). This indicates that nylon can be either solid or liquid at 160°C.

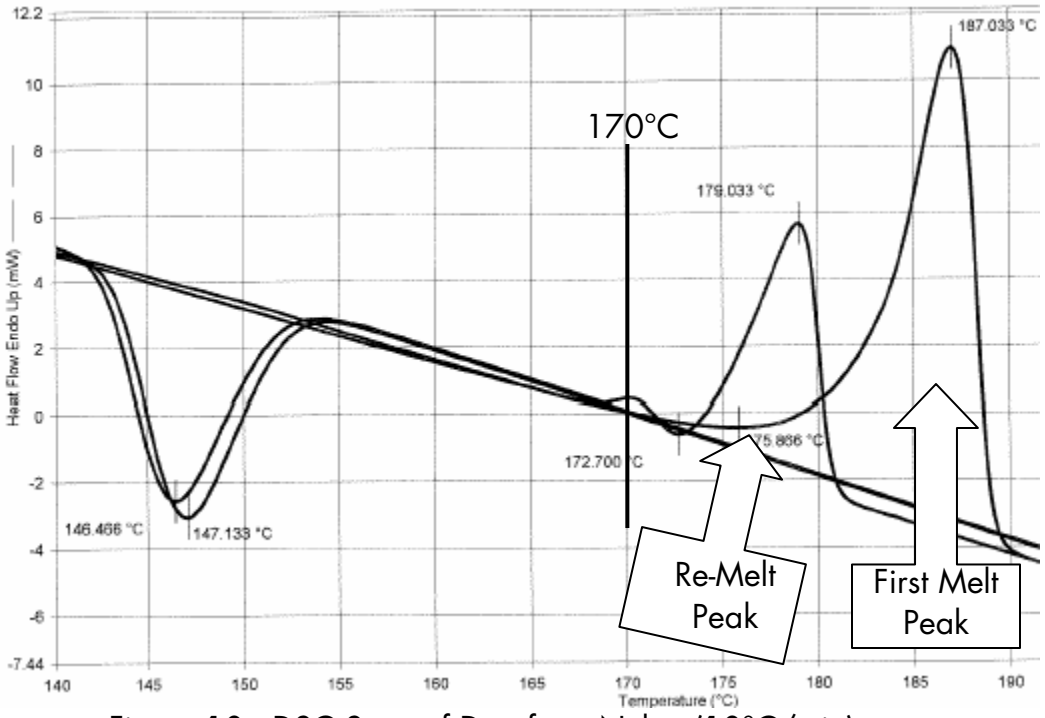

Figure 10 DSC Scan of Duraform Nylon (10°C/min)

The DSC forces a sample material to follow a prescribed temperature ramp while monitoring the necessary energy flow. An upward spike indicates that additional energy is being supplied to maintain the temperature ramp to overcome melting, as an example. The second trace in Figure 10 shows that the second melt of the same sample has a lower melting point (179°C) which is indicative of Duraform. The higher initial melt point is due to the molecular form of the powdered nylon which is formed by a precipitation reaction, rather than by grinding bulk material into a powdered form. The second melt on the other hand has a molecular structure determined by the cooling cycle within the DSC machine.

During the melting process, the smaller crystallites melt first with larger ones melting at higher temperatures. The shape of the melt curve is then related to the fraction of crystallites at various sizes. The size of "crystallites" is not directly related to the molecular weight, but rather relates to the crystalline engagement between polymer molecules. It is during the process of melting that the large difference in viscosity highlighted in Figure 9 occurs. Within a solid the viscosity is theoretically infinite, above the glass transition temperature the material will yield readily and then the viscosity falls through the melting process (again by several orders of magnitude). Nylon is semicrystalline. More fully crystalline materials like wax or ice melt to form very low viscosity fluids, while nylon retains a somewhat higher viscosity.

Since nylon can be solid or liquid within a range of temperatures, the scanned section of powder from one layer can remain partially molten while the next layer of powder is spread over the existing one. When the laser scans this next layer and the heat affected zone reaches the full thickness of it, molten powder bonds with molten powder. Then the bonded layers either cool slowly as they become buried deeper in the part bed or with a heated part bed chamber, as a whole when the build has been completed. As an empirical example of this process and its relationship to the sintering potential polystyrene, Duraform (nylon-12), and polypropylene wax may be considered. SLS processing of these three materials in a DTM 2500plus machine was observed during the research on this project. Polystyrene is an amorphous thermoplastic resin. Instead of melting, it more gradually softens at temperatures above its glass transition (a second order phase change process). Figure 11 shows a DSC scan for polystyrene. Parts can be made from polystyrene, but they are weak and porous: the higher viscosity limits the sintering rate and ultimately the final sintering potential of the parts.

Nylon-12 represents 85% of the material currently used in the SLS industry. It has the best SLS processing characteristics coupled with material properties of any commercially available SLS material. Polypropylene wax has an even larger temperature difference between its melt and re-solidification (at 59°C, seen in Figure 12) than Duraform (at 41°C). However, its viscosity falls so quickly (as it is more fully crystalline) above its melt temperature that it can almost instantly reach full sintering potential. It is difficult to keep scanned regions from becoming pools of low viscosity liquid. During the observed SLS testing of this material such pools were rounded and did not have the same shape as the scanned region of powder. The behavior of the material was dominated by surface tension. The key is that there are appropriate ranges of viscosity and surface tension that allow strong, accurate objects to be formed in the SLS process.

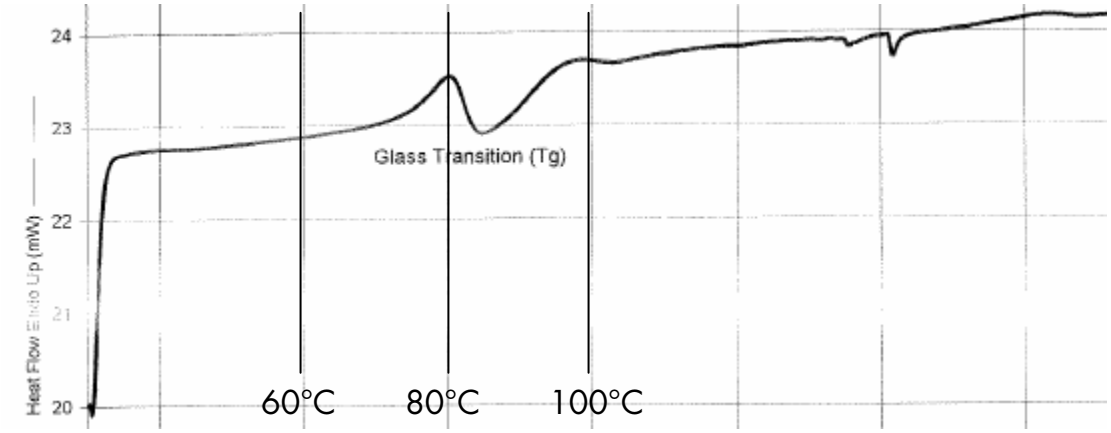

Figure 11 DSC of Polystyrene (glass transition, but no melt peak.)

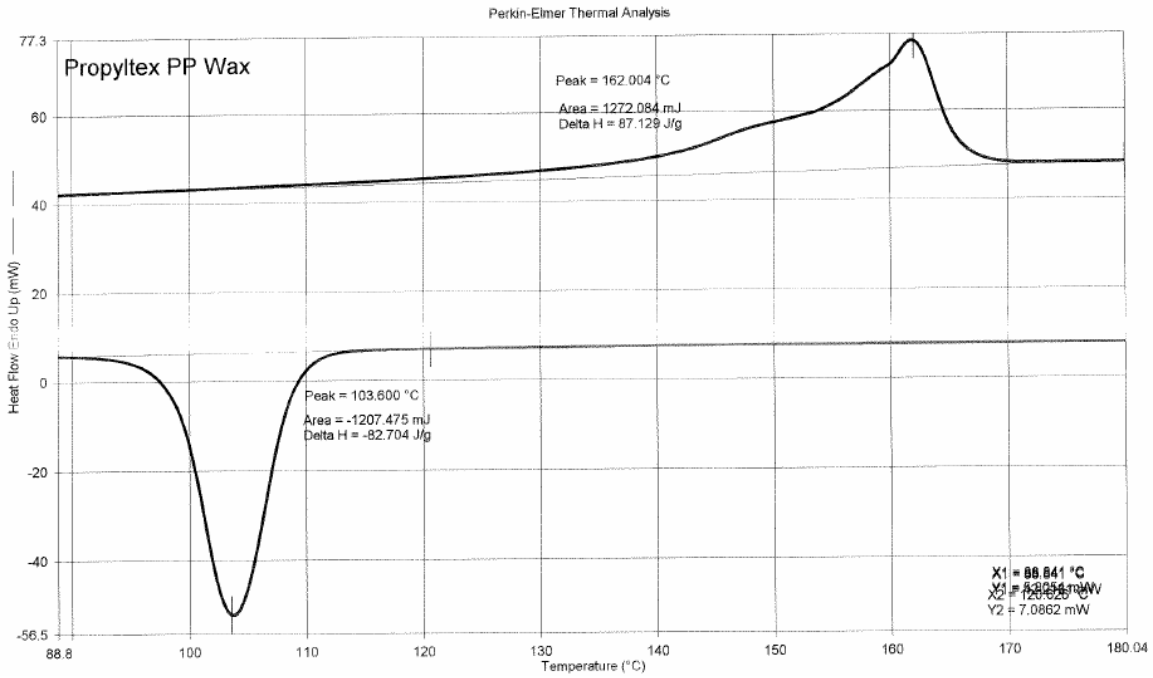

Figure 12 DSC of Polypropylene Wax (large difference between melt and recryst.)

Sintering is obviously important, but the management of shrinkage (exhibited by warping or "curl" in the parts) is a bigger challenge. The following expression, Equation (6), is from German, 1989. It relates a change in linear dimension, Δx, to the ratio of initial and final fractional density of a powdered material. The fractional density is relative to a theoretical, fully dense maximum density. In other words, a $\phi(\mathbf{x},t)$ of 1, would correspond to an f_f of 1. Obviously, an increase in density with the same amount of solid material results in a change in dimensions.

$$(6)\quad \frac{\Delta x}{x_0} = 1 - \left(\frac{f_i}{f_f} \right)^{1/3}$$

For reference, an initial fractional density of 0.5 and a final fractional density of .95 are typical for nylon powders used in the SLS process. Equation (6) relates this to a linear shrinkage ($\Delta x/x_0$) of 19.2%. As each layer of material is scanned within the SLS machine different regions receive laser energy at different times.

The thermal and sintering-based dimensional changes happen at different times in different locations. Further, since the laser heats the material from the top there is an inherent temperature gradient into the powder. These inherent properties of the SLS process can easily cause regions of layers, entire layers or multiple layers to exhibit shape distortion or curl. Interestingly, when the curl of the material is low, the shrinkage is exhibited predominately in the 'z' direction (perpendicular to the powder bed surface) creating a depression in the top surface of the powder which is filled in when the next layer of powder is spread. The sintering effect is in addition to dimensional changes from phase changes and thermal expansion. Basically, partially molten powder can accept the shrinkage of the above powder as it slowly melts and coalesces. If it does not, the top layer undergoes sintering and thermal shrinkage and the edges of the scanned area curl upward. This can happen gradually over the course of several layers and is called in-build curl. Post-build curl on the other hand sets up across the entire part during post-scanning cool down. Polypropylene, which has a rapid drop in viscosity when melting, solidifies rapidly, creating extensive curl across a scanned layer of powder (if it is not reduced to a pool of liquid by higher energy scanning). For binder systems, the shrinkage is less of a concern because of the low amount of material that is actually active under the laser and the stability of the inert material especially when it has more extensive particle-to-particle contact.

Even below its melt point, nylon does undergo chain-growth reactions that increase its molecular weight, and thus the viscosity, lowering the sintering rate of the material. There are also effects due to oxygen reactions. In short, nylon that has seen a significant thermal history does not sinter as well as virgin material. There is a visual indicator of poor sintering, called "orange peel," which is a pitting of the part surfaces. This is the reason for the powder blending and

recycling in commercial SLS operations. In existing commercial binder systems the part bed temperature settings are lower so that changes in the binder happen much more slowly (the powder can be almost completely recyclable), but there is no visible indicator other than part weakness for poor sintering in binder systems.

The key parameters set during SLS processing are laser scan power 'P_s', outline scan power, 'P_o', scan speed 'v_{beam}', scan spacing 'Δx', layer thickness 'z_{layer}', part bed temperature 'T_{pb}' and feed temperature 'T_f'. There are also settings for nitrogen flow and various temperature profile settings. Scanning parameters can be altered from one part to another and temperatures can be ramped across several layers. Laser fluence is a unit of laser energy dose, typically in units of J/cm^2. A similar, but less scientific, estimate of laser fluence called the Andrew Number is typically used in the SLS industry. The laser scan power, scan speed and scan spacing may be bundled together as shown in Equation (7). The 'f' in Equation (7) is a constant used to iron out units issues. The Andrew number can be used to guide changes in parameters to maintain the same basic part properties. As an example, doubling the scan spacing roughly halves the scanning time during a part build. Maintaining a similar Andrew number requires either a lower scan speed, which undermines the savings of scanning time, or higher laser power, which does not increase build time. Of course, small changes in transient conduction, radiation and sintering potential prevent different Andrew numbers from being associated with equivalent part properties. There are related effects on part strength, feature detail, curl, and surface finish, but these are not easily predicted. In practice the Andrew number is a guide for process improvement, but some iteration and testing is still required.

$$(7) \quad A_N = \frac{P \cdot f}{v_{beam} \cdot \Delta x}$$

Finally, thermosetting polymers add additional challenges to SLS processing, an exothermic chemical reaction and even more transient melt viscosities. The viscosities are a function of temperature cycle, not temperature alone. At one end of the spectrum, this reaction could be minimal and have little effect on the processing. On the other a large amount of crosslinking would occur under the laser changing the nature of layer-to-layer bonding and possibly undermining the recyclability of the powder. Additional heat transfer issues are also important. The basic behavior of thermosetting polymers is reviewed in Section 3.2.4.

3.1.2 Powder Mechanics

A review of basic powder literature and especially German, (1989), provides the main issues for understanding powder behavior. Building upon these an appropriate strategy for binders in SLS can be formulated. Average particle size, particle size distribution and particle shape, have a direct influence on the density and flow behavior of powder. Sand flows through an hourglass while dry flour tends to form clumps and will clog a funnel. In this document, the term 'flow' applied to powder is a qualitative term describing its tendency to cascade either while rolled in a cylindrical chamber or spread by the roller in the SLS machine. In addition, the effect of mixing different average particle sizes into multiple mode mixtures is an important consideration. As an example, flour particles can be mixed with sand and will, in part, fill the interstitial spaces between sand grains. Finally, one of the primary variables of binder function is the dispersion of that binder within the material to be bound. This is accomplished in industry by using attritor mills, ball mills and other mixing techniques.

The following is a synopsis of key elements in powder behavior. The flow of the powder is related to its tendency to freely form higher density compacts. In

practice this is quantified by assessing the tap density or measuring the angle (of repose) formed between a surface and the slope of a free, conical pile of the powder. This and other key powder processing characteristics may be found in Table 3

Table 3 Powder Processing Variables

Symbol	Name	Description
α	Angle of Repose	Angle of the side of a free-standing cone of powder
Nc	Coord. Number	The average number of touching neighbor particles in a powder arrangement
f	Fractional Density	Density as a fraction of the theoretical density of a material
-	Interparticle Friction	The friction that exists at the contact between adjacent powder particles
Ψ	Sphericity Index	The ratio of the surface area of a sphere with the same volume to the actual surface area of the particle
-	Porosity	Volume fraction of void space in a powder compact (equal to 1-f)
f_t	Tap Density	The density after vibration - the maximum density without compression

SPHERICAL PARTICLES: As a foundation for understanding the behavior of powder packing, consider an arrangement of monosized spherical particles packed into several typical crystal structure formations. Further consider that appropriately sized smaller spherical particles are arranged within the empty spaces of those structures, not altering the packing density of the larger spheres. Table 4 shows the coordination numbers and fractional densities for diamond, orthorhombic, cubic and face-centered cubic (or rhombohedral) structures. The effect of the smaller interstitial spheres is also shown. For the rhombohedral packing configuration, two interstitials exist. The last column will be discussed below in terms of determining appropriate binder characteristics. The purpose of

this table in terms of powder packing is to provide a range of fractional densities for perfectly arranged spherical particles. The rhombohedral configuration represents the highest unpressed powder packing density that is theoretically possible. In addition the general relationship between coordination number and density may be seen.

Table 4 Particle Packing + Interstitials (Adapted from German, 1989, p.138)

Particle Arrangement	Nc (# of tang.)	f (fract. dens.)	Smaller Diameter (Ds/D)	Added Volume	f (Combined)	Volume% of Smaller Spheres
Diamond	4	0.340	-	-	-	-
Cubic	6	0.524	0.723	0.391	0.729	28%
Orthorhombic	8	0.605	0.528	0.147	0.693	13%
Rhombohedral	12	0.741	0.225 0.414	0.019 0.070	0.810	8%

PARTICLE SIZE and PARTICLE SHAPE: When comparing particles of different sizes, the mass (volume) decreases faster, with D^3, than the area which decreases with D^2 (where D is the particle diameter or particle size). The result is that smaller particle sizes have higher friction (relative to gravitational forces settling the powder) and thus lower fractional densities. In practice, the same surface roughness exists for particles of various sizes, which tends to increase this effect. For the same interparticle friction (and other powder parameters to be discussed below), particles of higher density would have higher fractional densities. Figure 13 shows the relationship between particle size and the fractional density for Tungsten Carbide powder. Smaller particles have a lower packing density. This type of powder has a similar particle shape but a much higher density when compared to SiC.

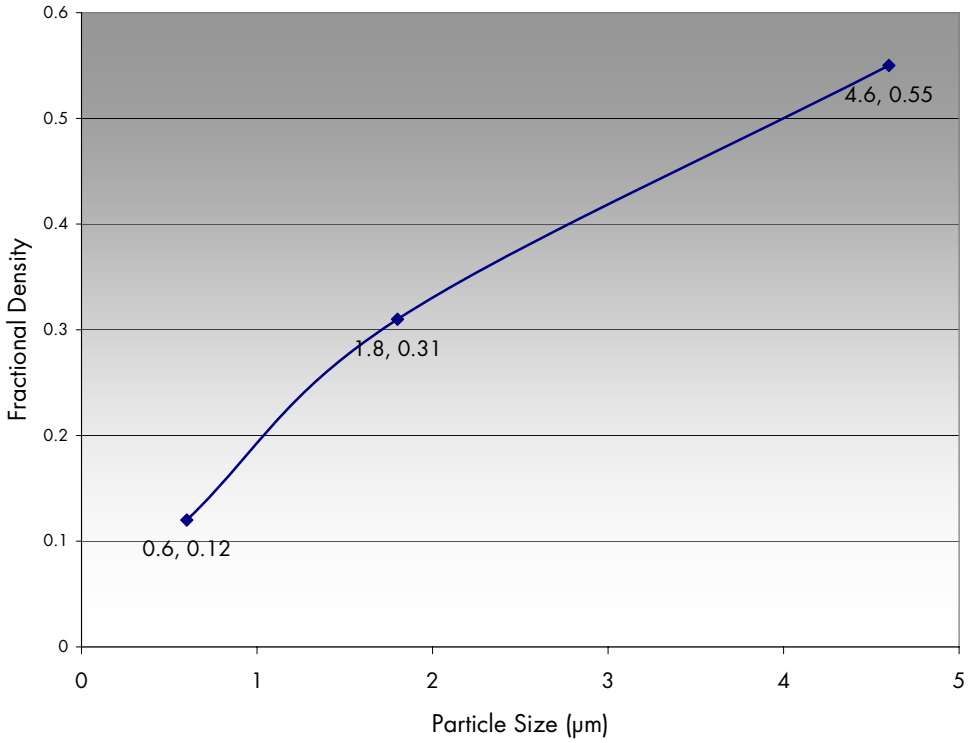

Figure 13 WC Packing Density versus Particle Size (German, 1989)

The shape of particles is also an important consideration. While regularly shaped particles can be arranged into high density packing arrangements (cubes to an 'f' of 1.0, as an example) irregular arrangement, or irregular shapes limit the powder to a density below that reached by ideally arranged spherical particles. As indicated in the previous paragraph, packing density is also decreased by increasing particle surface roughness.

PARTICLE SIZE DISTRIBUTION: The reality of powdered materials is that powders almost always exist in terms of a particle size distribution where the "particle size" is actually the *average* particle size. Although based on the properties of relatively spherical nylon powders, a general rule for SLS powders is that they should have only trace amounts of powder either above 80μm or below 10μm. Again, powders of a denser material can have less sphericity, greater

surface roughness or could have a larger fraction of small particles and still maintain appropriate behavior for SLS processing. Similarly, less dense materials, more irregularly shaped particles or greater surface roughness would tend to increase the minimum particle size limit and would probably tend to favor a larger average particle size as well. A greater percentage of large (>80μm) particles have a prominent effect on the surface roughness of finished parts while greater amounts smaller particles or "fines" inhibit the flow and alter the fractional density of the powder. "A high proportion of large, round particles, (German, 1989, p.197)," correlates with a high packing density. Further, a wide distribution (over several orders of magnitude) and more spherical particles have also been correlated to higher powder densities. Clearly, there is a balance to be made between maximum powder density and best flow characteristics with the processing characteristics of the SLS machine.

THE BEST BINDER POWDER: For the purposes of this project – it is the characteristics of a powdered binder that are of greatest interest. A related process is the sand casting process used to produce cast iron objects. The mold used to form such objects is often made from sand held together by a phenolic binder. The configuration of sand and phenolic particles produces stable parts capable of holding their shape even while in contact with molten iron. Thinking in terms of the phenolic and sand system, some guidance for SLS binders can be created.

If the sand and phenolic particles were both uniformly spherical and followed the relationships set forth in Table 4 the amount of phenolic needed would be relatively clear. Yet, the irregular shape of the particles prevents forming such a regular packing structure. Another baseline can be developed by imagining that each particle of sand is coated with a uniform layer of phenolic. Incidentally,

there are resin-coated sand materials that are commonly used for sand casting. Assuming spherical particles thicker layers would represent greater volume percentages of binder. This relationship may be seen in Figure 14.

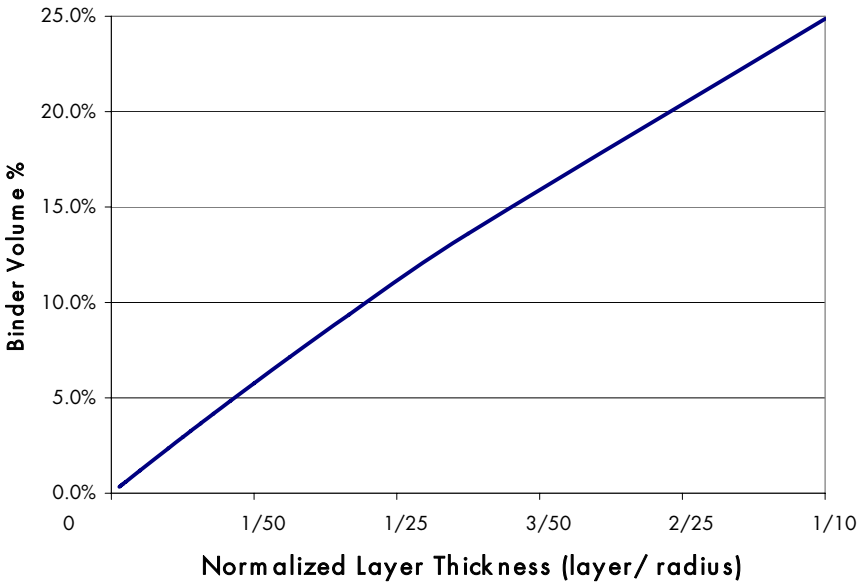

Figure 14 Binder Percentage for Coated Particles

For this model, thicker layers would represent greater shrinkage without significantly increasing the cross-sectional area of load bearing binder material between particles. It is not necessary to have a complete coating and still ensure a high probability of bonding between particles. Further, although powder coating is a commercially available and mature process, it does add significant costs over mixing powdered binders and base powders together.

Starting again from spherical particles, consider all sand particles to have a radius 'R' while the presumably smaller phenolic particles all have a radius 'r'. Let two such sand particles touch one another and one phenolic particle be tangent to them both, an arrangement shown in Figure 15. For this arrangement the upper 'sand particle' could be moved in a circular path with respect to the lower particle and still remain in contact with the phenolic particle. The same path would result

by revolving the line of length 'a' around the line connecting the centers of the phenolic and sand spheres, prescribing a region of the lower sand sphere called a spherical cap.

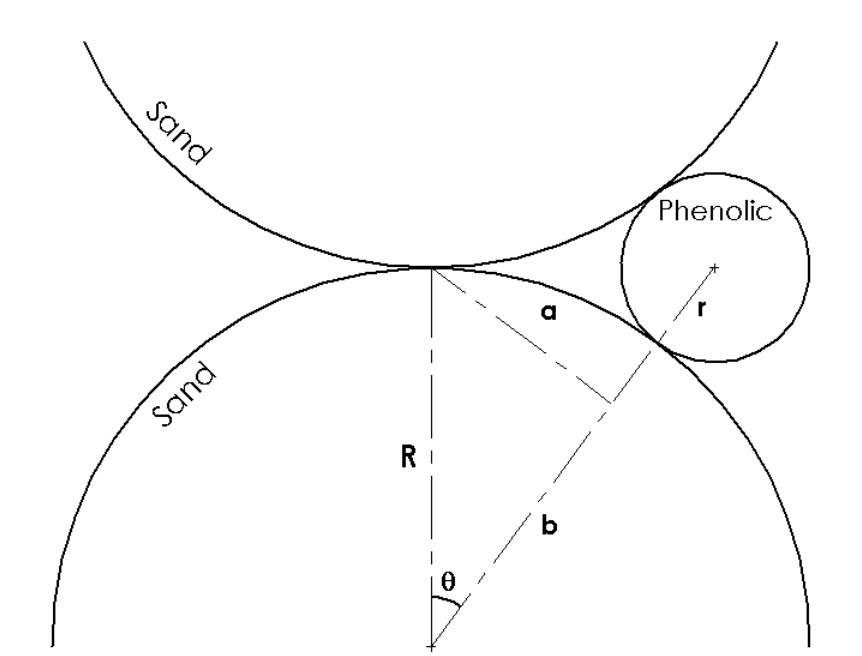

Figure 15 Theoretical Binder Geometry

In other words the phenolic particle presides over a certain area of the sphere and when heated will bind the two particles together. The ratio of the total sand particle area to that of the spherical cap region would determine the number of such particles needed to "coat" the entire surface of the sand particle, or at least make sure that if two sand particles touch they will very likely be bound together during an appropriate heating process. This assumption overestimates the amount of phenolic needed as the phenolic particle shown in Figure 15 presides over an area on each of the two sand particles. The area of a spherical cap adapted from Weisstein, 2004 is found in Equation (8). Combining this with the standard geometric relationships in Equation (9), Equation (10) can be created and used to estimate the number of phenolic (binder) particles needed for each sand (base)

particle. This can be used, in turn, to examine the relationship between the phenolic particle size (relative to the sand) and the volume percent of phenolic needed for high binding probabilities. This relationship is shown in Equation (11) and graphed in Figure 16. A similar type of relationship for establishing conductivity in a powder is shown as Equation (12) (German, 1989, p.265). The basis for this conductivity relationship is the connectedness between the conductive portion of the powder and how it establishes a reasonable conductivity in the material. In this equation, adapted from German, 1989, the base is insulating and for the purposes of this discussion, the binder is conductive. The value of this relationship is a critical value although initial conductivity readings may be found at 1/3 the value established by the equation.

$$(8)\quad A_{cap} = \pi\left(a^2 + \left(R-b\right)^2\right)$$

$$\frac{b}{R} = \frac{R}{r+R}$$

$$(9)\quad a^2 = R^2 - b^2$$

$$A_{sphere} = 4\pi R^2$$

$$(10)\quad \frac{A_{cap}}{A_{sphere}} = \frac{1}{2}\left(1 - \frac{R}{R+r}\right)$$

$$(11)\quad \frac{V_{Binder}}{V_{Total}} = \frac{2r^3}{\left(R^3 + r^3\right)\left(1 - \frac{R}{r+R}\right)}$$

$$(12)\quad \frac{V_{conductive}}{V_{total}} = \frac{1}{\left(1 + \frac{2.99R}{r}\right)}$$

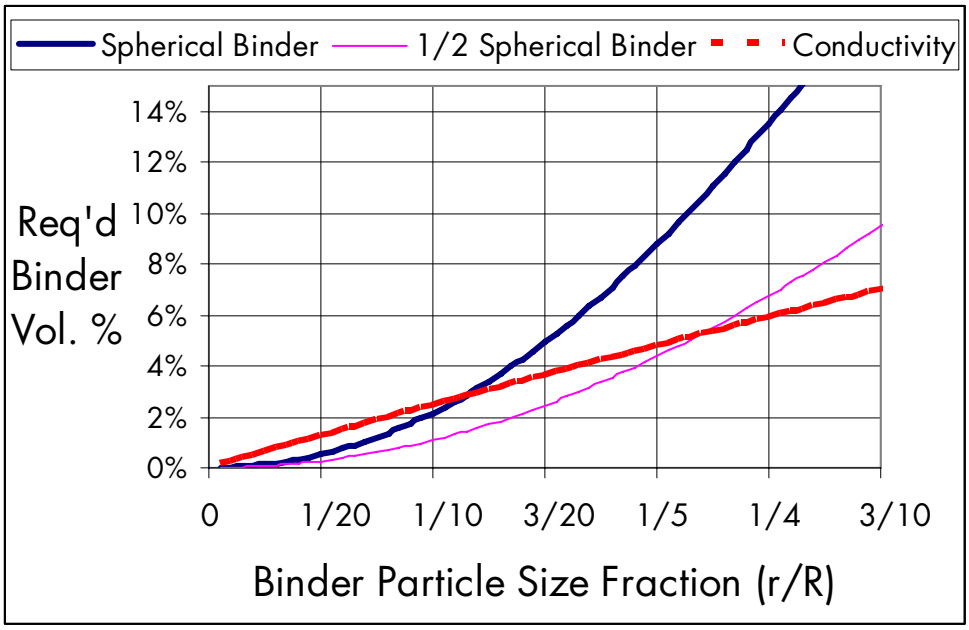

Figure 16 Required Volume Versus Binder Ratio

The solid thick line in Figure 16 is the graph of Equation (11) while the thin line is ½ of that value, representing one phenolic particle touching two sand particles. The dashed linear line is the conductivity model. The trend is clear. Smaller particles provide the same potential for binding with a lower volume fraction of material. While a larger amount of material between two touching particles might represent a stronger bond it also represents a larger proportion of the binder material. It is more important to have binding occur uniformly throughout the volume, than to have very strong bonds where they happen to occur. Another consideration is that smaller particles are more difficult to disperse evenly but also facilitate more connections between base particles and therefore less shrinkage upon sintering. Still, this provides a guide for choosing a binder size for a particular base particle size. It is also likely that certain powders will be readily available in only one particle size. It is also important to consider the effect of the particle size distribution here. The finer particles of a distribution are more valuable than the larger ones. The size guidelines for SLS powders introduced

above apply loosely to the entire powder and not just to the binder, which is intended to be present in a small fraction. If a particular sand material had a particle size of 40μm and a phenolic had an average particle size of 8μm an initial binder percentage to start with would be perhaps 7%, depending on the actual behavior of the powder mixture.

POWDER MIXING, GRINDING: There are several types of mixing and grinding operations used for powdered material. In some cases these two operations are done simultaneously. Rolling involves putting the binder and base powder into a cylindrical chamber which is placed on parallel rollers. As the chamber is rolled at an appropriate speed, the powder is circulated up one side of the chamber forming a standing cascade of powder. If the circulation and cascade can be set up, it is an efficient, low shear method of mixing. Ball milling is a variation on simple rolling where steel balls, as an example, are added to the mixture being rolled. The rolling speed is generally increased slightly to allow the balls (or other milling media) to fall into the rolling powder after being carried up the side of the chamber by the rolling motion. Finally, attritor milling involves a higher concentration of milling media and is actively stirred in a high-power mixing chamber – similar to a kitchen mixer. The attritor mill has a water jacket around the mixing chamber to minimize the temperature rise in the powder during mixing. More information about attritor milling may be found on the internet (www.UnionProcess.com). There are a variety of other temperature controlled industrial grinding methods as well.

POWDER SIZE DISTRIBUTIONS: The size distributions of powdered materials can be determined in several ways. First, sieves of various sizes can be stacked – the amount of material retained on each sieve indicates the relative amount of material that went through the previous sieve, but is retained on the

current one. Some of the notation for powders was derived from this process. A "-325" powder is one that would go through a 325 mesh screen, while a "+325" powder would be retained on it. Sieves can only be used as particle size indicators with materials that flow reasonably well and have specific gravities above about 2.0. This characteristic prevents their use for most polymer powders. Sieves are used to process polymer powders by using pore sizes significantly larger than the particle sizes. Powders of any type can be classified using an air classifier wherein the powder is lofted into a stream of air. The stream rapidly stratifies and is then split. A particle size distribution curve is generated by using a laser particle size analyzer, which are commonly coupled with air classifiers. The common means of reporting particle size distribution for powders is to list the D10, D50, and D90 sizes. D10 would be the particle size under which 10% of the powder's mass exists. D50 would represent the particle size under which one half of the mass exists.

POWDER TESTING AND COMPARISON: There are several simple tests to examine the behavior of powder. The first is to establish a tap density. When agitated (or "tapped"), powdered material will settle to a stable uncompressed density. By pouring a known mass of powder into a smooth cylindrical chamber and agitating the chamber the powder will settle to a stable density, the depth of which can be used to establish the fractional density.

3.1.3 Phenolic and Other Thermosets

In contrast to thermoplastics which can be remelted, thermosets undergo an irreversible crosslinking reaction where chains of the polymer are branched and bonded together into a 3D structure. This process, in general, allows thermosets to exhibit higher stiffness, adhesion and flame retardance than similarly priced

thermoplastic materials, though with less toughness. Incorporating and facilitating crosslinking into a manufacturing process presents additional challenges.

The curing of thermosetting polymers and the modeling of the curing process are mature subjects, but are also still actively researched. As an example, phenolic curing has been studied for over a century, but, "a detailed knowledge of the curing chemistry has not been achieved (Zhang et al., 1997, p.5835)." Kinetic models of the curing reactions of thermosetting polymers may be directly related to DSC data. The amount of curing that has occurred in a particular thermoset is defined by its "degree of conversion," 'α', where a value of 1 would indicate a fully cured sample. Equation (13) shows how the rate of conversion is related to the heat flow, 'dH/dt' and the total heat of reaction (the heat evolved during the curing process), ΔH_R (Ishida, et al., 1995, Montserrat, et al., 1993, Kosar et al., 2004). The total heat of reaction for the phenolic trace shown in Figure 30 would be the total area of the exotherm curve from 120°C to about 180°C. For each temperature in this region the position of the trace below the value at 120°C represents the heat flow. Finally, the temperature scan is linear with time.

$$\frac{d\alpha}{dt} = \frac{dH/dt}{\Delta H_R} \qquad (13)$$

While some analytical models of thermoset curing incorporate a coupled set of equations for each of several intermediate reaction compounds such as the 4 component model of epoxy curing discussed by Fouchal, et al., 2002, a simpler form, Equation (14) is more widely accepted. This is an empirical model set by the particular curing behavior seen on a DSC trace. And f(α) can be related to the shape of the DSC curve (which is a graph $dH/dt(T)$ versus 'T') by combining Equations (13), (14) and (15), as adapted from Montserrat, et al., 1993.

$$(14) \qquad \frac{d\alpha}{dt} = k(T)\, f(\alpha)$$

$$(15) \qquad k(T) = Ae^{\left(-\frac{E}{RT}\right)}$$

$$(16) \qquad \frac{dH}{dt}(T) = A\Delta H_R e^{\left(-\frac{E}{RT}\right)} f(\alpha)$$

The most common form of f(α) from the literature reviewed is found in Equation (17). The values of 'm', and 'n' in this relationship would be chosen to fit curves established from DSC data.

$$(17) \qquad f(\alpha) = \alpha^m (1-\alpha)^n$$

Finally, if the total heat of reaction for a particular thermoset, ΔH_R, is known then the degree of conversion, 'α', of a sample would be the amount of curing that a sample had undergone divided by the total heat of reaction, as seen in Equation (18). Or, the degree of cure of a sample can be established by knowing its curing exotherm (from a DSC scan), ΔH_{sample} and the total curing exotherm of the material, ΔH_R as seen in Equation (19).

$$(18) \qquad \alpha = \frac{1}{\Delta H_R} \int_0^t \frac{dH}{dt}(t)dt$$

$$(19) \qquad \alpha = \frac{\Delta H_R - \Delta H_{sample}}{\Delta H_R}$$

3.1.3.1 Phenolic Chemistry

Often called "the workhorse of thermosets," Phenol Formaldehyde resins (or phenolics) represent the earliest mass produced fully synthetic polymers (and only cellulose nitrate or "celluloid" predates it commercially). They are characterized by high strength (for a polymer), but like many thermosetting polymers also exhibit brittle fracture behavior. Although formed from very reactive precursors in phenol

(C_6H_5OH) and formaldehyde (CH_2O) the cured resin is extremely stable and nearly inert below the onset of decomposition (~300°C). There are two basic types of phenolic resins, resoles and novolacs. Resoles are usually liquid before crosslinking and are used extensively in the production of plywood. Novolacs exhibit more rapid curing and are the predominant type used for powder systems. Uncured novolac resins do melt. The onset of melting varies, but is typically complete after about 120°C. For example, the initial lot of phenolic examined during this project had a melt onset of 70°C while the sample was completely molten at 110°C. This may be seen in Figure 17.

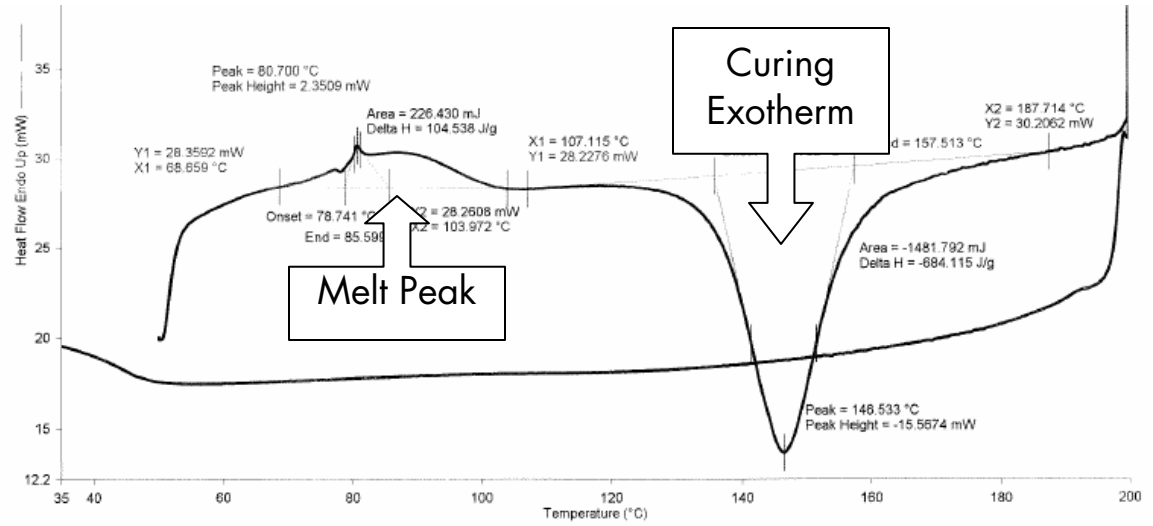

Figure 17 DSC Scan of Phenolic

According to Georgia Pacific, the manufacturer of the GP-5546 phenolic used extensively during this project, the onset of curing occurs at the same temperature as the onset of melting. The curing is relatively slow in the temperature range of the melting process, but the viscosity of the material (due to the increase in 'α') is transient and increasing when it is molten. In the GP-5546 resin system, Hexamethylenetetramine (HMTA, $(CH_2)_6N_4$), a common crosslinking agent, is compounded with a novolac resin. The GP-5546 resin was chosen in part because its relative melt viscosity was lower than other readily available

novolac powders. This is tested commercially using a heated (150°C) inclined plane and is not related to an actual viscosity. Lower viscosity was expected to increase the sintering rate, or binding ability of the material. GP-5546 also featured a relatively rapid curing reaction.

Fifteen different types of intermediate compounds were identified by Zhang, et al., 1997 in the curing reaction of phenolic resin with HMTA indicating the complexity of this process. The reaction rate increases with lower pH, hence the possibility of adding of acid catalysts for more rapidly curing resins. HMTA is alkali, so larger amounts tend to slow the reaction. Zhang, et al., 1997, also report that higher HMTA increases the higher-stability nitrogen-containing linkages, yielding stronger cured resin. "The reactivity of novolacs with HMTA increases with increasing water content. (Knop and Pilato, 1985, p.95)"

The usual chemical structure of novolac may be seen in Figure 18. During its decomposition in the range of 140°C, HMTA facilitates the rapid formation of a variety of linkages from CH_2 (Methylene) and Nitrogen groups within the curing resin. These are crosslinking reactions, creating a strong interconnected 3D structure while evolving heat, water and ammonia. Figure 19 and Figure 20 are diagrams of the most common nitrogen-containing linkages that form in the presence of HMTA decomposition products, although additional CH_2 linkages – as seen in novolac are also formed. Many other types of linkages have been identified as well. All of the linkages shown in these diagrams are 'ortho-ortho' linkages – indicating their adjacent position on the benzene ring of the phenolic relative to the OH group. The 'para' position, opposite the OH group, is also a potential binding site and in some cases the ortho and para positions can support linkages on the same ring. Finally one ring can rotate relative to adjacent rings to accommodate the creation of new linkages or to establish a lower energy

relationship relative to nearby molecules. There is an immense variety of interconnected, three-dimensional crosslinked structures possible in this polymer system. A more detailed discussion of the reactions may be found in Knop and Pilato, 1985, p. 52 and in Zhang, et al. 1997.

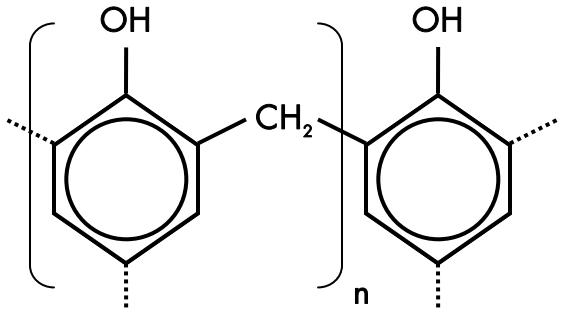

Figure 18 Chemical Structure of Novolac Resin

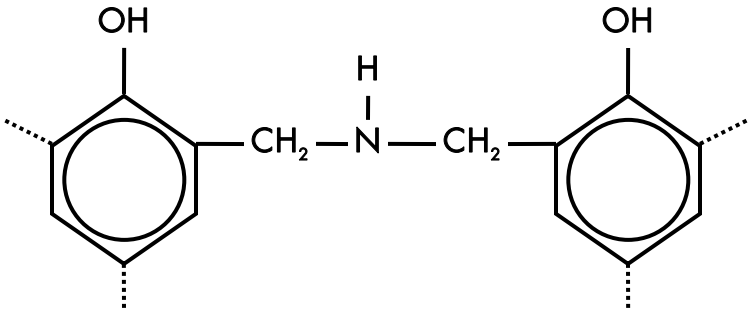

Figure 19 Lower Temperature HMTA Linkage

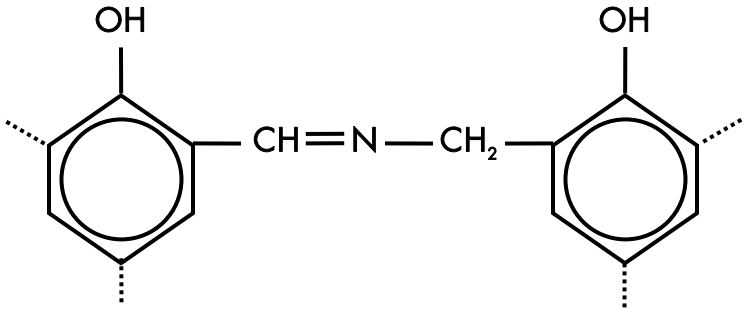

Figure 20 Higher Temperature HMTA Linkage

The usual analysis of phenolic resin and other polymers involves a Differential Scanning Calorimeter at scan rates of 10-40°C. Different scan rates

do influence the melt and crosslinking behavior as these processes are rate dependent. Under the laser the rate of temperature increase will be extremely high and again not easily considered with standard DSC testing. The crosslinking reaction in phenolics is accompanied by shrinkage, and the structure of the cured resin can be undermined in molded parts by the evolution of gaseous crosslinking products. However, if they are used in powdered form as binders then these effects should not play a significant role. Abhinandan et al., 1999, examined the behavior of an epoxy-polyester hybrid thermoset cured by IR laser. They observed several different final material states relating to the laser power and scanning rates used: these were unaffected powder, a smooth film, curing onset, fully cured and thermally damaged powder. The DSC of their powder showed a melting phase and a higher temperature rapid cure which are similar to the behavior of phenolic. The area of the curing peak was used in their study to determine the amount of curing in partially cured polymer samples. Finally, higher powers coupled with more rapid scan rates have been linked with lower melt viscosities (Abhinandan, et al., 1999)

3.1.4 Heat Transfer in SLS

The SLS process, whether polymeric or metallic materials are being used is fundamentally a heating process. A laser provides rapid local heating which induces a phase change, material flow and then rapid solidification. In this section a basic overview of relevant heat transfer issues is presented followed by a discussion of simple models that were used to characterize the process and ultimately guide the research.

Understanding the interaction of the laser and the powder is a complex, multi-physics problem, but one that is fundamental to the SLS process. Equation (20) is a standard transient conduction relation with the addition of a non-zero

convection term. The rapid heating under the laser coupled with the temperature change (~50°C for polymers, >150°C for binder systems) makes the temperature dependence of 'ρ'and 'c' significant.

$$\rho(T)c(T)\frac{\partial T}{\partial t}+v\rho(T)c(T)\frac{\partial T}{\partial x}=\frac{\partial}{\partial x}(k_x\frac{\partial T}{\partial x})+\frac{\partial}{\partial y}(k_y\frac{\partial T}{\partial y})+\frac{\partial}{\partial z}(k_z\frac{\partial T}{\partial z})+\dot{Q}_V'''(x,y,z,t) \quad (20)$$

The absorptance of materials changes with temperature and more significantly across phase changes. Further, infrared radiation is known to behave as a volumetric heat source, rather than strictly influencing the surface. This effect is more pronounced in transmissive or porous materials. The behavior of powders complicates this effect and the conductivity, 'k' as well. The sintering of powder particles has an influence on the heat transfer as well. "The increase in transmission as well as its dependence on the wavelength (of the laser) is observed only when (polymeric) powder particles start fusing (Abhinandan, et al., p.254)." In other words the coupling of the laser to the powdered material can exhibit significant changes during SLS processing. However, Kolossov et al., 2004, state that powder layers of metals thicker than 5 particle widths may be approximated as having surface heating when scanned by an IR laser. This should apply to binder systems where the base material has low transmissivity as well.

Fortunately, with a few assumptions it is possible to piece together useful analytical models. First, using a semi-infinite approximation and further assuming that an instantaneous pulse of energy, 'E', is delivered and completely absorbed at time t=0, results in Equation (21) (Mills, 1999, p.181). The expected dependence on time and depth, 'z' is clear here, but the model does not address the actual form of the incident radiation.

$$T-T_0=\frac{E}{\rho c\sqrt{\pi\alpha t}}e^{-z^2/4\alpha t} \quad (21)$$

Ion, et al., (1992), went further to incorporate the dynamics of a scanning Gaussian IR laser, similar to that used in the SLS process. They also introduce parameters to map the model onto actual scanning data while avoiding the infinite values at time t=0. The analytical model of the thermal cycle they created, Equation (22), relates beam power, scan speed and the depth into the substrate at the center of the beam path. In this equation, 'A' is absorptance 'a' is thermal diffusivity, 'q' is beam power, 'v' is beam speed and 'k' is thermal conductivity while 't_0' and 'z_0' are reference parameters of characteristic time and length respectively used to capture actual data. Equation (23) indicates that 't_0' is related to the beam radius and the thermal diffusivity of the substrate material. 'z_0' on the other hand is to be set by matching the output of the equation to the temperature at the *actual* surface of the powder. The dependence on depth is the same here as in the simple pulse example, but the dependence on time is slightly different even considering the effect of the velocity term. Unfortunately, the form of the equation with respect to 't' does not support closed form integration, which would allow this expression to be readily incorporated with the simplified expression for sintering potential, Equation (5).

$$(22) \qquad T - T_0 = \frac{Aq}{2\pi kv\sqrt{t(t+t_0)}} \exp\left[\frac{-(z+z_0)^2}{4at}\right]$$

$$(23) \qquad t_0 = \frac{r_B^2}{4a}$$

The influence of power and scan speed on the peak temperature are clear here, but a better understanding of thermal spreading across the powder, temperature profile and temperature decay are needed to understand the influence of SLS processing parameters. In SLS, the laser is scanned at high rates as it rapidly rasters over the surface. It is important to consider the effects of this scanning as subsequent passes near the same spot change the thermal cycle estimated by

Equation (22). This additional element was described by Nelson, et al. (1995) and incorporated into their development of an iterative FEM model for predicting the temperature profile. It is expected that the temperature of a point in the powder when scanned by a laser should rapidly rise while the radiation is incident and then decay and spread after the laser passes. When a narrow shape is being scanned, a point in the powder will be reheated before it has a chance to cool completely. The maximum temperature would then exceed that at the center of a single laser pass. Kolossov et al., 2004, and Dai and Shaw, 2004 observed a maximum temperature at the center of a scanned square region.

The next piece of the puzzle is to extend the laser scanning models above, which were prepared for solid materials, to a bed of powder. Within a powder, heat transfer happens relatively easily as conduction within a particle, but relatively slowly across the spaces between them. Kai and Shaw, 2004 suggest an effective thermal conductivity for the powder bed relating porosity and the respective conductivities of the solid powder 'k_s' and interstitial fluid 'k_f' as well as the radiation from one particle to another within the powder bed 'k_r'. φ is the fractional porosity and x_r is the average particle radius. Equation (24), a simplification assuming rigid, spherical particles allows the heat transfer equations above to be extended to powder. The remaining element of this analysis, which is left to the following research discussion, is to address the effect of the exothermic curing of phenolic on the thermal cycle of the powder.

$$\frac{k_{eff}}{k_f} = \left(1-\sqrt{1-\varphi}\right)\left(1+\frac{\varphi k_r}{k_f}\right)+\sqrt{1-\varphi}\left(\frac{2}{1-\frac{k_f}{k_s}}\left(\frac{1}{1-\frac{k_f}{k_s}}\ln\left(\frac{k_s}{k_f}\right)-1\right)+\frac{k_r}{k_f}\right) \quad (24)$$

$$k_r = \frac{4}{3}\sigma T^3 x_r \quad (25)$$

3.1.5 The Research Task

The task at hand is to establish a thermoset binder system for use in the SLS process. The base material (to be bound together by the phenolic binder) was limited to glass microspheres and silicon carbide due to the wide variety of potential applications and the relatively low cost of both materials. Similarly, although several types of thermosetting polymers were screened, phenolic was chosen as the binder for this project, again due to availability and also due to its ease of processing and low cost. In the discussion above the main subjects supporting this work were reviewed: powder mechanics, the SLS process, thermoset curing and heat transfer. From this, the basic structure of an SLS process for thermosetting materials can be created, as shown in Figure 21. The variables are within the boxes while the observables are shown in the rounded shapes below the main processes. Based upon this framework, thermosets were studied and a more general SLS materials testing method was pursued.

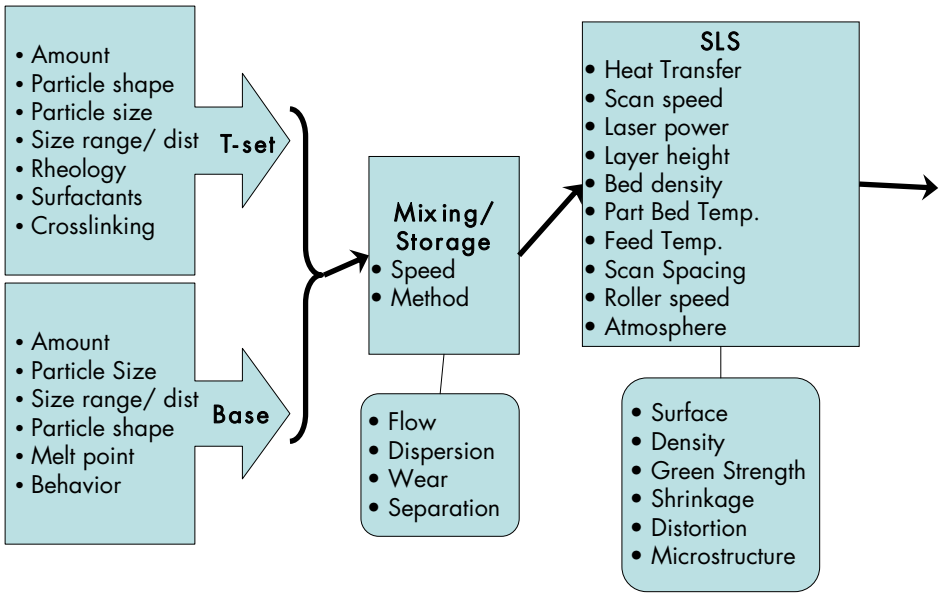

Figure 21 Thermoset Binder Processes and Key Variables

3.2 Method

3.2.1 Powder Behavior

A basic analysis of tap densities and powder behavior was performed on a variety of powder compositions including commercially available SLS powders. Duraform, the most common, is a nylon-12 powder. There are also steel powders, called Laserform, which have spherical particles. The Castform (polystyrene) material also features nearly spherical and smooth particles. Of the current SLS materials, Duraform is the material with the poorest packing and flow characteristics. The idea was to compare new powders to the behavior of Duraform.

Straight-sided glass jars commonly used for storing spices were used to test the tap density by comparing the height and weight values to that of water (see Equation (26)). The same solid volume of powdered material was placed in each jar. The jars were rolled on their sides to observe the powder's tendency to flow and to ensure powder uniformity. The jars were then literally tapped on a hard counter top, but not hard enough to disturb the top layer of the powder. After the powder settled to a static height in the jar, it was measured and related to a fractional density. 'm' is the mass of the powder sample, 'α' is the cross-sectional area of the jars, and SG is the specific gravity of the bulk material.

$$f = \frac{m}{\alpha \cdot h \cdot SG} \tag{26}$$

Three different relationships were examined during tap density testing. The first was the relationship of particle size and shape on tap density. The sizes of silicon carbide powder used may be found in Table 5 , below. Next, the effects of adding various fractions of fine powder to a coarser powder (bimodal mixtures) were examined to approximate the effect of adding binder to the SiC powder.

Finally, combinations of phenolic with both glass and silicon carbide powders were tested. This last test included powders prepared in a variety of ways, which is discussed in the following paragraph. In each of these tests a standard bulk volume was placed in each glass cylinder which facilitated comparison between different powders.

Table 5 SiC Powder Data (aaa-industrialsupply.com)

Grit Rating	D6 (μm)	50% in range (μm)	D97 (μm)
280	22	35 - 38	59
320	16.5	27.7 - 30.7	49
600	3	8.3 - 10.3	19
1200	1	2.5 - 3.5	7

The second main topic in this section involved mixing, grinding and the dispersion of the binder within the base material. Several different types of powder preparation methods were used. Phenolic (GP-5546) was used directly from Georgia Pacific and ground by the HJE Company, Queensbury, NY. The Base (SiC) and binder were mixed using rolling, attritor milling, ball milling (with ½" cylindrical alumina media) and for larger batches a cement mixer. The powder mixed in the cement mixer was subsequently sifted using a sieve attached to the lid of a barrel lined with a plastic bag, to retain the media. The attritor mill used had a damaged motor and chamber. The chamber capacity was about 1 quart of powder and it leaked profusely through a damaged valve. Powder was simply passed through it as if it were a continuous feed process to assess the effect of attritor milling. The alumina milling media was also added to the cement mixer. Visual comparisons, tap density and flow, SLS processing behavior and SEM images were used to analyze the various types of powder preparation.

A standard Hitachi scanning electron microscope (SEM) was used to examine microstructural features of powders and powder mixtures. This allowed macroscopic tap density and flow observations to be related to particle features and size distributions. SEM images were also used to identify micro-structural features throughout the research and images are found throughout the results section of this and subsequent chapters.

3.2.2 Polymer Analysis

A variety of readily available powder coating thermoset resins including polyester, polyamide-imide, acrylic, epoxy and hybrid resins were obtained and tested in a DSC from 50 to 200°C at ramp rates of 10 and 20°C/min. All DSC plots in this dissertation were run by the author except for polypropylene and nylon which were run by Chris Schaefer, an undergraduate research assistant, for this project. More details of these resins may be found in the result section to follow. These materials were chosen as their normal use involves rapid heating and curing, often with IR radiation, which is similar to SLS processing. The DSC allowed their melt and curing behavior of these resins to be compared with the phenolic which has previously been a component of an SLS binder system.

Differential scanning calorimetry (DSC) and scanning electron microscopy (SEM) analyses supported work in binder characteristics and SLS processing outlined in subsequent sections. Additional information on the DSC used and the type of data that may be obtained can be found in the polymer characterization lab section of the Texas Materials Institutes internet address (www.tmi.utexas.edu).

The DSC was also used to assess the degree of cure for thermally aged phenolic powders as well as various samples taken during actual SLS processing. Thermal aging was done using a standard lab oven. Pure samples of phenolic were aged at 60, 70 and 80°C for at least 2 hours. The longest soak was over 8

days. The soak temperatures were chosen to bound the 70°C melt onset found during DSC analysis which was expected to represent an upper bound for the part bed temperature in the SLS machine (to avoid turning the bed into a solid brick). The idea was to explore the changes in the phenolic both in curing exotherms and melt endotherms due to the heat aging. These observations were expected to inform the analysis of observed changes in SLS processing.

3.2.3 Basic Binder Characteristics

While actual SLS testing is the most informative way (currently available) to examine a particular binder, it requires several pounds of material to assess multiple layer builds and 50 to 100 pounds or more to explore the various transients associated with SLS processing. If a variety of materials and material ratios are to be explored SLS testing, is not an efficient testing method. To quickly examine a broad variety of binder mixtures, a Teflon powder mold was prepared, which is illustrated in Figure 22. The cavities are 5.5" in length and 0.5" in width and depth – this shape matched the largest beam specified in the ASTM D-790 bend test specification. Rockwell hardness testing (especially 15W, 15Y or 15N) was also planned. The purpose of the mold was to explore the effect of different binder formulations using small quantities of powder. Changes in cured strength and shrinkage were expected to be observed both qualitatively and during bend testing. It was assumed that the strength and shrinkage of the SLS parts would be less than the molded parts, but that the effect of powder constituents would still translate. As introduced in Section 2.2.1, previous Indirect SLS research at UT made use of a three-part binder consisting of Nylon, Wax and Phenolic.

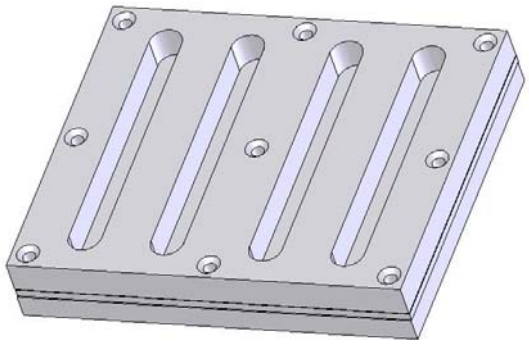

Figure 22 Bend Test Mold

280 grit SiC powder was mixed with 6, 10 and 14% Phenolic and was mixed by rolling only. The powder was lightly packed into each chamber, leveled and placed into a preheated standard lab oven at several temperatures. The best temperature for preparing phenolic/ SiC molds was 120°C and soaks of longer than 40 minutes did not improve final strength. The strength, color and other features of the molded parts were examined qualitatively. A more rigorous examination using the ASTM D-790 method for three-point bend strength was prepared by Bhandari, (2004) as a part of her examination of the original 3-part binder formula (nylon, wax and phenolic).

3.2.4 Heat Transfer Analysis

The thermal characteristics of several different materials were examined to put the materials of interest in this project in context. Table 6 shows the density, thermal conductivity, specific heat and thermal diffusivity for phenolic and SiC as well as for comparison materials. The most interesting aspect of this table is the high conductivity of the SiC ceramic material. The effective conductivities the powders examined during this project were found using Equation (24).

Table 6 Basic Thermal Properties of Selected Materials (azom.com)

Material	SG	k (W/m-°K)	cp (J/g-°K)	a (cm *cm /s)
Phenolic	1.30	1.46E-01	1.30	8.64E-04
Nylon	1.02	3.00E-01	2.60	1.13E-03
Alumina	3.80	2.50E+01	0.87	7.56E-02
Aluminum	2.74	2.40E+02	0.97	9.03E-01
Iron	7.87	8.02E+01	0.45	2.27E-01
SiC	3.16	1.10E+02	0.72	4.87E-01

A basic evaluation of heat transfer issues was performed to get an understanding of the temperatures ranges and thermal cycles expected within the SLS machine. This would then help examine the feasibility of running phenolic or other thermosets and hopefully guide the subsequent research. The first part of this involved bounding the temperature rise expected by considering the volume of powder heated by a scanning laser (modeled after the standard SLS laser) in a single second. The following assumptions were taken during the calculation. Basically, this estimates the temperature rise if the energy was distributed evenly through the powder heated during one second of scanning.

1. 1-second strip of powder, 4mils thick…
2. 1mm beam width
3. Flat beam profile
4. Adiabatic beam edge
5. 50% powder density
6. Constant temp across and into powder
7. 0.004" affected depth
8. 10W beam at powder surface
9. 10% phenolic/ 90% Silicon carbide powder

The results of this initial analysis and an assessment of the effective thermal conductivity for the powder supported the use of Equation (22) to determine the heat plume below the advancing laser. The temperature rise was matched with the more comprehensive FEM model described by Nelson, et al. (1995). The

other piece of information was the temperature spike observed when the laser scanned under the IR temperature sensor. These two analyses provided information about the phenolic melting, the time scales and the depth to which melting could be expected to occur.

3.2.5 SLS Processing

For all of the capability it does have, the SLS platform is not a robust, hands-free system. Instead, different machines have slightly different behaviors. Lasers require calibration and clean optics to have power levels read correctly. Temperature sensors are not routinely calibrated (except where this is automated in the newest SLS machines) and the thermocouples and IR sensors exhibit different fluctuations in their readings. There are significant thermal transients inherent in the process since the laser and IR heaters are adding energy while the volume of powder in the part bed changes. Each layer of new powder is typically cooler than the set temperature for the part bed. Different layers receive different amounts of laser energy. In addition, the machine components surrounding the powder beds have a significant thermal mass. There are temperature gradients from the center to the edge of the part bed which have been measured to be in excess of 30°C at times. There are different thermal cycles seen in scanned regions based on part placement, part orientation and the order in which different parts are scanned within a particular layer. The point is that there is some art involved in running an SLS machine: the process does not lend itself well to an elaborate, methodical plan of development. Instead, it is a case of carefully observing the operation of the machine and of parts produced to help evolve an appropriate set of parameters to reliably produce parts. Watching both the scanning and powder spreading for several layers allows early stages of in-build curl to be observed. Incidentally, this can be mitigated by lowering the laser

wattage, increasing the part bed temperature or increasing the feed temperatures. The other observations that are important are the feed and part bed temperatures as well as heater duty cycles (a measure of the power going to the heaters). The detailed notes from the initial multi-layer builds, found in Appendix 2 indicate observations and parameter changes made during that set of runs and provide a guide for running new materials in the SLS machine.

An understanding of the melting and curing characteristics of the phenolic and a basic analysis of the heat transfer characteristics within the powder bed supported decisions during the work in the SLS machine. The work to set upper and lower limits for appropriate powder mixtures was completed in the molds described in Section 3.2.3 above. The development of an appropriate SLS process for a new commercial material may be broken down into 4 main phases, which are described below. The organization of these phases grew both out of the current research project and by observing concurrent SLS materials development activities with Advanced Laser Materials, LLC.

Phase 1: Single Layer Scans

Before enough powder was mixed to fill the machine, some basic SLS parameters were explored using a small tray of powder placed in the center of the SLS machine which facilitated using a small amount of material during each test. In addition, the temperature of the part bed reaches its set point in seconds rather than 10-20 minutes for a fully charged machine. Iterations can happen quickly. For each test, the powder in the tray was carefully leveled and a single scan of the laser traced several shapes in the powder. Most of the powder used for the scans was milled using a Union Process attritor mill which size reduced the phenolic and also dispersed it evenly throughout the SiC powder. Other tests used powder that was simply rolled. The build height was set at 0.003" and the layer thickness at

0.004" to prevent the roller from moving. The piston was raised to just below the point that the powder tray would interfere with the roller if it accidentally moved during the scanning process. The tray, pictured in Figure 23, was 8" in diameter and was 0.1" deep. It was formed from Duraform in a Vanguard HS SLS machine.

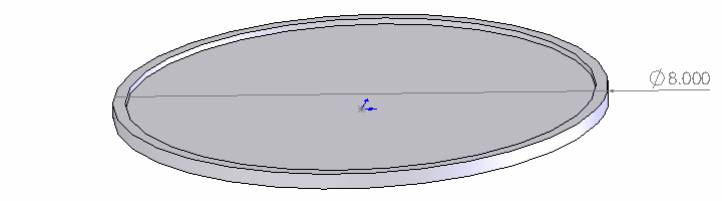

Figure 23 Single Layer Build Tray

A series of tests were performed to establish appropriate ranges for part bed temperature and laser power by observing the relative strength of the scanned regions. Each of the shapes scanned had sharp corners that allowed adhesion beyond the scanned regions to be observed as well. Finally STS-200 metals configuration (config) files were used as base setups for the single layer scans.

Polyester powder coating material (PAO-01189M from Becker Powder Coatings) not mixed with any silicon carbide was also tested in a single layer scan. Laser powers from 7 to 10 watts were examined with a bed temperature of 50°C, below the melt determined during DSC testing.

Phase 2: Initial Multiple Layer Builds

Aside from honing the various SLS parameters and accommodating full machine operation, the next step was to examine interlayer adhesion. To facilitate rapid iteration during this series of tests the metals (STS-200) config files were used initially in the machine to avoid waiting for the machine to inert after each time it was opened.

150 pounds of 280 grit (42 micron) silicon carbide was mixed in a cement mixer with 13lb of phenolic (8% by weight) ground to an average particle size of 17.6 microns with a standard deviation of 11.8 microns. The phenolic was commercially ground by the HJE Company. This was done to facilitate processing larger batches of material without having to use the attritor mill. The attritor mill was difficult to use and represented additional equipment for supporting this process in a manufacturing setting. The scan speed was constant at 49.5 in/sec for all builds.

The main parameters for the builds are shown in Table 7 , below. The limited part bed temperatures, laser powers and scan spacing for the initial build is attributable to the single layer scan work. The parameters for each build were determined from the results and observations of the previous build. Again, detailed observations (coupling the method and results) from the initial series of builds may be found in Appendix 2.

Table 7 Initial Series of Multi-layer SLS Builds

#	Part Bed	Feeds	Feed Dist.	Layer	Scan Spacing	Power	Other
0	80°C	50°C	.008″	.003″	.003″	6-10W	Multiple scans, 4-layers only
1	60°C	30°C	.008″	.003″	.003″	8-10W	
2	60°C	35-55°C	.008-.010″	.003″	.003″	8-10W	
3	40-55°C	30-40°C	.009″	.004″	.003″	8-10W	Duraform Config.
4	70°C	R35, L40°C	.009″	.004″	.003-.004″	8-10W	1 layer of BTB parts
5	75°C	R35, L40°C	.008″	.004″	.003-.004″	6-10W	Spacing/ Low Power
6	75°C	R35, L40°C	.008″	.004″	.004″	8-10W	Breakout Testing
7	75°C	R35, L40°C	.008″	.004″	.004″	8-10W	Low part spacing
8	75°C	R35, L40°C	.008″	.004″	.004″	8-10W	Bend Test samples

Within this initial series of tests several builds were made of simple prismatic bars to examine part spacing and directional effects. Other parts were designed to help develop the process development further. One of these parts is shown in Figure 24. This part allowed the ease of part removal from the bed as well as relative part strength, and dimensional stability to be qualitatively assessed without actual mechanical testing. Directional effects were also expected to be further examined. SiC with its high thermal conductivity was expected to cause the parts to grow with the spreading of the laser heat. This could be observed as growth of the fins or the narrowing of the small channels in the breakout part. To limit the atmospheric variation from one build to another, the Duraform config was used (which maintains the chamber under nitrogen during the builds).

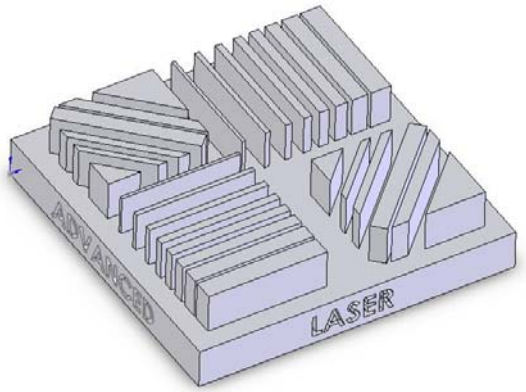

Figure 24 SLS Breakout Part

Phase 3: Breakout Capability, Dimensional Stability and Material Properties

The purpose of Phase 2 is to establish a fairly robust set of parameters for building SiC parts. The next set of builds revolved around manufacturability, material properties and issues with longer builds, such as heat buildup, laser window fogging and powder degradation. Additional parameters were explored in scan spacing, temperature ramps and outline scan parameters. Three-point bend samples, tensile blanks, heat deflection temperature blanks and several other types of parts were built during several different builds with new powder. A newer breakout part was designed to provide a greater challenge in getting the parts out of the bed and removing the loose powder. It is shown in Figure 25 and was also used to examine furnace infiltration which is discussed in the following chapter. The narrowest cylinders were designed to be too fragile to get out of the machine. The two feet at one end were designed to allow this part to provide additional information during post processing, which is discussed in the following chapter.

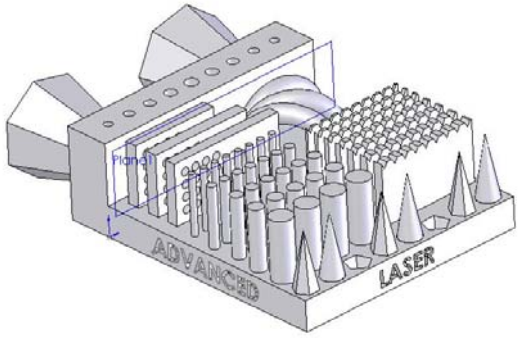

Figure 25 More Intricate Breakout and Infiltration Part

Several different types of parts were placed along side the breakout parts during a series of builds. Three-point bend test parts (per ASTM D-790) were built in primarily the 'X' (in the direction of the roller motion) and 'Y' directions. No beams were built vertically. 2.5 x 0.5 x 0.5" blocks were also oriented in the 'X' and 'Y' directions to examine the dimensional stability both in the SLS machine and during post processing. These blocks were built with glass and SiC base materials and at 8, 10 and 12W with constant 0.003" scan spacing.

There was a concurrent assessment of strategies to make the machine run faster, such as by varying the scan spacing or changing the temperatures in the feed beds during the course of the build.

Phase 4: Reliability and Long-term variation

To actually create a material that can be run commercially the variation from run to run, in different areas of the part bed, due to powder life and from machine to machine must be understood, particularly if that material is to be sold to SLS service bureaus. The robustness of the process must be known before it can be exported to another fabrication facility. These issues are more stringent if finished parts, rather than prototypes are to be fabricated from that material. This

final phase addresses these issues with a series of builds made with aged powder, in different machines and over the course of several weeks. In addition representative parts for display to potential customers are built during this phase. Several representative parts were prepared and shown to a variety of customers. These parts will be discussed in the following chapter. No research directed to establishing process reliability and robustness were completed during this research project. These tasks are left for future work.

Other Materials Systems

Two other base materials were also explored, graphite and glass microspheres. They were processed based on the SLS parameters created during Phase 2 for the SiC base material. The formula for the graphite was determined by Ssuwei Chen in an effort to prepare Bipolar Plates for fuel cells using SLS technology. The graphite runs within this research tested the basic SLS method developed during this project and also established an alternate set of process parameters for Mr. Chen's work. Several bars, beams and model bipolar plates were made during three separate builds.

The glass microspheres were examined more extensively. After initial builds to establish appropriate parameters, a variety of parts were prepared. Dimensional stability parts and three-point bend parts were built and tested to provide some context for the behavior of the SiC base material. The combination of the glass microspheres and the phenolic also represented an extremely cost effective material. The cost structure of SLS processing is reviewed in Chapter 5.

3.3 Results

3.3.1 Powder Behavior

The basic effects of particle size, particle shape, size distribution, and density were known, but the assessment of powders has shown the degree of these effects for the powders of interest to the current project. Figure 26, below is a diagram of the tap densities for a variety of different powder mixtures. The complete data for the tap density testing may be found in Table 21 in Appendix 1. The value of the test can be shown by making several comparisons referring to the numbers on the bars in the figure below. The effect of size can be seen by looking at 6 and 10. The effect of an interstitial smaller particle is seen comparing 2, 3, 4 and 6. As expected the smaller particles can occupy interstitial spaces, increasing the fractional density. What are also seen are the diminishing returns – with increasing volume fraction the smaller particles begin to separate the larger particles and eventually will dominate the powder decreasing the fractional density. Particle shape and smoothness gives the difference between 1 and 6. Finally, the effect of adding phenolic for SLS processing is shown in the difference between 1 and 7 as well as 6 and 8. The fractional tap density of Duraform is shown by column 9.

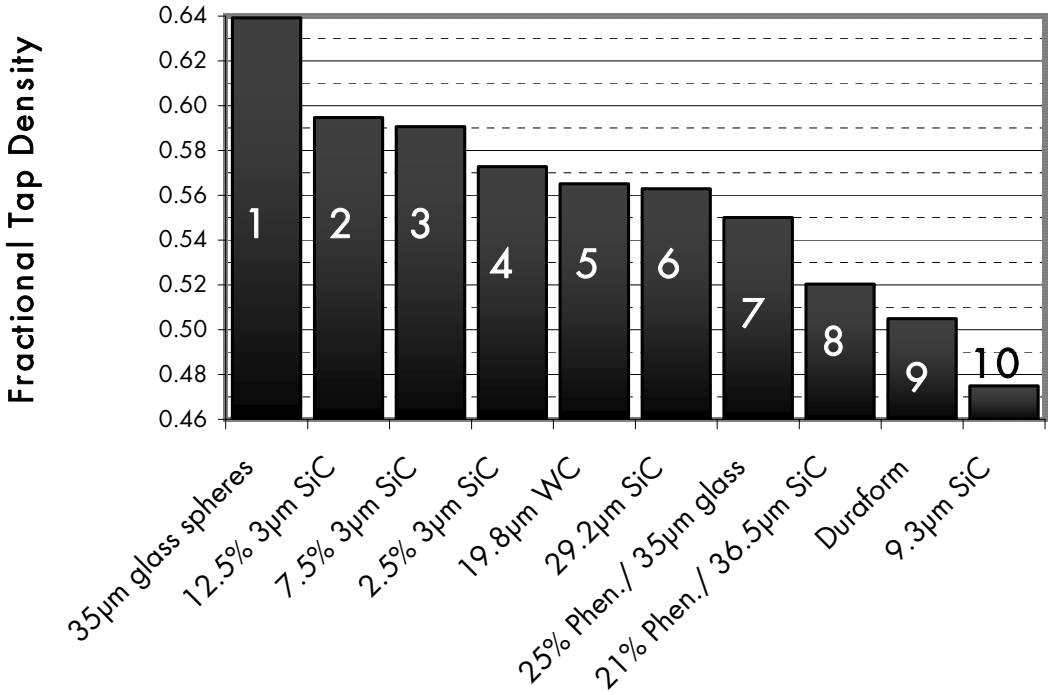

Figure 26 Tap Densities of Various Powders (mixture % are volumetric)

The following SEM images provided additional insight into the behavior of the powders and an initial benchmark into later microstructural analysis. The features of 280 grit silicon carbide (36.5µ) are typical for brittle ceramic materials, as shown in Figure 27. Some of the particles are chard-like while others exhibit large smooth areas. There are few fines (particles less that 10µ) and aside from the shape variation from particle to particle, the material is uniform and has no visible fine-scale texture.

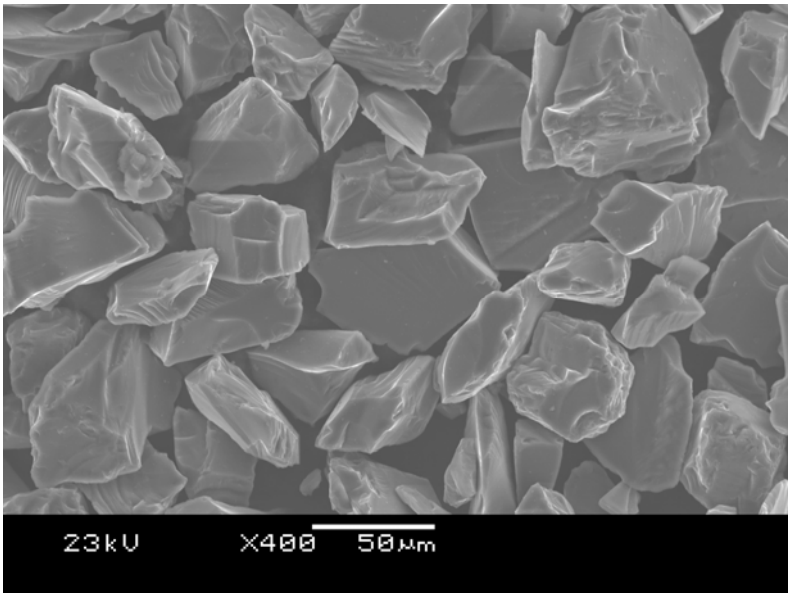

Figure 27 280 Grit SiC Powder

In contrast, the 20µ A6 tool steel powder pictured in Figure 28 (at 10X the magnification of the SiC image above), has uniform particle shape, but also surface roughness. The smaller white clusters are a nylon 6/12 binder used for SLS processing.

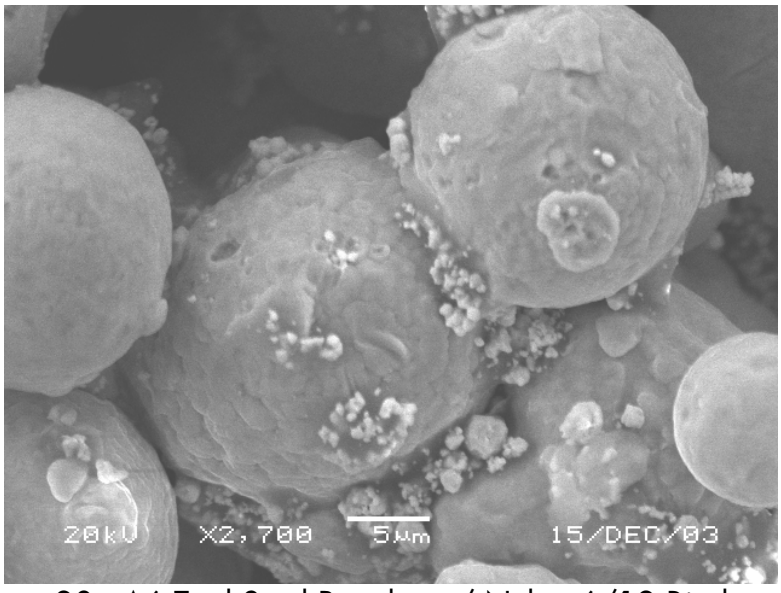

Figure 28 A6 Tool Steel Powder w/ Nylon 6/12 Binder

Phenolic is shown in Figure 29. The larger particles are about 10μ across. Many sub-micron particles and agglomerates can also be seen. The phenolic powder flows very poorly due to the particle shapes and large fraction of fine particles.

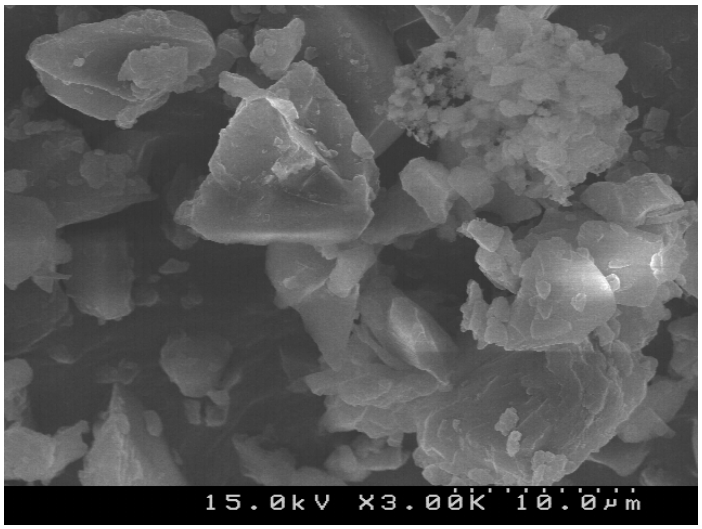

Figure 29 GP-5546 Phenolic

Samples of phenolic and silicon carbide placed in the same jars used for tap density testing showed differences based on preparation. Simple rolled powder (placed in a chamber and rolled for 6-24 hours) looked and flowed like silicon carbide alone. The phenolic coated the glass. When alumina media was added to a cement mixer and the powder mixture was mixed for 12 hours, the powder had a lighter color and less phenolic coated the glass on the jar. When powder prepared in an attritor mill was observed, the powder flowed more like a finer particle size powder and little phenolic coated the glass. It was expected that this difference was due to finer particle sizes, greater dispersion and phenolic particles tending to stay on the surface of the SiC particles. This expectation was verified in later SEM images after SLS scanning, as may be seen in by comparing Figure 34 (rolled powder showing agglomeration) and Figure 35 attritor milled powder indicating widely dispersed small phenolic particles. Phenolic was also ground separately (to the specifications shown in Table 8) and then mixed with

SiC powder. That powder was similar to the powder prepared in the cement mixer with media. Similar size reduction was seen with the media/ cement mixer and the attritor mill made the outside grinding unnecessary.

Table 8 : Ground Phenolic Data (From HJE, New York)

Powder	Mean (µm)	Std. Dev (µm)	Size of particle capping certain mass pcts. 10% (µm)	50% (µm)	90% (µm)	95% (µm)
Raw	31.0	23.7	4.1	24.8	64.1	78.9
Ground (-325 Mesh Cut)	17.6	11.6	3.4	15.5	33.3	41.1
Ground (Fines)	10.6	6.8	2.6	10.0	19.8	23.4
Raw Powder Oversize	62.2	19.0	35.1	56.4	85.7	102.8

The attritor mill was run with a bucket to catch the powder freely flowing out of the chamber, though this was due to the damaged valve. After two complete runs through the machine the powder was compared to powder prepared using other methods and also used for single layer scanning. It was decided that the $2500 for the new bucket was not worth the cost and the attritor mill was not used to prepare powder for multilayer SLS processing.

3.3.2 Polymer Analysis

The initial polymer analysis was a DSC scan on several promising powder coating thermosets which may be seen in Figure 30. Each of the powder coating resins had average particle sizes within the range for SLS processing. Further, they were all designed to sinter into smooth, uniform layers during heating processes. These samples were examined as a screening process for appropriate binder materials. The traces have been normalized and also moved to make them more easily comparable. In each trace a melt curve may be seen between 50 and 110°C and a curing exotherm starts to draw the curve downward at about 130°C even though the chemistries of these resins vary dramatically. The most notable

difference in these materials is the large curing exotherm in the phenolic resin, and the significant melt spikes of the Polyesters and DuPont RRBS-9 resins. The large phenolic exotherm is in part due to a relatively rapid curing reaction, although the DuPont resins feature a full cure in 5 seconds under IR heating. Phenolic had the most favorable combination of relatively high melt and a strong curing reaction a reasonable temperature above the melt. The area of the curve during that curing reaction represents the curing exotherm (in joules per gram) for the phenolic.

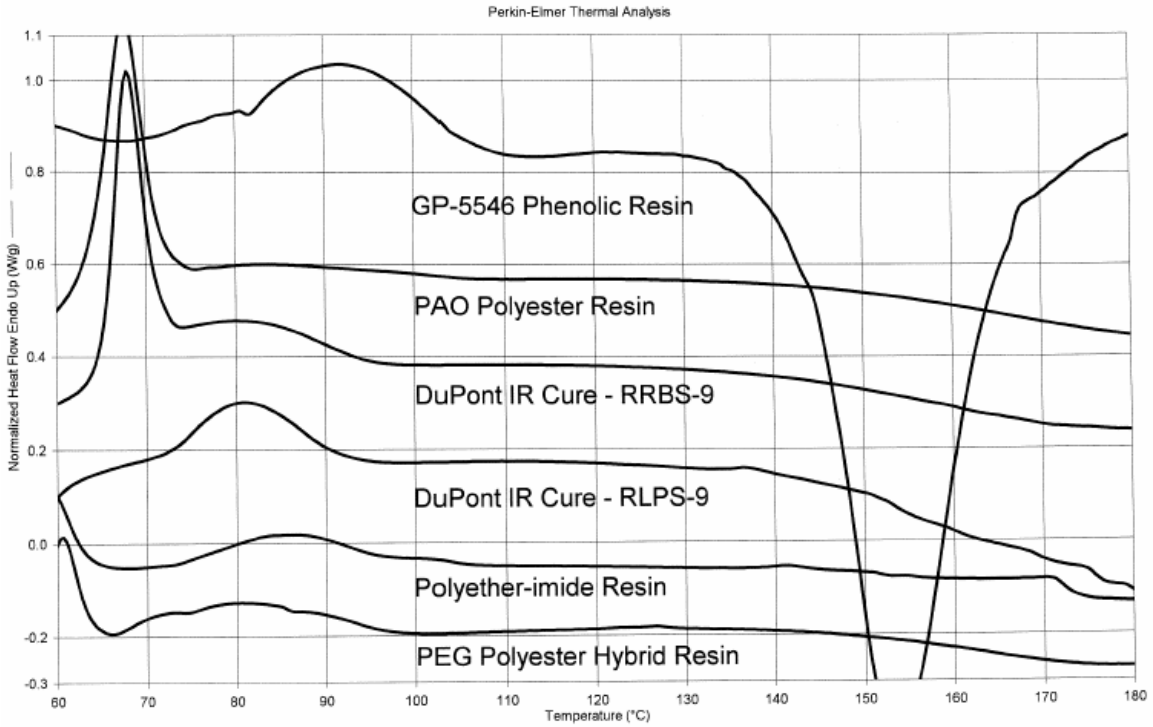

Figure 30 Melt and Curing Behavior of Various Thermoset Resins

In terms of SLS processing, the melt behavior was expected to determine the temperature limitations on the part bed. If significant melting or softening occurs, the powder in the bed will begin to fuse together or cake. If curing is desired during the SLS process, a broad melt point with a narrow curing curve is desired. In addition, a small difference between the melt and curing temperatures is also desirable. Most of the resins tested had a sharp portion to their melt curve

indicating sensitivity to thermal variation and a rapid onset of part bed caking. The remaining resins were the DuPont RLPS-9 IR cure resin and phenolic. The rapid cure described in the product literature for the DuPont resin was not clear on the DSC analysis and the difference between melt onset and cure onset was greater for the DuPont resin. The reaction characteristics of the phenolic, in contrast, have been studied extensively and several models were found in literature. The phenolic is very inexpensive (at $1.80/ lb.), shows an obvious curing reaction in the DSC and can be easily ground using a variety of methods. Further, the phenolic curing reaction can be modified easily. The addition of salicylic acid, which can be added as powder, enhances the curing kinetics of the resin. Still, the large exotherm represents either an advantage in promoting curing, or a disadvantage in undermining the part geometry.

The information from the samples tested may be found in Table 9 , below. Some adhesion and color changes were associated with longer aging soaks and higher temperatures. The larger mass loss for the longer soaks at 70°C was expected to be associated with curing and more uniform losses for the other samples with drying only. This was confirmed by the DSC results found in Table 10 . Graphs of representative DSC runs may be found in Appendix 1. The curing exotherms of the 60 and 80°C samples were larger. This was expected to be a combination of water inhibiting the reaction and also absorbing the energy. However, as was described in the background section of this chapter, water enhances the curing reaction in phenolic. In addition, there was ample time between oven heat aging and DSC testing for atmospheric water to return to the samples. The identification of the effect would require additional testing. The DSC data of ~240 minute soaks did not show a correlation between temperature and curing (within the range examined).

Table 9 Phenolic Heat Aging Study

Temp. (°C)	Time (min)	Initial Mass (g)	Final Mass (g)	Mass Loss (%)	Comments
60	120	5.85	5.73	2.05%	No visible change in powder appearance
60	240	6.20	6.11	1.45%	
60	360	7.74	7.57	2.20%	
70	235	4.09	3.99	2.44%	No caking of powder - light color remains
70	7326	5.08	4.74	6.69%	Slight caking esp. at bottom - slightly darker color
70	11789	7.26	6.69	7.85%	Slight caking + slightly darker than above sample
80	122	7.85	7.69	2.04%	All samples of powder form loose cakes - longer soaks have slightly harder caking and slightly more amber color
80	245	10.29	10.05	2.33%	
80	521	11.35	11.01	3.00%	

In addition to these heat aging samples, mixtures prepared in a variety of ways and across two separate lots of powder were examined. Phenolic mixed with SiC did not exhibit the same curing exotherm per volume of phenolic that was found with the 100% phenolic samples. All exotherms listed in Table 9 , below represent joules per gram of phenolic. The two lots of powder had significantly different exotherms having 59.8 and 72.3 J/g respectively. The phenolic ground at the HJE Company showed the highest curing exotherm possibly due to increased surface area or better HMTA dispersion.

It was hoped that some meaningful data could be created for a degree of cure as introduced in Section 3.1.3, above. Because of the effect of drying and mixing with SiC a total exotherm could not be established except for the powder samples aged at 70°C. The 5 and 8 day samples had a degree of cure that was approximately 0.5 ($\alpha \cong 0.5$) with respect to the dried sample aged only 4 hours.

The Part Bed powder sample from Lot #1 represented powder taken from the SLS machine after the first series of 8 build runs had been completed. Lot #2 samples were taken after a much more extensive series of higher depth builds amassing over 10 inches of powder into the feed bed (~120 hours of scanning)

with several overnight soaks at temperature. Part samples were taken from the interior of parts prepared in the final builds before the part bed samples were taken. Comparing Lot #1 and Lot #2 powder there was a mixed result for whether curing happens under the laser within the SLS machine. Additional study would be necessary to verify the result.

Table 10 DSC Curing Study

Powder	Preparation	SLS Processing	Curing Exotherm (J/g)
Lot #1 : GP-5546 Phenolic	Raw Phenolic	-	59.837
	60°C - 120min	-	56.499
	60°C - 240min	-	66.817
	60°C - 360min	-	75.699
	70°C - 235min	-	60.347
	70°C - 5d, 2h, 6min	-	31.436
	70°C - 8d, 4h, 29min	-	30.826
	80°C - 122min	-	58.503
	80°C - 245min	-	60.088
	80°C - 521min	-	75.699
	HJE Ground	-	88.400
	Attritor Milled (10% Phenolic)	-	21.047
	Cement Mixer (8%, no media)	Part Bed Powder	23.652
	Cement Mixer (8%, no media)	Bend Test Bar	24.225
Lot #2 : GP-5546 Phenolic	Raw Phenolic	-	72.260
	Cement Mixer (10%, w/ media)	-	24.447
	Cement Mixer (10%, w/ media)	Part Bed Powder	26.304
	Cement Mixer (10%, w/ media)	Bend Test Bar	19.707

3.3.3 Binder Characteristics

Using the same mold setup described in Section 3.2.3 above, the influence of different ratios of nylon, wax and phenolic on the bending strength of green (directly from SLS) and brown (after carbonization) samples was performed by

Bhandari, 2004. The influence of the wax (N,N' Ethylene Bis-Stearimide powder metallurgy lubricating wax) on the Green strength was confirmed. The molded parts cracked due to shrinkage when processed in a pre-heated oven at temperatures high enough to melt the nylon (>195°C). The surprising result of the study was the indication that the presence of wax also slightly increased the brown strength of the parts. The actual physical or structural cause of this increase was not identified. The lowest viscosity component of the three-part binder system was the wax. Its tendency to flow and coat other elements could have improved the connections that formed between particles and served to improve the microstructure of the phenolic prior to decomposition.

The coating of the three-part binder system on SiC particles may be seen in Figure 31. There are significant pores and unbonded surfaces despite the significant strength of the part examined.

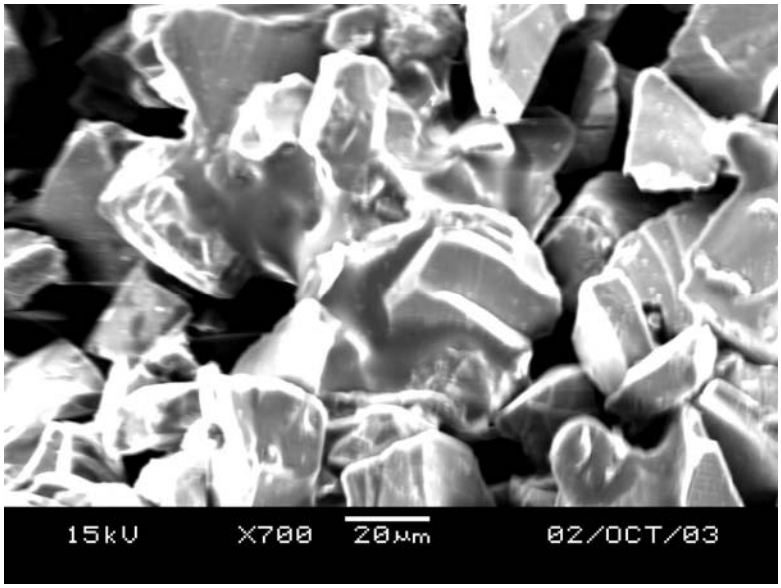

Figure 31 10% NWP Binder with 280grit SiC

The design of the mold incorporated shrinkage from the powder as the phenolic binder cured. The shrinkage appeared as cracks in the bars and all parts were difficult to remove from the molds. The molds were modified to allow each chamber to be opened to allow part removal. Hardness testing including Rockwell 15X, 15Y and 15N did not produce any relevant data and nearly all samples tested were simply fractured.

The relative effect of binder loading for an all-phenolic binder system was identified. 12% (by weight) of binder, even with unground and unmilled phenolic, yielded a powder with visibly inhibited flow characteristics. Higher loadings also featured more cracks from shrinkage in the parts, but the pieces were harder. The best strength while often maintaining unbroken parts was with 8% phenolic by weight.

3.3.4 Heat Transfer Analysis

Using the method described in Section 3.2.4, the temperature rise of the powder under the laser was estimated. In addition, the effect of an entire curing exotherm from the phenolic was also examined as seen in the table below. The curing reaction was not significant enough to promote significant thermal spreading or auto-catalysis of its own curing reaction. The estimate of curing energy was taken from the DSC of phenolic only while the mixtures showed a lower energy per unit of phenolic. At the center of the beam the temperature would be higher than this estimate. It would also be higher if the rastering heated the powder during adjacent sweeps of the laser. The peak temperatures seen during SLS scanning of the powder (when the scanned region was within the view of the IR temperature sensor) ranged from 120 to 150°C. However, the timescale of sampling was too large to be accurate. It is also unknown how much of the signal is averaged with the cooler regions of the sensor's viewing area and how

much laser energy is reflecting into the IR sensor directly. The estimates from the table below are considered low since the beam width of 450μ (.017") represents a multiple of 2.5 to 5 times the scan spacing seen during SLS processing. The model (for PMMA coated SiC) developed by Nelson et al. (1995), predicted surface temperature peaks (above ambient) that ranged from 130 to 180°C for scanning parameters ranging from 8W with 0.005" spacing to 12 W with 0.003" spacing.

Table 11 Powder Heat Estimate

Inputs	
Beam Speed (in/s)	49.5
Scan Spacing (in)	0.004
Ambient Temp (°C)	73
Beam Power (W)	10
Specific Heat (J/kg*°K)	774
Absorptivity (%)	50
Specific Gravity	1.505

Calculations	
Volume (mm^3)	127.74
Mass (g)	0.10
Single Scan Temp (°C)	140.20
Single Scan Delta T (°C)	**67.20**
Curing Energy (J/g of mix)	7.22
Delta T (w/ curing) (°C)	**9.70**

The next piece of the puzzle was to explore the effective thermal conductivities of various powders using the relation found in Equation (24). The effect of particle size, powder density and several materials can be seen in the following table. The most striking feature is that large differences in bulk conductivity translate into much smaller differences in the effective powder conductivity. Also, coating the SiC particles as described by Nelson, et al., (1995), rather than mixing powders resulted in a lower conductivity.

Table 12 Effective Powder Conductivities

Material	Avg. Size (μm)	Fract. Dens.	k (W/m-°C)	k_{eff} @70°C
600 Grit SiC	9.3	0.47	110.0	0.27
320 Grit SiC	29.2	0.56	110.0	0.29
280 Grit SiC w/ 10% Phen	36.9	0.52	99.0	0.28
10% Phen - Untapped Dens.	36.9	0.45	99.0	0.26
PMMA Coated SiC (Nelson et al., 1995)	Multimode	0.57	0.03(PMMA)	0.20
Glass Micro-spheres	35.0	0.64	1.1	0.12
Duraform	40.0	0.50	0.3	0.07

The effective conductivity of the 10% phenolic powder was put into the model from Equation (22) (heat plume under a scanning IR laser) and built up in Excel. By iteratively varying the value of z_0 in the model the maximum temperature rise was set to 140°C which represents double the energy density used in the estimate above, without the effect of curing. This number also corresponds with the temperature rises modeled by Nelson et al., (1995), which provides a good benchmark for the validity of the simpler model used here. The time to peak temperature was similar but did not incorporate multiple passes. The temperature decay behavior was almost identical. The following graphs (Figure 32 and Figure 33) indicate that the phenolic easily melts at a layer depth and also show that the time at curing temperature is extremely short. The curing exotherm of phenolic as seen during the DSC testing ranged over 40°C which represented 2-4 minutes of cure time. More rapid scan rates (to model laser heating) require extensive calibration of the DSC instrument and were avoided. While more rapid temperature ramps tend to increase the speed of the cure even a step increase in temperature would still require perhaps several dozen seconds for the curing

reaction to take place. Unless there is some type of autocatalytic reaction that laser heating initiates, little curing during SLS is expected to occur.

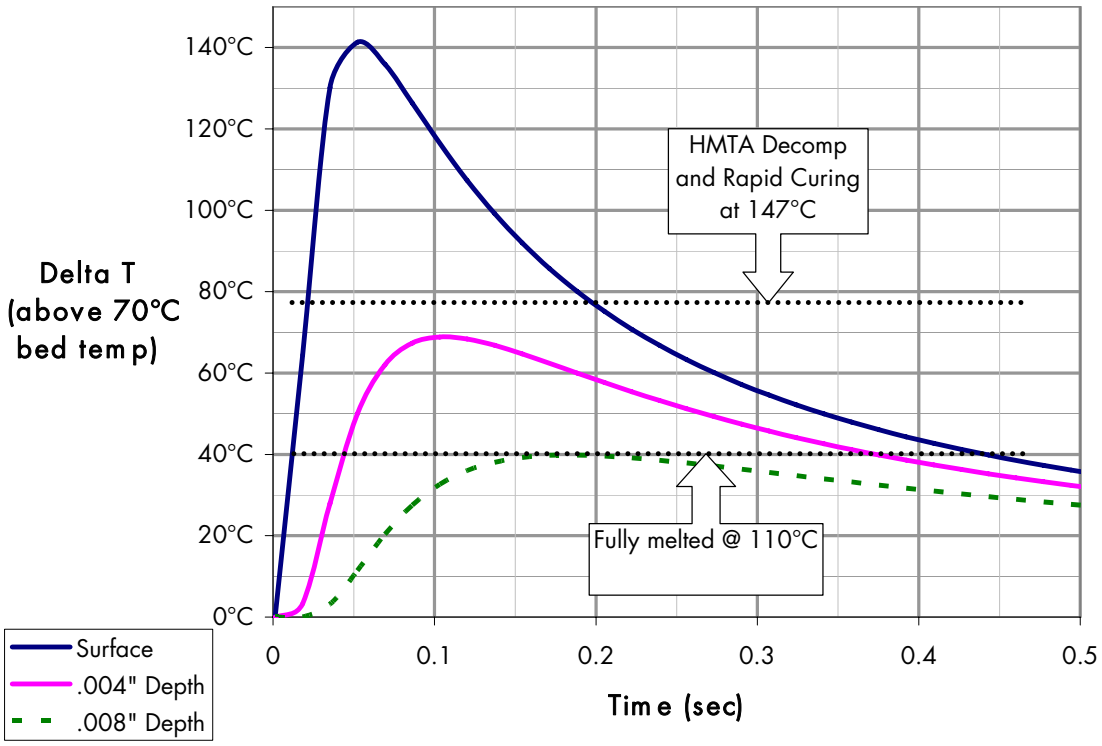

Figure 32 Laser Scanned Heat Transfer Model : Temp vs. Time

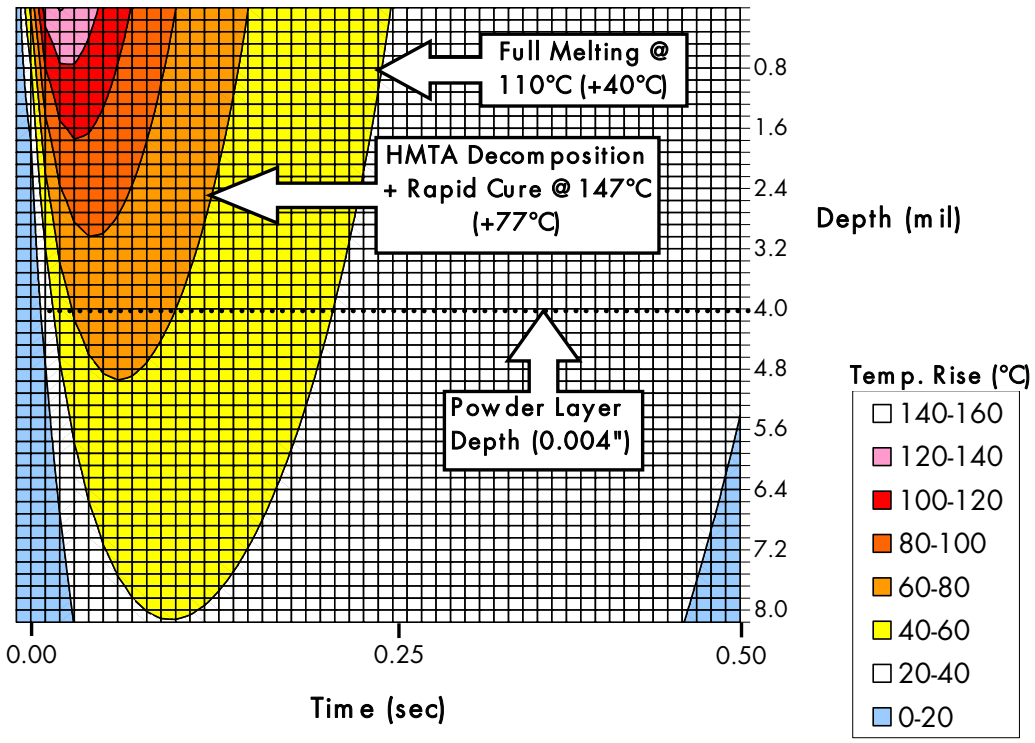

Figure 33 Laser Scanned Heat Transfer Model : Heat Plume

There is enough energy flow to facilitate bonding between layers, but compared to the beam width of 450μ (or 0.017") is not very significant spreading into the powder. It is expected that the same scale of spreading will occur across the powder. Since the model was built to accommodate a Gaussian beam and the spreading seen in the z-direction is below the center of that beam, it was not expected that significant spreading would occur with a 10W beam unless the effect of adjacent passes of the laser was significant. Many observations of adhesion extending beyond the area scanned were made during actual builds in the SLS machine particularly into cavities and the narrow slots designed into test parts.

3.3.5 SLS Process Development

Phase 1: Single Layer Scans

Above 80°C the powder in the tray began to have a faint vapor rising from it and it began to cake. At 100°C the vapor was more visible and the powder formed a firm cake. The range of powers that provided acceptable strength and acceptable levels of spreading was from 8-10W (all at 0.003" scan spacing). Multiple scans had a small effect, but not nearly as large as even a 10% increase in laser power. No curl or z-direction shrinkage was seen in any scanned regions. The lack of z-direction shrinkage indicated that SiC to SiC particle contact was significant and that the binder was not providing extensive shrinkage during SLS scanning.

The polyester scanned showed extensive shrinking in the z direction and curled readily. The affected regions extended well beyond the parts especially at interior corners. Where the laser returned to fill in a region of the part there was a seam, which was not seen in any of the phenolic/ SiC scans.

SEM images of two different types of powder may be seen below. Figure 34 shows two SiC particles bonded near the center of the image. At the top center there is a large conglomerate of phenolic and SiC particles – which uses a relatively large volume of phenolic to bond a handful of particles. Two smaller spots of phenolic which spread out on the surface of the SiC can be seen near the bottom-right corner. The scanned powder pictured in Figure 35, was milled in the attritor mill and looks very different. The phenolic spots cover nearly every particle. It is unlikely that any two SiC particles touching would not have at least some adhesion between them. The amount of phenolic covering each particle is very low compared to the volume of phenolic contained in the conglomerate shown in the previous figure. These microstructural observations supported the

background discussion favoring smaller binder particles. The other main feature seen in these images is that the sintering rate was high (high surface tension and low viscosity) during SLS scanning.

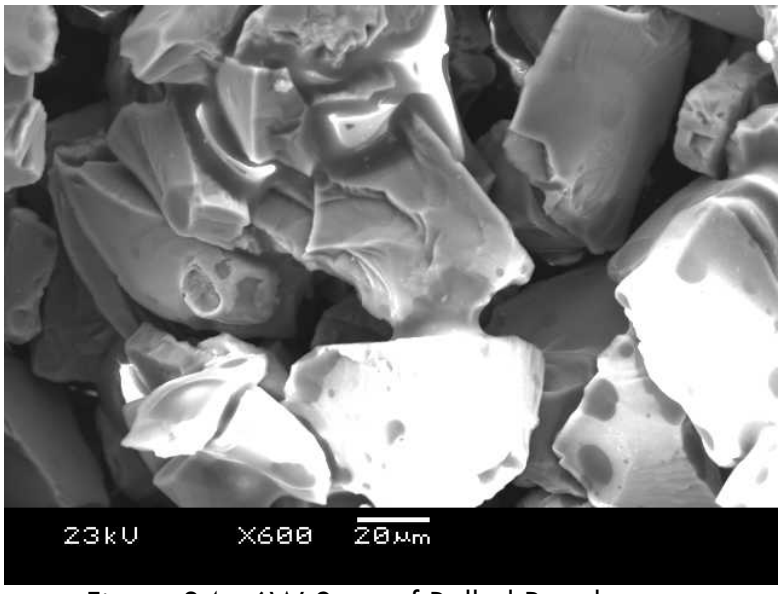

Figure 34 6W Scan of Rolled Powder

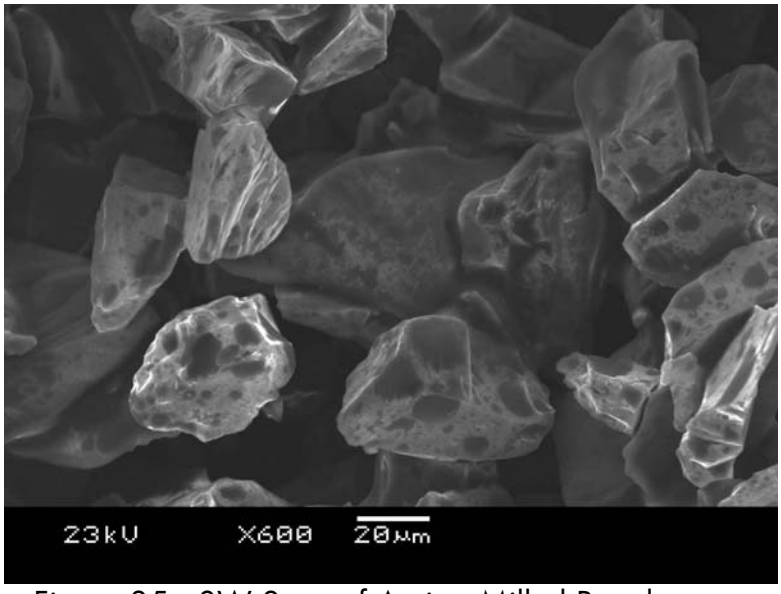

Figure 35 8W Scan of Attritor Milled Powder

Another pair of SEM images indicates the difference in phenolic behavior at the center of a scanned region and its edge. There is a difference in the temperature

reached, melt viscosity and clearly the strength of bonding. Figure 36, shows two SiC particles bonded together. The phenolic is seen to flow along the surface of both particles. The characteristic distribution of small phenolic particles from attritor milling is also visible. Figure 37, on the other hand is from a sample of rolled powder and is from the edge of a scanned region. The lower temperature seen in this region is clear. The phenolic does not extend along the surface of the SiC and the bonding does not appear to be as effective.

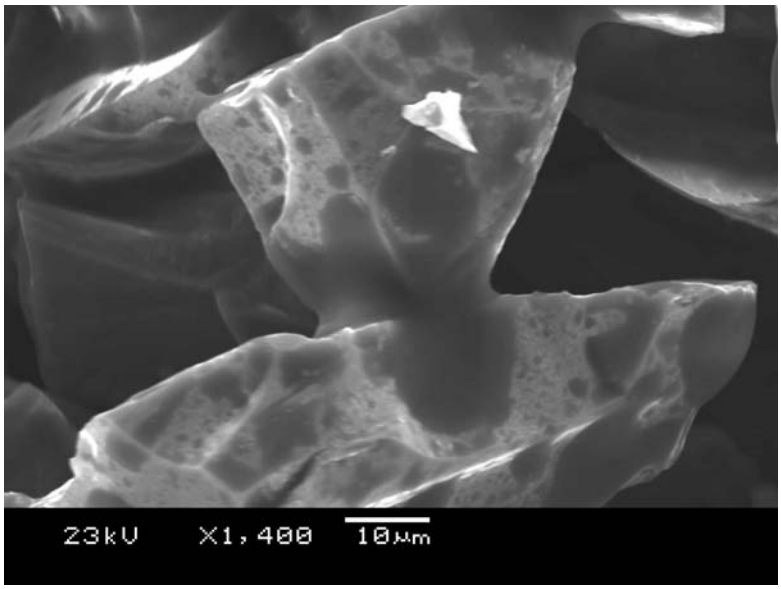

Figure 36 8W Scan, .003" Spacing

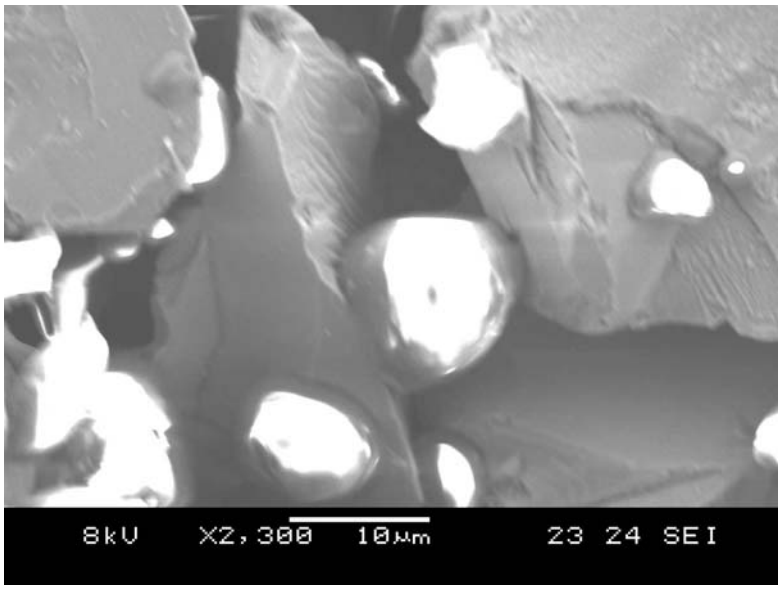

Figure 37 High-viscosity Phenolic

Phase 2: Initial Complete Builds

Again, the details of this phase may be found in Appendix 2. The main results the of 8 different build setups is reviewed below.

4-Layer Build

Interlayer adhesion was adequate even for low (6W) power. A double scan at 8W is significantly weaker than a single scan at 10W. The second scan does not provide a significant strength advantage. The time spent scanning during a build represents about 80% of the total build time – further diminishing the value of double scanning. Some small fissures were visible along the parts having 8W scans and above indicating either some X and Y direction shrinkage or curl within the layer.

Build #1: Curl versus strength

With lower bed temperatures curl was seen after 4 layers. In the 10W parts the curl was severe enough to allow the parts to be disturbed by the motion of the roller.

Build #2: Increasing feed bed temperatures

Feed temperatures were increased incrementally from 30 to 55°C. Although the curl decreased with increasing feed bed temperatures, there were other issues. With the feeds at 50°C the feed distance (distance feed piston rises to deliver new powder in front of the roller) had to be increased as the powder was not covering a new layer completely (it was exhibiting "short feeds"). At 55°C there were visible cavities within the feed beds, a thin layer of powder was sticking to the roller and there were further problems with short feeds. The build was stopped. The feed beds had become hard and caked in the middle. With the temperature sensor at the edge of the beds it is hard to determine the temperature reached at the center. It was clear that the feeds should be kept below 50°C to prevent caking.

Build #3: Thicker powder layers/ Duraform config.

The feeds were set at 40°C and the part bed to 40°C. Curl was seen as fissures at part corners after the 5th layer. With the part bed set to 55°C the beginnings of curl was seen after the 7th layer. The duty cycle of the right feed bed heater was at a higher level than the left – this indicates a problem with the sensor. The right thermocouple was found to be lower in the powder than the left. If the right temperature is set lower – this can be mitigated without trying to bend the thermocouple. The thermocouples are easily broken and notoriously difficult to replace.

Build #4: Wider scan spacing/ different powers/ 8, 9 &10W

A single layer of parts each with different scanning powers was setup, the right and left feeds were set to 35°C and 40°C respectively. The part bed was set to 70°C. All parts were 0.125" thick and all were successfully made. Some layering was visible on the sides of the parts, but it did not become worse with brushing – indicating adequate interlayer adhesion. All parts were slightly warped – especially along the downward facing side due to in-build curl.

Build #5: Part bed to 75°C

The first set of logo parts was built along side bend test beams. They are pictured in Figure 38 and Figure 39. The relative strength of the bend test beams may be judged by the apple seen in Figure 38, which was stronger than the samples of commercial steel powders bound with a nylon binder donated by Harvest Technologies, Inc. of Belton Texas. None of the parts exhibited curl. There was a trade-off between strength and growth of the parts. The 10W parts were stronger, but also had some part growth especially at internal corners.

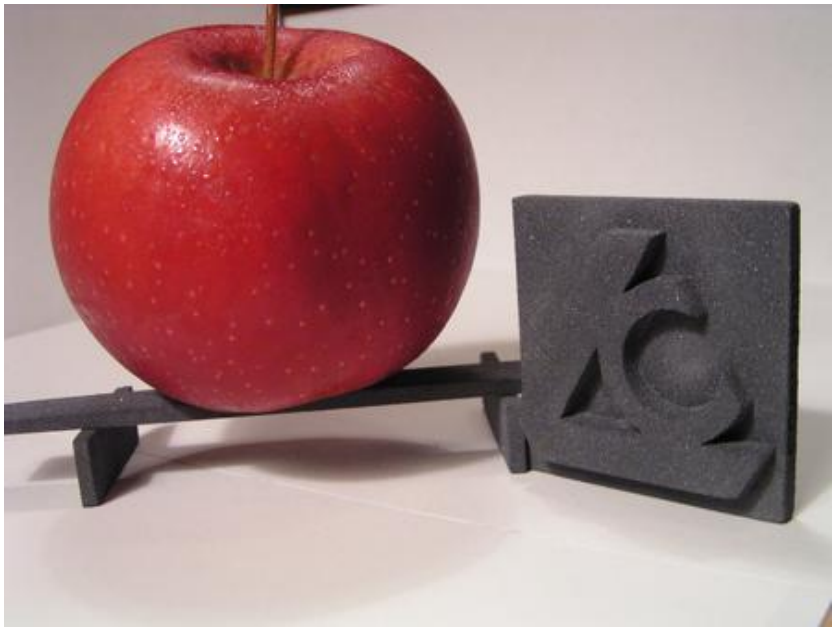

Figure 38 Green Parts – Illustrating Green Strength

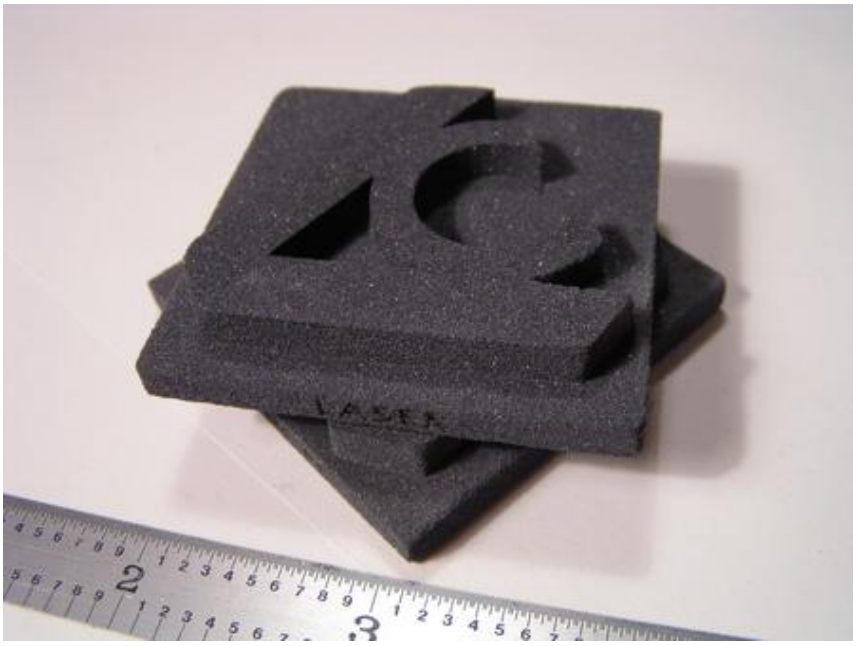

Figure 39 Green Parts – Illustrating Scale and Surface Finish

Build #6: Breakout parts

Breakout parts with fins and gaps of various sizes were made and examined. This provided a more thorough qualitative analysis of laser power versus part growth. Even at 8W the smallest gaps of 0.020" were filled in. The

10W part filled in the 0.060" and there was a small gap in the 0.080" space. The growth of fins was not nearly as pronounced as the filling in of thin gaps. The 10W parts were much easier to break out without losing the thinnest fins.

Build #7: Assessment of part spacing

The spacing between parts both within a layer (X and Y) and into the powder bed (Z) has an effect on the heat loading within the powder. With too many parts too close together it is possible for the powder bed to exhibit behaviors similar to higher temperatures in terms of caking and at the same time lower temperatures with increased curl. This was first seen in the loss of several parts during this build. By increasing the spacing of the parts to 0.150" from 0.100" the build was completed without incident. The beams prepared were used to examine the carbonization process which is discussed in the following chapter.

Build #8:

The final build in the series was for show-and-tell parts and also parts for bend testing after a variety of post processing steps, also discussed in the following chapter. These final two builds indicated that a set of basic parameters had been established for building parts in the SLS machine. It became possible to set up the machine, observe a few layers and then return when the build was complete.

Phase 3: Breakout Capability, Dimensional Stability and Material Properties

During the series of builds the effect of altering the scan spacing (to make the scanning operation faster was examined). A 0.500" build was run twice with an array of different parts – first with 9W and 0.003" scan spacing and again with 18W and 0.006" scan spacing (preserving the same Andrew number). The build times were 9:18 and 5:16 respectively. Significantly more vapor rose from

the scanning front during in the 18W build. There was also a degradation of the feature detail and a slight, but observable increase in part growth at interior corners. The strength of the parts as exhibited by breakout parts (Figure 25) in each build was equal. The build was then run a third time with a laser power of 15W and a scan spacing of 0.005." This provided a balance between build time (which was 6:38) and part quality. For higher quality, very complex, or finely structured parts lower spacing (0.003") and power (8-9W) was found to be more effective.

To manage the transient effects of machine warm-up and also thermal loading from part scanning the temperature was ramped from 77°C to 68°C during the series of builds. This allowed for a tighter spacing between parts, which was increased during Phase 2 tests. The heat loading from scanning can be managed via larger part spacing or by ramping the part bed temperature. The most universal ramp began with setting the part bed to 77°C during warm-up and then included ramping it down to 71°C in 0.100" (25 layers or about 1:40). The spacing was set to 0.125" in X, Y and Z. Longer ramps were used for lower scanning density builds, but the temperatures were kept the same.

The outline scan power was also varied during the series of builds. There was an interesting effect when the glass base material was tested, which is discussed below. In the SiC material 4W was universally found to be the best outline scan power regardless of interior scanning parameters or temperature ramps.

The dimensional stability of the SLS process for both the glass and SiC based parts may be found in Figure 40 and Figure 41 below. In each figure, the y-axis represents a percent change from the dimensions of the original CAD file. There is a separate line for the length, width and thickness and overall volume of

each part, represented as 'L', 'W', 'T' and 'V' respectively. There are software and scanning control issues that influence these dimensions as well as material issues. Still the trends related to part orientation and scanning power are clear. The comparison between the glass and SiC base material is also interesting. The higher conductivity SiC material had a much larger directional variation. It is also interesting to note that the fractional densities of the parts were significantly different. The tap density of the glass phenolic powder was 0.55 while the density of the green parts was 0.58. In contrast the tap density of the SiC based powder was 0.52 and the green parts were 0.44. The parts produced by Nelson et al., (1995) using a multimodal SiC powder with a higher tapped density (0.57) had part densities that ranged from 0.44 to 0.46 with similar energy densities. These observations indicate that the influence of the particle shape on the powder behavior was compounded during the SLS process. This is partly caused by the roller spreading the powder and the phenolic flowing to bind the particles together.

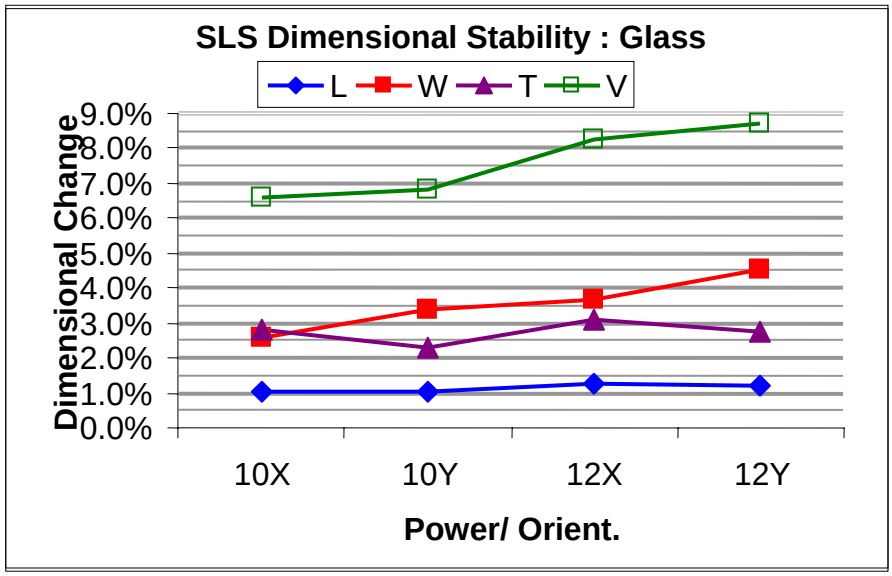

Figure 40 Dimensional Stability in SLS Process for Glass Base

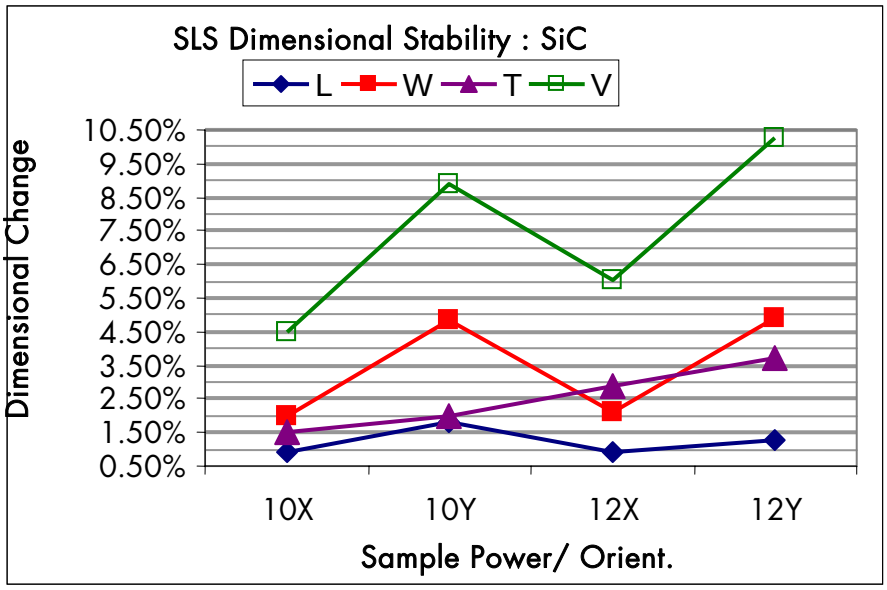

Figure 41 Dimensional Stability in SLS Process for SiC Base

Phase 4: Fabrication of Commercial Parts (No Long Term Reliability)

Although the long term effects and reliability of the phenolic binder system were not addressed, several parts were made and delivered to a variety of potential customers. This will also be addressed in the following chapter as each of these parts received some type of post processing prior to delivery.

Other Base Materials

Graphite and Glass Microspheres were also mixed with phenolic and run in the machine. The graphite material was borrowed from the research project performed by D. Bourell and S. Chen, but run with the setup established using the SiC base material. During a single build run in the machine it was found that the same temperatures (40°C for the feeds and 73°C for the part bed) were appropriate for the graphite as well. The laser spacing was decreased to 0.003" and the laser wattage was ranged from 8 to 10W. All parts were removable.

Higher wattage corresponded with higher strength and the part growth was not as extensive as in the SiC material.

Several runs were completed with the glass as a base material. The percent of phenolic by volume was 30%, in contrast to 21% for the most of the SiC builds. The same basic temperature parameters as the SiC also worked for the glass base material confirming that the temperatures are primarily determined by the binder material. The temperature ramps developed during the Phase 3 builds were also applicable, however, they were found to be more effective when the ramps ranged from 35 to 50 layers rather than 25 layers as found with the SiC material.

When high outline powers (12-20W) were used in conjunction with chamber oxygen contents of about 5%, the phenolic blackened creating a laser writing effect in the material as seen in Figure 42. Since this laser writing effect did not inhibit part strength or promote curl in the parts, it could be useful in keeping track of parts or measuring part tolerances. To take advantage of this effect a separate writing program would be necessary to add lettering instead of being limited to outlining parts.

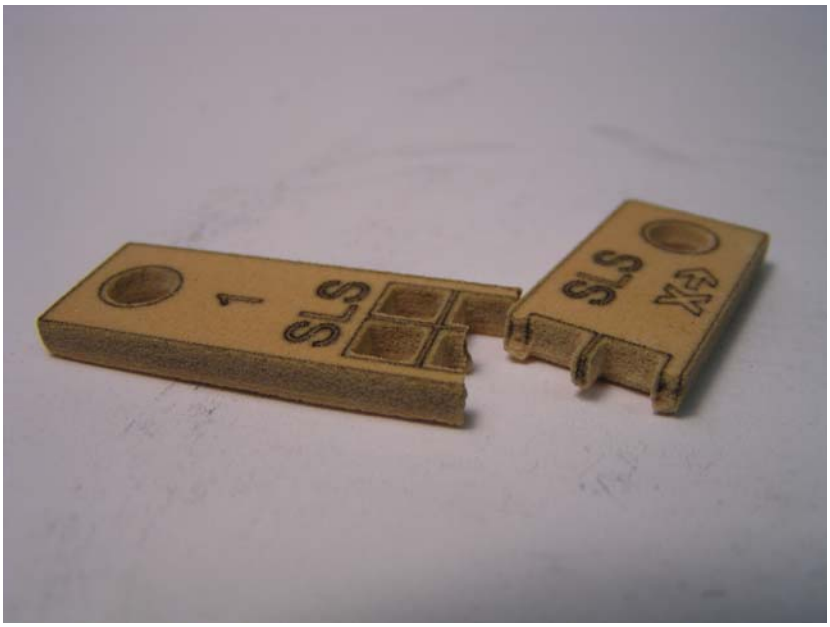

Figure 42 Laser Marking of Phenolic/Glass Part

3.4 Discussion

3.4.1 Thermoset Binders

With regard to glass, silicon carbide and graphite powder base materials, phenolic powder can be easily dispersed. In the case of silicon carbide in particular, phenolic is easily size reduced either via attritor milling or ball milling (using media within a cement mixer). Under the laser the GP-5546 phenolic melts and flows - readily binding base powders into firm compacts. Those compacts compared favorably to currently used SLS binder systems and were found to be stronger, opening up the potential for parts with finer features and more challenging geometry. As a binder, phenolic provides an effective and low cost material easily processed in the SLS machine. The expected advantages of having curing occur under the laser, however, were not realized. No substantial evidence of curing under the laser was discovered. The first hypothesis of this chapter is thus partially supported.

Phenolic and most of its derivatives are basically adhesives. Since at least certain types of Novolac resin can be processed via SLS, many different base materials can also be used. Ceramics and graphite were tested. Graphite, in particular is very difficult to bind. It is expected that few base materials, satisfying the powder constraints of SLS processing could not be bound together with a phenolic binder. For lightweight parts hollow phenolic microspheres (as a product called Phenoset) or hollow glass microspheres might be very useful. Flexible materials such as silicone powders might also be useful, but might conflict with the brittle nature of phenolic. Metal base powder should also be possible. The influence of and desired properties for post processing are discussed in the following chapter.

Returning to the mixing and storage issues highlighted in Figure 21, the speed and other features of the mixing method were parameters while the flow, dispersion and separation were observables. Although the attritor mill prepared the best powder in terms of dispersion and size reduction, the time and facilities costs did not seem to present an overall advantage to using a cement mixer with alumina media. The flow of the powder and tap density was shown to be comparable if not superior to the most widely used SLS material for a wide range of binder loading and powder preparation techniques. The separation of powder which was identified as a concern prior to the research was not found to be an issue since the powder was actively mixed and sifted prior to being loaded in the machine. The process of rolling the powder in the SLS machine also mixes it. The strength of the green parts was not tested quantitatively within this research project but was instead related directly to an ability to handle the parts. The fine features of the breakout parts were a more direct test of what is actually required from the parts. Green parts from the current research compared very favorably to green

parts prepared using the RapidSteel material from 3D Systems. Parts were stronger, but did show more significant part growth. The flexural testing of brown parts by D. Bourell and S. Barrow did establish a flexural strength of 540psi for brown parts observed to have similar strength to the green parts (shown in Table 17 , below). This compared very favorably with the strength of ~150psi reported from the work of Nelson, et al. using a PMMA binder.

Going forward there are two avenues of binder exploration: 1) pursue more curing under the laser and 2) abandon curing as a necessary element of processing thermosets within the SLS machine. Pursuing the first, the GP-5546 phenolic can be enhanced with the simple addition of salicylic acid. The effect could be explored using a DSC in a couple of ways. First, a rapid ramp to an appropriate hold temperature (perhaps 130°C) would allow the observation of relative changes in the curing kinetics in terms of the time for the exotherm to expire. Second the effect would still be visible, though not as clearly characterized via more traditional DSC scans. The amount and effect would require several single layer scans and multiple layer builds to determine. It is likely that there would be an effect on the aging of the powder with the addition of salicylic acid. Typically curing modifiers are *compounded* rather than simply mixed. The key to modification is intermolecular contact with the modifying agent, which may be difficult to achieve with powder mixing. Georgia Pacific and other phenolic producers might need to prepare sample batches of custom resins. This might support a more extensive analysis of appropriate phenolic materials for SLS processing. Going further still, it is very unlikely that phenolic is the only thermoset polymer that can be used in the SLS process. There is an entire thermoset powder coating industry. Powder coating materials have similar powder size and rheological constraints when compared to SLS materials. For some portion of

these materials, curing may not be possible under the laser. Even so post-processing or uncured thermosets might still offer useful SLS materials. The DuPont RLP-S9 material should be at the top of the list for the next materials to explore. It is a powder coating resin designed to rapid cure under IR heating.

3.4.2 Screening Method for SLS Materials Development

One of the overarching results of this project is the realization of a preliminary screening method for new SLS materials. This grew out of the sequence of research tasks performed to examine the thermosetting binder material. Ultimately, the organization of the chapter was organized around this concept. Materials in the SLS machine must be powders with appropriate properties and some appropriate portion of the powder must respond favorably to laser scanning. This requires an assessment of powder behavior and the thermal characteristics of the material. It is important to note that traditional DSC analysis provides an assessment of the temperature at which melting or curing occur, but does not inform the effect of rapid laser heating. There may be a way to have a microscale DSC examine the effects of more rapid temperature ramps. Following this, some understanding of the heat transfer characteristics of the laser scanning process is important. Then the basic parameters of the SLS process can be established in the range of process temperatures and laser powers can be determined. More detailed parameters, part spacing, temperature ramps, etc. can then be established. Finally, the reliability and longer term behavior necessary for commercial application can be assessed. These stages can be organized into flow chart, seen on the left side of Figure 45. At each stage the material is either fit to undergo additional testing or found to fail the test for SLS materials.

One of the limitations of the current project was that a range of powder formulas has not been examined due to the cost and time associated with

preparing large enough volumes of powder to allow for large representative builds in the SLS machine. This was to be enhanced by the creation of an insert for the SLS machine allowing for smaller volumes of powder to be used for making actual multiple layer parts. This Small Volume Insert (SVI) was designed and built during the course of the research. The basic idea is to have a smaller cylinder within the main bed of the machine that allows all of the controls of the SLS machine to be used. The center and feed bed inserts are shown in Figure 43 and Figure 44 respectively. By the time the SVI was ready the basic parameters for running phenolic with SiC and glass base powders had been established. It was also realized that significant characterization of the thermal characteristics of the inserts remained to be done particularly in terms of the SLS machine operation still retaining characteristics of being an art.

Figure 43 SVI : Part Bed Insert, Piston and Alignment Rails

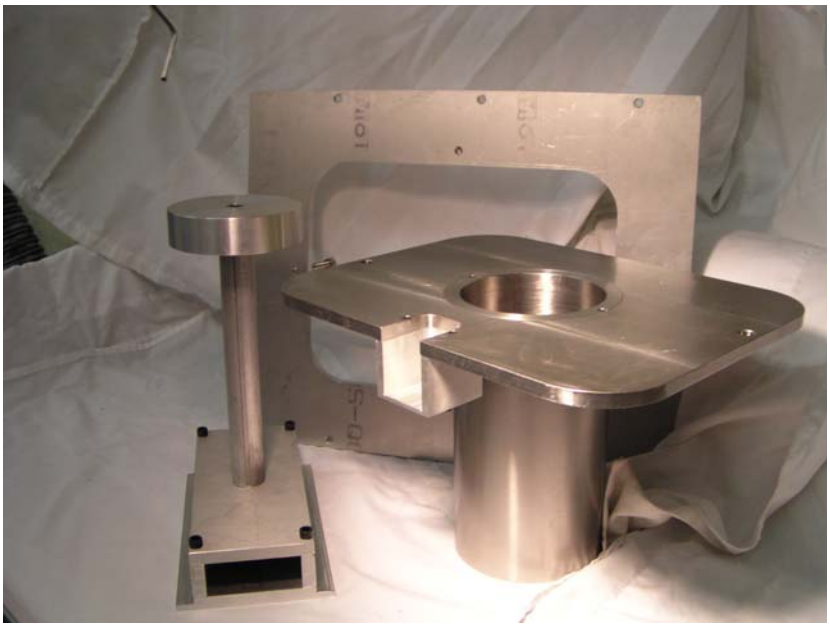

Figure 44 SVI : Feed Insert, Piston and Mounting Plate

Several additional technical pieces would support a more effective, efficient and generalized method for screening materials to work in the SLS machine. The first is to better establish the actual temperature cycles seen by powders in the SLS machine via experimental and numerical methods. This would support additional work linking the temperature/ rheology behavior of polymers with their tendency to sinter or bind inert materials within the SLS thermal cycle. With these two pieces and a more extensive library of SLS materials it would become possible to have a predictive model of SLS processing. This model (or set of models), could be used for a much more effective SLS material screening method. This and other additional development projects necessary are listed in the central column of Figure 45. It would still be necessary to verify the results of the model, but developing a preliminary set of operating parameters would not require iterative builds in the SLS machine. Coupled with the SVI, very little time and test material would be needed. The advantages of more rapid materials screening and development for SLS are clear, but this would also facilitate work with higher cost

materials than are currently feasible with material consumption in the machine and the large minimum material requirement. It is also often the case that samples of experimental new polymers or custom polymer blends can be obtained either in samples of less than 5lb. or more than 1000lb. The intermediate amounts of several dozen or several hundred required for current SLS development activities are not generally supported.

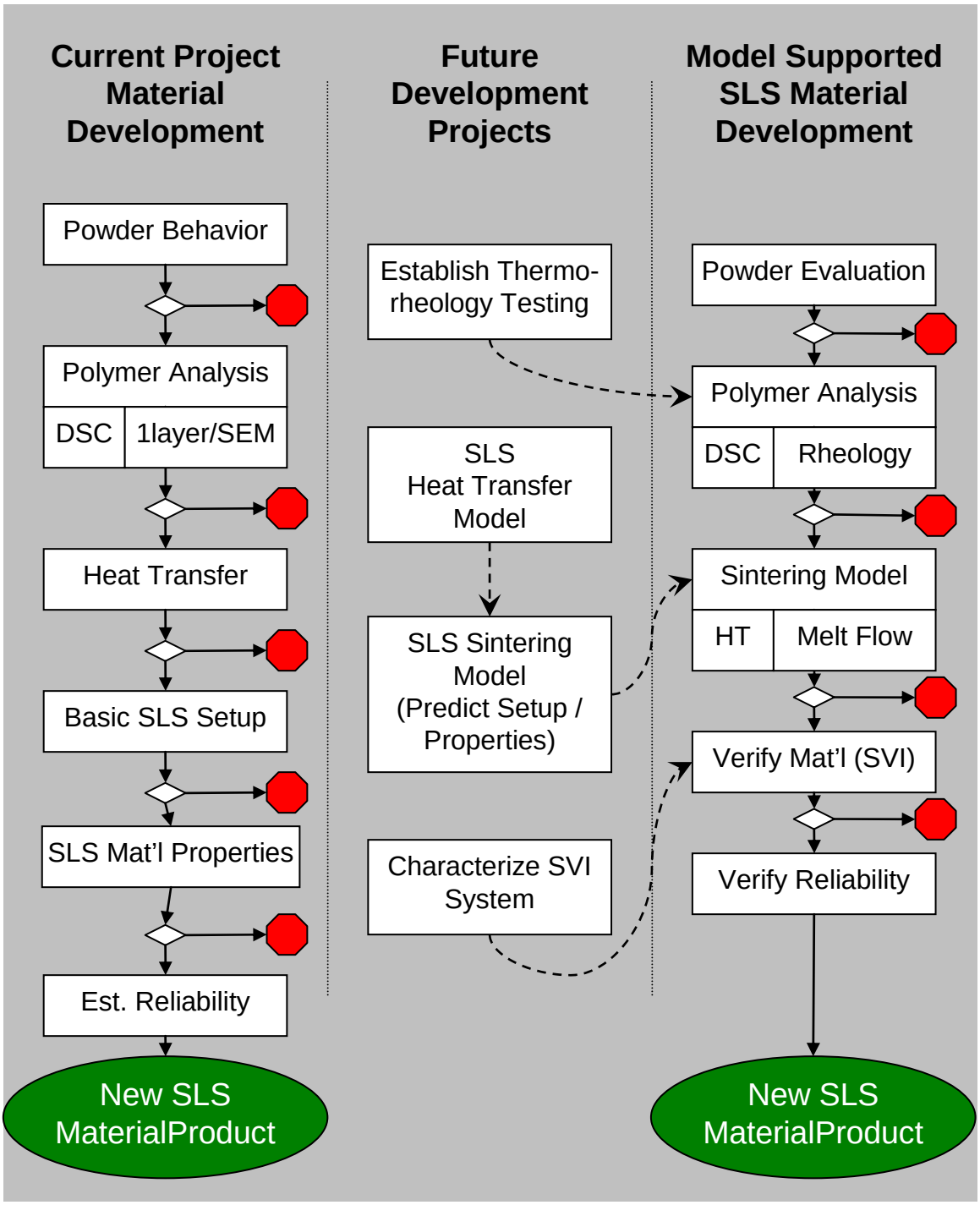

Figure 45 Current and Future SLS Materials Development Processes

3.4.3 SLS of Thermosetting Materials

Looking at the patent claims on the current SLS material patents a certain conventional wisdom about the SLS process can be assembled. The conventional wisdom is that semicrystalline organic polymers, having a significant difference between melt and recrystallization temperatures represent the best materials for SLS processing. Thinking instead of rheology, heat transfer and a sintering potential opens up the potential material set available to SLS.

When asked to list the most important things required of new SLS material, a representative of Boeing listed high temperature resistance, flame retardance and low cost. The advantages of thermoset materials, in general, are high temperature resistance coupled with low cost. Many of them are also inherently flame retardant. There is a clear opportunity in creating SLS parts from thermosetting polymers alone (not just as binders).

Phenolic is not a likely candidate as it emits a vapor during SLS processing, exists as a brittle powder and forms a brittle solid. Other types of materials, such as powdered epoxies or cyanate ester would offer better material properties. It was also suggested by engineers at Cymetech that Poly-Dicyclopentadiene, a polymer used to form large high-impact resistant parts for trucks and snowmobiles, as an example, could be prepared in a powdered form.

The best type of thermosetting material for SLS would be one for which the laser initiated a curing reaction rather than having high temperature necessary for curing to occur. With this type of system the region scanned would continue to cure after the laser had scanned the surface. This might be some type of A/B material that is mixed under the laser. One part could be coated over another as an example. Upon melting these phases would mix and cure. There are single component silicone materials that contain an inhibition chemical that changes into

a curing catalyst when heated. Perhaps a similar chemical system could be found in a powdered form.

3.4.4 Toward Rapid Manufacturing

The overarching context for the entire research project was to think in terms of rapid manufacturing, which will be explored in the following chapters. In this chapter, however, there were several relevant issues. The first is the need for more capable materials and a wider variety of materials. Thermoset binders, and even phenolic specifically, are stronger binders than current industry standards. They are effective with a wide variety of base materials or mixtures of different base materials. Laser marking might also be a very desirable feature in terms of identifying parts.

It is clear from the current work that the while the current embodiment of the SLS machine is capable of making a variety of parts, it was not created to support manufacturing. The temperature differences across the powder beds, changes in thermal cycle due to the scanning method and large time-scale transients do not support the level of reliability and ease of use necessary for manufacturing operations. Rapid manufacturing will not be realized if the part geometry changes by several thousandths depending on part orientation, placement in the bed and order in which it is scanned relative to other parts being built simultaneously. Other possible improvements to the machine are clearer in terms of the costs of producing parts using the SLS process which is reviewed in Chapter 5.

None of the parts produced during the tests described above were strong enough directly from the SLS machine to be prototype parts or certainly to be used as a finished product. They required additional post-processes to enhance their mechanical properties. The post-processing examined during the course of the research is discussed in the following chapter.

Chapter 4 Post Processing of SLS Parts

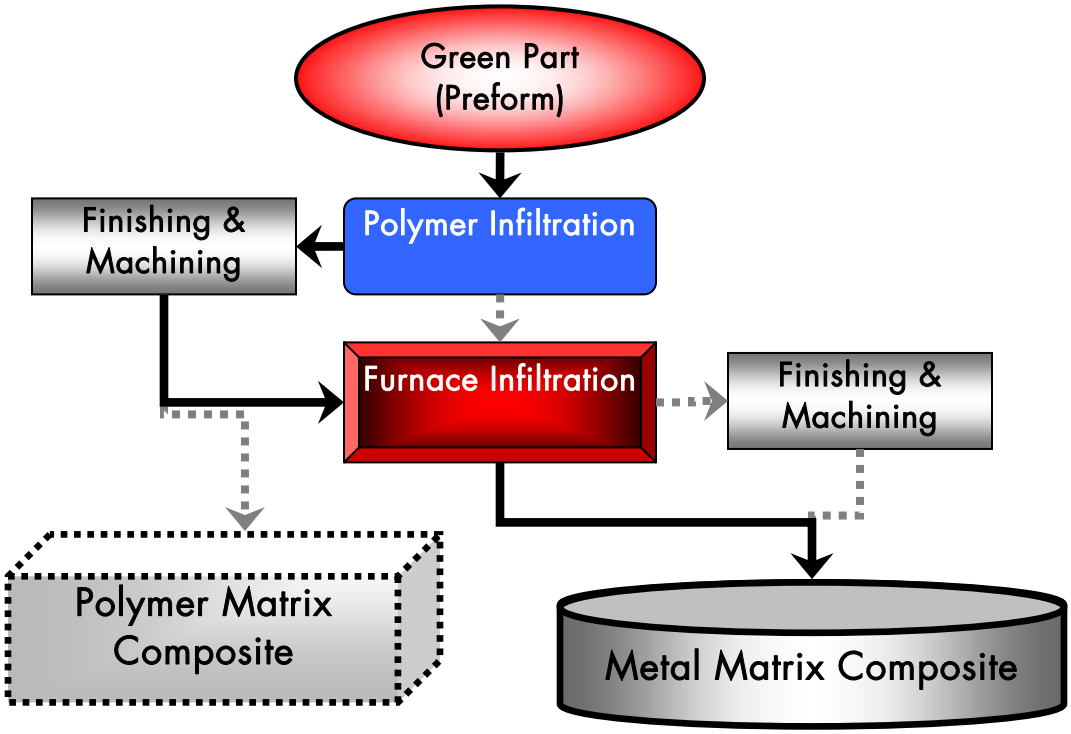

Figure 46 Post Processing Operations for SLS Preforms

In this chapter several processes are described that add value to the green preforms described in the previous chapter. Many different types of manufacturing processes are often followed by additional steps to prepare finished, fully functional parts. Flashing is removed from molded parts, machined parts are deburred and finished and both types of manufacturing processes are routinely followed by heat treatments, surface treatments or coating processes. These processes improve the accuracy, surface finish and materials properties of manufactured parts. Commercially prepared SLS are similarly post processed. Nylon parts are sanded and bead-blasted. CRP Technology (www.crptechnology.com) offers a family of SLS materials called Windform. In addition to improved strength and abrasion resistance with respect to standard

nylon SLS parts, these materials can be finished to a surface smooth enough to be used for F-1 racing components.

In other cases post processing of SLS parts is used not just for material improvement but to create significantly different material composition. Many materials currently used in the SLS industry form porous parts (herein described as green parts) which are subsequently infiltrated to form a final material composition. The concept of using SLS for the object shape and subsequent processes for material properties is called "Indirect SLS." This is a common strategy used for commercial SLS materials. Castform is infiltrated with wax to create a solid part which can then be sanded to a smooth surface and used for lost-wax metal casting. Somos 201 is infiltrated with polyurethane for toughness and color while preserving flexibility. The steel powders are held together by nylon binders and with a bed of alumina powder providing transitional support, infiltrated with bronze.

The current chapter describes two infiltration processes. The first is infiltration with functional polymers such as epoxy. The second involves a high-temperature furnace and free-standing, spontaneous infiltration with silicon as an example of metal infiltration. This particular infiltration process includes the simultaneous, reactive formation of additional SiC. The work with the two infiltration methods supports three different hypotheses within this chapter: 1) Polymer infiltration is an effective method of producing indirect SLS parts with properties not obtainable via current SLS methods; 2) By using a char-yielding polymer, high-accuracy, free standing, spontaneous infiltration may be achieved; 3) Indirect processes form a flexible rapid manufacturing platform capable of supporting a variety of material systems.

4.1 Background

4.1.1 Infiltration of Porous Compacts

The dynamics of fluid wicking into porous compacts is a mature, well understood subject. Here, the equations were taken from German, (1989), but many other sources exist on the subject. Equation (27) is called the Washburn Equation, and provides a relationship between the height the fluid has wicked into the porous compact, h, and the time, t. In this equation $\bar{d}_p$, is the average pore size, ρ and μ are the density and viscosity of the fluid respectively. With a simple wicking test the time and wicking height can be measured for a particular fluid and porous compact combination and related to unknown parameters of the materials using the following equations. The maximum height the fluid will reach, $h_{\max}$, may be determined from Equation (28). The relationship between fractional density, f, the particle size of the powder, $\bar{D}$, and the average pore size is shown in Equation (29). Finally the underlying model for the Washburn wicking model is the Poiseuille Capillary Flow equation seen in Equation (30).

$$\frac{h^2}{\left(h_{\max}-h\right)}=\frac{\bar{d}_p^{\,2} g t \rho}{32\mu} \tag{27}$$

$$h_{\max}=\frac{4\gamma_{LV}\cos(\theta)}{\bar{d}_p g \rho} \tag{28}$$

$$\bar{d}_p=\frac{2\bar{D}\left(1-f\right)}{3f} \tag{29}$$

$$\frac{dh}{dt}=\frac{\bar{d}_p\gamma_{LV}}{8\mu h}-\frac{\bar{d}_p\rho}{32\mu} \tag{30}$$

One final variable of interest in these relations is the driving surface tension, γ_{LV}, which exists only where the fluid/ atmosphere surface intersects dry compact material. This is related to the contact angle, θ, (and therefore the surface energy

gradients) between the solid and the liquid material interface. The contact angle can range, theoretically, from 0 to 180°. 0° would represent complete wetting while anything above 90° would indicate an adverse surface energy gradient, requiring pressure to drive an infiltration process. The contact angles between molten metals and ceramics have been experimentally determined and are available in a variety of metals processing handbooks, offering an ability to match base and infiltrant materials that will facilitate spontaneous infiltration. The surface energies of infiltrant polymers could be used in the same way but are not readily found in literature.

4.1.2 Binder Decomposition

When heated in an anoxic atmosphere polymers will decompose. Some form entirely gaseous byproducts while others tend to form various amounts of carbon ash. For polymers with silicon in the polymer backbone, silica and other ceramics can be a part of the remaining ash or char material. Crosslinked polymers, in general, do not melt since the linkages between chains prevent viscous flow. This allows them to retain greater strength at higher temperatures and in many cases to leave a significant amount of ash or char that can still be structural even after the polymer has decomposed. Phenolic polymers crosslink and leave between 30 and 75% of their initial weight as carbon. Both of these characteristics have supported the wide use of phenolic for ablative coatings, carbon-carbon composites, friction creating and friction resistant materials. For the current work residual carbon is needed to retain the shape created by the SLS process during high-temperature processing and metal infiltration. A preform held together by carbon from thermally decomposed polymers is referred to as a brown part.

Knop and Pilato, (1985), describe two basic stages of phenolic decomposition. From 3-600°C gaseous compounds are evolved including H_2O, CO, CO_2, CH_4, and various phenols. This is accompanied by chain scission (the breaking of bonds between the phenol base structures in this case), but relatively little shrinkage. Above 600°C the carbon structure begins to organize into lower energy, higher density, and higher conductivity structures. Gaseous emissions continue with CO_2, CH_4, and H_2O but also include benzene and toluene at these higher temperatures. The evolution of benzene and related compounds can be captured by filtering furnace exhaust with activated carbon.

The oxygen in the phenol hydroxy structure in the phenolic chain itself can be an oxidation factor even in an otherwise inert environment. Choe and Lee, (1992), describe the evolution of the microstructure during the decomposition process mapping both the density and the strength of the resin across the most active decomposition temperatures (300-1000°C) and for different ramp rates. For all ramp rates the strength of the decomposing resin decreases to 500°C. For ramp rates of 30°C/hr and below the strength increases to between 2.5 and 4 times the original strength with a 40% unsupported linear shrinkage. For higher ramp rates they observed a continued reduction in strength above 500°C. Ko et al. (2001), observed nearly identical density changes with a minimum at 500°C of 1.199g/cm^3 rising to a density of 1.536g/cm^3 at 1000°C. They further observed no increase in strength or density with additional heating from 1000°C to 2400°C.

4.1.3 Furnace Operation

A 2300°C horizontal graphite vacuum furnace was built by The Furnace Source, LLC in Terryville, Connecticut. The furnace features separate purge and process gas lines, a mechanical vacuum pump and a Yokogawa programmable

temperature controller. Aside from the controller all main furnace operations are manual including purge cycles, cooling water control and gas flow rates. The basic structure of the hot box is a high density graphite bottom plate with large graphite heating elements along the side walls. Surrounding this is a 3" thick low density graphite wall which is suspended ¼" inside a steel water jacket. The water jacket isolates the high temperatures and also provides the structure for establishing the vacuum. The hot box has dimensions of about 11 x 11 x 16". The basic concept of the furnace is to dump heat into the center while removing it from the exterior of the evacuated space. After a test firing in Connecticut in December of 2003 the furnace was shipped to the University of Texas. It was installed by the UT Physical plant in only 19 weeks.

The other important features of the furnace concern safety. There are two thermocouples coming through the top of the hot box; one in the center for temperature control and another near the top of the right-hand heating element that provides over-temperature control. All ports into the hot box are water cooled including heating elements, gas supply, vacuum ports and thermocouple leads. The most dangerous situation for furnace operation would be to lose cooling water with the furnace at high temperature. There is a pressure release valve on the furnace and the water drain would also release some of the pressure from boiling. The supply manifold for the cooling water has several flow sensors that will shut down the power if a minimum threshold flow rate is not met. The flow rate used for all furnace runs was 58gpm.

The temperature controller is a Yokogawa Green Series UP550. A manual for this controller may be found online. The temperature cycles may be managed using a computer with an associated LL100 software package. The other useful feature is that the controller can set its own PID settings for each of several set point

temperatures. The controller will automatically scan through the set point to determine the best parameters for temperature control at that temperature. This feature is especially necessary as the transient behavior of the furnace is very different at 500°C and 1500°C, as an example.

4.1.4 Reactive Infiltration of Silicon

When liquid silicon (Si) meets carbon it reacts to form silicon carbide (SiC). When a porous SiC preform (with 320grit SiC powder) is placed in contact with liquid silicon, the silicon has been calculated to have a maximum wicking height of 2m (Wang, 1999). The concept examined in the related previous research at UT was to provide molten silicon to a brown part so that a fully dense composite of Si and SiC can be formed. The best embodiment of this process would be the growth of new SiC in place of the structural carbon, as illustrated in Figure 47. Building from a review of the literature, there are several significant challenges to be overcome in practice.

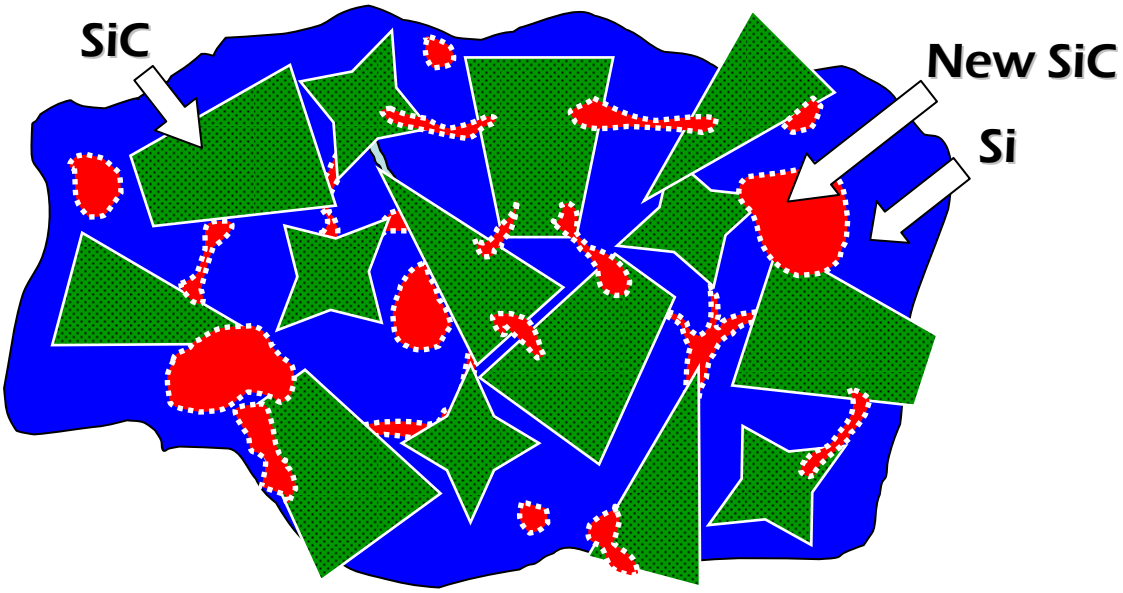

Figure 47 Diagram of RBSiC

A rather significant ~116 kJ/mol (~2600 J/g) is released when this reaction occurs (Rajesh and Bhagat, 1999). To put this into perspective the phenolic examined in Chapter 3 exhibited a curing exotherm of only 72J/g. Wang, (1999), observed a local temperature increase of 400°C. This heat of reaction, which changes based upon the structure of the carbon, influences the infiltration parameters (especially the melt viscosity and solubilities), formation of SiC and several characteristics of the final parts. This combined with the significant changes in permeability observed by Rajesh and Bhagat, (1999), indicate an influence on wicking kinetics and therefore final composite microstructure based on temperature at the onset of wicking. Introducing molten Si rather than allowing Si to melt near the preforms is expected to support more rapid and more effective infiltration. SiC formation from "solution reprecipitation" due to the increased exposure of C to Si melt, likely due to carbon diffusing from higher temperature regions of the Si melt and supersaturating others leads to rapid SiC growth. Favre et al., (2003), observed similar significant SiC growth at the liquid atmosphere boundary, away from the interface between carbon and silicon which they attributed mainly to the diffusion of $CO_{(g)}$ to the SiC grains within the Si melt. Figure 48 illustrates this behavior. The effects of heat from reactions, dissolved carbon and other transport phenomena all influence the processing of RBSiC via melt infiltration. If the Si is introduced to the preform as a melt, the main SiC formation occurs within the first minute of contact and proceeds to a stable thickness of 10-12 μm at carbon surfaces (Favre, et al., 2003). After this thickness has been reached further growth is inhibited by the extremely low diffusion of carbon or Si through SiC. High compression forces at the grain boundaries cause crystals to break away, causing periodic growth and local breaks (Favre, et al., 2003). These breaks obviously can cause a sudden exposure of carbon to Si and

also cracks in the carbon surface itself. These effects are also illustrated in Figure 48.

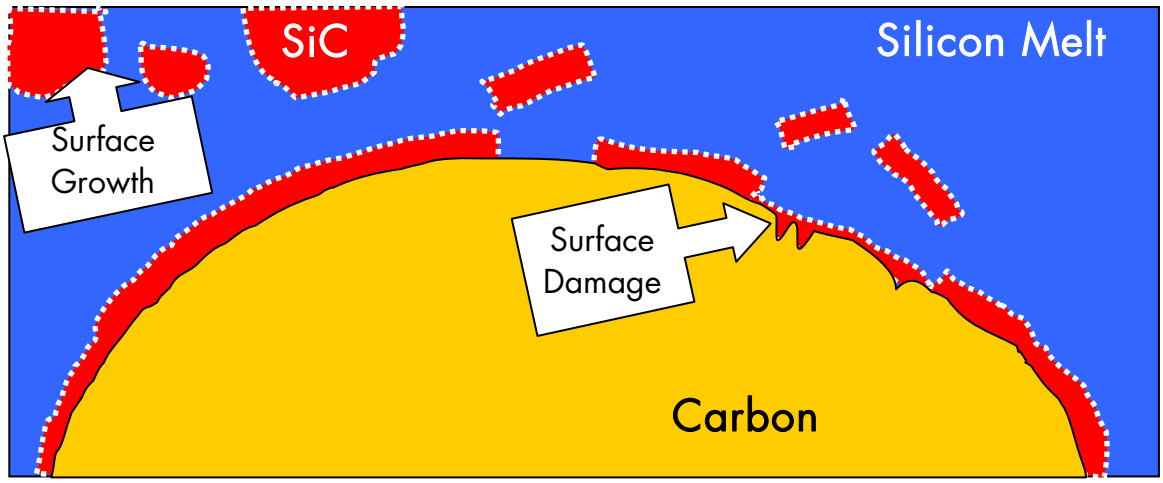

Figure 48 SiC Formation

A thorough understanding of the wetting characteristics and the driving capillary action from the previous work coupled with a newly available model of transient permeability within preforms for reaction-formed SiC materials (Rajesh and Bhagat, 1999) provides insight into the expected infiltration mechanics. In small capillary channels the growth of SiC can choke off the subsequent flow of liquid Si. SiC growth can also occur in other regions where liquid saturation or gas-phase (specifically $Si_{(G)}$, $SiO_{(G)}$ CO and CO_2) transport supports growth. The quick initial boundary growth and the liquid surface growth are both promising SiC formation avenues. Unless the furnace used for the work has a diagnostic capability for the actual atmospheric composition during operation, any gas-phase SiC formation paths would be unknown. The obvious reaction is the first one listed in Figure 49. The other reactions listed involve gas-phase reactants. The last reaction in the list described the reaction for the Acheson process which is used to prepare SiC commercially from powdered mixtures of silica and coke above

1500°C. For some of these reactions the products of one are the reactants for another creating a complex SiC formation system.

$$Si_{(l)} + C_{(s)} \Rightarrow SiC_{(s)}$$
$$SiO_{(g)} + 2C_{(s)} \Rightarrow SiC_{(s)} + CO_{(g)}$$
$$2Si_{(l)} + CO_{(g)} \Leftrightarrow SiC_{(s)} + SiO_{(g)}$$
$$Si_{(l)} + CO_{(g)} \Leftrightarrow C_{(s)} + SiO_{(g)}$$
$$2C_{(s)} + SiO_{(g)} \Leftrightarrow SiC_{(s)} + CO_{2(g)}$$
$$2Si_3N_{4(s)} + 3CO_{(g)} \Rightarrow 3SiC_{(s)} + 4N_{2(g)} + 3SiO_{(g)}$$
$$SiO_{2(s)} + 3C_{(s)} \Rightarrow SiC_{(s)} + 2CO_{(g)}$$

Figure 49 Common Reactions for SiC Formation

Compared to sintered SiC, a composite material retaining a silicon matrix (such as reaction-bonded SiC) has weaker the mechanical properties and a lower service temperature (Paik et al., 2002). The behavior of RBSiC is dominated by the failure of the Si matrix (Fernandez et al., 2003). This influence is also seen in weaker acid resistance and fracture toughness. The sintering study by Suyama et al., (2003) generated a remarkably strong sintered material by, "controlling the residual Si size under 100 nm." Fernandez, et al., (2003) also observed a significant strength when a continuous SiC structure from carbonized wood was a feature of the infiltrated material. Another strengthening mechanism was noted by Dyban, (2001 & 2002) and Paik, et al., (2001) where larger SiC particles (~100μ) maximized the connection of SiC to SiC within the structure of the infiltrated material. Paik, et al., 2001, and Basu, et al., (1999) (who reported sintering reactions at as low as 1400°C) also used phenolic as a carbon source and binder in the preparation of reaction bonded silicon carbide. Clearly the characteristics of the finished parts are strongly dependent upon the structure of the

preform parts. Overall, the literature indicates that a very capable material may be made, especially if an interconnected or at least touching SiC phase can be established. For a more comprehensive treatment of the fabrication methods and applications of silicon carbide see Roewer, et al., (2002).

4.1.5 Toward Functional Matrix Composites

If other metals were wicked into the preforms, a process called "Liquid Phase Sintering", particulate reinforced metal matrix composites would be formed. For combinations having an appropriate relative surface energy gradients free standing, spontaneous infiltration is possible allowing the shape of the article to be preserved during the infiltration process without special tooling. As an example molten iron or cobalt have a contact angle of 0° when in contact with Tungsten carbide indicating very strong spontaneous wicking. Titanium and aluminum will both wick into silicon carbide with careful avoidance of oxygen. The advantages of SLS processing could be extended to a set of very capable materials. The formation of additional SiC during infiltration (promoting reaction bonding) is another important feature of the current process. Titanium, as an example, also forms a stable carbide when the melt encounters carbon. Aluminum instead forms unstable carbide that reacts with atmospheric moisture, leaving surface defects in finished parts. Ultimately, there are three issues that govern the success and behavior of liquid phase sintering; 1) the surface interactions between the powder and the melt, 2) relevant chemical reactions and 3) the evolution of material microstructure. The microstructural evolution is a more complex subject, beyond the scope of the present work. There is a wide array of research describing the effects of base material size, reaction infiltration, multimodal particle sizes and other characteristics on the final properties for many different types of material combinations.

In terms of preparing products from SiC powder (with an appropriate binder) it is possible to pursue a high SiC content finished part by adding carbon during intermediate infiltrations with carbon yielding materials. On the other hand 40% loadings of SiC powder are common for commercially prepared SiC composites. This indicates that the SiC powder tested in the previous chapter would naturally settle to an appropriate fractional density for these types of material systems. Phenolic-matrix composites are prepared with reinforcement loadings of up to 75% by weight (with materials of similar density).

Table 13 , below lists the properties of several ceramic and metallic materials from a variety of sources. The key comparisons are the contrast between pure SiC and RBSiC and the high thermal conductivity of the SiC materials.

Table 13 Ceramic and Metals Material Properties

Material	Density (SG)	Tensile Modulus (GPa)	Flexural Strength (MPa)	Thermal Cond. (W/mK)	Soften. Temp. (°C)
Silicon Carbide	3.1	>400	550	120	2800
RBSiC	2.9	200-375	40-450	110	1375
Alumina	3.69	300	330	18	1925
Aluminum	2.7	62-70	240	150-210	550-650
Steel	7.8	~195	750-2500	15-35	300-650
Titanium	4.43	114	-	22	1660

4.1.6 Research Task

The research tasks associated with this chapter are broaderin some respects than in the previous chapter. In line with the themes listed in Section 4.1.1 of this chapter, the first task is to establish an appropriate understanding of polymer infiltration and curing using a variety of infiltrants. The curing task is tied to the curing of the phenolic binder discussed in the previous chapter. Next, the issues associated with free standing, reactive infiltration are explored by using silicon

infiltration as an example. Finally these results are applied to the overall discussion about rapid manufacturing and to the concept of a platform for a variety of different functional materials.

Figure 50 is similar to the diagram introduced in Section 3.1.5 and outlines the variables and observable characteristics for the post processing stages that will be discussed below. It is possible to leave out the intermediate machining step if improved dimensional tolerances or surface finishes are not desired.

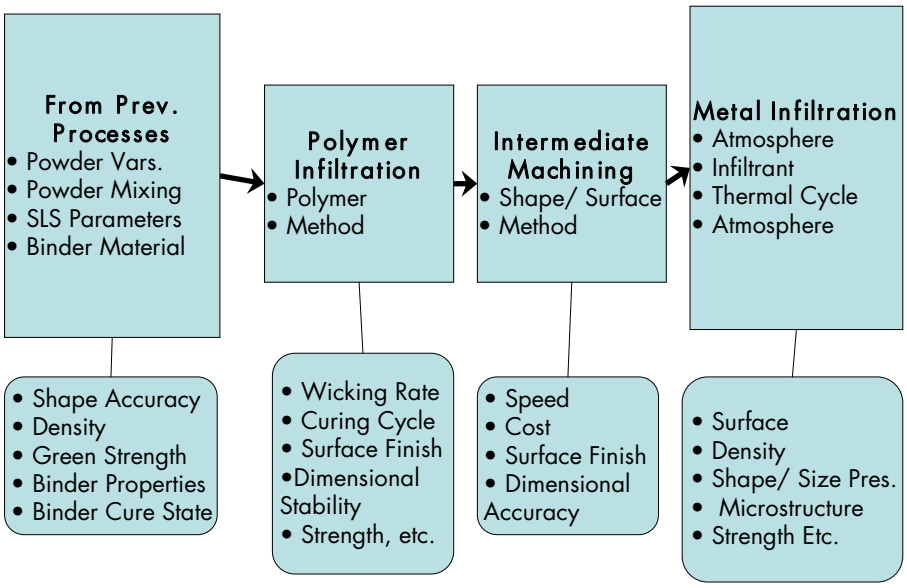

Figure 50 Post Processing Variables

4.2 Method

4.2.1 Polymer Infiltration and Curing

The examination of polymer infiltration covers a variety of polymers and infiltration methods. The different methods of infiltration are listed below. Next, the polymers tested and their basic properties and curing cycles are outlined.

Infiltration Methods

1 – Drip: This term describes applying the infiltrant to the outer surface of the part using a dropper, as an example. The infiltrant is allowed to soak into the part and is added until the part is uniformly wetted and the soaking of newly applied infiltrant becomes very slow.

2 – Dip: Predictably dipping is soaking the parts in infiltrant. At least the top surface of the part should be kept dry to allow air to escape during the infiltration process and to provide a gauge of progress.

3 – Wick: Similar to dipping, but with only the bottom surface of the part in contact with the infiltrant. This method was used to examine the relative speeds of infiltration for different polymer infiltrants.

4 – Vacuum Bag: In this method the part is sealed in a small plastic bag with two valved tubes attached. One is provides an inflow for the infiltrant while the other is attached to a vacuum pump. After the bag is evacuated infiltrant is allowed to flow into the evacuated bag from one end to another driven by additional vacuum pumping. The bag is then removed. The purpose of this method is to promote complete and rapid infiltration.

5 – Vacuum Soak: In this method the part is immersed in infiltrant completely. A surrounding chamber containing the parts and the container of infiltrant is slowly evacuated. Pumping is stopped when bubbles begin to appear in the bulk infiltrant fluid – indicating the vaporization of solvents in the infiltrant. The chamber is held under vacuum for several minutes to allow bubbles to dislodge from the parts and rise to the surface. At this point, only a small amount of infiltrant has penetrated the part. When the chamber is repressurized the infiltrant is forced into the part from all directions – leaving a small void at the

center of the part. Similar to using a vacuum bag, the purpose is to increase the speed of the infiltration process.

Infiltrant Polymers

Polydicyclopentadiene (DCPD) is a thermosetting polymer that has a very low viscosity (similar to glycerine) in its uncured state. The curing process occurs after mixing a Ruthenium-based crosslinking agent into the liquid. The base material is very pale yellow while the crosslinking agent darkens it to a yellow-amber color. The polymer has a variable pot-life from about 30 seconds to about 15 minutes depending one the formulation of precursor and crosslinking chemistry. The mixed liquid gels and then rapidly hardens with very little volume change over the liquid state. Curing is strongly exothermic and several ounces of polymer will evolve enough heat to reach 180°C-200°C and completely cure. Infiltrated parts divide the bulk DCPD and also add thermal mass which tends to limit the auto-curing. The polymer has a very strong, sweet, unpleasant aroma in its uncured state which is only removed at a completely full cure.

DCPD from Cymetech was infiltrated into several green SiC preform parts. The drip, dip and vacuum bag methods were examined. The infiltrated SiC parts were expected to reach only a partial cure spontaneously due to the thermal load of the SiC itself and were post cured in an oven at 140°C for 80minutes.

Two different types of epoxy were examined. Both were chosen for their relatively low viscosity, long pot lives (~1 hour) and high solids content (lack of solvents) compared to most epoxies Even so their viscosities resembled Karo® syrup. They were both two-part resins that featured room-temperature curing with more rapid and complete curing at higher temperatures. The first was System Three Clear Coat. After curing the resin is designed to be colorless and nearly clear. It has a heat deflection temperature (often considered the maximum

continuous use temperature) of 127°C. Additional information about the material may be found at the System Three website (www.systemthree.com). The material will reach a full cure at room temperature in 7 days or a more rapid 4-hour cure at 70°C. The second epoxy was BJB TC-1622 A/B, a higher strength and higher temperature (177°C) two-part epoxy. The fully cured resin resembles butterscotch candy. This resin partially cures and hardens at room temperature, but heat (66°C and 120°C for two hours and 177°C for 2 hours) is needed for a full cure. The final yellow color is seen only after the final higher temperature soak. Additional information is available through the company website, (www.bjbenterprises.com). The curing behavior of epoxy can be modeled in the same way described for the phenolic in the previous chapter as described by Montserrat and Málek, (1993).

Green parts with SiC and glass base materials were infiltrated using both epoxies. A more extensive study was conducted with the BJB material which included dimensional stability testing, outlined in the following section. Parts were infiltrated by wicking, dipping and vacuum soaking.

Imprex (www.imprexusa.com) is a company that specializes in low-viscosity thermosetting infiltrants. The infiltrant tested was Imprex 95-1000A Superseal which cures to a clear and flexible final form. Its final form has strength similar to that of styrene (the material used in disposable wine glasses), significantly lower than the BJB Epoxy. It is a single component resin. The curing cycle can be accomplished over 3-6 hours at a relatively low 80°C, but no curing occurs at room temperature. The low viscosity comes in part from solvents.

Similar to the epoxies, glass and SiC base material parts were infiltrated. Brown parts were also tested for comparison. Parts were infiltrated using the dip, drip and wick techniques outlined above.

One specific test was performed to quantify the spontaneous wicking of Imprex and BJB Epoxy into SiC base parts. Both infiltrants were wicked into 1" SiC base material cubes. After 1, 2 and 5 minutes of wicking the height of the each infiltrant was measured to obtain the unknown surface tension. This was put into Equation (27) to allow height versus time graphs to be prepared for the two resins.

Phenolic Curing

As discussed in the previous chapter, the phenolic was not cured significantly under the laser of the SLS machine. The phenolic would instead be curing at the same time as the infiltrant polymers. There were three issues expected. The first was the outgassing of the phenolic curing reaction. The second was due to the fact that without a significant cure the phenolic would begin to soften at 70°C, lower than the curing temperature of several of the infiltrants studied. This same issue was addressed in terms of the furnace testing to be discussed in the Section 4.2.3. The final issue was adverse chemical reactions with or solubility in the infiltrant materials which can contain solvents. Uncured phenolic is soluble in alcohols and aromatic solvents (such as benzene, xylene and toluene).

A quick curing examination was carried out in a standard lab oven at 80, 90, 100 and 160°C. Green parts (5" beams, 1/8" thick, 0.5" wide) were suspended between stainless steel blocks and observed at appropriate intervals.

4.2.2 Dimensional Stability

As introduced in the previous chapter, 0.5 x 0.5 x 2.5" bars were built to examine the dimensional stability of the SLS and infiltration processes. The bars were oriented in both the X and Y directions within the SLS machine and had different laser powers. The parts were distributed randomly within the part bed.

The first set of tests was completed with glass powder as the base material. A more focused study was then completed with SiC base material. The length (long dimension), width and thickness (aligned in the Z direction of the part bed) were measured for all parts before and after infiltration with the BJB Epoxy. The complete details of the part setup may be found in Table 22 and Table 23 in Appendix 1.

4.2.3 Surface Preparation and Machining

Parts were filed and sanded in green, polymer infiltrated and silicon infiltrated conditions. Filed and sanded surfaces of green and polymer infiltrated parts were examined after being processed in the furnace into brown and silicon infiltrated parts.

4.2.4 Mechanical Testing

Mechanical testing consisted of subjective observations SEM analysis and three-point bend testing. Sample beams with glass (5" length, ¼" thick) and SiC base materials (5" length and $\frac{1}{8}$" thick) were infiltrated with BJB epoxy. Fully and partially cured samples were examined. Three point bend testing was completed to the ASTM D-790-03 specification.

5" Green and epoxy infiltrated bend test beams (again to ASTM D-790-03 specifications) were prepared during the related work of D. Bourell and S. Barrow. The parts were bend tested to examine the strength of the final RBSiC material produced during this project.

4.2.5 Furnace Processing and Metal Infiltration

Before the more sophisticated graphite furnace was installed molded compacts were carbonized (the binder was reduced to carbon) in a tube furnace with a Nitrogen forming gas (4% Hydrogen) at 700°C. Compacts were placed in

alumina boats. The boats were placed in a cold furnace and the temperature was raised at 50°C/hour to a final temperature of 700°C, which was held for 2 hours. The furnace was allowed to cool naturally and the flow of gas was limited to about 1scfh (by setting the flow to have 2 bubbles per second in an outbound water flask) after an initial purge of 5scfh for 5 minutes. The ends of the tube were sealed with appropriate clamps and gaskets.

Phenolic powder was packed into one of the molds used to characterize it as a binder. During curing it expanded from outgassing to resemble a loaf of bread. One half of the cured phenolic was placed into the graphite vacuum furnace and carbonized to 1100°C. The structure of the part was observed using an SEM and also measured to assess the weight loss and shrinkage due to binder decomposition.

After the graphite furnace was installed, process gas connections were setup so that one bottle could be attached to both the purge and process inputs. Before each run the furnace was sealed and pumped down to below 5mtorr, purged and repumped at least once. The purging cycle used most of the process gas during operation. After running a drying cycle soak of 500°C for one hour followed by 700°C for 3 hours (to remove the water from the walls of the furnace), the furnace was setup for the initial infiltration test. Water dissociates at high temperatures (above roughly 1200°C) becoming a source of oxygen contamination. During the initial infiltration run the cooling cycle of the furnace was monitored which allowed the numbers to represent cooling with a thermal load present..

Next, a set of green parts were placed in graphite crucibles along with 125% of the silicon metal necessary to fill the voids of each part. The graphite crucibles were sprayed with Boron Nitride mold release to prevent silicon

infiltration. This setup may be seen in Figure 51. The bottom plate, rear wall and heating elements are also visible in the image. The left, rear part has been notched with a file to test the effect of intermediate machining. The bars in the foreground were setup to provide the most aggressive test of part slumping.

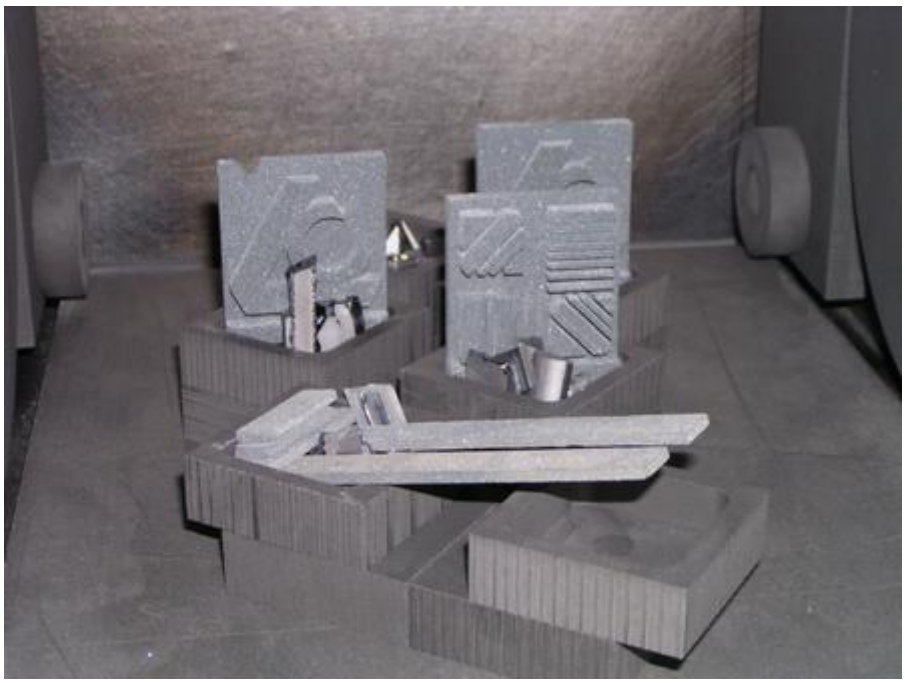

Figure 51 Setup for Furnace Infiltration (Si is arranged within the crucibles)

The initial temperature cycle was borrowed from the runs completed at the University of Rhode Island during the previous research (Wang, 1999). It included 5 steps (listed below) and both Nitrogen and Argon were used as inerting gases during separate runs.

1 – Room Temperature to 450°C:	90min
2 – Hold at 450°C:	30min
3 – Ramp to 1650°C:	120min
4 – Hold at 1650°C:	90min
5 - Shutdown	

The parameters of the temperature cycle evolved during the series of furnace runs that followed. After each run the parts were observed and changes

were made to the cycle. That evolution pursued the appropriate temperature cycles for 3 main phases; curing (ambient – 200°C), polymer decomposition (300-1100°C) and infiltration (1420-1600°C). The temperature cycle also had to address several overarching issues. The first of these is that there are long term advantages to having the total cycle, including the cooling, have a length that allows one-day turn-arounds. The other issues identified were exposure to oxygen contamination and also an appropriate temperature cycle for SiC formation. The relative amount of silicon was also altered during the runs.

The parameters for the polymer decomposition came from the literature discussed in the background section above. In particular, later ramps were held to 30°C per hour from 3-500°C. The ramp from 500-1100°C was run from 100°C/hour up to 300°C/hour.

A variety of approaching ramps and soaks were examined for the infiltration phase. This included rapid ramps from 1100°C to the peak temperature as well as soaks just below the 1420°C melt point of silicon. In all cases the ramp from the melt point to the peak temperature was rapid, 1000°C/hour as an example. The peak temperatures were tested at 1550, 1600 and 1650°C. Peak temperature soaks ranged from immediate shutdown to 1 hour.

Different types of fixtures were also explored. This included vertical and horizontal orientation and several different types of supporting pieces and part features to support infiltration. Graphite crucibles and graphite plates were used to prevent silicon contact with the furnace base plate.

In addition to the silicon infiltration that is outlined below two other metals were tested. By changing the peak temperature, iron was melted in proximity with

a part. It was not expected to infiltrate due to the adverse surface energy gradient that exists between iron and SiC. Other parts were placed into a nitrogen-inerted furnace used for commercial bronze infiltration into steel SLS parts. These parts were buried in alumina powder prior to being placed in the furnace. This allowed the bronze to be placed atop the parts to examine a gravity feed for a milder adverse wicking situation.

4.3 Results

4.3.1 Polymer Infiltration and Curing

Several properties of the infiltrants examined may be found in Table 14 Essentially, two low and two high viscosity materials were tested. This had a large effect not only on the amount of time required to perform the infiltration, but also the difficulty associated with handling, storage and cleanup. The basic procedure for wicking, regardless of method used, included removing the excess material from the parts before placing them in the oven for curing. This was accomplished using paper towels and typically took longer than the infiltration itself. It also required carefully putting some of the fine features of the parts tested in contact with the paper towels. Fine feature breakage was a problem. Lower viscosity materials did not require contact on all surfaces to remove excess material.

Table 14 Polymer Infiltrant Information

Infiltrant		Visc.	Pot Life	Cure	
Company	Description	(cp)	(min)	(°C)	(Minutes)
System 3	High-clarity Epoxy	600	120	70	240
BJB	High-strength Epoxy	~750	45	177[1]	300
Imprex	100%-solid semi-elastomeric polymer	1	360	106	60
Cymetech	Ruthenium catalyzed DCPD	3	15[3]	140[2]	80

1 BJB recommends a 66°C and 120°C soaks for 2 hours prior to 177°C curing
2 Bulk DCPD is self curing in bulk due to its strong curing exotherm
3 Material tested had a 1min pot life - up to 15 minutes is available commercially

The Imprex and DCPD materials did not require either bagged or immersed vacuum processing for the small parts tested. Wicking or soaking allowed parts to be fully infiltrated within the 1 minute pot life of the DCPD material tested. Several parts including dimensional stability bars and cubes were made using the glass base material and were infiltrated with both infiltrants. The time and wicking height were used to create a curve fit from Equation (27), since γ_{LV} and θ were not known for these material combinations. The results of this curve fitting infiltration study may be seen in Figure 52. For parts thicker than a centimeter it is impractical to simply wick the BJB Epoxy. The Imprex on the other hand was not tested with vacuum aided infiltration since all of the parts tested were rapidly filled. Even the slower wicking BJB Epoxy coated the surface of the SiC particles completely, as seen in Figure 53. This image is of the top of a wicked SiC part and shows that the Epoxy is drawn to cover the SiC particles completely even at the top outer surfaces of the part.

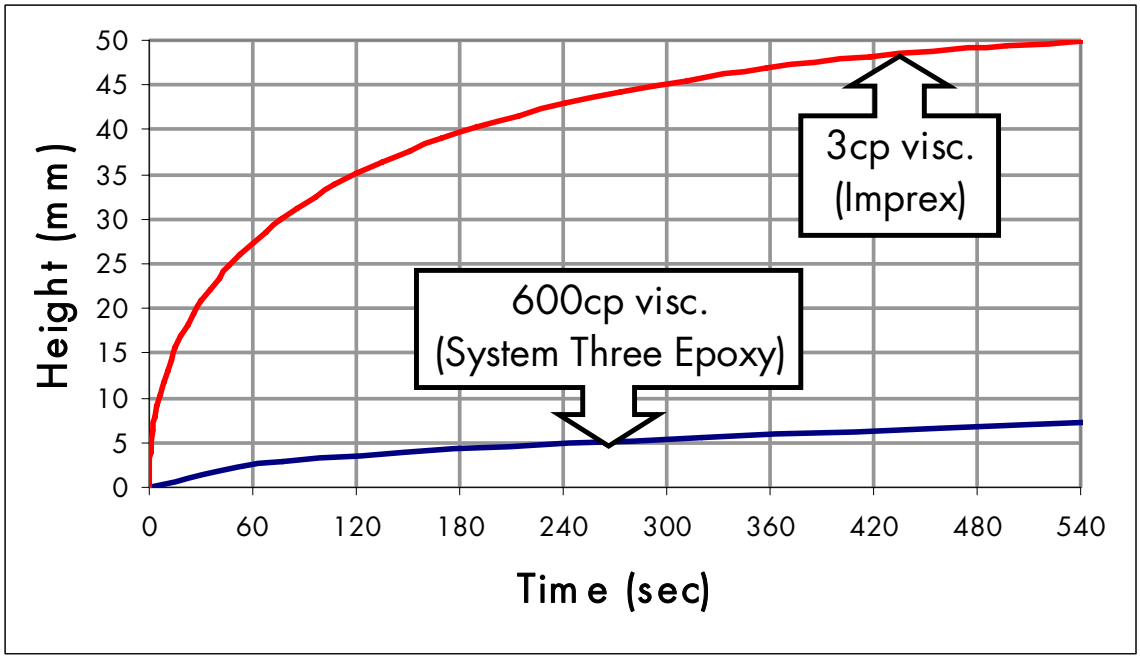

Figure 52 Infiltration Model for Polymer Infiltrants

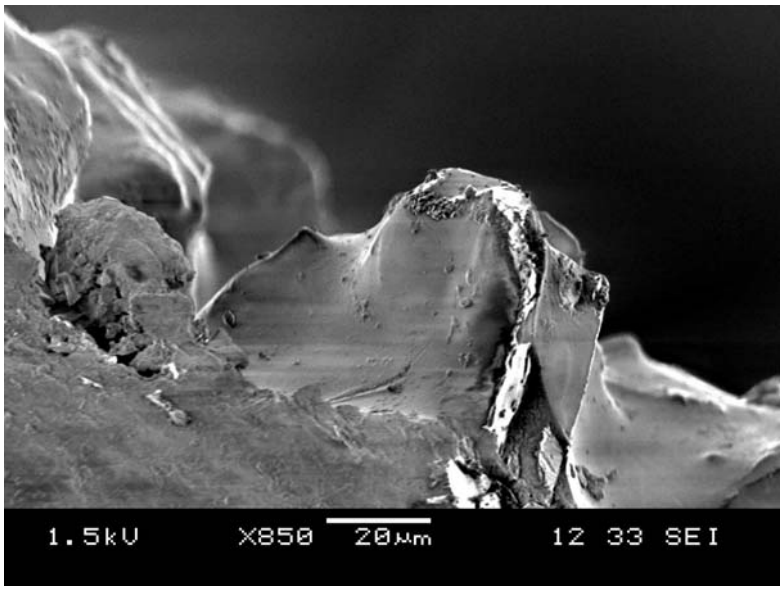

Figure 53 BJB TC-1622 Epoxy Coating SiC Particles (at top edge of part)

Both methods of vacuum-driven infiltration allowed the process to be more uniform between parts and in the case of the BJB Epoxy in particular, far more rapid. Using a bag for the DCPD infiltration required building appropriately sized

vacuum bags for each part. These were then cut away and the excess material was removed from each part. With vacuum assistance infiltration could be performed closer to the gel state of the polymer. The excess time and part-specific bags did not seem to represent a viable infiltration method in manufacturing practice since the bags pressed on the parts, limiting the features of the parts to be infiltrated. The other problem was the labor intensive and messy practice of building and tearing down the bags. Immersing parts in the BJB Epoxy proved more effective since there was no loading on the parts. The parts still required extensive cleanup to remove the excess material and there was an inherent uninfiltrated cavity inside the parts. The size of the cavity was explored using 0.5, 1 and 2″ cubes, as seen in the halved samples in Figure 54. The green and infiltrated volumes were compared to determine the volume change associated with the infiltration process. The 2″ cubes tested had the least variation. 1″ and 0.5″ cubes showed a wider range of cavity sizes. Data from one of the 2″ cubes examined and representative samples of the 0.5 and 1″ cubes may is contained in Table 15 . A more detailed examination of the dimensional stability of the infiltration process may be found in Section 4.3.2 , below.

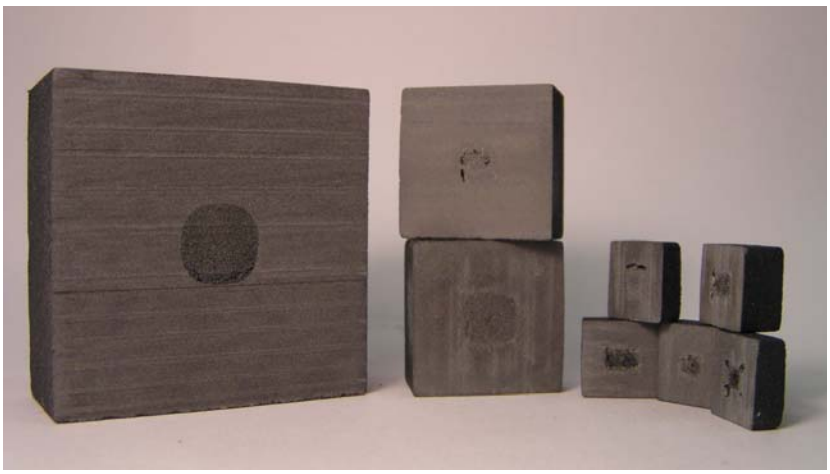

Figure 54 2″, 1″ and 0.5″ Infiltrated Cubes (BJB TC-1622 Epoxy)

Table 15 Vacuum Infiltration Pore Analysis

Cube Size	Green Vol.	Infil. Vol.	Pore		Pore Volume Fraction
			Minor Dia.	Major Dia	
2	102.8%	102.3%	0.488	0.503	6.23%
1	103.6%	103.3%	0.160	0.240	3.63%
	-	103.7%	0.398	0.440	29.93%
0.5	-	108.2%	0.156	0.173	13.90%
	-	107.4%	0.140	0.234	24.28%

Phenolic Curing

There were two issues associated with phenolic curing found during the polymer infiltration experiments. The first was slumping. Uninfiltrated green parts began to soften above 80°C. At higher oven temperatures the parts sagged predictably more rapidly and the phenolic became softer. Attempts to quick cure the surface regions with quick soaks in high temperature ovens (at about 200°C) did not achieve improved results. Although the phenolic will theoretically cure very slowly at 75°C, soaking parts for several days is not an effective method for part production. For reference parts soaked for over 8 days at 70°C (described in the previous chapter) showed a degree of cure of only 0.50. Fortunately, the epoxies and DCPD tested both achieved a partial cure at ambient conditions which was capable of supporting the parts through the curing cycle that was appropriate to the infiltrant. The second issue was the outgassing of the phenolic during its curing cycle. If the infiltrant was still pliable and the oven temperature was relatively high (>125°C) the outgassing was seen to distort the parts. As seen in Figure 55, with more curing of the infiltrants (in this case simply leaving the part on the left at room temperature for 8 hours) and a lower dwell temperature this was not an issue.

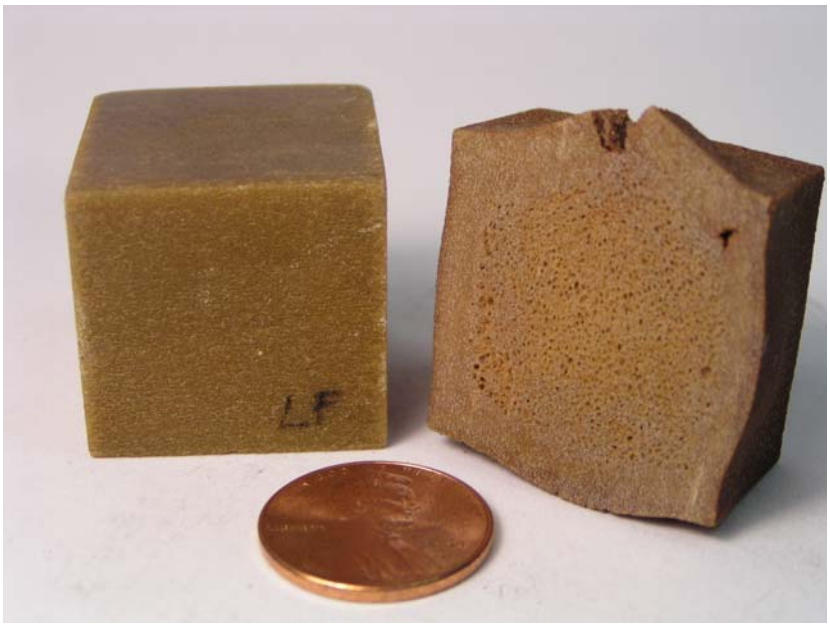

Figure 55 Aged (L) and Immediate (R) Heat Cure (1" cubes, System Three Epoxy)

Polydicyclopentadiene (DCPD)

A monomer aroma was still present on the parts after post curing. The infiltrated parts exhibited relatively high strength and 2 x 2 x 0.5" parts could be dropped from 6' onto concrete without visible damage. This was in contrast to the strength of the green parts which was similar to that of firm sugar cubes. The DCPD represented the best infiltrant material in terms of rapid wicking and high cured strength. The actual makeup of the material tested had a 1 minute pot life, which was too short for large parts or extensive testing. The wicking testing was done at Cymetech to limit the cost of infiltration and to support the training recommended for handling the polymer.

Epoxy

The epoxies tested had roughly the same processability. The BJB epoxy showed higher strength in early tests and with a continuous use temperature 50°C higher than the System Three material was preferred for more extensive testing.

The dimensional stability parts as well as those prepared as sample parts for potential customers (both described below) were made using the BJB epoxy.

Imprex

Imprex illustrated another potential problem with uncured phenolic – solvent attack. Figure 56, below, shows a green beam drip infiltrated on one end and placed in a lab oven at 80°C for curing. Green parts soaked with Imprex were slowly softened at room temperature, but quickly liquefied upon heating. In contrast, a 5" brown part did not slump during curing, as seen in Figure 57. While Imprex has the most rapid infiltration and was the easiest to handle, the interaction with uncured phenolic and the low strength of the final cured polymer made it unacceptable for this particular application.

Figure 56 Green Part Partially Drip Infiltrated with Imprex

Figure 57 Brown Part Infiltrated with Imprex Infiltrant

4.3.2 Dimensional Stability

Again, Appendix 1 contains the complete data for the dimensional stability testing. Examples of glass and SiC based parts may be found in Figure 58. The part orientation and scanning power was marked on the upper surface of the parts themselves.

Figure 58 Dimensional Stability Beams (0.5x0.5x2.5")

Figure 59, Figure 60 and Figure 61 show the volume, density and dimensional stability through the infiltration process for the glass parts. The dimensional stability calculations represent the change in dimensions between the green and brown parts. The trend through 8 and 10W is expected, but the 12W parts show a much larger difference between X and Y orientation in the infiltrated

parts. The density of the parts decreases with the 12W power as well. The lower density was likely due to inflation of the phenolic due to rapid surface curing containing the outgassing from within – which is supported by the carbon structure seen later in Figure 73. The decomposition of the HMTA would also be a source of outgassing. If the source of the outgassing were HMTA it would indicate that only in the 12W samples did the temperature reach ~147°C. If that were the case it certainly supports the lack of laser-induced curing found in the DSC testing described in the previous chapter. The cause of the increase in volume between the infiltrated12X and 12Y samples is unknown. Regardless, this test suggests that 12W with a spacing of 0.003" is too high an energy loading since it causes a large directional change in dimensions and part density. Early tests showed that this threshold did not happen until 13 or 14W with the SiC base material. The tests with the SiC material were confined to 10 and 12W parts. The parts swelled during the infiltration process adding to the part growth observed during SLS processing.

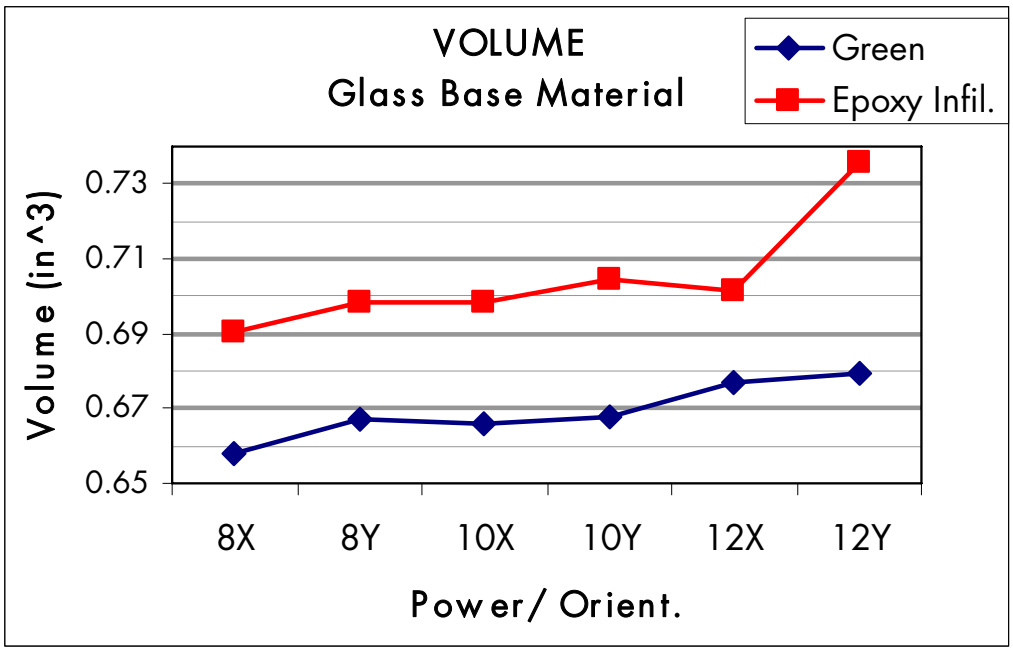

Figure 59 Phenolic/Glass Volume Trending

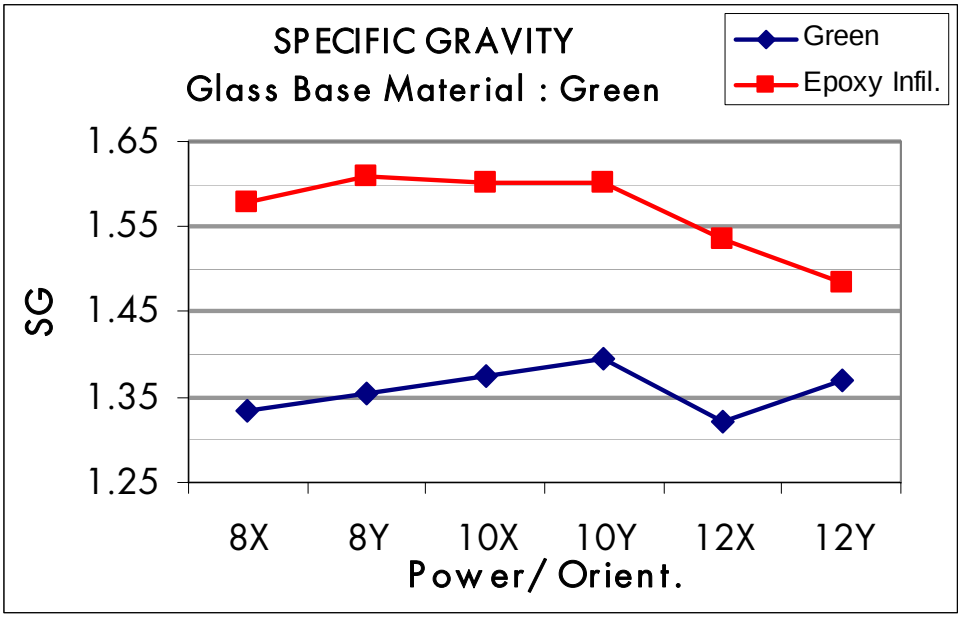

Figure 60 Phenolic/Glass Density Trending

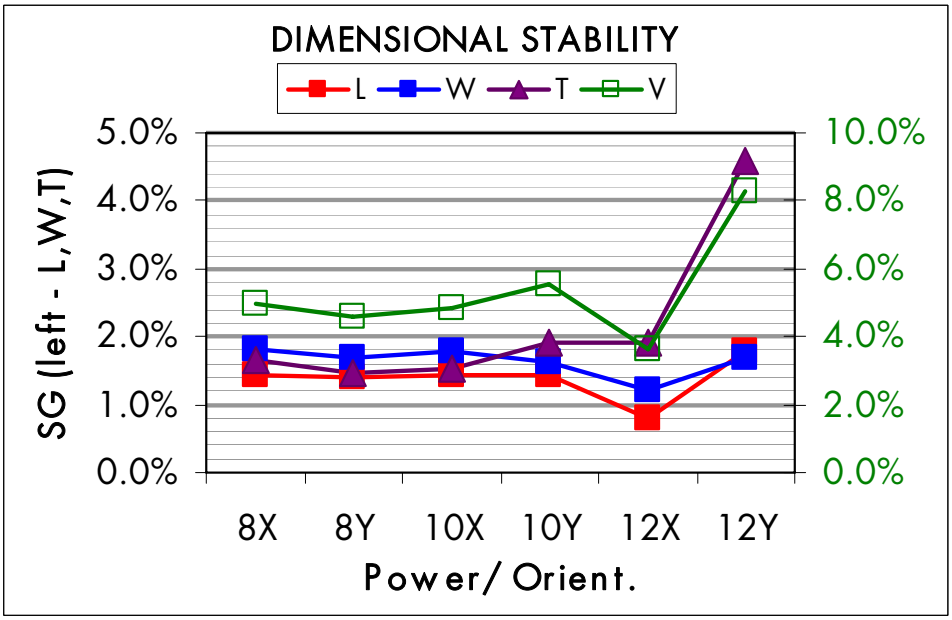

Figure 61 Phenolic/Glass Dimensional Stability

Figure 62, Figure 63 and Figure 64 illustrate the volume, density and dimensional effects of infiltration for the higher conductivity SiC material, respectively. The parts actually shrank during the infiltration process which removed some of the part growth from the SLS process. However the infiltration

shrinkage was uniform while the dimensional changes from SLS processing were more dependent upon part orientation and the width of a particular region being scanned. In terms of the infiltration process alone – an appropriate mixture of glass and SiC base material might facilitate an infiltration with very little dimensional change. The directional variation was more significant with the SiC base material. There was higher growth (increased part volume) in the regions aligned in the Y direction indicating part distortion. Along with the part growth was a variation in density which leads to different material properties in different regions of the part.

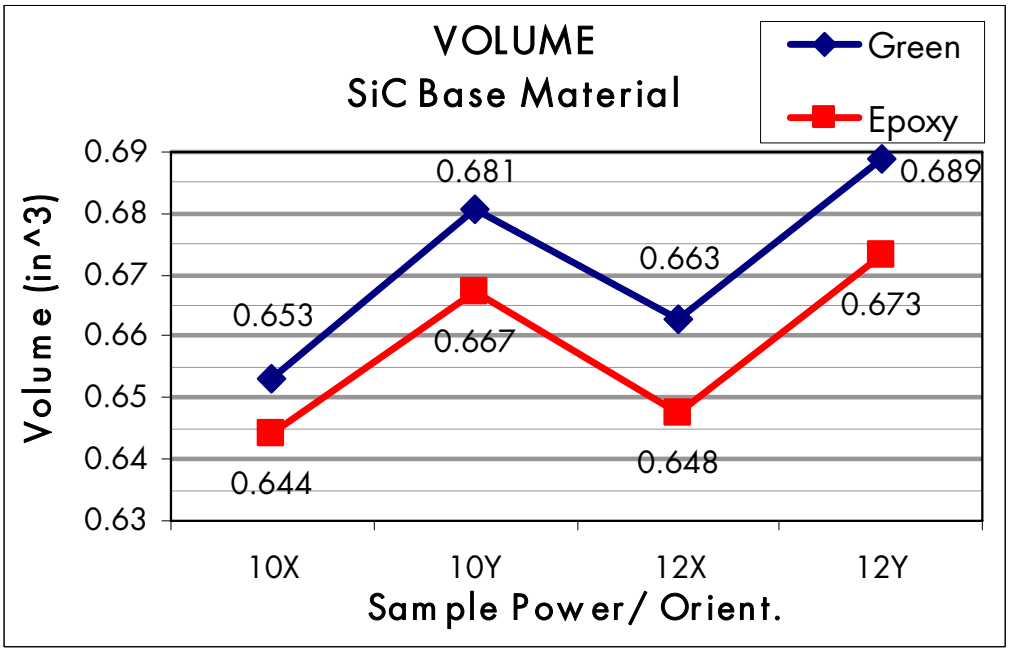

Figure 62 Phenolic/SiC Volume Trending

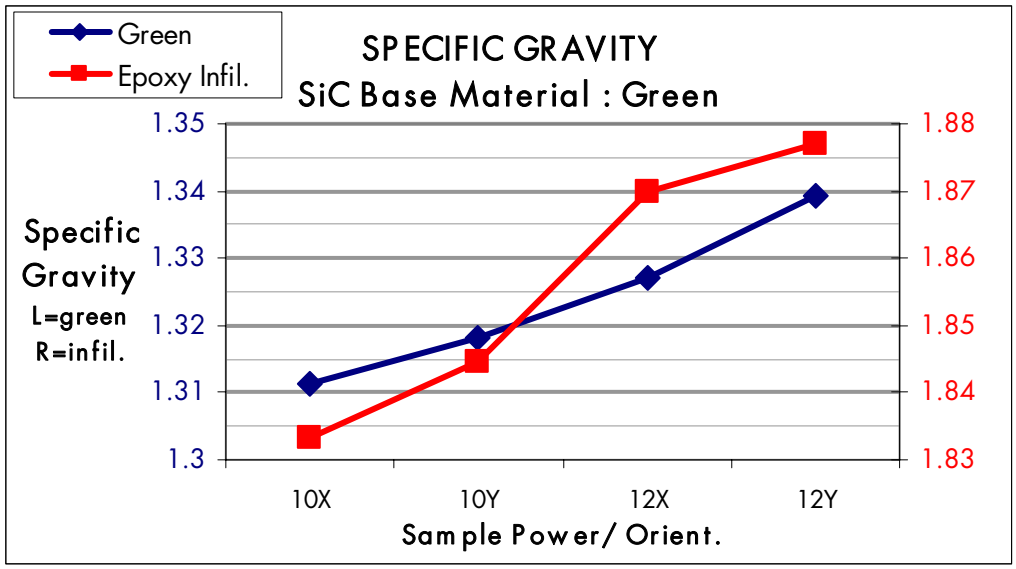

Figure 63 Phenolic/SiC Density Trending

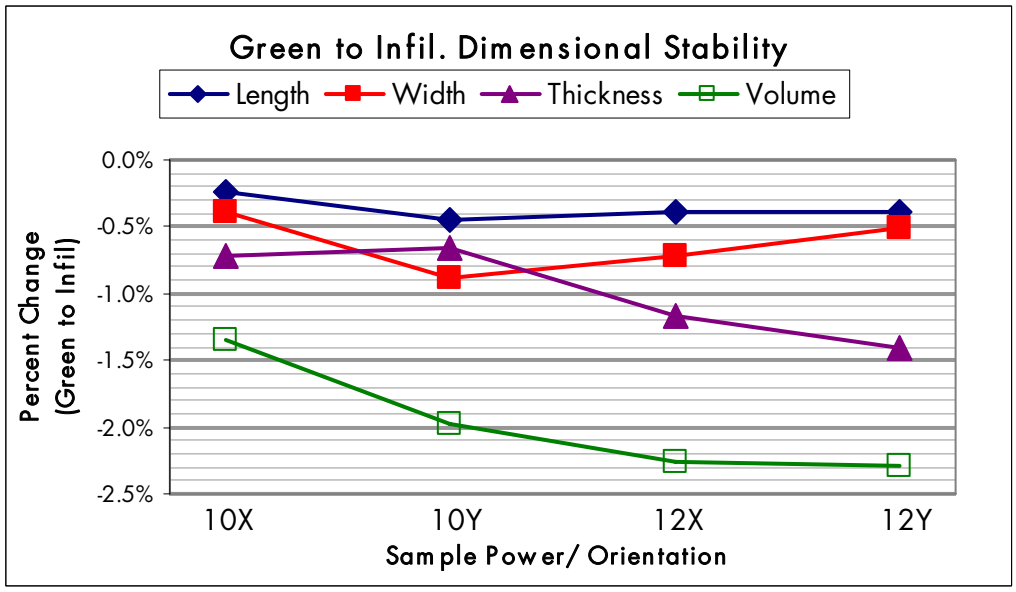

Figure 64 Phenolic/SiC Dimensional Stability

4.3.3 Intermediate Machining

During the DCPD infiltration testing, a standard metal file removed surface material easily to a smooth surface. Additional material removal required more significant pressure and effort. Similar behavior was found with the Epoxy materials. This indicated the potential of intermediate machining for achieving

closer tolerances and surface finish. The application for such a material might include low-energy wear resistance (meaning that local impact was not enough to remove SiC particles from the matrix). RBSiC and MMC's are notoriously difficult to machine due to the inclusion of abrasive ceramic particles. Even in the case of an easily machined matrix there are still concerns from high tool wear due to the abrasive ceramic particles. Still epoxy and the polymer matrix materials exhibit brittle behavior which facilitates a better sanded surface finish, but limits the ability of machining operations. Limited ductility in a material causes chipping at part edges or limits machining operations to very thin depth of cut.

A variety of BJB Epoxy infiltrated parts were filed, sanded and ground with a standard grinding wheel for steel. During these operations there was a slight phenolic aroma that came from the parts. Sanding with SiC sandpaper left a smooth finish similar to filing and there was also a slowing of progress after a smooth surface had been reached. With SiC base parts, alumina-based sandpaper quickly lost its sanding capability. Improvements in surface smoothness were noticed up to 400grit paper which is smoother than sanded SLS parts formed from nylon. Nylon-12 tends to form small filaments during sanding which is the same property that facilitates the formation of nylon filaments and fibers. This tends to limit the smoothness achievable. Grinding left a finish similar to that found on ground steel. The grinding wheel also removed small chips at part edges with heavier pressure on the wheel. In all cases glass base parts were more easily processed. One SiC base part was machined with a 0.5" end mill, at 0.010" depth of cut and at speeds used for aluminum. Climbing cuts at the edges limited but did not stop chipping. The surface was similar to 240grit sanded surfaces.

4.3.4 Mechanical Testing of Polymer Infiltrated Parts

Following the study of dimensional stability, the flexural strength and fracture behavior of SiC and glass-based parts were also examined. The purpose was to establish a means of placing the behavior of the materials in context of other polymers and polymer-matrix composites. The strength of metal infiltrated parts is discussed within the furnace processing section below. The brittle fracture behavior of the parts is illustrated in Figure 65.

Figure 65 Dimensional Stability Part – Illustrating Brittle Fracture

There are several comparisons to be made in Table 16 that put the polymer infiltrated material into an appropriate context. First, the strength and flexural modulus are both increased with the addition of fiber reinforcement in Nylon and ABS polymers. Next, SLS nylon is weaker than molded nylon, illustrating the material property trade-offs currently associated with SLS processing. Particulate reinforcement (with the same glass microspheres used in this project) increases the stiffness of the final material to a lesser extent than fiber reinforcement. Particulate reinforcement is not expected to yield significant advantages in flexural strength. Then, the strength and stiffness of epoxy may be compared to the infiltrated parts. There is a large increase in the stiffness (flexural modulus) similar to the fiber

reinforced nylon and ABS materials, but the strength increases only moderately. The strength of the infiltrated parts, however, is much higher than SLS processed nylon. Finally, there is a significant difference in part strength based on part orientation. In practice, this will establish different strengths in different regions of the part. The parts were prepared using a 15W laser with 0.005" spacing which is a slightly lower power density than the dimensional stability parts which were scanned with a 10W beam and 0.003" spacing. Still the directional density variation of the dimensional stability parts was 0.5% while the difference in strength seen in the two directions was roughly 15%. It is clear from the results that the epoxy provides the strength while the filler adds stiffness. The complete flexural strength data for the infiltrated parts may be found in Appendix 3.

Table 16 Flexural Strength Comparison

Material	Flexural Strength (Mpa)	Flexural Modulus (Mpa)	Source
ABS (Molded)	47.8-107	1606-5903	www.matweb.com
ABS (40% Carbon Fiber Filled)	152-173	15200-15900	
Nylon-12	14-60	260-1600	
Nylon-12 (30% Glass Fiber Filled)	134-160	4000-6900	
Nylon-12 (Duraform, SLS Processed)	~5-10	1290	
Nylon-12 (Glass Filled/ SLS Procs.)	-	3300	
Epoxy (System Three Clear Coat)	82.7	2590	www.systemthree.com
Epoxy (BJB TC-1622 A/B)	86.9	2620	www.bjbenterprises.com
SiC Base (Soft cure/ X-direction)	74.8	-	-
Glass Base (Full Cure/ X-direction)	64.2	16900	-
SiC Base (Full Cure/ X-direction)	105.4	11100	-
SiC Base (Full Cure/ Y-direction)	89.4	11400	-

The fracture faces of SiC and glass parts were observed after 3-point bend testing. Figure 66 and Figure 67 show SiC particles embedded in a BJB epoxy matrix. Figure 68 and Figure 69 offer similar views of glass microspheres in the

same matrix. The glass part shows a higher incidence of porosity than the SiC part. Features of brittle fracture are visible on the surface of the epoxy in the higher magnification views (Figure 67 and Figure 69). The effect of different particle shapes or significantly different adhesion between the epoxy and the two base materials is not seen in these images.

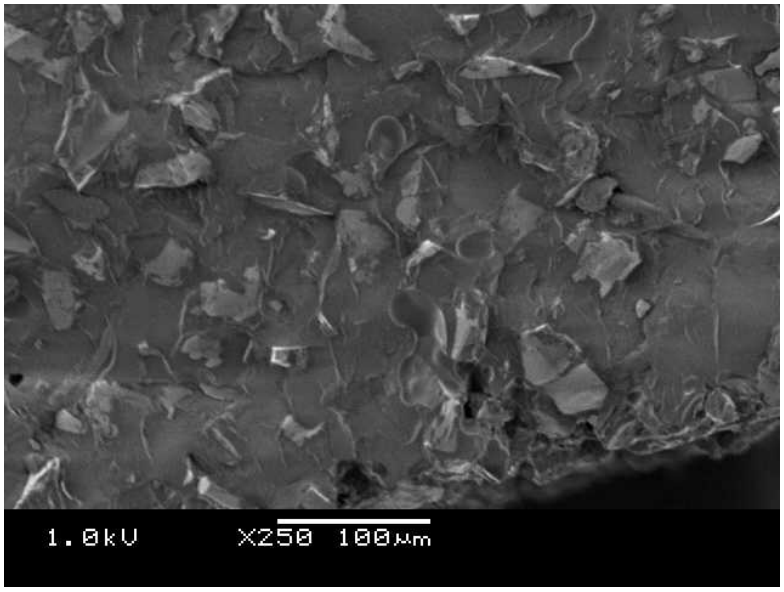

Figure 66 Fracture Face of Epoxy Infiltrated SiC

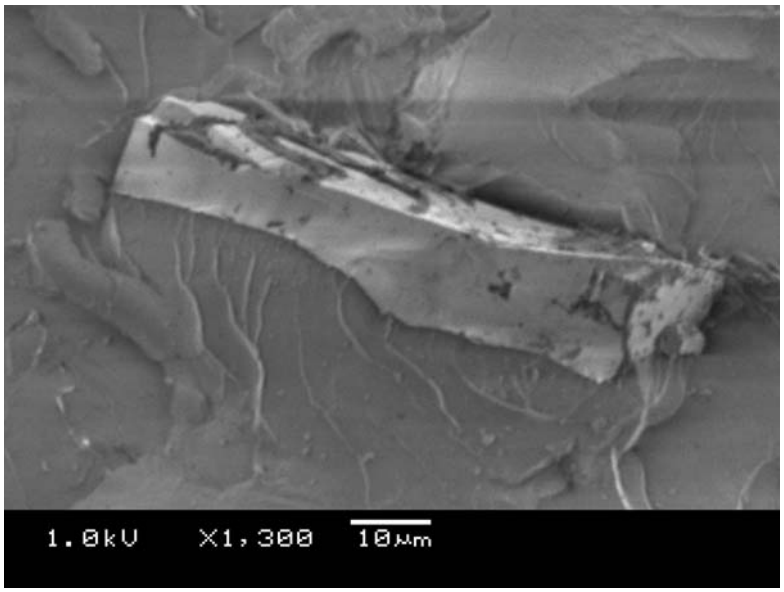

Figure 67 SiC Particle Embedded in Epoxy (Fracture Face)

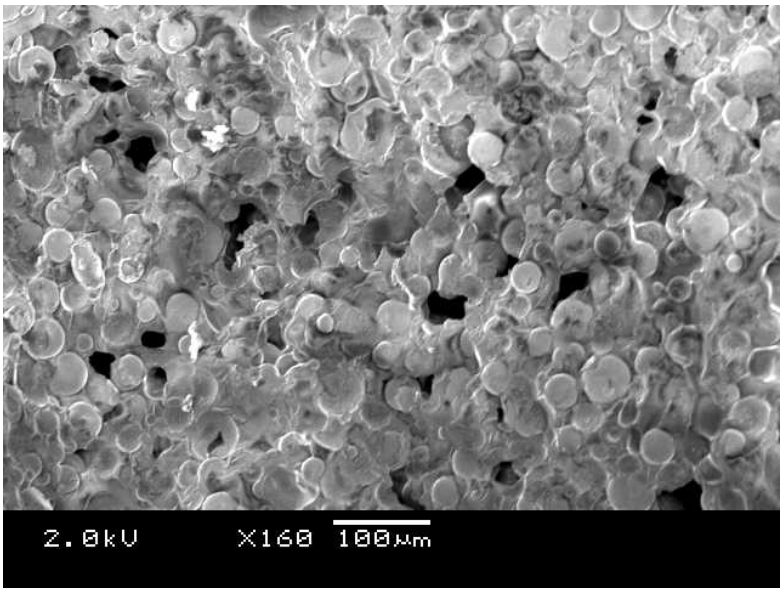

Figure 68 Fracture Face of Epoxy Infiltrated Phenolic-Glass

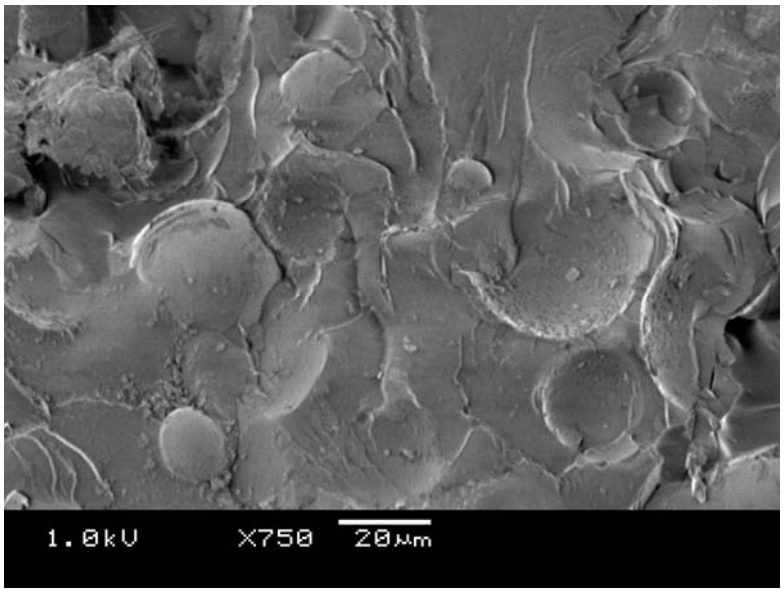

Figure 69 Glass Beads and Cavities (Fracture Face)

4.3.5 Part Analysis by Potential Customers

There are four main advantages to the epoxy infiltrated parts over nylon-12 (the most prevalent SLS material); better strength, smoother sanded surface finish, higher maximum temperature and lower material cost. Still, the actual value of the material must be measured in terms of its desirability for use in certain applications. As an example, the ventilation ducting for the Boeing F/A-18 (E and

F models) is made using SLS technology. The key material parameter for this particular application is elongation and there is far less concern for cost, strength or use temperature. During the course of the research several parts were made to get feedback in terms of potential applications for the epoxy infiltrated SLS parts. In addition, the polymer infiltration process itself was assessed by current SLS industry experts. Both of these feedback channels helped to assess indirect SLS as a manufacturing method. The parts included both research parts as well as parts made specifically for certain applications. Almost all parts shown to potential customers were formed from SiC-base material. In addition, this effort helped incorporate the opinion of SLS experts and end users into the analysis of these materials and recommendations for future work.

Some of the parts used to show the features of the infiltrated SiC parts may be seen in Figure 70. The cylindrical part is a pump seal while the right-most part was used for testing the flex strength of silicon infiltrated parts. The pump seal part was finished on all surfaces with 400 grit sandpaper to illustrate the surface quality possible with this material.

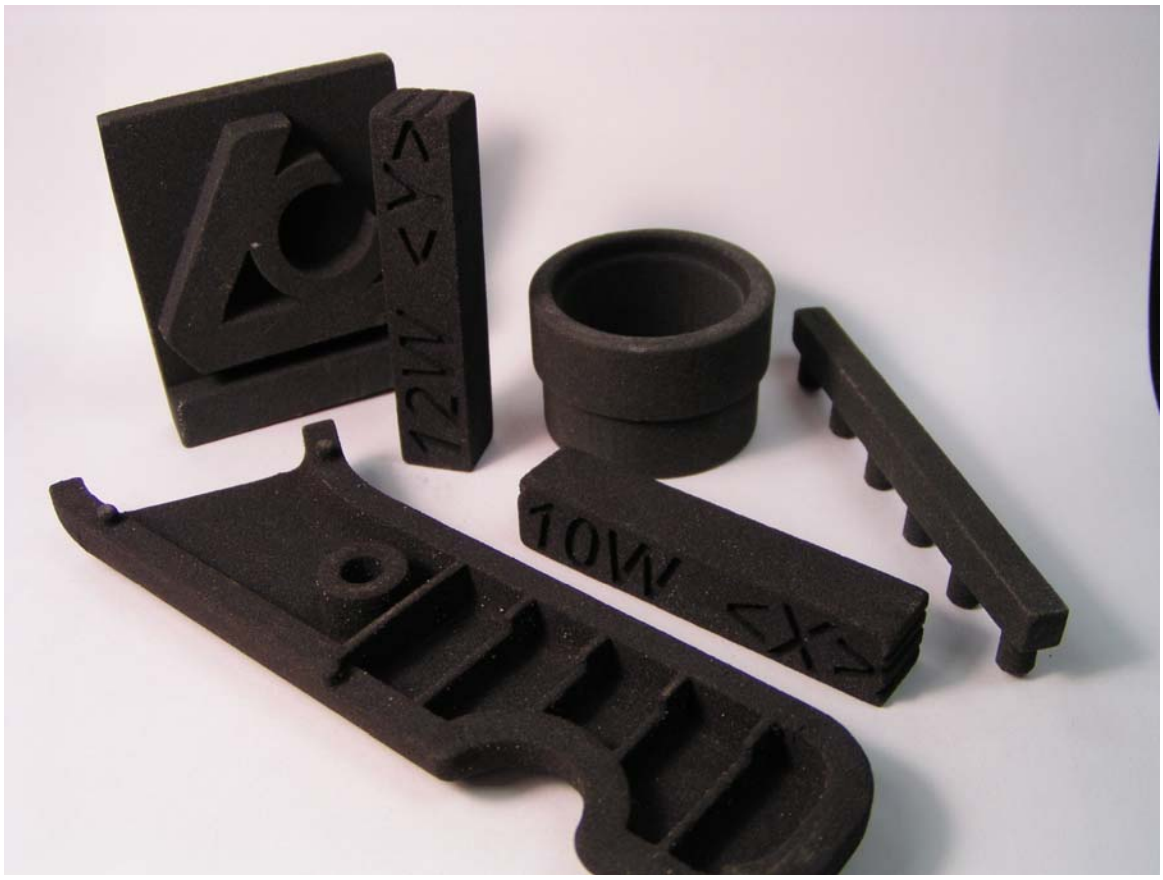

Figure 70 Various Epoxy Infiltrated SiC parts (lettered beams are 2.5" in length)

Other parts were built from customer supplied CAD files. Figure 71, shows a solder mask prepared for a customer of 3D Systems, Inc. The part shown is used to cover a circuit board during a soldering process so that only certain regions are exposed to molten solder. The side shown goes against the circuit board. The feature detail was appropriate for the application but the unsanded surface finish was too rough. In addition the overall flatness of the part was not accurate enough for immediate use (although additional work could correct this). The use temperature of the epoxy was also adequate, but the relatively high thermal conductivity from the SiC would cause too much heat transfer to the covered areas of the circuit board. A part with glass, alumina, phenolic microspheres, or another low-conductivity base material would be more appropriate for this application.

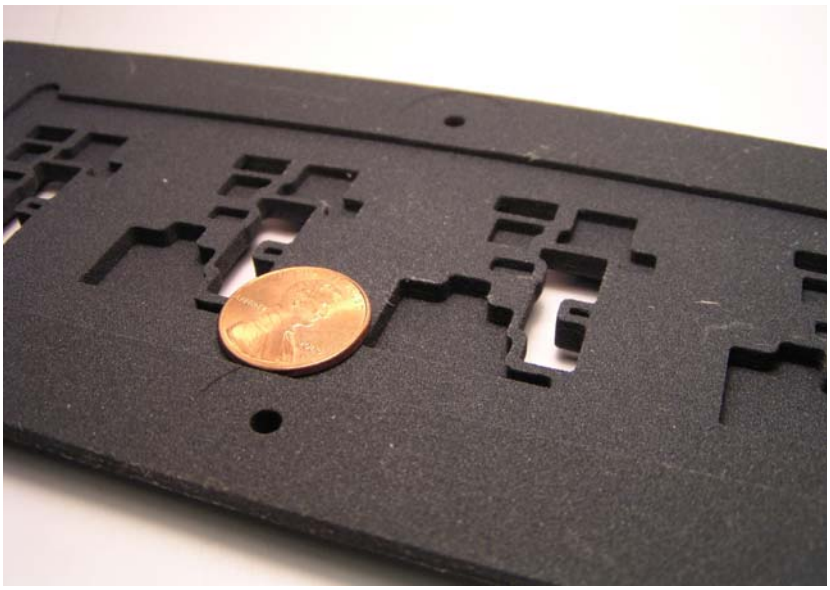

Figure 71 Epoxy Infiltrated Solder Mask

Figure 72 shows two other files that were made and infiltrated. The angled stamp was a part prepared for Lockheed Martin. The brittleness of the material did not work well with the requirements of a hand tool, but the surface finish on the handle was an advantage over the injection-molded version. In addition the critical surface of the stamp itself was easily sanded to an appropriate smoothness. The critical detail and dimensional tolerances of the blower impeller made it a challenging part to build, and the SiC base material was too dense for a typical blower application. It was also difficult to ensure that the part was dynamically balanced. The parts were sent to the appropriate companies and were not photographed prior to being sent.

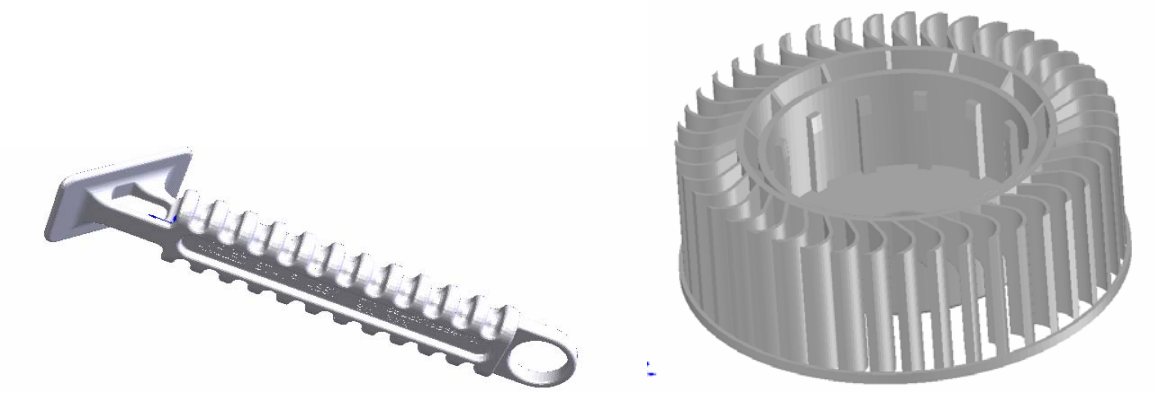

Figure 72 4" Angled Stamp (L) and 3"OD Blower Impeller (R)

Finally, the infiltration process for some of the example parts was performed at Harvest Technologies, Inc. of Belton Texas. Experts in their current SLS post processing operation were able to observe the infiltration and provide an important perspective on the viability of polymer infiltration in terms of current industry practice. The Castform material is dipped in red wax while the Somos flexible resin is vacuum soaked in polyurethane. The dip and vacuum infiltration used during this project was very similar. The handling of the epoxy was similar to the polyurethane. There were no potential problems indicated with regard to implementing higher function polymer infiltration into current industry practice.

4.3.6 Furnace Processing

Tube Furnace Testing

The work with the tube furnace shed light on three main areas. First, oxygen contamination is difficult to remove without a good seal at either end of the furnace tube. Even very high flow rates (emptying a T-size high pressure bottle in 6 hours) cannot make up for an imperfect seal. Even small amounts of oxygen remove measurable amounts of carbon. Before a specialized seal was placed on both ends of the tube the best char yield was 30%. Afterwards, char yields rose to 45-55%. Second, a single layer scan part was carbonized and then examined

using an SEM. Figure 73, shows a carbon structure bridging two SiC particles. The lattice structure is likely due to bubble formation during the scanning process. The smooth outer surface of this structure is an easily observed trait of phenolic and phenolic char in SEM images.

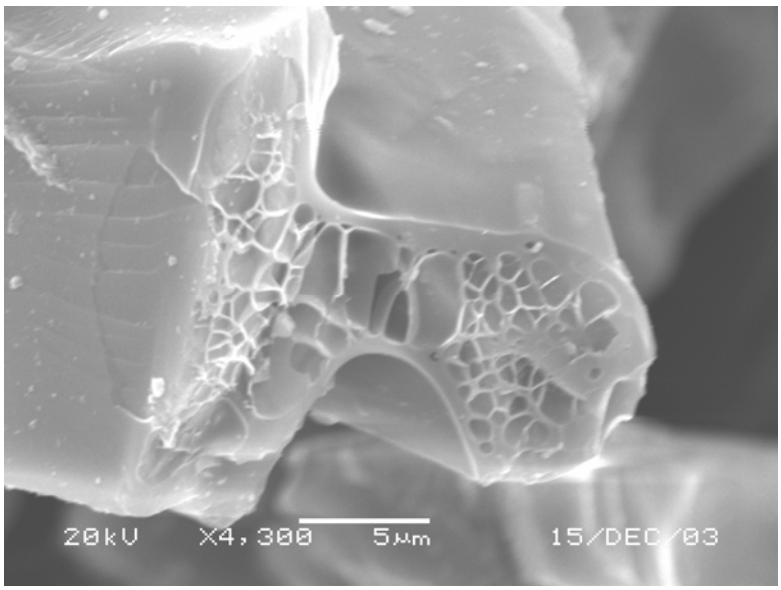

Figure 73 Carbon Structure Between SiC Particles

Third, a portion of the all phenolic part was also carbonized. The shrinkage can be seen by comparing the phenolic to the carbonized part in Figure 74. The effect of outgassing is clear and as seen in Figure 75, the carbon features are similar to those seen in Figure 73. The width of the phenolic part that came out of the 0.500" mold (at the bottom of the figure) was 0.461". The carbonized part had a width of 0.393". Some shrinkage occurs after the expansion due to outgassing. The carbonization process involved an additional 15% shrinkage. This is roughly appropriate since Ko, et al. (2001) observed a 22% volume reduction going to 1000°C instead of the 700°C temperature reached in the tube furnace.

Figure 74 Raw and Carbonized Phenolic (Illustrating Outgassing and Shrinkage)

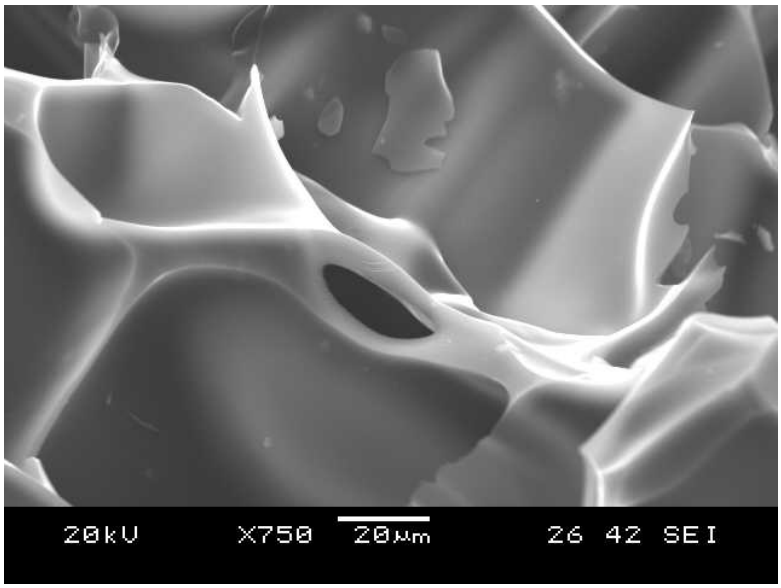

Figure 75 Carbonized Phenolic

The brown strength observed in previous research, Wang, (1999), was observed to be noticeably higher than the green strength. The strength observed

in brown parts made using the tube furnace was approximately equal to the green strength. This was expected as glassy carbon does not carbonize (or form stronger interconnected glassy carbon) until about 1100°C.

Graphite Furnace Cooling Cycle

The natural cooling cycle of the furnace (again loaded with parts for infiltration) is shown in Figure 76. The cooling follows an exponential model after about 30minutes. This graph represents an unavoidable step in the infiltration heating cycle. In terms of silicon infiltration it takes 15 minutes for the furnace to cool from 1600°C to the recrystalization point of 1420°C.

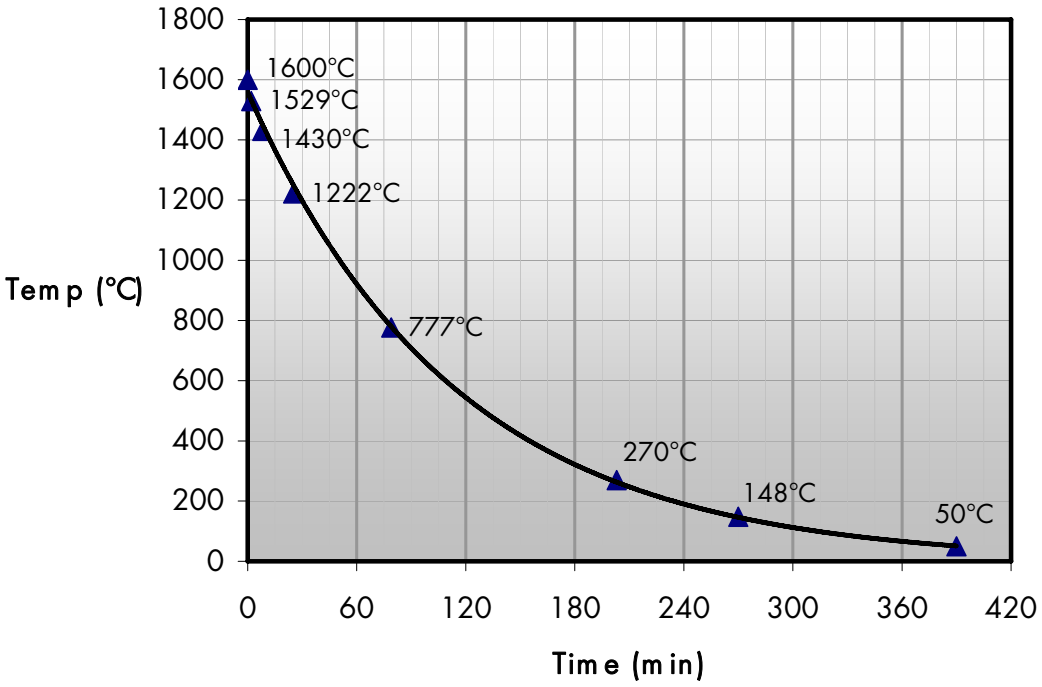

Figure 76 Furnace Cooling Cycle

Brown Parts (Polymer Decomposition)

One furnace run to 1100°C was run to examine brown parts formed in the graphite furnace. Epoxy infiltrated and green parts were examined. Parts tested from the initial test showed a 53% char yield for phenolic and an 8.5% yield for

DCPD. Epoxy was not assessed for char yield, but is known to have a yield below 10%. Figure 77 shows cracked carbon attaching several SiC particles. Both the shrinkage of the carbon and the value of particle to particle contact are visible. On the whole the surfaces of the SiC particles were visible and the carbon was intermittent. An infiltrated part on the other hand shows more widespread carbon, as seen in Figure 78. Thin carbon structures wind across the surface of several adjacent SiC particles. It also appears that the surface features of the SiC have been smoothed over, possibly with a thin, conformal layer of carbon.

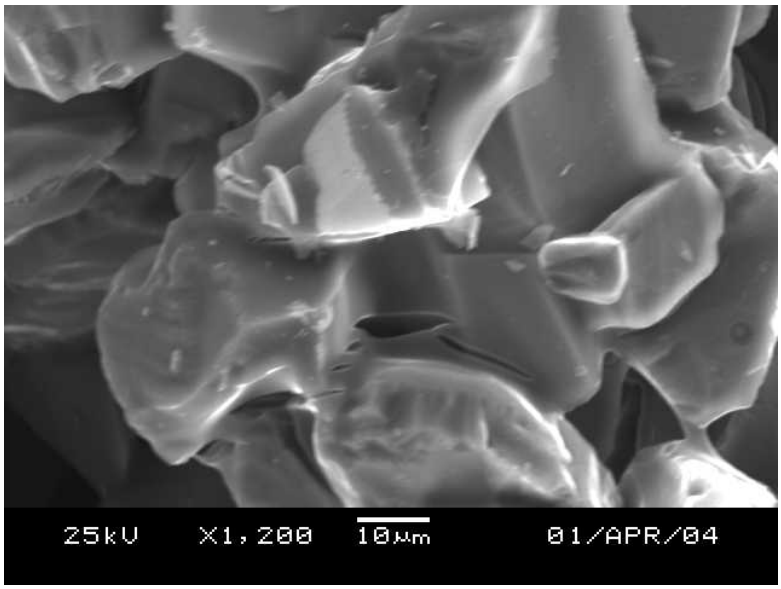

Figure 77 Brown Part Surface Showing Cracked Carbon Features

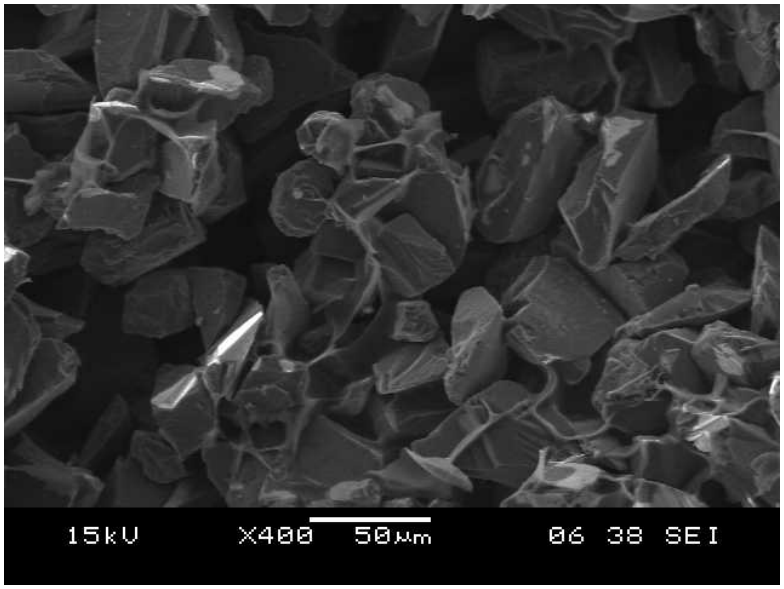

Figure 78 Widespread Carbon Coating Brown Part Particles (from epoxy infil)

Temperature Cycle Development and Infiltration

The temperature cycle for the furnace was developed to support three phases; phenolic curing, polymer decomposition and silicon infiltration. Slower initial ramps such as going from ambient to 140°C in 3 hours offered small improvements over more rapid ramps for green parts. Fewer of the thin walls and cylinders on the breakout parts tended to bend with slower ramps. With epoxy infiltrated parts, on the other hand, 30minute ramps in the same temperature range showed no slumping. The transition region between curing and decomposition at 300°C was spanned rapidly in all cases.

The 30°C/hr recommended by Choe and Lee, (1992) gave a 6:40 time for the ramp from 3-500°C. However this recommendation was for solid phenolic. For green parts and for polymers with lower char yields, the porosity and lack of solid barriers to outgassing would allow for faster ramps. This ramp was reduced to 2 hours with no effect observed in component deformation. Choe and Lee also only recommended ramps of 100°C/hour up to 1100°C to allow the carbon to form a higher strength structure. This was initially followed, but again shortening

this from 6 to 2 hours did not have a noticeable effect on the amount of slumping observed in the parts. Changing the overall decomposition cycle from the recommended 12:40 to the later 4:00 version actually increased the strength of brown parts significantly (based on qualitative observations only).

Since SiC formation is relatively rapid at interfaces of liquid silicon and carbon the time above the melt was kept low. Another consideration was that molten metal has a lower viscosity at higher temperatures – and thus more rapid infiltration. Finally, if the carbon is simply dissolved by the silicon then the part could slump as it would become a slurry of molten silicon and SiC. Ramps that waited at 1400°C, just below the melt point of silicon, before going to 1600°C did not show any obvious differences compared to those that simply went from 1100 to1600°C (usually in 30minutes). However the prevalence of gas-phase formation of SiC, discussed below would favor 1400°C holds. It was unclear if ramping to 1600°C with a 15minute hold or ramping to 1650°C with no hold was a better strategy.

Parts tended to have regions falling into 4 categories; 1) un-infiltrated (dark grey), 2) lightly infiltrated (light grey, not shiny), 3) fully infiltrated (shiny surface with roughness from SiC particles) and 4) overfilled (smooth silicon surface). In some cases there were also regions that had darker crystal-like regions within the over-infiltrated areas. These tended to form on downward facing areas of parts and were more prevalent when the infiltration happened with the parts oriented horizontally. The first three regions may be seen in the part shown in Figure 79.

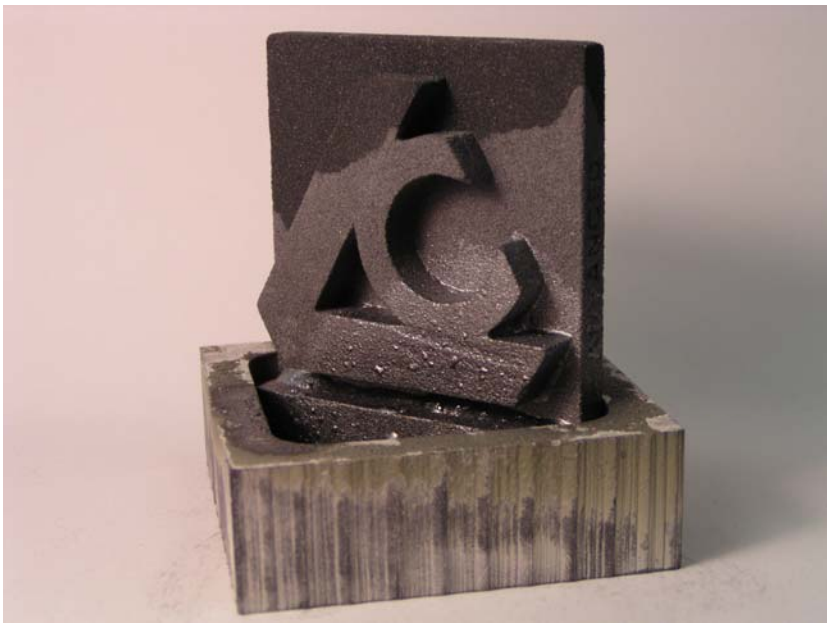

Figure 79 Partially Infiltrated Part (crucible BN coated)

The silicon infiltration front became visible when partially infiltrated parts were bead blasted. Figure 80 illustrates the structure of the infiltration front within the part. The surface of the silicon has a characteristic roughness and there is a thin seam at the interface of the Si and the SiC. The surface of the lightly infiltrated region, shown in Figure 81, shows both silicon and SiC at the surface of the part. The silicon exists as smooth regions between the SiC particles in contrast to the silicon seen at the infiltration front. There was no evidence of choked flow from SiC formation. The large round chipped region on the surface of the SiC particle on the right side of the image is discussed in terms of SiC formation below. On the surface of the silicon there are lighter-colored feather-shaped regions that seem to have a similar shape to the grooves seen in the infiltration front, although they are more localized. A closer image of this type of structure may be found in Figure 82. These tended to grow from the center of a large region of silicon or from the edges of SiC particles. The actual material comprising these formations is unknown.

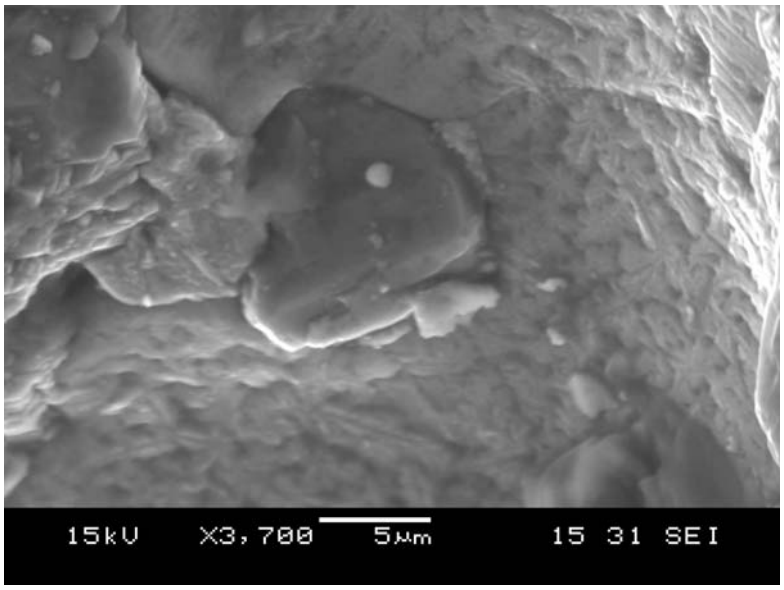

Figure 80 Si Infiltration Front with SiC Particle

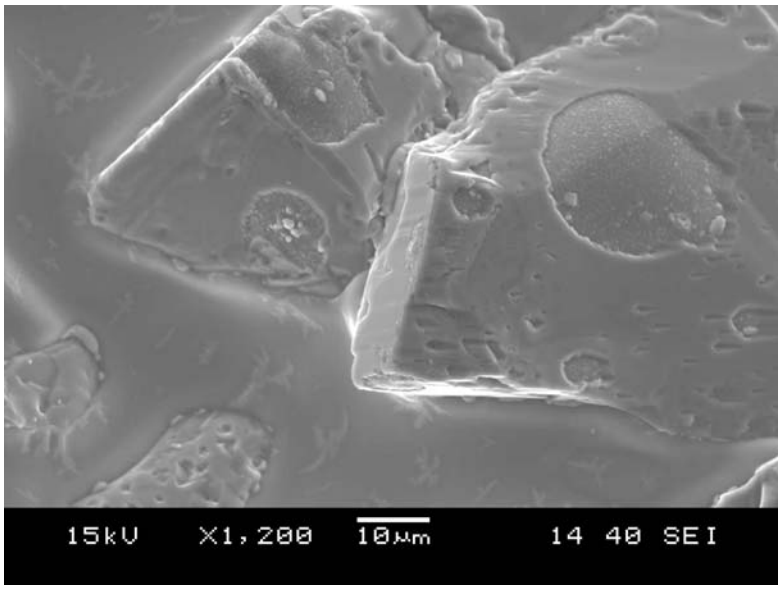

Figure 81 No Luster Surface of Si Infiltrated Part

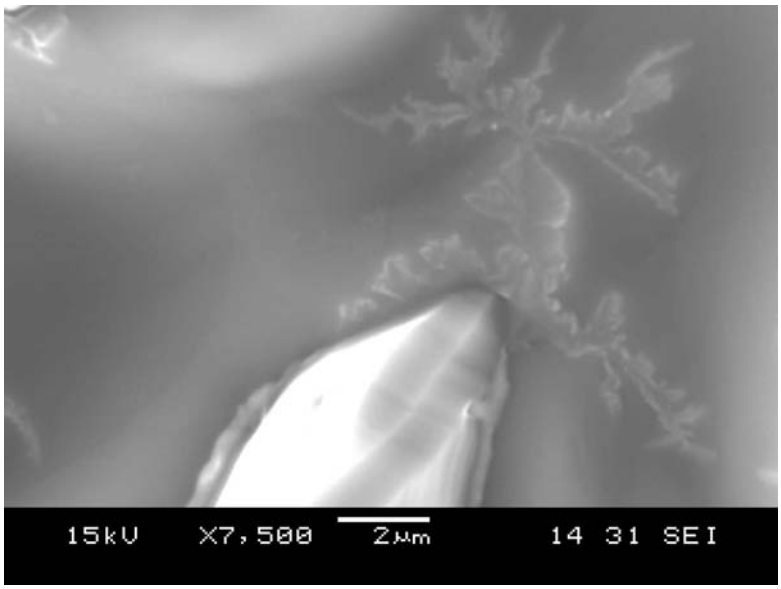

Figure 82 SiC Particle (white) With Si Surface Pattern

The part in Figure 83, shows both fully and over infiltrated regions. The over-infiltration tended to occur at corners and toward the center of parts. This indicates a likely dependence on both heat transfer and fluid wicking. There seems to be a strong surface force between molten silicon and silicon – which may provide the force necessary to draw the silicon to fill large cavities external grooves in the parts. In some cases over-infiltration was much more widespread. In many breakout parts silicon filled the cavities between the thin walls across the entire part. The shiny regions of fully infiltrated parts have a different appearance in an SEM, which is shown in Figure 84. In this image, the large darker regions are silicon crystals. The type of material comprising the more irregular interstitial regions is not known. It may be a more amorphous form of silicon or new SiC or a combination of the two.

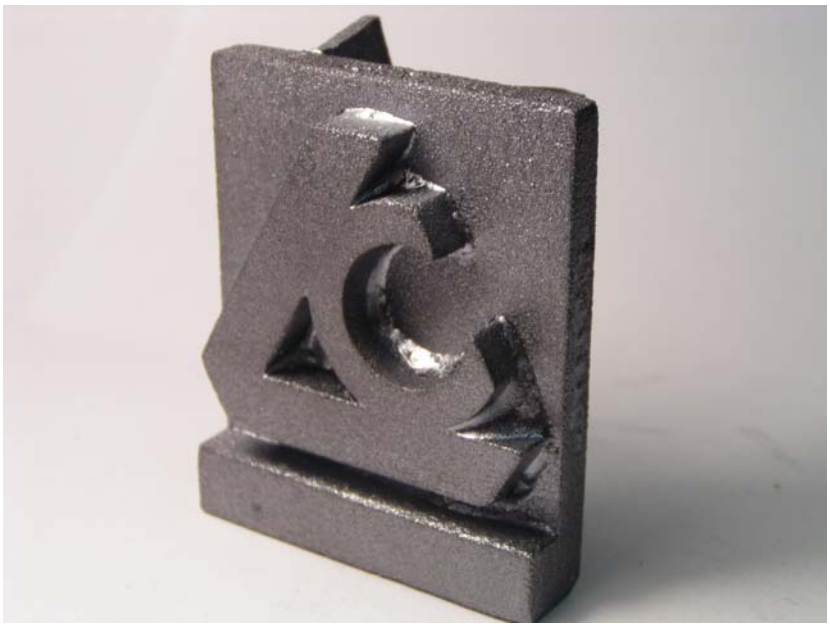

Figure 83 Shiny Silicon Infiltrated Part (RBSiC)

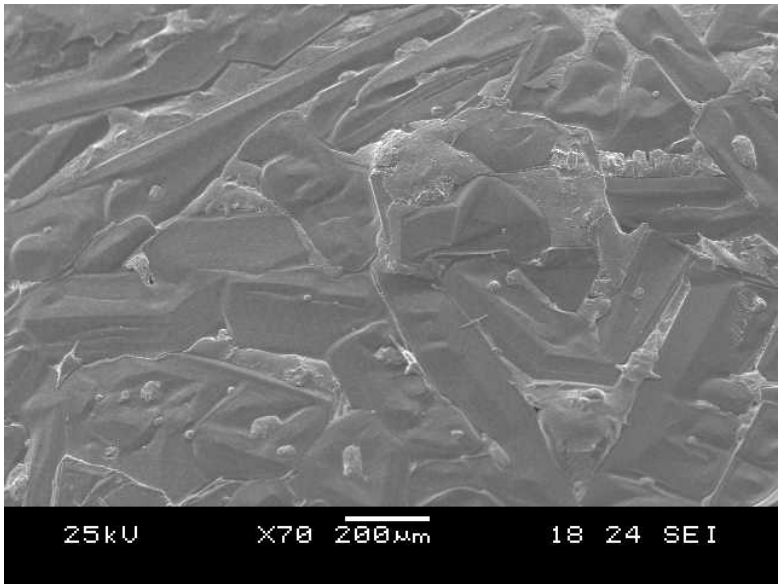

Figure 84 Shiny Surface of Si Infiltrated SiC Part (Note Feature Scale)

Infiltration Fixtures

Several different strategies were used to facilitate infiltration. 2.5″ graphite crucibles sprayed with Boron Nitride (BN) aerosol were used to support vertical infiltrations (Figure 85). The crucibles held the silicon for infiltration and the BN

prevented the silicon from wicking into the crucibles. More parts were prepared by supporting them on 1/8" bend test beams that were infiltrated at the same time. The beams were used to support the parts and enclose an area of a graphite plate, again covered with a thin layer of BN. Examples of parts prepared using this method may be found in Figure 83, Figure 87 and Figure 89.

Figure 85 Fully Infiltrated Part with Slumped Features

Slumping During Furnace Processing

The most difficult problem encountered is part slumping. Over several experiments and from several literature sources four sources of slumping were identified; 1) phenolic softening, 2) rapid phenolic decomposition, 3) oxygen depletion of structural carbon and 4) silicon dissolving the structural carbon without leaving structural SiC. Phenolic softening was observed as curved parts, like those seen in Figure 86 and Figure 87. This problem was almost completely mitigated by infiltrating epoxy into the green parts before furnace processing.

Figure 86 0.125 x 0.5 x 5″ Beam Showing Slumping

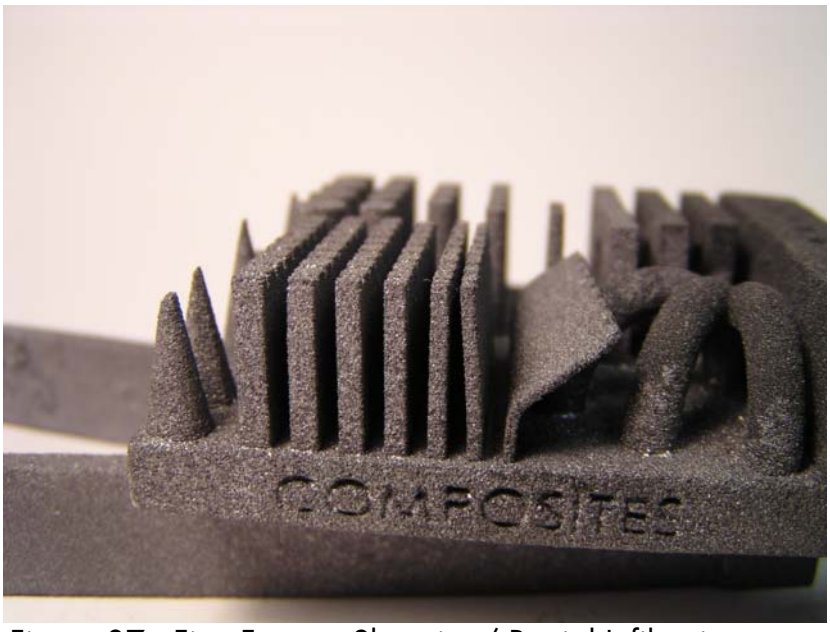

Figure 87 Fine Feature Slumping/ Partial Infiltration

Appropriate ramps prevented damage to the carbon structure from rapid polymer decomposition. The depletion of carbon either by oxygen contamination or silicon interaction were harder to diagnose. The broken features seen on the left side of Figure 88 and in Figure 89 did not show the same curving, but rather broke at the

point of maximum stress. The lack of curving indicated an effect that occurred after the phenolic had cured. The prevalence of this type of slumping was diminished by decreasing the ramp from 500-1100°C to 2 hours from 6. The use of higher purity Argon or 4% Hydrogen in Argon (the highest hydrogen concentration recommended by the furnace manufacturer) should decrease this effect further.

Figure 88 Lightly Infiltrated (L) and Uninfiltrated Slumped (R) Breakout Parts

Figure 89 Slumped/ Partially Infiltrated Part

SiC Growth

SiC growth was expected to be seen within the parts and also on the surface of the silicon. It was also found on the surface of SiC particles not directly exposed to silicon and not coated with carbon. This required both gas phase silicon and gas phase carbon sources to be present within the furnace. It is likely that all of the SiC formation reactions listed in Figure 49 are occurring within the furnace. Figure 90 is a comparison between raw SiC particles and those found in un-infiltrated "brown" parts. What appear to be chipped regions on the right-hand image are not seen on raw SiC particles, nor is the surface texture within those regions. Figure 91 shows additional features of un-infiltrated parts. The "chipped" regions are visible again. The same roughness within these regions is also visible on the linkage between two SiC particles at the upper left-hand side of the image (formed from phenolic char). The linkages between particles consisting of phenolic and carbon char shown in previous images were smooth.

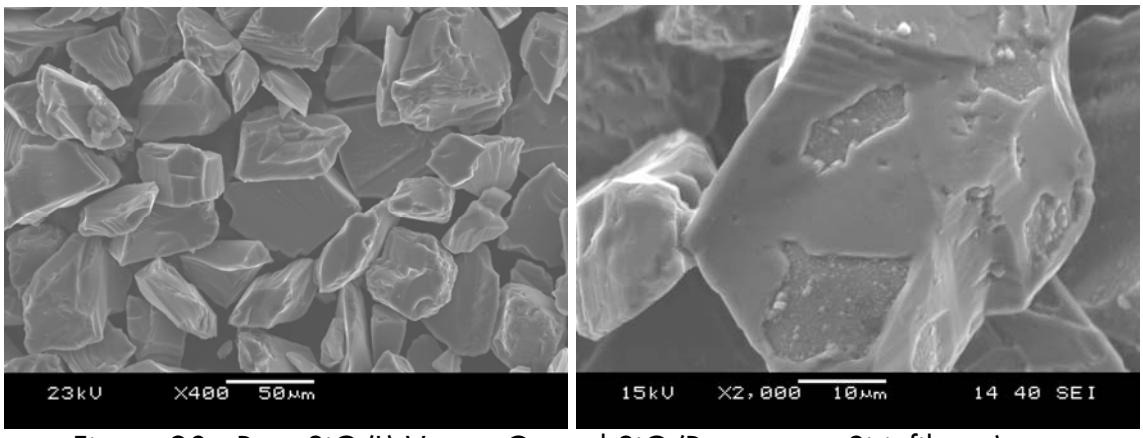

Figure 90 Raw SiC (L) Versus Coated SiC (R, not near Si infiltrant)

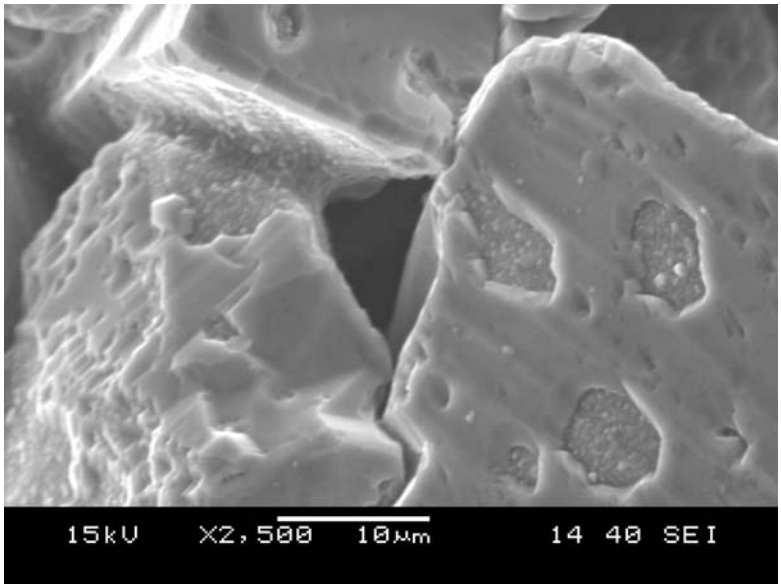

Figure 91 Coated Particles from Uninfiltrated Part

The graphite crucibles that came into direct contact with molten silicon cracked, as shown in Figure 92. This was an indicator that SiC had formed within the crucible causing localized expansion. Even the microstructure of crucibles not touched by silicon was changed during furnace processing, which is clear from Figure 93. The SiC crystals in the right-hand image are very different from the structure seen in the left image of an unheated crucible. This observation further supports the prevalence of gas-phase reactions forming SiC during the furnace processing, and not other materials such as SiO_2. Another factor is that SiO_2 has a much lower

surface energy (310mN/m) than SiC (3800mN/m) which does not promote spontaneous infiltration. The infiltration microstructure would be visibly different with the presence of SiO_2. Unfortunately the cause of the rough surface of the linkage between two particles (seen in Figure 91) remains unclear.

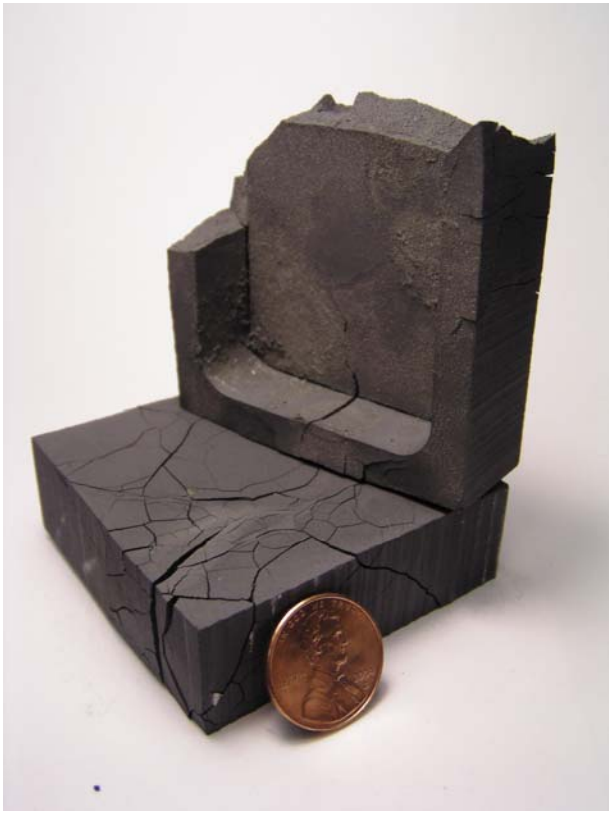

Figure 92 Crucibles Cracked During Si Infiltration

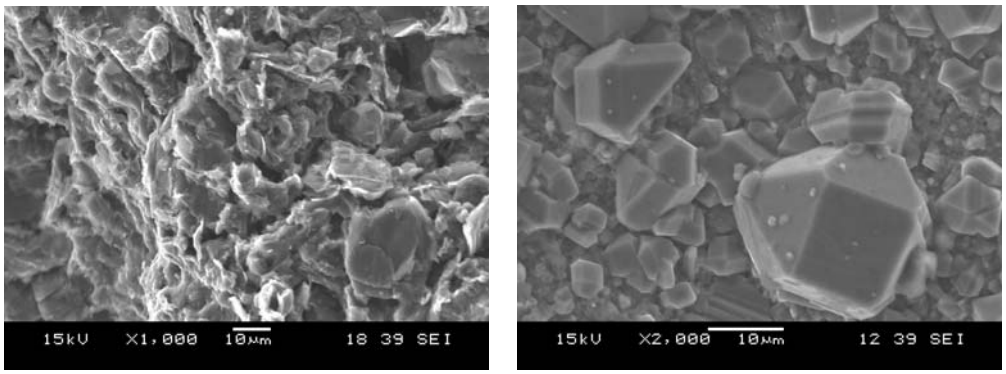

Figure 93 Graphite Crucible Before (L) and After (R) Heating In Presence of Si

The formations on the surface of silicon, as seen in Figure 82 above and Figure 94 below show SiC particles providing a possible seed for crystal formation. However these formations might be silicon alone and derived from the Marangoni effect (surface tension driven flow). Surface tension flow is due to temperature gradients along the surface of a liquid where fluid is driven from higher to lower temperature regions. The Marangoni effect adds the influence of upwelling to surface tension driven flow. Upwelling replaces fluid driven away by surface tension and also maintains a higher surface temperature. It is expected that this occurs near heat sources or at the center of metal regions, which were both observed. SiC formation is exothermic and the combination of gas-phase source with the Marangoni effect could be responsible for the surface growth of SiC observed by Favre, et al. (2003). Hibiya, et al. (2003), found that the melt transport of oxygen was more dependent on surface tension flow than on diffusion. They further found that thermocapillary (from ΔT at crucible walls), solutocapillary (from oxygen concentration gradients), surface tension flow and buoyancy were nonlinearly coupled with molten silicon. The final element of interest was their finding that even oxygen at 10ppm in the evacuated atmosphere led to a 10% oxygen concentration at the surface of the silicon melt. Together the findings of Hibiya et al. (2003) in conjunction with observations made during the research show a very complex infiltration process that is extremely sensitive to atmospheric conditions. High reliability silicon infiltration would require extremely high purity process gases and lengthy purge cycles in the furnace. One early question was whether the gas-phase formation of SiC or the liquid infiltration would allow structural SiC to form between particles. Figure 95 is a cross section of an infiltrated part viewed with an optical microscope. The widespread dark features are SiC indicating significant formation of new SiC. There are several regions

where small SiC particles are clustered between larger regions from original SiC. Starting from the lower left-hand corner of the image it is possible to trace connected SiC to the top of the image – a distance of greater than 200μ. Other particles seem to have bridges of SiC between them as well. Structural, interconnected SiC growth seems prevalent in this image.

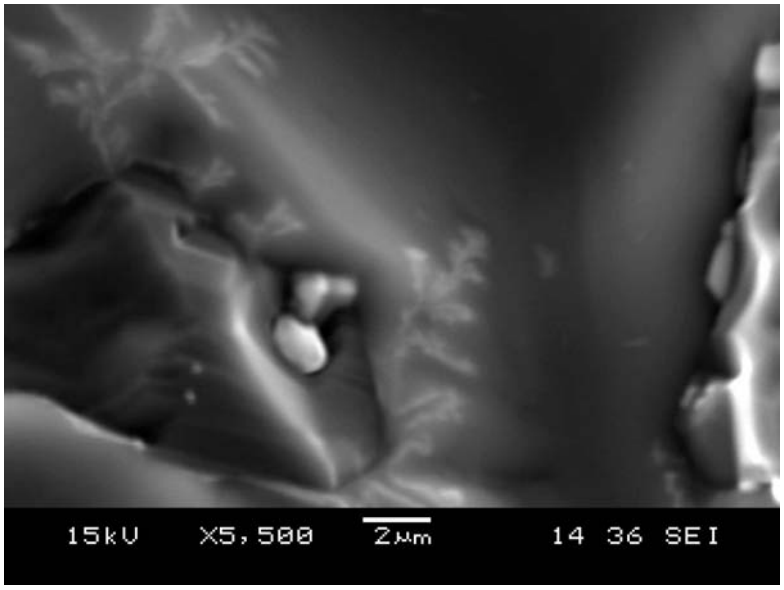

Figure 94 SiC particle in Si Showing Crystal Growth

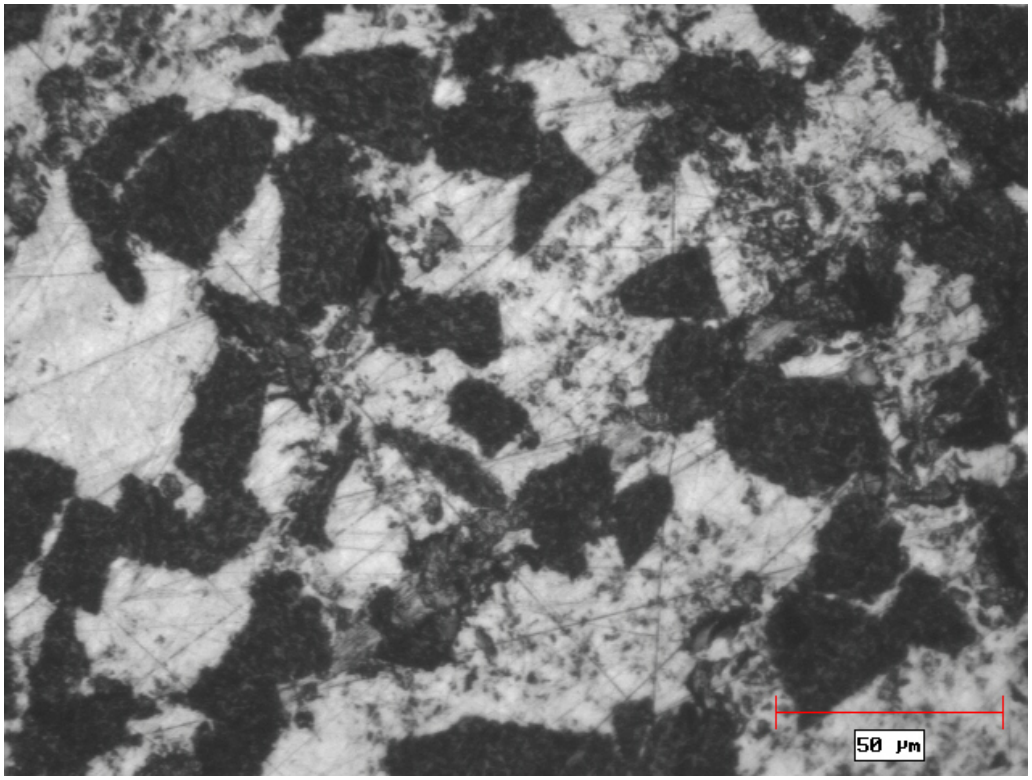

Figure 95 Cross-Section of Si Infiltrated SiC Part (courtesy D. Bourell and S. Barrow)

The flexural strength of infiltrated parts is shown in Table 17 . The most striking feature is the lower final strength of the epoxy infiltrated parts. If the epoxy tended to leave a layer of carbon on the surface of the SiC particles, the formation of new SiC might be prevented from having widespread direct contact with the surface of the SiC particles – causing a lower strength. With a carbon coating the gas-phase growth of SiC would be disconnected from the original SiC particles as well. Both strength measurements are well within the range 40-450MPa range found in literature. The prevalence of SiC interconnects is a significant factor here.

Table 17 RBSiC Flex Data (Courtesy of D. Bourell & S. Barrow)

Part Description	#	Flex Strength (Mpa)	Average	Std. Dev.
RBSiC w/ Epoxy Infiltration	e1	140.03	147.26	14.06
	e2	140.67		
	e3	172.36		
	e4	140.76		
	e5	142.47		
RBSiC w/o Polymer Infiltration	n3	170.99	163.60	12.93
	n4	144.28		
	n5	168.52		
	n8	170.62		
Brown Part	b1	3.35	3.70	0.55
	b2	4.52		
	b3	3.49		
	b4	3.42		

Alternate Infiltrants

As expected, iron beaded up on the surface of the SiC as seen in Figure 96. Upon cooling the iron crushed the lower end of the part causing the break visible at the part/ iron boundary. A large bead of iron chipped from the floor of the furnace is seen in the foreground of the image. The tests with bronze were also not successful. The weight of the bronze stacked atop the parts was not enough to drive infiltration.

Figure 96 Ductile Iron Infiltration (With Iron Bead from Furnace Wall)

In the end there are two problems that were not solved during the experimentation. The first is the issue of over-infiltration. In one run of the furnace two parts were connected by the same 1/8″ beam. One was partially infiltrated while the other was over infiltrated. It was hoped that parts would equalize in such a case. Instead the appropriate amount of silicon must be in proximity with each part. In addition, longer ramps and soaks near the melt point of silicon tended to increase the number of parts that were partially infiltrated. Silicon was being depleted by sublimation or gas phase reactions. The correspondence between temperature cycle, gas phase reactions and the appropriate amount of

silicon to just fill the part, has not been not established. The other problem is the lack of characterization of the gas phase reactions that occur within the vacuum furnace at high temperatures. Several effects of these reactions were observed and included carbon depletion, silicon depletion and SiC formation effects. A capability for analyzing the output from the furnace box during processing would be necessary to do this effectively.

4.4 Discussion

4.4.1 High-Function Polymer Infiltration of SLS Preforms

Polymer infiltration is an effective means of creating fully dense parts with characteristics not currently achievable through direct SLS. While the raw surface finish is similar to current SLS practice, the polymer infiltrant allows a finer surface finish. The added processing time per part is not significant compared to the part finishing that is common to current commercial SLS materials. The actual costs associated with this process are compared to current SLS methods in the following chapter. The advantages in part strength and maximum use temperature may be very useful for certain applications. One possible example would be for under-the-hood applications requiring 200°C continuous use temperatures.

The importance of the key parameters shown in Figure 50 has been explored. Since all polymer infiltrants tested readily infiltrated both glass and SiC base parts, the most important parameter for wicking is low viscosity. The largest effect of low viscosity is faster and easier cleanup prior to curing. A low enough viscosity negated the need for vacuum assisted infiltration and allowed for much more rapid infiltration. This coupled with an appropriate curing cycle that supported the phenolic and limited outgassing made for several different successful

material combinations. The dimensional stability of the process and flexural strength were also characterized.

Additional work would be necessary to limit the directional variation of strength and density. The most promising infiltrant tested, DCPD, would require additional testing especially with a compound having a longer pot-life. While flexural strength does help characterize the material, additional tests are needed to facilitate the identification of applications and the optimization of the process to meet those applications. These tests would include determining tensile and impact strength along with heat deflection temperatures.

The materials tested are certainly not the only ones available. Polyurethane, as an example, might provide better performance for applications requiring greater toughness. The more obvious avenue for further work lies in additional base materials. Hollow phenolic spheres (sold under the name Phenoset), as an example, would yield a low density green part. Silicone microspheres, with an appropriate binder might allow for parts with higher elongation.

4.4.2 Intermediate Machining

A fine surface is possible on the epoxy, but with the decomposition of the epoxy this surface is lost. Intermediate machining did seem to be an appropriate method for improving dimensional accuracy, but not for improving final surface roughness. The particles limited the smoothness available at an intermediate phase. The additional penalty of infiltrated part strength seems to indicate that intermediate machining does not offer significant advantages. The per-part costs associated with high accuracy machining also limit the potential. The full effect of this type of processing would need additional examination of various MMC's before the concept is abandoned, however.

4.4.3 RBSiC Composites

While structural SiC was formed during the furnace cycle, the formation seems to be more related to gas-phase reactions than to infiltration of silicon. The chemical makeup of the material formed in place of the structural carbon remains uncertain, but is most likely SiC. This eliminates one of the sources of slumping as the SiC can be formed before molten silicon infiltrated the parts. This finding also boosts the potential for free-standing infiltration. The combination of managing the infiltration and the gas-phase reactions would require additional research. Many of the key issues influencing free-standing infiltration have been identified, but consistent full infiltration has not been achieved during the current research project. With reference to the goals described in the opening section of the chapter, free-standing infiltration is possible, but not yet at high accuracy. The reliability of the infiltration was not established to a degree that would have facilitated a dimensional analysis like that completed for polymer infiltrants.

One direction for future work would be to increase the carbon content of the preforms with infiltration of liquid resole phenolic instead of epoxy. The additional carbon would increase the amount of SiC in the final part. Multiple infiltrations and burnouts are common in the formation of bulk SiC material and could be extended to a process preserving the original preform shape.

The other direction is to examine other reactive or non-reactive systems using higher-function matrix materials. One of the advantages of this process is that the reinforcing particles are held in place during infiltration – especially if a gaseous reaction changes the carbon into a more stable material before infiltration. There are infiltrant polymers, such as the family of polymers from KiON (www.kioncorp.com) that yield silica and SiC instead of carbon char during decomposition. These could provide additional benefits to this process. Titanium

could be wicked into the preforms forming TiC with the carbon and producing an interesting SiC, TiC, Ti composite with interconnected ceramic reinforcement. Aluminum could be wicked into preforms prepared using silica yielding (ceramic precursor) polymers, mitigating the undesirable formation of aluminum carbide.

4.4.4 Indirect SLS Rapid Manufacturing

For fully functional parts, the material must fit the application. Traditional manufacturing has evolved to encompass an immense number of different materials. The significance of Rapid Manufacturing will be measured in part by the variety of functional materials that can be processed. In the previous chapter a new family of materials has been explored for use in the SLS process. With the addition of polymer infiltration and free-standing metal infiltration there is a far greater body of materials that can be considered in terms of rapid manufacturing. More importantly the current work has been done within the constraints of standard industry equipment. Post processes did not mitigate the material issues driven by the SLS process itself, however. Additional research might explore the potential for having a limited number of base materials, binders and infiltrants reach a wide variety of different applications. Additional discussion about rapid manufacturing and the indirect process examined during this project may be found in the following chapter.

Chapter 5 Indirect Rapid Manufacturing

Indirect selective laser sintering has been advanced during this project as a platform capable of building parts from combinations of a variety of materials. Examples of base materials (SiC, glass and graphite), binders (Phenolic and other thermosets) and several infiltrants (polymers and silicon) have been explored and related to the concept of indirect SLS as a platform for the fabrication of a variety of material systems. In the first section of this chapter the main technical elements of the binder study and the work with infiltration from the previous two chapters are briefly reviewed. Within the technical scope of the project there are several immediate implications as well as clear avenues for further development. Since the thesis of the dissertation went a step further to address rapid manufacturing, the second section of the chapter broadens the scope of the discussion. Examining the current research in terms of manufacturing highlights the main issues related to the implementation of Indirect SLS in actual engineering practice. This is followed by a discussion about valuable future work. The last section of the chapter returns to the thesis proposed in Chapter 1 and concludes the dissertation.

5.1 The Indirect SLS Fabrication Platform

By combining the operations discussed in Chapter 3 with those reviewed in Chapter 4 an overall fabrication platform may be considered, as pictured in Figure 97. The solid arrows indicate the process that was described in Chapter 1, while the dotted arrows indicated alternate routes supported by research observations. On one hand intermediate machining has not been found to be as useful as expected. On the other hand favorable feedback from potential customers indicated that polymer matrix composites might find application as finished goods for certain applications. Using Figure 97 as a guide, the key achievements of the

current project may be reviewed. For each of the main technical areas the key contributions are reviewed followed by a discussion of the future work highlighted by the current project.

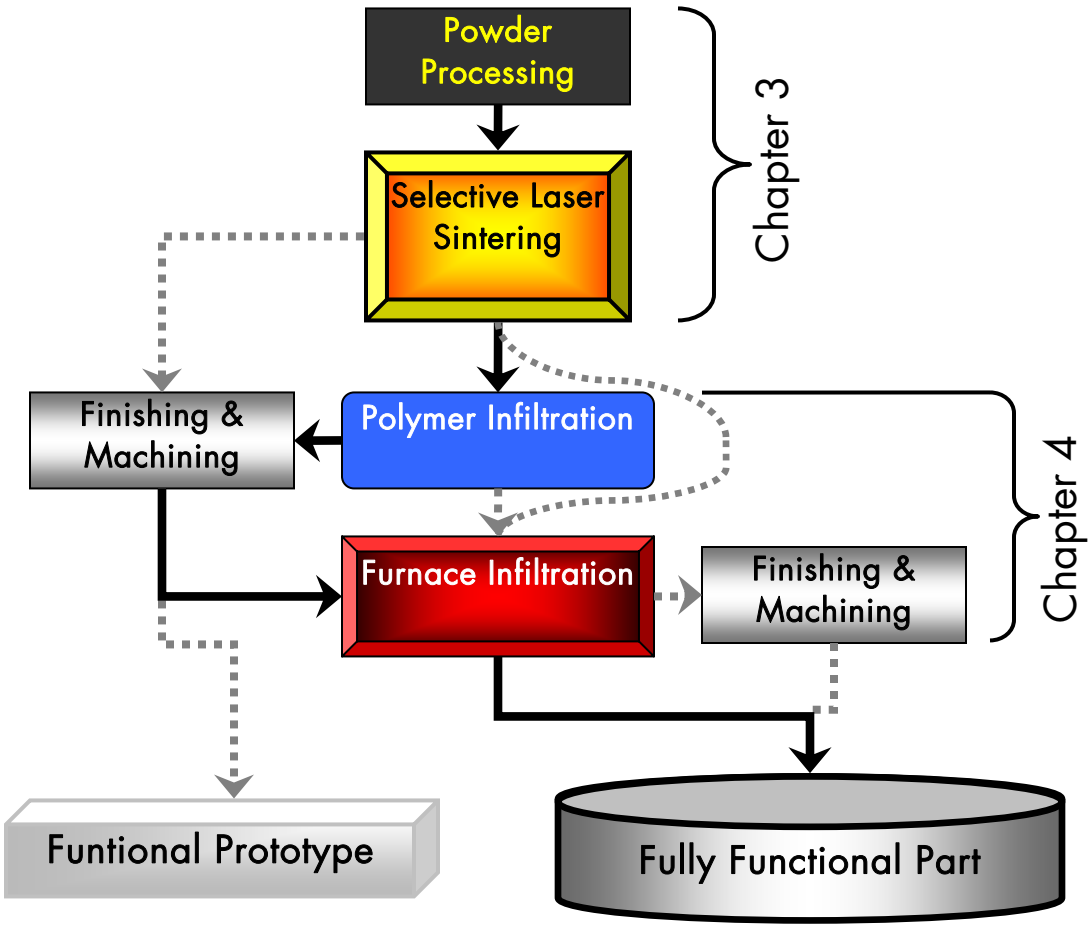

Figure 97 Indirect SLS Process Diagram

5.1.1 SLS Materials Development

Main Technical Contributions

The conventional wisdom from the SLS industry is that reasonably spherical particles ranging from about 20 to 80μm work well in the SLS machine. While this remains a reasonable baseline for lower density polymer powders, denser

materials and binder systems require additional considerations. The tap density of a particular mixture can be roughly correlated to suitability for SLS processing, but the settling and flow behavior of a powder mixture are more important. When two base powders have identical tap densities, the one with smoother, more spherical particles will provide a denser green part. The roller influences these two different powders differently and the binder tends to promote greater shrinkage in smoother particles. Binders are more effective as smaller particles that are well distributed throughout the mixture. The best case is where the binder particles effectively coat the surface of the base particles which establishes widespread adhesion and powder behavior is more like the larger particles (at appropriate binder percentages). When the binder particles are small enough they can occupy interstitial spaces and increase the density of the overall powder.

Within the SLS machine, heat transfer and polymer rheology are the central technical issues. As Choi and Chan (2003) mention, predicting "the effects of shrinkage and warping may require complex models of thermodynamics and binding forces, which are not yet available." While models of particle sintering have been developed, they have not been linked to a comprehensive model of the SLS process. In particular, the effect of adding multiple layers has not been incorporated into analytical models is that post-build curl cannot be considered. Extending the model to predict binder behavior would be an additional step.

The characteristics of current SLS technology provide another main set of considerations. Still, if an appropriate surface temperature can be estimated, the temperature profile within the powder can be easily modeled using Equation (22) in conjunction with Equation (24) which captures the heat transfer characteristics of the powder. This has been shown to yield results very close to those obtained from a much more complicated iterative FEM method described by Nelson, et al.

(1995). The behavior of phenolic under the laser was shown to be very conducive to binding. SEM and DSC analysis helped set appropriate SLS parameters and characterize the behavior of the polymers under the laser. While concurrent curing has not been found, other thermosetting materials may exhibit heat initiated rather that heat catalyzed reactions. One the main advances of the current work is the creation of a broader definition of what types of materials can be processed in the SLS machine. This is no longer limited to semi-crystalline thermoplastics with large differences between melt and recrystallization temperatures. Instead, it is a question of appropriate thermo-rheology. In terms of the sintering model reviewed in Chapter 3, SLS materials simply need to have an appropriately low viscosity coupled with a low surface tension to promote the formation of a dense, flat, low residual stress, sintered layer at temperatures reached under the laser. Further modeling could help assess the appropriate parameters further and might lead to a predictive model for SLS processing which would support materials development and virtual prototyping.

The systematic SLS materials method described in Chapter 3 is based on knowledge gained during the characterization of the SLS process and the series of builds that followed. This includes powder characteristics and the details of the SLS process. This process will facilitate more rapid screening of potential SLS materials including single component resins and those used as binders. This method could be rapidly transferred to the commercial sector to promote the development of new commercial materials. A larger library of useful SLS materials would be related to a better understanding of the SLS process, better practices and embodiments for the SLS machine and better models for predicting material behavior within the SLS process.

Another interesting discovery was that the phenolic could be laser marked with appropriate atmospheric oxygen content. This could open up part tracking or enhancing the appearance of the parts with a simple change in the CAD file.

Promising Future Work

There are several promising avenues of future work. The first is to examine additional materials using the screening method outlined in Chapter 3. This includes additional thermoset binders and especially thermosetting powder coating materials such as DuPont RLPS-9 IR curing resin, non-outgassing thermosets alone and highly functional thermoplastic polymers such as polyphenylene oxide. Some polymers leave silica rather than carbon ash upon decomposition. If such a polymer could be developed as a binder it would support metal matrix composites better than residual carbon. Silica ash is less reactive and does not influence the behavior and properties of metals as much as carbon. Next, other types of base materials could be explored. In particular, there is a hollow phenolic microsphere product called Phenoset would yield very low density preforms. Other materials appropriate for reinforcing metal matrix composites will be discussed later.

Development efforts in materials will only go so far toward creating a greater role for SLS technology. Machine development is also critical and may be divided into several areas. The first area is instrumentation. There is a difference between the older DTM Sinterstation 2000 machine used for this project and the newest machine, which has a built-in part bed calibration, yet even in the newest machines the temperature profile across the bed is not managed. The laser power reaching the bed is also not instrumented. In terms of a research machine, there should be an extensive amount of instrumentation to monitor the temperature across the top of the part bed and down into it as well. This would facilitate more precise process control and also validate process modeling. The physical layout

for the machine limits its capability as well. Powder storage, handling and delivery all promote variation in the current process. As described in Chapter 3, the scanning method used in the current SLS machines supplies significantly different thermal cycles to different regions of the part. This causes distortion (part growth, and curl) and also differences in material strength. In the future this effect could be used to increase strength in critical areas, but it is currently dependent on part geometry, the particular path the scanning actually takes and the orientation of the part. Since the laser sweeps back and forth and overlaps previous sweeps, the edges tend to have longer contact with the laser. This causes the X-direction facing edges of parts to have higher energy doses. In the end, the current project shows that there are opportunities for significant improvement in the SLS machine in temperature control, powder handling and scanning.

Creating a comprehensive model for the process is also an important future goal which ties into the virtual prototyping work discussed below in terms of product design issues. The key to this is to capture the behavior under the laser using both a model and experimental validation of the thermo-rheological processes. Such a system would greatly enhance the development of new material systems for use within the SLS process.

Finally, a scanning overlay (additional writing scan) would be necessary to explore the concept of laser marking further.

5.1.2 Polymer Infiltration

Main Technical Contributions

Polymer infiltration is a widely used technique, even within current SLS industry practice. Yet, the exploration of a new family of materials for use with SLS preforms brings new capabilities to the existing process. In particular, the

177°C service temperature of the epoxy is significant compared to the100°C service temperature of Duraform nylon. Although the infiltrant polymers were brittle, they did allow for a better surface finish compared to Duraform. The infiltrant materials were found to provide excellent support for parts during subsequent furnace processes. Finally, customer feedback has been positive in terms of part accuracy, but the brittleness of the parts significantly limits the potential applications.

More importantly, the appropriate characteristics of infiltrants and the processes to get them into SLS preforms have been established. The effect of the infiltration process on the dimensional stability of the parts has been characterized. The variation in the properties of the infiltrated preforms that stemmed from the SLS process was larger than expected. This underscores the importance of developing a more tightly controlled SLS process. Infiltrants could allow preforms with light colors to be colored without having to clean colored powder out of the SLS machine.

Promising Future Work

Additional infiltrants coupled with less brittle base materials could provide a final material that is less brittle. Another avenue for development is to promote other features such as low density or flame resistance. Potential base materials include silicone for flexibility and flame resistance and hollow phenolic microspheres for low density. Silicone might also provide an interesting infiltrant for preform parts.

While the dimensional effects and basic part properties were established, additional work would be necessary to establish more general behavior and create a process capable of supporting the reliability necessary for manufacturing.

Following this, very high stability infiltration processes could be developed which would be necessary to provide manufacturing reliability.

The last arena for additional work is high-temperature metal infiltration. Pre-ceramic infiltrants would further promote the development of structural SiC in route to metal matrix composites. It may also be possible with the addition of pre-ceramic infiltrants to produce strong and reliable porous ceramic parts. One interesting application of such parts would be to serve as burner media for gas turbine engines.

5.1.3 Metal Infiltration

Main Technical Contributions

Previous research also explored infiltration of silicon into porous SiC preforms and focused on the characterization of the fluid mechanics associated with infiltration. The current work has more broadly characterized the infiltration process, including the chemical reactions that are critical to the development of the final material properties. This included the variety of chemical reactions present during infiltration as well as the complex coupled flow effects within the silicon melt. The gas-phase reactions were found to play a more significant role than was previously reported for this process.

The next main contribution is the identification of four different sources of part slumping and their solutions. With additional work to establish general best practices for infiltration especially in terms of metal handling, free-standing infiltration would be possible.

Promising Future Work

Additional work could establish a more reliable method for silicon infiltration. The most promising application of the silicon infiltration is to create

ceramic materials which could be explored at the same time. The key elements of this additional work would be to match silicon flow characteristics to thermal cycles and to the gas-phase chemistry within the furnace. The gas-phase reactions themselves would need to be minimized via the use of high-purity gases or to be carefully characterized by monitoring the makeup of the furnace atmosphere during the infiltration process.

Outside of the microscale, silicon is not a useful structural material due to its brittleness. There are two paths toward more useful materials: ceramics and metal matrix composites. For ceramics, a high SiC content part could be prepared by increasing the carbon content of the preform. One method of accomplishing this would be to add multiple infiltration and burnout cycles with liquid resole phenolics. Other infiltrant metals offer a broader set of potential applications. Titanium, as an example spontaneously infiltrates SiC preforms and also forms a stable carbide. If the use of pre-ceramic polymers or an intermediate heating (with Si in some type of gas-phase) could eliminate the residual carbon from the preform, aluminum infiltration would also be an interesting alternative. SiC reinforced aluminum is widely used as highly conductive and dimensionally stable electronics packaging. Preceramic polymers would also support infiltration with iron alloys (but not into SiC, of course). Other base materials such as TiC, WC or alumina increase the number of matrix and reinforcing material pairings that can be pursued.

A reachable goal of additional work could be to create a viable method for producing fully functional parts. Future work would need to address several issues to make this possible. While several different types of fixtures have been examined during the current research, additional work would be necessary to establish best practices for designing and building parts to support free-standing

infiltration. The final properties of the infiltration process would need to be characterized for a variety of materials. The mechanical behavior of parts that were prepared via free-standing metal infiltration would need to be carefully characterized as well. This would allow the process and the materials produced to be placed into context with currently available engineering materials – which is absolutely critical if the process is to be adopted in actual engineering practice.

5.1.4 Platform Overview

Much of the work to develop SLS materials in the past has been focused on creating a single material type. In contrast, the underlying goal of the current work has been to prepare a more general system that would support a variety of materials using the same basic overarching fabrication process. The most important element of the current work has been the characterization of a phenolic binder, which is essentially a powdered adhesive. Graphite, which is notoriously difficult to bind, was easily formed into preforms using the phenolic binder. This paves the way for many other base materials to be used. Other types of binders could be developed as well. The different combinations of bases and binders coupled with a variety of polymeric and metallic infiltrants also promote material variety using the same basic process. With the future development of higher carbon content preforms ceramic materials can be formed as well. Using the basic process established by the current project, parts can be fabricated in metallic, polymeric, ceramic (via reaction formation) and particulate reinforced composite materials.

The vision for rapid manufacturing is that finished and fully functional parts will be possible directly from the fabrication process, such as SLS. This would mean that no tooling or post processing would be necessary and hence manufacturing would be at once simplified and generalized. Mass customization

and continuous process improvement would be attainable. The advances in technology to bring that type of capability to engineering practice will likely happen eventually. However, with indirect methods fully functional parts can be realized in the nearer term and the necessary infrastructure and changes in engineering practice can be addressed sooner. The current technology can be considered in terms of a bridge to complete rapid manufacturing or it might become a more permanent family of technologies. The perspective of rapid manufacturing is explored in greater detail below.

5.2 Indirect SLS Rapid Manufacturing

The technical perspective of the current project was presented in the previous section. Additional work that was completed during the project related to cost analysis and product design. These subjects are discussed below in terms of rapid manufacturing. By developing the broader rapid manufacturing perspective the current project can be shown to have additional contributions. The RM perspective also highlights additional future work.

5.2.1 Overview of Rapid Manufacturing

Groover (2002), describes manufacturing in terms of material shaping, material property enhancement and assembly. Issues of process planning, tooling and machine design play a supporting role. In practice, manufacturing logistics (materials, parts, scheduling and capacity management) and quality control (specification and customer expectations) are also a part of the manufacturing effort. With regard to the creation of a new manufacturing system, concepts of technology transfer also become important. Mansour and Hague (2003) describe rapid manufacturing as the creation of fully functional parts directly from a CAD file using layered fabrication techniques, such as SLS. The central tenet of their definition is the capability to, "create parts of any geometry and complexity

automatically without any tooling or skilled craftsman." They also describe rapid manufacturing as, "the next industrial revolution." The most common technical hurdles to rapid manufacturing from a survey of current literature are material properties and the limited range of available materials. Hopkinson and Dickens (2003), claim the largest barrier to be the costs of machines, maintenance and materials, while Mansour and Hague (2003) describe low dimensional accuracy and poor tolerances as the "Achilles' heel" for RM. The slow speed of the machines relative to mass production also limits any application of economies of scale. The critical developments needed to realize rapid manufacturing are briefly reviewed in the following sections including RM machinery and processes, materials development, cost structures and product development. The purpose of this is to highlight the value of indirect methods in terms of rapid manufacturing and show additional work that will support Indirect RM in the future.

5.2.2 Processes and Machinery

The keys to manufacturing are speed, low cost and repeatability. For RM this translates into limiting the amount of human intervention during the creation of parts. Current SLS methods touted as having low labor costs still require significant adjustment and monitoring by experienced personnel.

> The performance of an RP process is affected by a multitude of process parameters. It is not an easy task to choose an appropriate combination of these parameters for optimal fabrication of a prototype… Hence a significant degree of expertise is required to produce prototypes of consistent quality. The process is of a trial-and-error basis and is therefore both time-consuming and very costly. –Choi and Chan, 2003

The importance of SLS temperature control, powder handling and laser scanning improvements coupled with better process modeling have been discussed above

but are perhaps more critical in terms of supporting manufacturing operations. The directional variability of the epoxy infiltrated parts as an example, would not allow manufacturing processes without significant part redesign to accommodate the dimensional effects of SLS scanning. Altering the CAD files to accommodate the SLS process (if it could be currently predicted) would freeze the orientation and part placement. Instead, the ultimate goal is to have a process that is capable of producing parts from a standard CAD file without adjustment and human intervention. This will likely be a combination of machine improvement coupled with modeling capable of quickly modifying CAD files to produce accurate, high precision parts.

5.2.3 Materials Development

The "dearth of information about even the limited number of currently available materials," is described by Hague, et al. (2003) as a critical issue. Hopkinson and Dickens (2003) state that simply knowing the properties of materials in detail would alone facilitate the advent of RM. Part of this need is in terms of simply examining the properties of the finished materials in detail. More important, however, is characterizing how they behave within RM processes and what range of properties is possible.

This underlines the value of creating a systematic materials development method for SLS materials. Building a more comprehensive understanding of the materials would also facilitate more accurate modeling of the processes associated with RM. The other valuable element of the current research is that the post processing allows well understood material properties to be integrated into current rapid prototyping processes. In other words, not only are the materials available to indirect rapid manufacturing well understood, but the ability to make them is based on current technology and not technology that will be developed at some

time in the future. As new combinations of materials are explored, the focus should be on material "beachheads" that would either service wide applications, high demand or are populated with materials not easily processed in another way.

5.2.4 Cost Structure of Rapid Manufacturing

While Pham and Dimov (2003) claim SLS as a cost effective technology for the production of 1-5 parts, other estimates place this number much higher. Hopkinson and Dickens analyzed the costs for SLS parts versus injection molding and other RP processes. The break-even point for SLS in terms of cost per part versus injection molding in their study was 14,000 units for a particular 1.5" plastic lever part. The material costs of the phenolic binder, glass base material and DCPD infiltrant is compared to their results in Table 18 . The significantly lower material costs of the glass base material composite has a significant effect on the amount of production needed to reach a break-even cost per part compared to injection molding. This increases the advantages of the SLS technology over FDM and SLA, also shown in the table. If this number can be increased further with improvements in machine speed there is an additional advantage to RM over traditional mass production. With a relatively constant cost per part there is no burden to produce and sell large numbers of products to amortize the tooling cost. There is also no restriction on either mass customization or continuous improvement which tooling establishes for traditional manufacturing processes.

Table 18 Cost Comparison of RP Methods (Hopkinson and Dickens, 2003)

	Fused Deposition Modeling	Stereo-lithography	Selective Laser Sintering	Phenolic/ Glass/ DCPD	Injection Molding
#/ Machine Run	75	190	1056	1056	$35,294 tool
Machine Cost/ Part	$3.41	$5.06	$0.67	$0.67	$0.30 per part
Labor/ Part	$0.10	$0.05	$0.05	$0.05	
Material Cost/ Part	$2.26	$1.66	$2.10	$0.53	
Unit Cost	$5.77	$6.77	$2.83	$1.25	
Breakeven # of Parts vs. Molding	6,457	5,453	13,977	37,227	

It is important to consider two things to put Table 18 into perspective. First the capability of the materials themselves is not considered. Injection molded polymers are fully dense while SLS materials are inherently porous and do not reach full strength. The DCPD infiltrated composite, as discussed above, is brittle. In other words, the material properties must be established before this type of cost analysis indicates real manufacturing potential. Second, smaller parts, like those examined by Hopkinson and Dickens (2003), allow the SLS machine to process parts in parallel giving it a certain economy of scale. An examination of larger parts would represent a less favorable analysis for SLS processing. On the other hand parts of greater complexity would increase the cost of tooling without increasing the cost of SLS processing.

The commercial potential of the current research was explored with the creation of a cost model for Indirect SLS. The costs of SLS processes were based on those quoted for outsourcing in industry. Actual costs to SLS manufacturing houses would be slightly lower. Furthermore, fairly large parts were used for the analysis, in comparison to the 1.5" parts examined by Hopkinson and Dickens (2003). A complete version of the cost model may be found in Appendix 6. The first analysis, shown in Table 19 , is a comparison of two base materials to both

Duraform (3D Systems, Inc.) and the higher priced Windform (Cevolini) material. Costs per part and per full build of a Sinterstation 2000 machine are compared. The product "prices" were changed to yield approximately the same profit per machine build. The difference in base material cost between the glass base material and the Duraform is particularly striking. Again, it is important to consider that cost and material properties are both important. As an example, if parts would be expected to withstand impact loading the additional cost of Duraform would be preferred in many cases to the lower cost epoxy infiltrated parts.

Table 19 Cost Analysis for Traditional SLS Materials

Product	4x4x4" Duraform Block	4x4x4" Phenolic/ Glass/ DCPD	4x4x4" Windform	4x4x4" Phenolic/ Alumina/ DCPD
Margin	21.84%	36.36%	18.20%	22.76%
Profit per Build	$ 4,371.28	$ 4,372.13	$ 4,374.55	$ 4,377.46
Product Price	$ 1,500.00	$ 901.00	$ 1,801.50	$ 1,441.00
Mfg. Cost (/ Part)	$ 1,172.44	$ 573.38	$ 1,473.70	$ 1,112.98
Mfg. Cost ($/ build)	$ 15,646.28	$ 7,651.75	$ 19,666.55	$ 14,852.74
Base Materials ($/build)	$ 9,022.57	$ 132.30	$ 13,042.83	$ 7,333.29
Setup ($/build)	$ 565.00	$ 565.00	$ 565.00	$ 565.00
SLS Procs. ($/build)	$ 5,625.00	$ 5,625.00	$ 5,625.00	$ 5,625.00
Infil. Matl's ($/part)	$ -	$ 7.12	$ -	$ 7.12
Infil./ Curing ($/ part)	$ -	$ 60.00	$ -	$ 60.00
Post Processing ($/part)	$ 32.50	$ 32.50	$ 32.50	$ 32.50

The same cost model was used to examine several commercial products that could be formed from RBSiC. One application that unites the advantages of part complexity with those of difficult material processing is molds and dies for injection molding and metal casting. This particular application was explored extensively during the course of the research and is the subject of the Idea to Product entry

and business plan materials found in **Error! Reference source not found.** and Appendix 5 respectively. Market numbers for aluminum casting and polymer injection molding were used to estimate the price of representative products. The low complexity heating element holder also analyzed cannot be manufactured profitably using the indirect SLS method developed during the current research. However, even with the majority of costs occurring in post processing, indirect SLS can make molds and dies effectively. For the sizes of parts chosen, the larger advantage for smaller parts was not seen. Design costs, additional furnace fixtures and any facilitating elements within the design of the parts themselves were not considered in this model.

Table 20 Cost Analysis for Matrix Composite Products

Product	(10x3x0.5") RBSiC Heating Element Holder	(4x4x3.5") RBSiC Small Aluminum Die	(4x4x3.5") DCPD Small Polymer Die	(6.5x6.5x5") RBSiC Large Aluminum Die	(6.5x6.5x5") Large DCPD Polymer Die
Margin	-12.49%	71.26%	57.57%	76.60%	64.29%
Profit per Build	$ (1,362.40)	$ 37,456.80	$ 17,290.35	$ 38,954.55	$ 20,807.39
Product Price	$ 350.00	$ 3,500.00	$ 2,000.00	$ 5,500.00	$ 3,500.00
Mfg. Cost (/ Part)	$ 393.72	$ 1,005.74	$ 848.63	$ 1,287.10	$ 1,249.70
Mfg. Cost ($/ build)	$ 12,268.63	$ 15,103.37	$ 12,744.03	$ 11,901.15	$ 11,555.33
Base Materials ($/build)	$ 566.21	$ 566.21	$ 566.21	$ 566.21	$ 566.21
Setup ($/build)	$ 565.00	$ 565.00	$ 565.00	$ 565.00	$ 565.00
SLS Procs. ($/build)	$ 5,625.00	$ 5,625.00	$ 5,625.00	$ 5,625.00	$ 5,625.00
Infil. Matl's ($/part)	$ 3.40	$ 12.70	$ 6.23	$ 28.59	$ 14.02
Infil./ Curing ($/ part)	$ 126.00	$ 323.14	$ 222.50	$ 87.83	$ 165.00
Post Processing ($/part)	$ 47.50	$ 220.00	$ 170.00	$ 440.00	$ 340.00

While the visionary approach is to consider the time when no tooling would be necessary and the material for a particular application would be within the capability of RM, there is room to consider the advent of Rapid Manufacturing as

a more gradual evolution starting with the capabilities available today. As reviewed above current technology allows small, complex, polymer parts to be produced cost effectively. The addition of post processing retains the same basic cost structure for creating parts but with the additional features of a broader set of more functional materials. The effect of also being able to produce complex custom parts could be addressed in future work. In short, there are commercial opportunities for indirect SLS methods. However this only emphasizes the need for additional work in process development, materials development, model development and the indirect method in general.

5.2.5 RM Product Design

Rapid prototyping has already had an influence on product development. Usher, et al. (1998) estimate a time cost of product development that is 10 to 50% of traditional methods when using RP techniques. Figure 98 is adapted from their diagram and shows both the compression of time and the facilitation of concurrent tasking compared to the linear organization of standard product development.

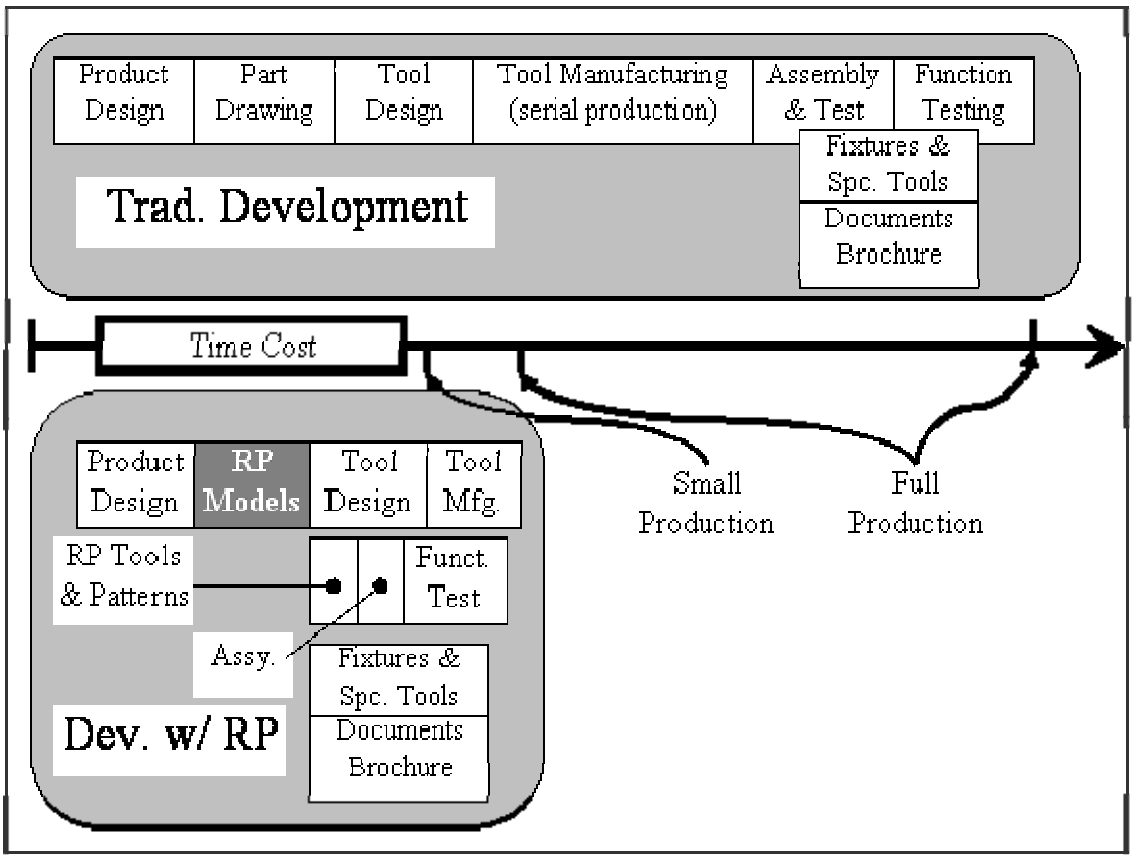

Figure 98 Product Development Process Comparison (Usher, et al., p.155)

Thinking in terms of fully formed RM, the above diagram is very different. In particular there are no tools or patterns to consider. As Hague et al. (2003) point out, this avoids the constraints established by traditional manufacturing methods and simultaneously incorporates mass customization. With RM, the design would be no longer bound by the need to create tooling and special fixtures. Complexity is nearly free, which has broad effects on current engineering design methods. As an example the "information axiom" of Nam Suh's Axiomatic Design might need to be revised. It may no longer be necessary to minimize the information content to create the best design. The ease in iterating a CAD file and the lack of some manufacturing limitations draws the customer closer to the design process, thus facilitating "collaborative design." It is unlikely that true mass production will ever be completely replaced by RM. Thus RM parts and more traditionally mass-

produced parts will be assembled into final products. This will require the creation and design of interfaces to accommodate mass produced parts into assemblies. The need for modeling RM processes is perhaps even greater, though, since iteration though RP or fully functional RM methods will remain time and cost prohibitive. Choi and Chan recommend a greater emphasis on virtual prototyping, where the RP processes themselves are modeled, due to the processing challenges of current RP systems including SLS (which do not currently exist). With additional work virtual prototyping would more accurately represent parts produced in more advanced RM systems. This would advise the part orientation and process parameters for desired surface finish or dimensional stability. The attainable accuracy and precision of machine improvements coupled with better models cannot be currently predicted. Choi and Samavedam (2002) also describe a virtual prototyping system and place it in a prototype development model that also can be considered in terms of RM processes. Instead of the traditional or RP modified methods shown in Figure 98, RM would allow the simpler and more collaborative system shown in Figure 99.

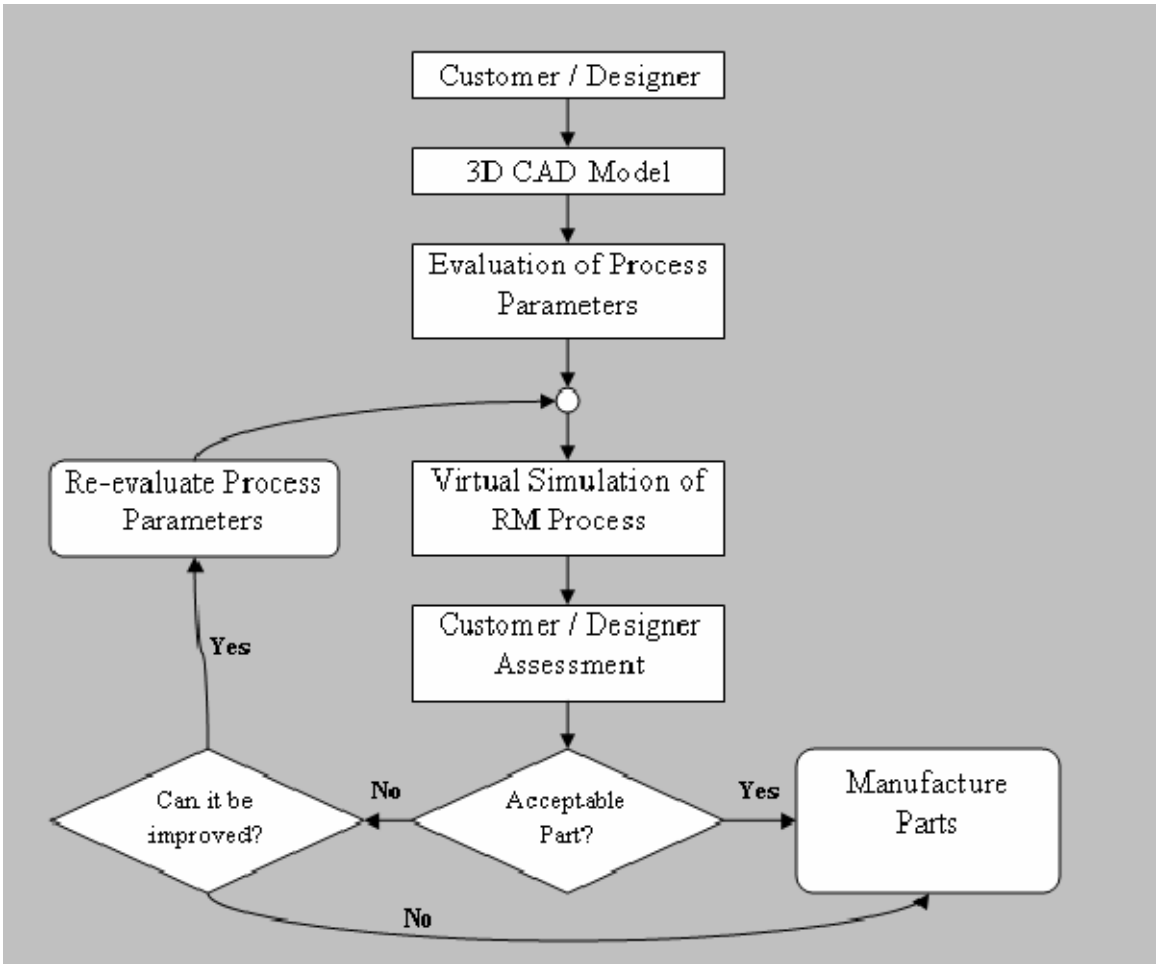

Figure 99 RM Design Flowchart (adapted from Choi and Samavedam, (2002))

Clearly there is significant work within product design to accommodate the advantages of RM into actual engineering practice and to realize the "next industrial revolution." The adoption of Rapid Manufacturing into engineering practice is not limited to material development, machine and process development or modeling. There are also cultural changes to consider in terms of product design and the roles necessary for the creation of new products. This will take time. Since the technical hurdles for Indirect SLS are similar, the same basic issues also apply.

5.3 Return to the Thesis

Indirect Selective Laser Sintering with thermosetting binders is a platform for commercially driven rapid manufacturing of polymer and metal matrix composites.

The thesis is true, but requires some elaboration in terms of the hypotheses proposed in Chapter 3 and Chapter 4. The basic theme of these hypotheses was to promote a greater variety of more functional materials while preserving the advantages of the SLS process. The perspective on Rapid Manufacturing developed within Chapter 5 is also important. Finally, the current work did not create a manufacturing system capable of being used commercially. However the future work proposed establishes several clear paths to making Rapid Manufacturing a more widespread alternative to traditional manufacturing methods.

In Chapter 3 the following hypotheses were addressed.

1. Thermosetting polymers can be used as effective binders for SLS processing and can be crosslinked under the laser, representing a significant advantage over the use of thermoplastic resins that simply solidify.
2. By combining the basic principles of powder mechanics, SLS heat transfer, and polymer rheology, a systematic material screening method can be prepared for assessing new SLS materials.

In using phenolic mixed with SiC, glass and also graphite a range of parts have been created to support these hypotheses. Thermosetting polymers represent a family of highly capable polymers by themselves. It is important to consider that as a family they are relatively brittle and many products formed using

thermosetting polymers are reinforced in some way. Still, the use of thermosets, and even just for binders, supports using SLS for a larger array of applications. More importantly, a more universally capable binder facilitates the use of a wide variety of base materials. Systematic materials development will continue to increase the number of applications that can be satisfied with Indirect SLS and possible with additional work direct SLS as well.

The following hypotheses were addressed in Chapter 4.

1. Polymer infiltration is an effective method of producing indirect SLS parts with properties not obtainable via current SLS methods
2. By using a char-yielding polymer, high-accuracy, free standing, spontaneous infiltration may be achieved
3. Indirect processes form a flexible rapid manufacturing platform capable of supporting a variety of material systems.

The service temperature, cost and strength of epoxy infiltrated parts represent a significant advantage over current SLS processes. The causes for part distortion and their solutions during the burnout and infiltration have been identified. The nature of the infiltration process has been characterized. Additional work is necessary to achieve reliable, high-accuracy infiltration, however. The binder system developed coupled with the infiltration methods does establish a method that supports the development of ceramic, polymeric, metallic and composite materials.

Chapter 5 contained a review of the technical achievements of Chapters 3 and 4, but also included additional material about the nature of Rapid Manufacturing. This helped place the achievements of the project in a broader context and ultimately allows the thesis to be addressed in terms of the entire

project. The cost analysis described above indicates that while full manufacturing may not be feasible in the near term there are certain applications where Indirect SLS can be applied when the reliability of parts improves.

In the end, with the support of the hypotheses in Chapter 3 and Chapter 4, the thesis is true. The real potential of the Indirect SLS platform will not be clear until a much greater variety of materials has been established. And, with the completion of additional work, it will not be commercially driven, but simply commercial.

Appendix 1 Thermoset Binder Research Data

Table 21 Tap Density for Various Powders

Powder Desc.	SG	Avg. Size	Sample (g)	Tap height(in)	Powder Dens.	Fract. Dens.
Phenolic (HJE)	1.30	10.8	30.47	1.955	0.567	0.44
600 grit	3.20	9.3	75.00	1.797	1.520	0.47
DFPA	1.02	40.0	23.91	1.690	0.515	0.50
8% Ph (280/ roll)	3.05	31.0(phen)	71.44	1.656	1.571	0.52
10% Ph (280/media)	3.01	-	70.55	1.640	1.566	0.52
10% Ph (280/att.)	3.01	-	70.55	1.598	1.608	0.53
Phenglass	2.38	31.0(phen)	55.78	1.557	1.305	0.55
320 grit	3.20	29.2	75.00	1.516	1.801	0.56
-270 WC	15.70	19.8	367.97	1.510	8.873	0.57
2.5% 1200 + 320	3.20	3.0 (1200)	75.00	1.490	1.833	0.57
5% 1200 + 320	3.20	-	75.00	1.459	1.872	0.58
10% 1200 + 320	3.20	-	75.00	1.450	1.883	0.59
7.5% 1200 + 320	3.20	-	75.00	1.445	1.890	0.59
12.5% 1200 + 320	3.20	-	75.00	1.435	1.903	0.59
Potters glass	2.50	35.0	58.59	1.335	1.598	0.64

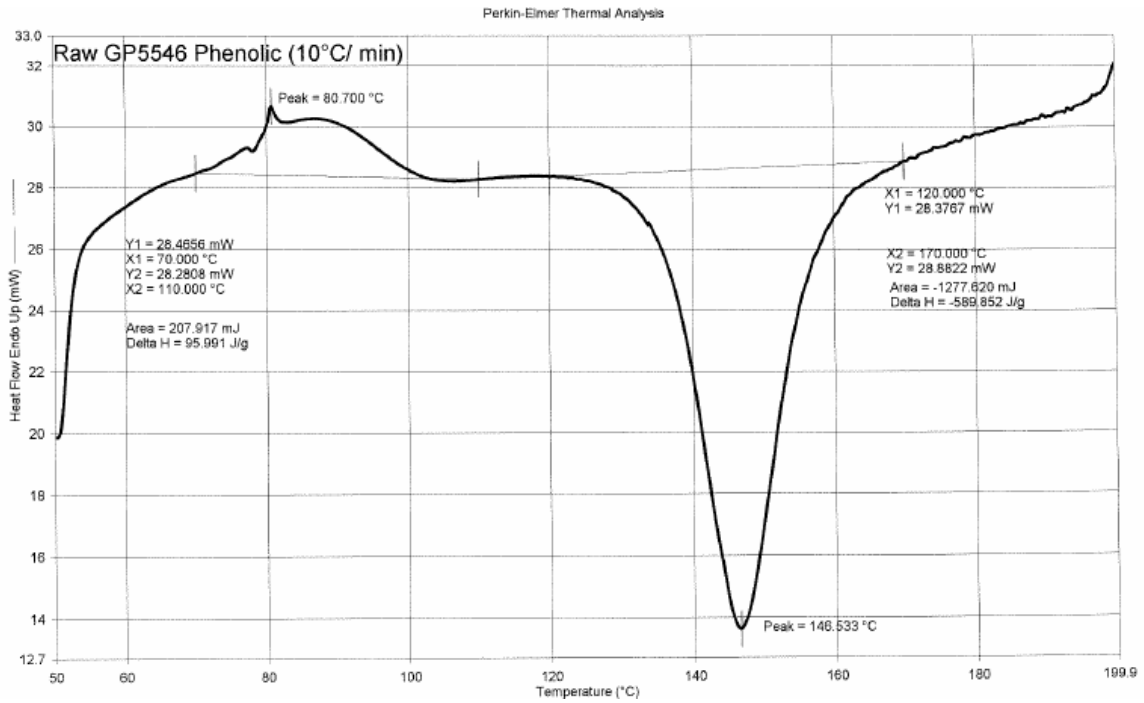

Figure 100 DSC Curve for Lot#1 Phenolic (ΔH numbers should read 1/10 values)

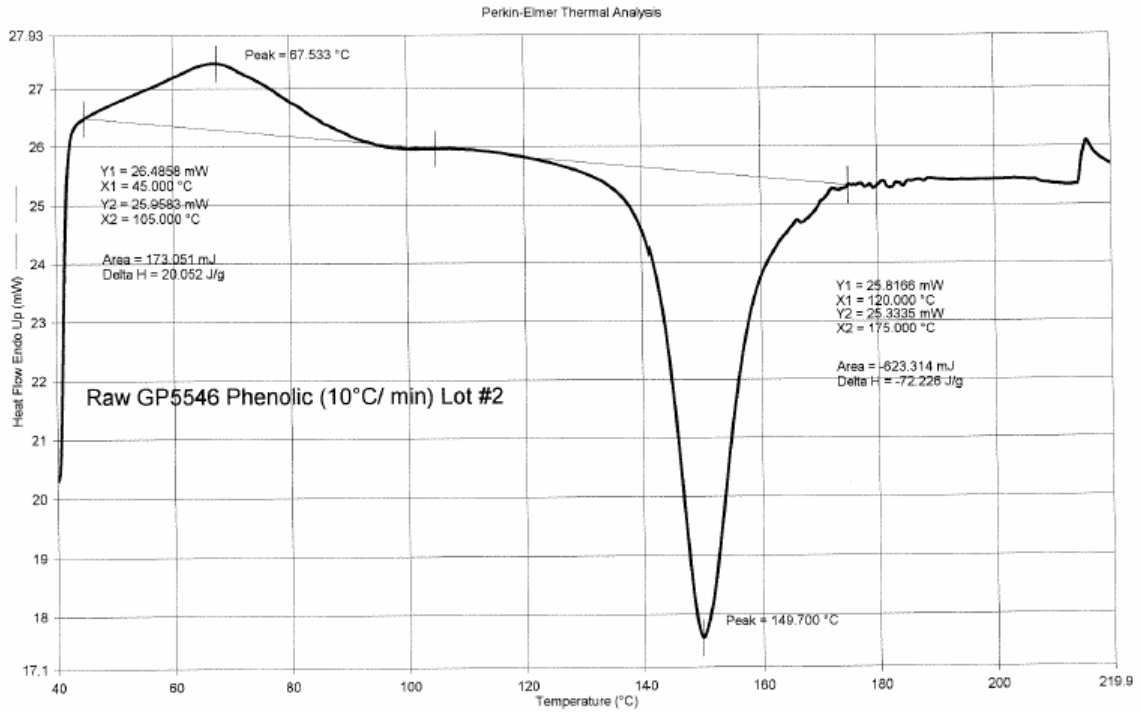

Figure 101 DSC Curve for Lot#2 Phenolic (10°C/minute scan)

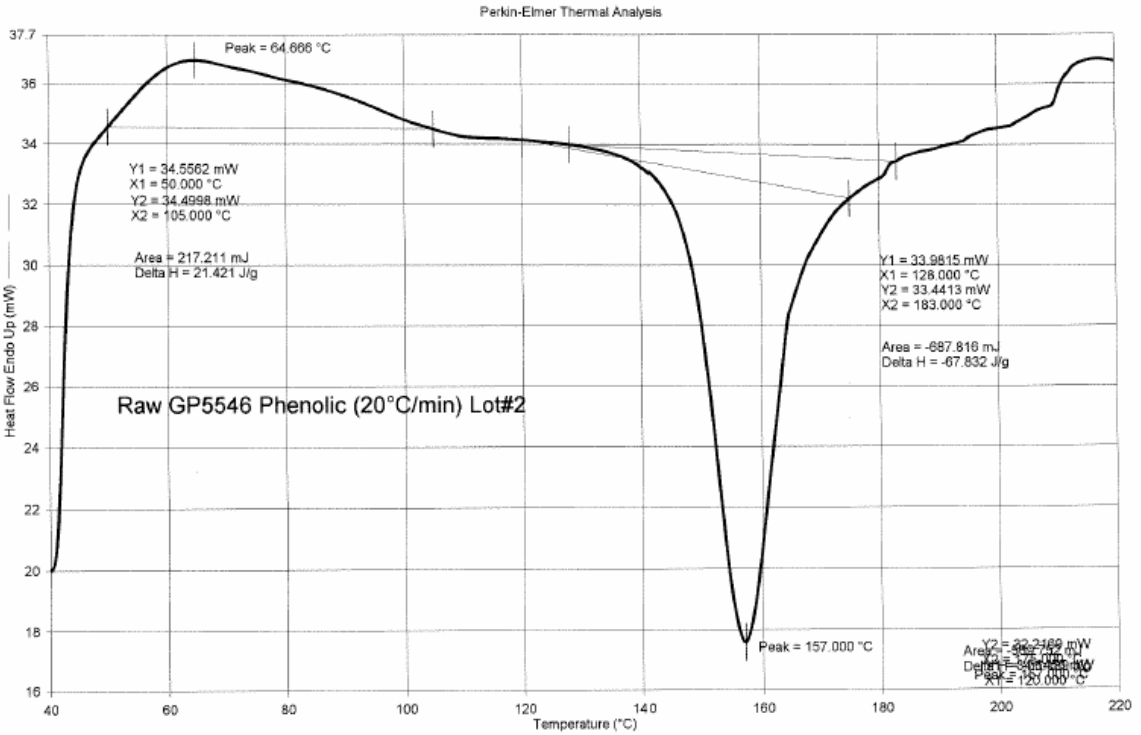

Figure 102 DSC Curve for Lot#2 Phenolic (20°C/minute scan)

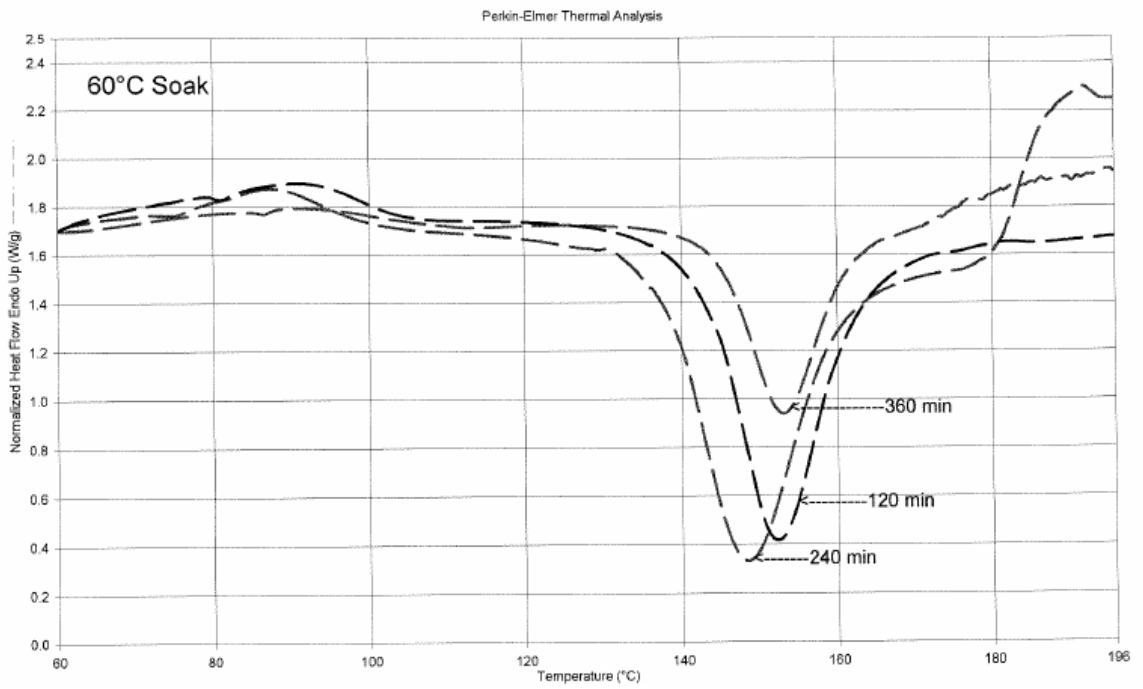

Figure 103 Comparison of DSC Curves for 60°C Soaks of 120, 240 and 360 minutes

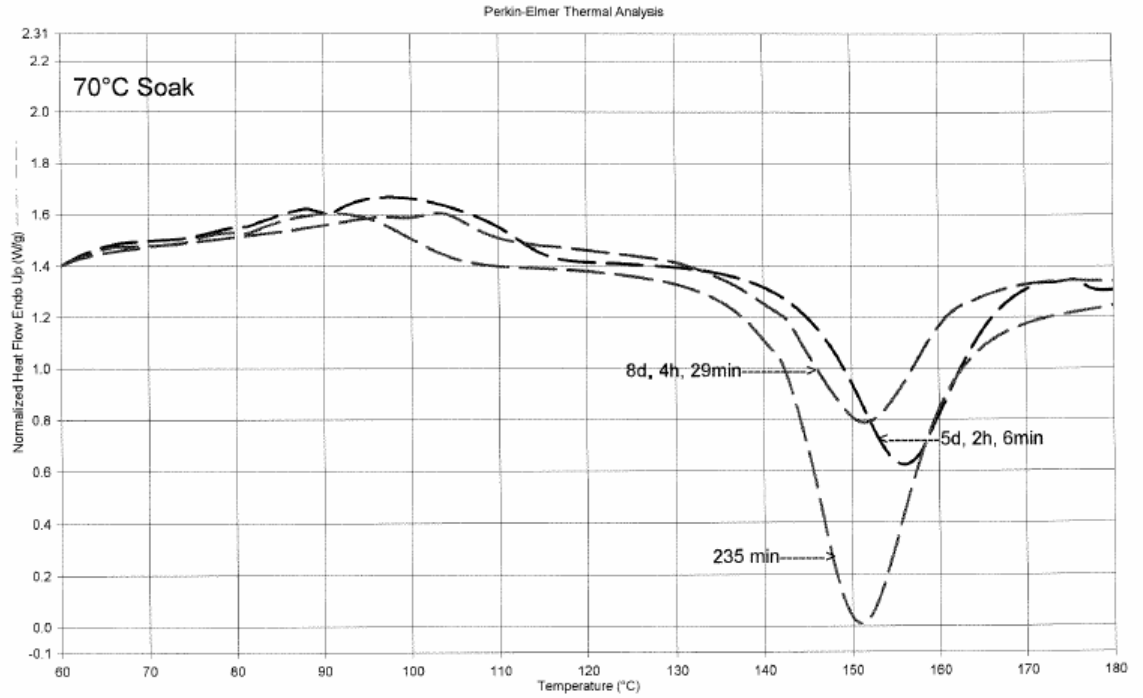

Figure 104 Comparison of DSC Curves for 70°C Soaks for 235min, 5days-2h-6min and 8days-4h-29min

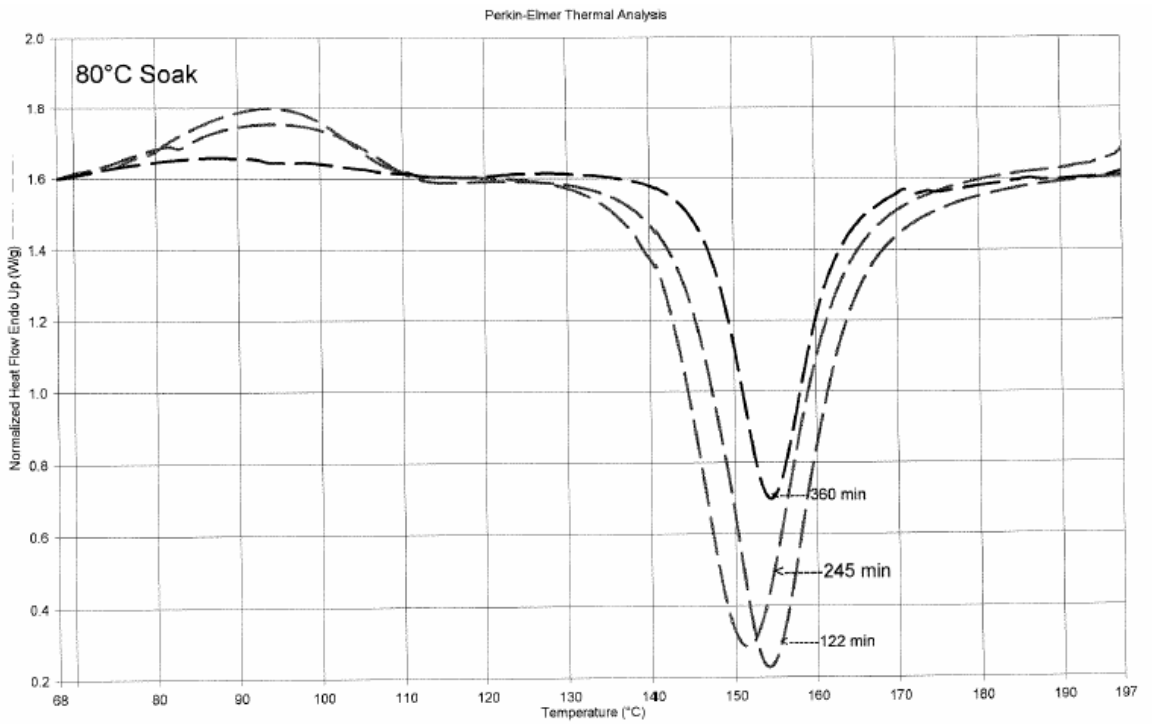

Figure 105 DSC Curves for 80°C Soaks of 122, 245 and 521minutes ("360min" should read "521min")

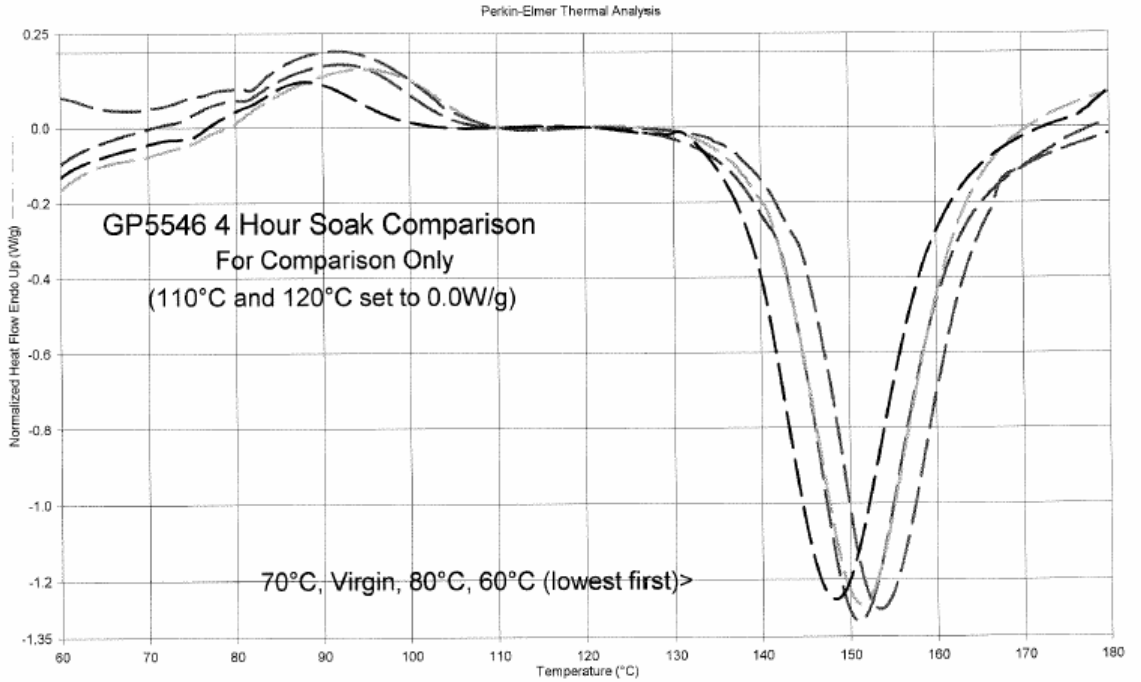

Figure 106 Comparison of DSC Curves for 4-hour Soaks at 60, 70 and 80°C

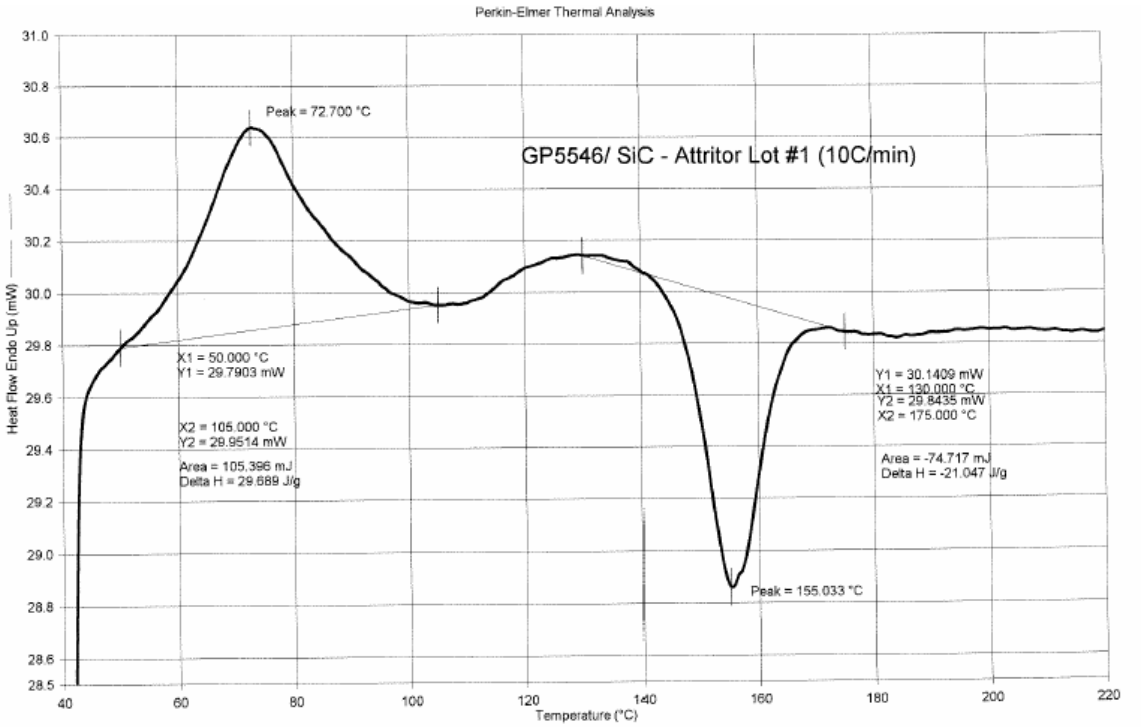

Figure 107 DSC of Lot#1 Attritor Milled Powder with Melt and Curing Data

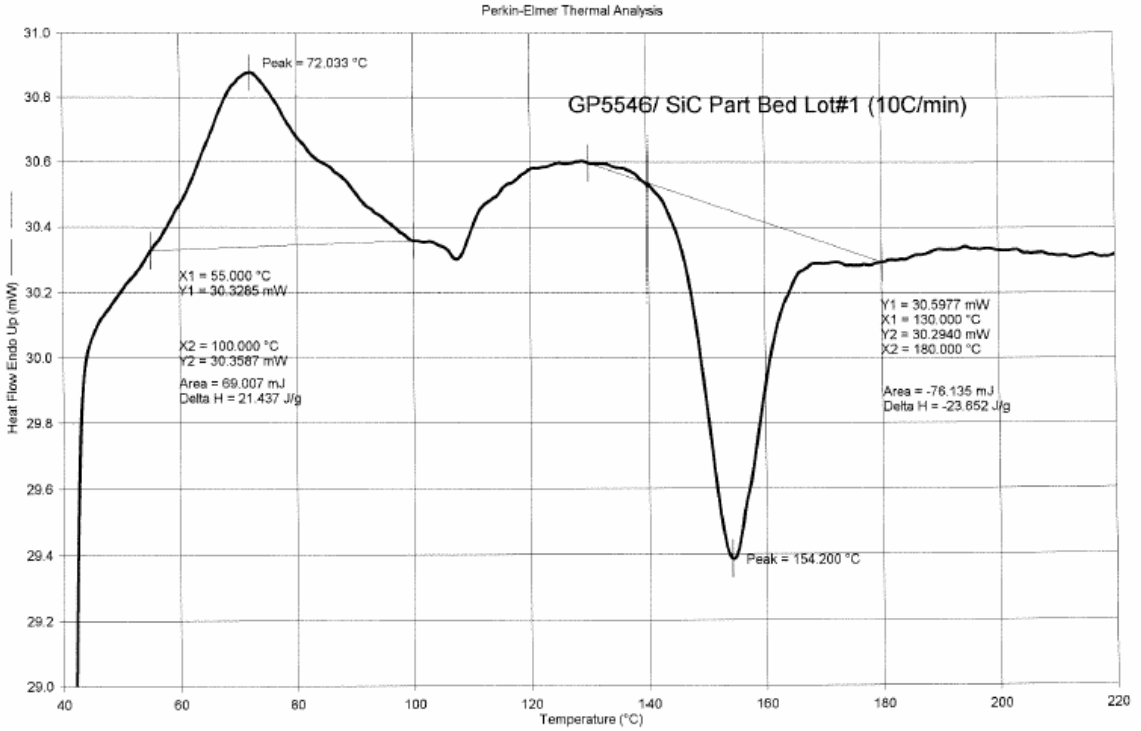

Figure 108 DSC of Lot#1 Part Bed Powder Showing Melt and Curing Data

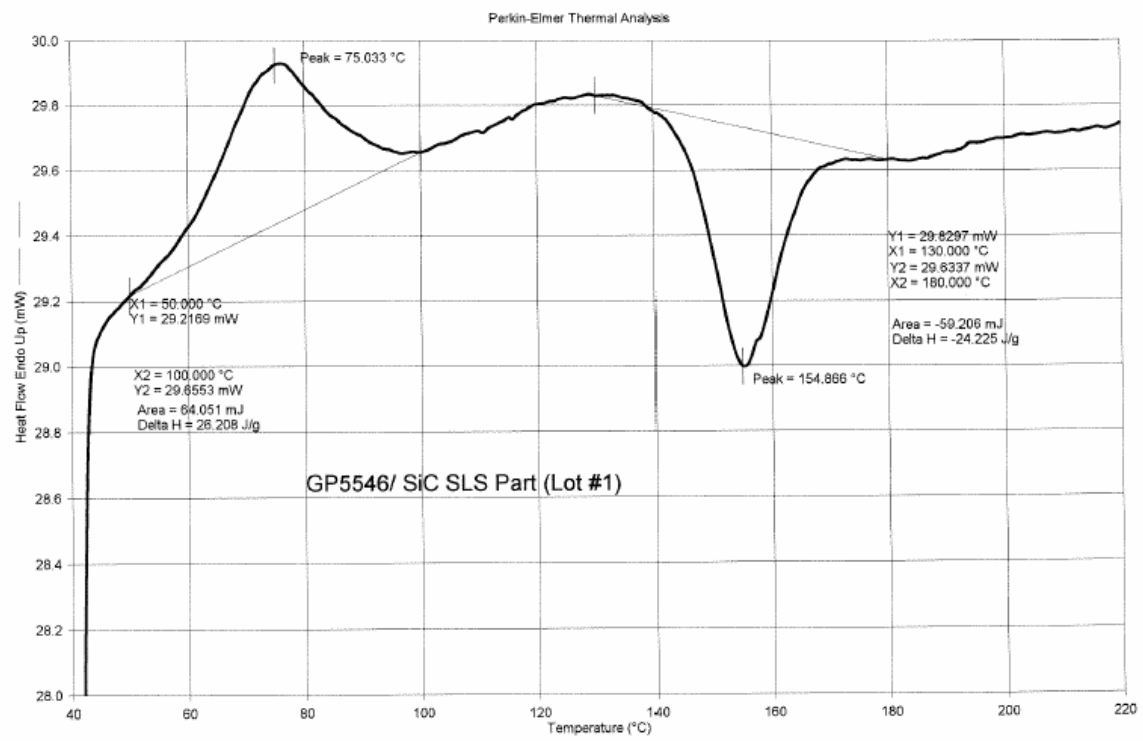

Figure 109 DSC of Lot#1 SLS Part Showing Melt and Curing Data

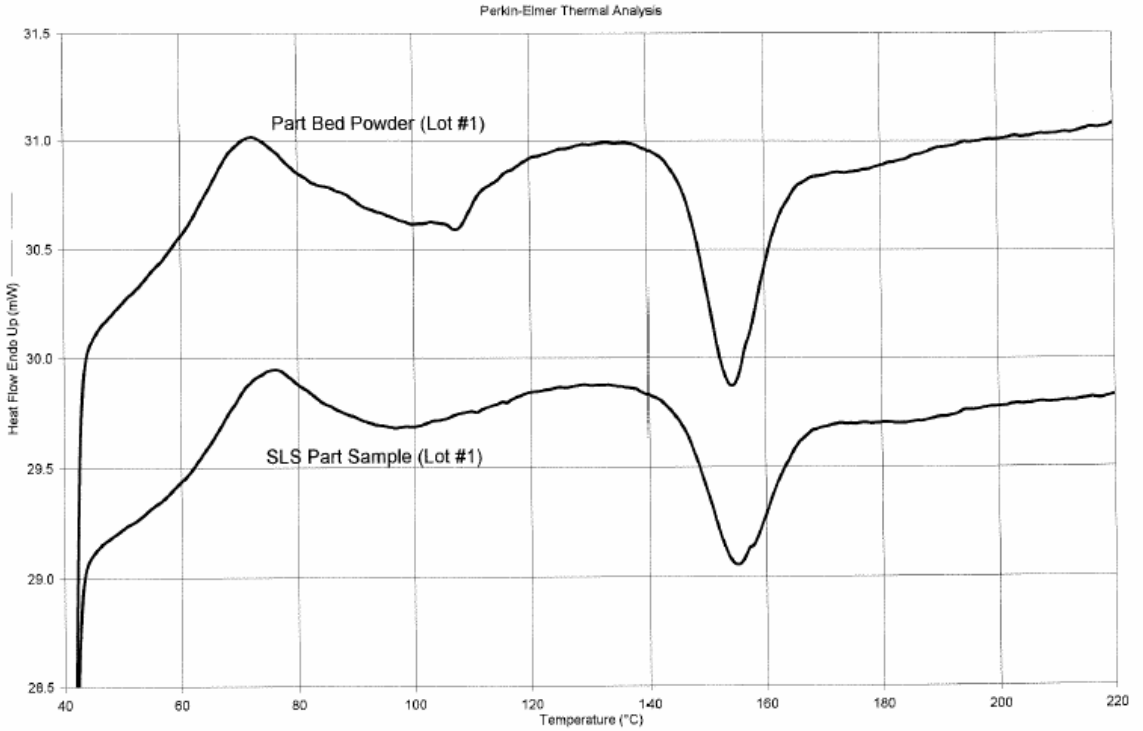

Figure 110 DSC Comparison of Lot #1 SLS Part Versus Part Bed Powder

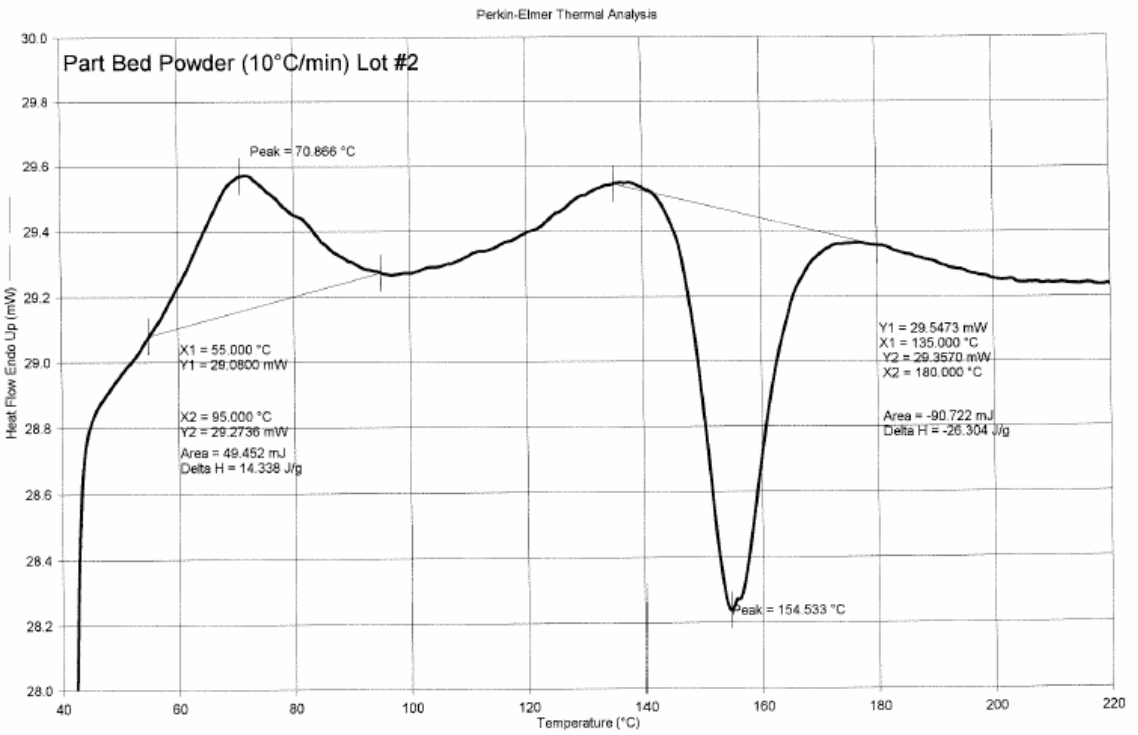

Figure 111 DSC of Lot#2 Part Bed Powder Showing Melt and Curing Data

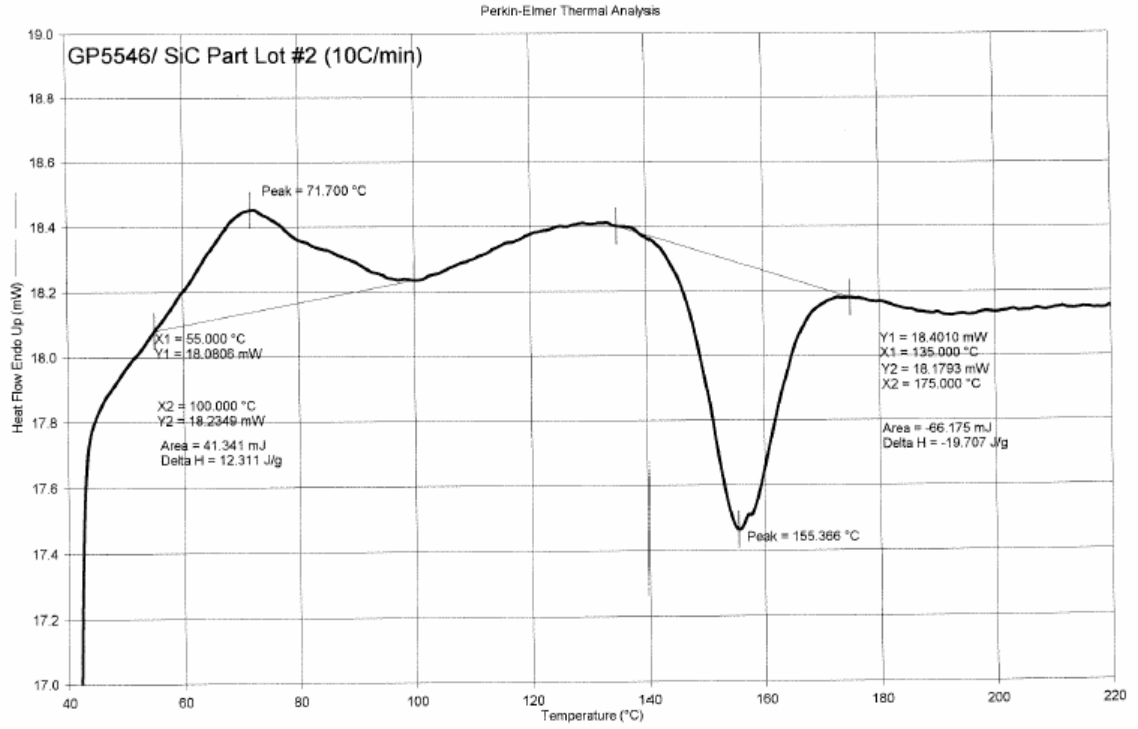

Figure 112 DSC of Lot#2 SLS Part Showing Melt and Curing Data

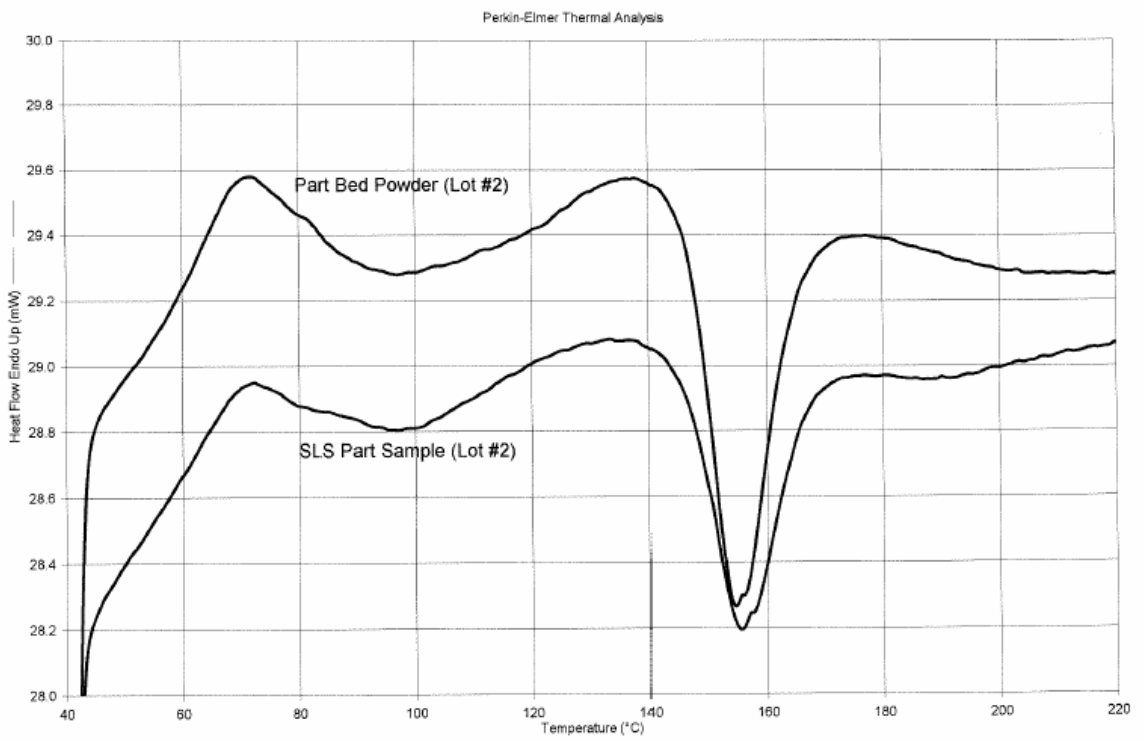

Figure 113 DSC Comparison of Lot #2 SLS Part Versus Part Bed Powder

Table 22 Dimensional Stability of BJB TC-1622 Epoxy Infiltrated Glass

TEST OVERVIEW : Glass/ Phenolic parts (33% by volume) were prepared, prior to the above test, using 8, 10 and 12 W. Bars similar to those described above were used and also distributed throughout the part bed. The 12X samples were dropped - the masses and SG values are skewed.											
		GREEN					EPOXY INFILTRATED				
Power/ Orient.		m (g)	W (in)	L (in)	T (in) mid	T (in) end	m (g)	W (in)	L (in)	T (in) mid	T (in) end
8X	21	14.4	0.508	2.514	0.516	0.504	17.7	0.518	2.550	0.522	0.514
	22	14.3	0.513	2.521	0.513	0.504	17.8	0.521	2.557	0.521	0.511
	23	14.4	0.515	2.527	0.512	0.507	18.0	0.524	2.565	5.220	0.509
	24	14.4	0.513	2.531	0.516	0.500	18.0	0.523	2.565	0.524	0.516
8Y	26	14.9	0.516	2.523	0.517	0.506	18.3	0.524	2.560	0.528	0.514
	27	14.8	0.517	2.547	0.514	0.499	18.5	0.527	2.583	0.522	0.504
	28	14.7	0.517	2.541	0.514	0.497	18.3	0.525	2.575	0.523	0.503
	29	14.9	0.517	2.549	0.515	0.506	18.5	0.526	2.583	0.522	0.511
10X	1	15.0	0.511	2.520	0.530	0.514	18.4	0.519	2.555	0.536	0.522
	2	14.9	0.514	2.526	0.521	0.505	18.3	0.524	2.561	0.532	0.510
	3	14.8	0.508	2.514	0.523	0.501	18.0	0.516	2.555	0.531	0.508
	4	15.1	0.515	2.535	0.519	0.503	18.4	0.525	2.568	0.530	0.513
	5	15.3	0.517	2.533	0.522	0.503	18.5	0.527	2.571	0.529	0.509
10Y	6	15.5	0.521	2.558	0.519	0.501	18.8	0.527	2.598	0.531	0.508
	7	15.2	0.511	2.524	0.522	0.503	18.3	0.523	2.560	0.532	-
	8	15.3	0.518	2.524	0.521	0.503	18.4	0.526	2.560	0.532	0.511
	9	14.9	0.516	2.501	0.522	0.500	18.2	0.523	2.537	0.532	0.509
	10	15.5	0.518	2.525	0.521	0.502	18.7	0.527	2.560	0.534	0.513
12X	11	15.1	0.514	2.532	0.541	0.523	18.2	0.519	2.550	0.548	0.528
	12	14.2	0.516	2.532	0.523	0.489	17.1	0.523	2.555	0.533	0.501
	13	14.4	0.523	-	0.524	0.498	17.3	0.529	-	0.535	0.507
	14	8.8	0.520	-	0.527	0.498	10.6	0.527	-	0.539	0.511
12Y	16	15.2	0.522	2.528	0.527	0.507	17.9	0.533	2.570	0.569	0.529
	17	15.0	0.519	2.515	0.527	0.501	17.4	0.529	2.564	0.564	0.522
	18	15.5	0.526	2.546	0.528	0.496	18.2	0.531	2.594	0.543	0.509
	19	15.3	0.524	2.529	0.530	0.495	18.0	0.533	2.572	0.548	0.516

Table 23 Dimensional Stability of BJB TC-1622 Epoxy Infiltrated SiC

TEST OVERVIEW : SiC parts (25% phenolic by volume) were prepared using two different laser powers (10 and 12 W) to determine the effect on dimensions and final part strength, if any. 0.5 x 0.5 x 2.5" bars were oriented along the X and Y axes for									
Power/		GREEN				EPOXY INFILTRATED			
Orient.		m (g)	W (in)	L (in)	T (in)	m (g)	W (in)	L (in)	T (in)
10X	1	14.02	0.509	2.526	0.507	19.30	0.507	2.522	0.504
	2	14.16	0.513	2.522	0.510	19.37	0.509	2.515	0.505
	3	13.93	0.508	2.520	0.506	19.24	0.508	2.513	0.503
10Y	1	14.77	0.522	2.542	0.513	20.20	0.521	2.533	0.508
	2	14.74	0.529	2.550	0.510	20.17	0.519	2.535	0.508
	3	14.60	0.522	2.545	0.507	19.98	0.519	2.535	0.504
12X	1	14.25	0.510	2.520	0.508	19.61	0.505	2.511	0.504
	2	14.45	0.510	2.523	0.514	19.84	0.507	2.514	0.510
	3	14.53	0.512	2.526	0.521	19.93	0.509	2.514	0.511
12Y	1	14.99	0.525	2.528	0.513	20.51	0.523	2.521	0.510
	2	15.08	0.521	2.524	0.524	20.58	0.520	2.514	0.513
	3	15.30	0.528	2.544	0.519	20.87	0.523	2.532	0.511

Appendix 2 SLS Development Notes

Overview

During the past two weeks (from about 2/25/04 to 3/10/04) we have run several SLS builds. During this time very significant progress has been made getting through some potentially fatal troubles in the SLS machine including interlayer adhesion, part curl and breakout strength. Previous tests established powder bonding during scanning. The following is a more detailed discussion of the testing completed, the results of those tests and the experiments that will support another round of SLS work.

Research Synopsis 2/25-3/10 (The SLS Builds)

Several single layer scans indicated that 90°C was too hot for the bed – some caking was observed. Above 90°C some darkening of the powder was also noticed. A range of scanning parameters were examined during these tests. The strength of the single layer crust was weak at laser powers of 7W and below. Above 11W the heat started to noticeably spread into lettering and corners. Some double scans (retracing each layer twice) had some effect, but not as much as increasing the power. The next issue to address was interlayer adhesion.

150lb of 280 grit (42 micron) silicon carbide was mixed in a cement mixer with 13lb of phenolic ground to an average particle size of 17.6 microns with a standard deviation of 11.8 microns. The scan speed was constant at 49.5 in/sec for all builds. The main parameters for the builds are in the table below. More details are in the following discussion.

#	Part Bed	Feeds	Feed Dist.	Layer	Scan Spacing	Power	Other
4-layer	80°C	50°C	.008″	.003″	.003″	6-10W	Multiple scans
1	60°C	30°C	.008″	.003″	.003″	8-10W	
2	60°C	35-55°C	.008-.010″	.003″	.003″	8-10W	
3	40-55°C	30-40°C	.009″	.004″	.003″	8-10W	Duraform Config.
4	70°C	R35, L40°C	.009″	.004″	.003-.004″	8-10W	1 layer of BTB parts
5	75°C	R35,	.008″	.004″	.003-	6-	Spacing/ Low

		L40°C			.004″	10W	Power
6	75°C	R35, L40°C	.008″	.004″	.004″	8-10W	Breakout Testing
7	75°C	R35, L40°C	.008″	.004″	.004″	8-10W	Low part spacing
8	75°C	R35, L40°C	.008″	.004″	.004″	8-10W	BTB samples

2/25/04 : Initial multi layer to test scanning parameters and interlayer adhesion

The parts were standard laser power testing parts scaled in 'Z' to only have 4 layers. The first layer had lettering in it.

Part	Power	# of Scans	Results
1	6	3	Color change, vapor on all scans, weak parts won't hold weight/ can't be removed from the bed in large pieces
2	7	2	Stronger part, still weak
3	7	3	No noticeable difference in strength from double scan
4	8	2	Significantly stronger than the 7/3 part. Much easier to remove from the powder
5	10	1	Another step up in the strength. The powder in the lettering on the first layer is firmer than the 8/2 part. The vapor coming off was heavier on this part.

No significant problems with interlayer adhesion were seen on any of the parts, but 4 layers does not offer much insight. Taller builds were necessary to more closely examine any periodic strength variation in the 'Z' direction, including interlayer effects. On a later build over 80% of the time was spent on scanning (this is reported on the 2000 machine at the end of the build). Fortunately, increasing the power had a much greater effect on the strength than multiple scans – the extra scanning time could really undermine the manufacturing capability of this process. There were faint fissures in the powder along the long edges of the parts in the 8/2 and 10/1 parts which indicate mild curl. No noticeable curl was seen in the single layer builds or in the lower power parts. The next issue is to minimize part curl while getting acceptable green strength. Degradation of the

phenolic was also a concern, but curl and strength were considered first. Some materials that have been tried in SLS have failed because the curl could not be controlled at any parameter settings.

2/26/04 : 1st Full build : Focus on curl reduction and 8-10W single scans

The build parameters were based on the ST200 metals parameters. 5 x .125 x .5" bend test bars were organized into 3 layers; 8W, 9W and 10W scans. The parts were spaced in X and Y by .25" and in Z by .125". 8 bars were placed in each layer. A fourth layer was added with logo parts and also breakout parts (Figure 1). The breakout parts have walls and cavities of various aspect ratios aligned in several directions to examine part spreading (due to excessive heating) and the difficulty of getting the parts out of the power bed. Later when we have bend testing data, strength numbers can be correlated with breakout confidence. All of the parts allowed dimensional testing. Numbers are nice, but we also need to be confident that we can reliably manufacture parts.

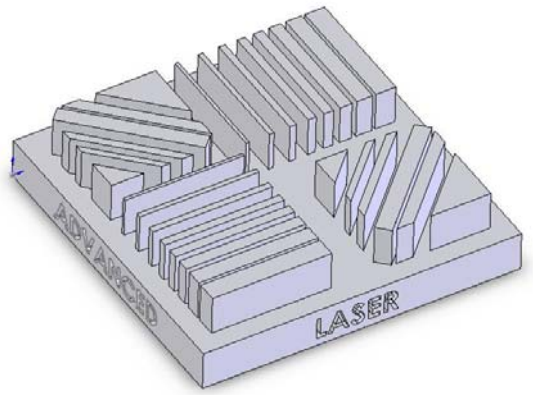

Figure 1: Breakout Part

The part warmup height was 0.1". No shrinkage was observed in the first 4 scanned layers. After an hour (about 20 layers) the roller had moved the parts and canyons ran down the length of all parts in the bed. The build was stopped.

This roller bumping could be caused by plowing (the powder ahead of the roller shearing the previous layers in the bed) or by the onset of more significant shrinkage after the first 4 layers. Since plowing was not a problem on the 4-layer build and the powder was observed to 'roll' or cascade down the front of the pile at the bottom of the roller, the issue was most likely shrinkage and curl. In nylon, laser scan spacing and part bed temperature (with an appropriately matching feed temperature) are key variables for controlling curl.

2/26/04): Build #2

The feed temperatures were raised from 35 to 40°C. Still, fissures were visible along the parts in the first few layers and became visible after the next layer of powder was rolled, not during the scanning.

The feeds were then set to 50°C and allowed to reach temperature over an hour pause. During rolling short feeds became a problem. The feed distances (raise dist. before each roll) were increased from .008" to .010" even though this tends to shorten the available total build height during production. Faint lines were still observed during scanning.

After increasing the feed temps again to 55°C and allowing for temperature stabilization – short feeds became a problem again. Also, the plumes coming from the scanning front only reach ½ the chamber height instead of reaching the heater plate during the early phases of the build. In addition more powder seemed to ride the face of the roller. Although curl seemed to decrease, short feeds persisted. After a crevice opened in the right feed the build was stopped. The powder feeds had caked in the center but loose powder was still found at the edges.

The instrumentation in the feeds are near the edge of the powder. They are heated by a radiant heater. The center of the feed bed was clearly much hotter than the reading coming from the thermocouples. Also, there seemed to be a long-term thermal transient in the build chamber. If the chamber is inerted there will be gas flow during the build stabilizing the atmosphere. Further strategies for mitigating curl include increasing the layer thickness (from .003") and building a low-power base part to support the real build parts.

3/3/04 : Build #3 (Based on Duraform config.)

The hardened powder was removed from the feeds (.5" was affected, 1" removed). The layer thickness was set to .004". The part bed was set to 40°C, the feeds to 30°C . The feed distances were set to .009" and the scan speed was 49.5 in/sec. In the 5th layer fine lines appear next to parts and alternate sides with the roller. Similar behavior was observed with a subsequent build having a 45°C part bed.

After a soak with a part bed at 50°C the build again curled, but was improved. Additional improvement was seen with the part bed at 55°C and the feeds at 40°C . The duty cycle of the right feed indicates some problem with the

temperature control. The thermocouple was noticed to be lower in the powder than the left. Fissure still appear after 7 layers.

It was noted that a lower shrinkage powder preparation (attritor milled) might be needed for this binder to work. Wider scan spacing can also influence curl.

3/3/04 : Build #4 (Scan spacing, new temperatures, range of powers)

A single layer of bend test bars was prepared. The right feed was set to 35°C, the left to 40°C and the part bed to 70°C. This was the first completed build. All parts were easily removed from the bed and exhibited solid strength. The parts were examined with a brush and an X-acto blade for delamination or layering effects. The sides of the parts showed some layering, but layering did not worsen with brushing.

Part	Power	Scan Spacing	Results
1	8	.004″	Least visible curl
2	8	.003″	
3	8	.003″	
4	9	.003″	
5	9	.003″	
6	10	.003″	Worst curl (small fissures visible at end of build)
7	10	.003″	
8	10	.004″	Comparable appearance to #2 & 3

3/4/04 Build #5: (New part setup)

A new build was prepared. 5 bend test bars were aligned along the X axis (the direction the roller moves) in two layers. Logo parts were also added in ¾ height versions (.375″ high) to coincide with the two layers of bars. The part bed temperature was increased to 75°C. No curl was visible on any of the parts. Upon breakout a layer of powder clung to the parts but was easily removed with a brush. The layer cycle time was 2:30.

Part	Power	Scan Spacing	Results
1	6	.004″	Weak part. Powder easily scraped off. Brush shows deep layering.
2	7	.004″	Stronger, but still somewhat weak. Brush shows layering on sides.

3	8	.003″	Strong, sidewalls smooth brush does not deepen appearance of layering.
4	8	.004″	Still strong same as above.
5	10	.003″	Stronger than 8W parts
Logo	8	.004″	Clear logo. Strong part
Logo	10	.004″	Clear logo. Slightly darker in color.

3/4/04 : Build #6 Breakout test parts

A layer of logo and breakout parts was prepared and left for the evening with previous parameters intact. Breakout parts were built with 8, 9 and 10W scans at .004″ scan spacing. The smallest features of the breakout parts (.020″) were easily broken, but were noticeably more resilient in the 10W parts. The smallest cavities (.020″) were slightly more filled in on the higher power parts.

3/5/04 : Build #7 Parts for bend testing

Labled BTB parts were prepared for 8-11 W and for green, post-cured, brown and infiltrated conditions. The spacing between the bend parts was changed to .100″ in all directions. Eight ¾ size logo parts were also added to the build. The powder sat at temperature for 5-6 hours before the build began.

The parts bumped and were progressively worse throughout the build. The logo parts showed pitting on the side facing the BTB part array, but were otherwise in good shape. The close spacing caused curl and other problems.

3/8/04 : Build #8 Bend testing array

The same parts were re-arranged and spread over a larger area of the part bed. Although a small fissure was visible at the right front of the build at the 8th layer, non was observed at several junctures later in the build.

The build completed and the parts show good shape. However the strength of the parts is significantly lower than similar powers in previous builds. The powder is degrading. More research is needed before another build can be prepared.

Brown Parts (3/8-3/10) :

Previous brown parts had been weak and carbon had obviously been lost. This was expected to be caused by the presence of oxygen, in other words a leaky furnace. Even forming gas (containing hydrogen to grab oxygen) had not fixed the problem. The furnace was sealed more carefully with vacuum grease and a

new tubing setup. A bubble tank was added to the outlet to measure outbound flow rate. Another lab running similar furnaces uses 2 bubbles/ sec as a rule-of-thumb inerting flow. An 8W BTB was placed across a 4″ long alumina crucible which left 3.75″ of the 5″ part suspended between the walls. The furnace was purged for 10 minutes and the temperature was ramped from ambient to 800°C at 1°C/ min. After a soak for 4 hours the furnace was shut down. When the temperature fell below 300°C the gas was turned off and the furnace was opened for more rapid cooling to ambient. The part completely collapsed and the remaining form was nearly powder. The weight loss needed assessment and the gas flow was not constant throughout the build – it stopped for a time at temperature.

Another 8W BTB part was weighed along with a cured piece phenolic. Each was placed in a separate crucible. The furnace was sealed and the regulator was set for more consistent operation. The weight loss of the BTB part matched the expected 50% weight loss of the phenolic exactly. The phenolic part lost 43% of its weight and experienced and isotropic shrinkage of approximately 20%. The BTB part retained its strength.

Appendix 3 Infiltrated Parts Data

Table 24 ASTM D-790 Data for Epoxy Infiltrated Parts

Part Desc.	#	Width (in)	Depth (in)	Force (kg)	Deflection (mm)	Flexural Strength (Mpa)	Flexural Strain (mm/mm)	Flexural Modulus (Mpa)
Soft Cure BJB Epoxy	1	0.513	0.141	13.67	-	76.40	-	
	2	0.513	0.136	12.85	-	77.20	-	
	3	0.508	0.139	12.45	-	72.30	-	
	4	0.510	0.139	12.70	-	73.47	-	
AVERAGES		0.511	0.139	12.918		**74.84**		
Bars Oriented in X-Direction	1	0.523	0.150	20.83	1.547	100.90	8.770E-03	11504.6
	2	0.531	0.150	24.00	1.801	114.50	1.021E-02	11214.4
	3	0.525	0.148	22.38	1.729	110.93	9.672E-03	11470.1
	4	0.519	0.149	21.08	1.600	104.28	9.010E-03	11573.7
	5	0.524	0.150	22.11	1.701	106.90	9.643E-03	11084.8
	6	0.526	0.147	20.40	1.654	102.30	9.189E-03	11132.8
	7	0.518	0.153	19.78	1.531	92.98	8.853E-03	10502.5
	8	0.525	0.150	21.90	1.697	105.68	9.621E-03	10984.4
	9	0.518	0.152	22.38	1.643	106.59	9.439E-03	11293.0
	10	0.518	0.151	22.02	1.658	106.27	9.462E-03	11231.0
	11	0.522	0.152	22.86	1.829	108.04	1.051E-02	10282.7
AVERAGES		0.523	0.150	21.795	1.672	**105.40**	9.489E-03	**11115.8**
Bars Oriented in Y-Direction	1	0.533	0.156	17.49	1.122	76.86	6.615E-03	11618.3
	2	0.531	0.153	21.61	1.610	99.10	9.310E-03	10644.1
	3	0.525	0.150	19.25	1.373	92.89	7.784E-03	11933.7
	4	0.532	0.152	19.16	1.301	88.85	7.474E-03	11888.4
	5	0.532	0.148	16.43	1.532	80.37	8.570E-03	9378.4
	6	0.527	0.151	19.30	1.289	91.55	7.356E-03	12445.4
	7	0.521	0.140	17.22	1.515	96.12	8.016E-03	11990.7
AVERAGES		0.529	0.150	18.637	1.392	**89.39**	7.875E-03	**11414.1**
Phenglass Full Cure	1	0.521	0.260	21.07	1.734	68.20	4.260E-03	16010.1
	2	0.531	0.268	22.71	1.645	67.88	4.166E-03	16296.3
	3	0.527	0.265	19.06	1.376	58.71	3.445E-03	17040.9
	4	0.529	0.271	20.79	1.391	61.01	3.562E-03	17127.8
	5	0.529	0.271	21.30	1.349	62.50	3.454E-03	18094.3
	6	0.519	0.258	20.42	1.608	67.39	3.920E-03	17190.2
	7	0.532	0.262	22.25	1.737	69.46	4.300E-03	16152.9
	8	0.526	0.265	19.01	1.353	58.67	3.388E-03	17318.0
AVERAGES		0.527	0.265	20.826	1.524	**64.23**	3.812E-03	**16903.8**

Table 25 ASTM D-790 Testing on Si Infiltrated SiC (courtesy of D. Bourell and S. Barrow)

Part Description	#	Flex Strength (Mpa)	Average	Std. Dev.
Epoxy Infiltrated Green Part	e1	140.03	147.26	14.06
	e2	140.67		
	e3	172.36		
	e4	140.76		
	e5	142.47		
Raw Green Part	n3	170.99	163.60	12.93
	n4	144.28		
	n5	168.52		
	n8	170.62		
Brown Part	b1	3.35	3.70	0.55
	b2	4.52		
	b3	3.49		
	b4	3.42		

Appendix 4 Int'l I2P Presentation

The International Idea to Product Competition was held on Nov. 7&8, 2003. Donnie Vanelli and the author prepared the following presentation based ontheir entry in the local competition and additional industry research and interviews. They were awarded second place.

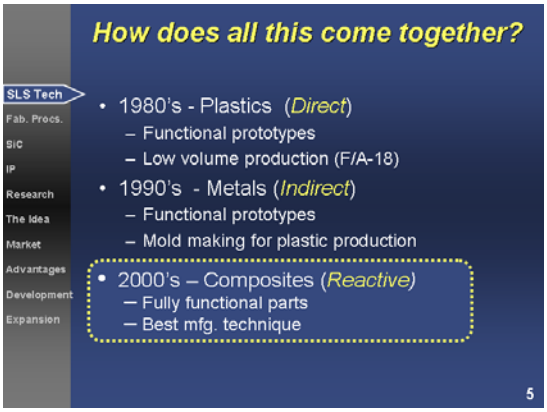

What's your manufacturing process?

SLS Tech.
Fab Procs.
SiC
IP
Research
The Idea
Market
Advantages
Development
Expansion

SLS Final Part Shape (Green Part)

Turn the Binder to Carbon in a Furnace (Brown Part)

Infiltrate with Liquid Metal to Form MMC

7

What's special about Silicon Carbide?

SLS Tech.
Fab. Procs.
SiC
IP
Research
The Idea
Market
Advantages
Development
Expansion

- Hardness
- Heat resistance
- Abrasion resistance
- Thermal conductivity
- Corrosion resistance

Critical for Metal Casting

Very Difficult to Manufacture Products ($400/cubic inch)

But, the powder is cheap ($2/pound), and readily available

8

Proprietary Position

SLS Tech.
Fab. Procs.
SiC
IP
Research
The Idea
Market
Advantages
Development
Expansion

- SLS & SLS Materials
  - Invented at UT
  - Leading licensing revenue technology
  - Advanced Manufacturing Center
- SiC Patent
- Binder
  - Trade Secret
  - Enables reactive MMC formation

9

Spring 2003

SLS Tech.
Fab. Procs.
SiC
IP
Research
The Idea
Market
Advantages
Development
Expansion

- Faculty Researchers
- Commercialization Grant
- Semiconductor Application
  - Tough qualification process
  - Needing a commercial partner

10

The Idea

Selective Laser Sintering of Silicon Carbide

11

The US Metal Casting Industry

"Revolutionary technologies should be investigated."

Cast Metals Coalition
A Vision for the US Metal Casting Industry
May, 2002

The Product

Silicon Carbide Tooling for Metal Casting

Metal Casting Market

SLS Tech.
Fab. Procs.
SiC
IP
Research
The Idea
Market
Advantages
Development
Expansion

Metal Casting Industry

- 90% of a manufactured products contain cast metal parts
- $120B in cast metal parts produced worldwide
- $30B in cast metal parts produced in the U.S.
- Trend to increasing complexity parts in U.S.

Casting Trade, 1999

15

Market Focus

SLS Tech.
Fab. Procs.
SiC
IP
Research
The Idea
Market
Advantages
Development
Expansion

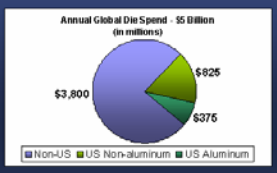

- $5B annual global die spend
- $1.2B die spend in the U.S.
- $375 million on aluminum casting dies

World Foundry Congress, 1999

16

Competitive Advantage

SLS Tech.
Fab. Procs.
SiC
IP
Research
The Idea
Market
Advantages
Development
Expansion

Rapid production

- Design Time for Die – 7-13 days
- Delivery Time for complex dies = 78 - 112 days
- ***Our time – 15-20 days***
- ***Simultaneous builds of dies***

"We offer our customers three levels of speed, at three different prices... 95% of the time they choose the fastest with almost no regard to price difference"
Solidiform
Aluminum Casting

17

Competitive Advantage

SLS Tech.
Fab. Procs.
SiC
IP
Research
The Idea
Market
Advantages
Development
Expansion

Superior Material

- Increased die life
  - Current die life 200,000 cycles
  - *Resistance to thermal shock, abrasion, and chemical attack*
- Improved Cycle Time
  - Cooling without loss of die life

"If you quench the tool steel dies to improve cycle times, you reduce their life by a factor of ten..."
Casting Engineer
LA Aluminum, Inc.

18

SLS Tech.
Fab. Procs.
SiC
IP
Research
The Idea
Market
Advantages
Development
Expansion

Cost Pressures in Aluminum Casting

"SciCast recently bid on a 550,000 piece job, offering to make the tool for $28,000 and the pieces for 42 cents each…The overseas price was $5,000 for the tool, less than 20 cents per part…."

Harold Brubaker
Philadelphia Inquirer, 2/9/03

19

SLS Tech.
Fab. Procs.
SiC
IP
Research
The Idea
Market
Advantages
Development
Expansion

Compare the numbers…

Aluminum Piston Part
0.86 lb part, 1,200,000 part run
1" thick, 5" diameter part

Average Offshore Quote
Tool cost: $28,726
First article lead time: 14.5 weeks

National American Die Casting Association
2002 Quotation Benchmarking Study

SLS Tool Quote
Total $4,940
First article lead time: 4 weeks

Harvest Technologies, Inc.
SLS Production

20

SLS Tech.
Fab. Procs.
SiC
IP
Research
The Idea
Market
Advantages
Development
Expansion

Launch

- New Intellectual Property
  - SLS of SiC Die
  - Additional MMC materials
  - New applications
- Team
  - 2 Phd Engineers
  - Faculty Inventors
  - Angel Investors
  - SLS Manufacturing Partner

21

SLS Tech.
Fab. Procs.
SiC
IP
Research
The Idea
Market
Advantages
Development
Expansion

Development

Completed
- '01 - Proof of concept, SiC/SLS
- '01 - Grant funding
- S'03 - Market analysis
- Su-F'03 - Business formation
  - License and funding
  - Development partnerships
  - New Product Target supported Grant Matching

Going Forward
- F'03 - Binder optimization
- S'04 - Infiltration study
- Su'04 - Casting qualification and expertise
- F'04+ - Market expansion
  - Materials
  - Application expansion

22

SLS Tech.
Fab. Procs.
SiC
IP
Research
The Idea
Market
Advantages
Development
Expansion

Expansion options…

- Other Applications
  - abrasion resistant seals, bearings
  - blast nozzles, ceramic armor
- Technology Development
  - semiconductor processing equipment
  - high performance brakes
  - turbine blades
- Follow-on Materials
  - other SiC infiltrants (aluminum, titanium)
  - other Metal Matrix Composites (tungsten carbide)

23

SLS Tech.
Fab. Procs.
SiC
IP
Research
The Idea
Market
Advantages
Development
Expansion

The brass tacks…

- The Idea
  - Reactive SLS
  - Binder Technology
- The Product
  - Large Market
  - Burning Need
  - Significant Advantages
  - Wide Expansion Opportunities

24

Questions

- Metal Casting Market
- Aluminum Casting Market
- Tooling Materials Comparison
- Reactive MMC Formation
- SLS
- Team, Barriers, Business Ops.

25

The Process : #2- SLS Carbonization

SLS Tech.
Fab. Procs.
SiC
IP
Research
The Idea
Market
Advantages
Development
Expansion

- Powders are mixed and layered via SLS

26

The Process : #4 - Infiltration

SLS Tech.
Fab. Procs.
SiC
IP
Research
The Idea
Market
Advantages
Development
Expansion

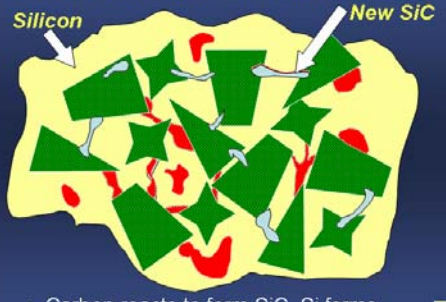

- Carbon reacts to form SiC, Si forms matrix

27

How does SLS work?

SLS Tech.
Fab. Procs.
SiC
IP
Research
The Idea
Market
Advantages
Development
Expansion

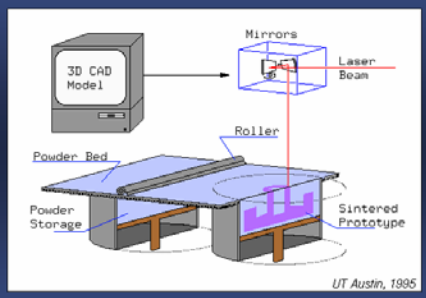

28

SiC versus Tool Steel

SLS Tech.
Fab. Procs.
SiC
IP
Research
The Idea
Market
Advantages
Development
Expansion

Reaction Bonded Silicon Carbide (Si2C)

- Thermal conductivity (145 W/m K)
- Thermal expansion coefficient (4.3 x 10 -6 /C)
- Maximum use temperature (1375 C)
- Hardness (2500 VHN)

Tool Steel (Traditional Aluminum Mold Material)

- Thermal conductivity (20 W/m K)
- Thermal expansion coefficient (12 x 10 -6 /C)
- Maximum use temperature (850 C)
- Hardness (700 VHN)

29

Tooling Cost Comparison

SLS Tech.
Fab. Procs.
SiC
IP
Research
The Idea
Market
Advantages
Development
Expansion

SLS Process

- Setup
- Hourly SLS Usage
- Materials
- Furnace
- Finishing

Tool Steel (Traditional Mold Material)

- Multiple milling machines
- Annealing Furnaces
- Machinist on each mill
- Annealing technicians

30

SLS Tech.
Fab. Procs.
SiC
IP
Research
The Idea
Market
Advantages
Development
Expansion

Industry Composition

Metal Casters

- 2,950 US Facilities
- Average employees : 60-70
- Less than 200 employ over 250

Mold Making Industry

- 4,200 companies
- Traditional heavy industry geography
- Average shop employs 37 workers
- $2,000,000 average shop revenue

31

Casting Industry

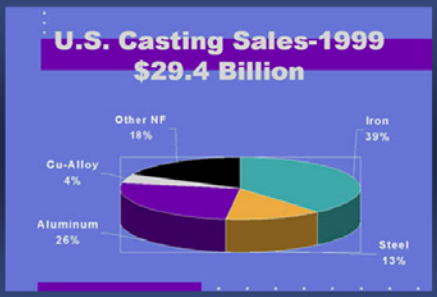

32

Supply and End Use

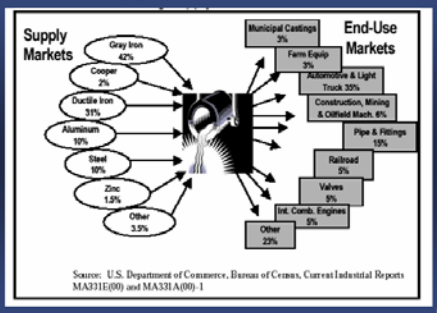

33

Why Aluminum?

- Common material - $9B in US castings
- Used in many small parts
- Higher complexity cast parts
- Lowest tool life among non-ferrous metals
- Lowest disparity in tool costs to offshore source
  - Aluminum – 57% lower
  - Magnesium – 70% lower
  - Zinc – 81% lower

34

Aluminum Market Trends

Foundry survey – 44% expect increased demand

35

How does casting work?

- Press the mold
- Inject molten metal
- Allow metal to harden
- Open press
- Remove parts
- Repeat

36

SLS Tech.
Fab. Procs.
SiC
IP
Research
The Idea
Market
Advantages
Development
Expansion

Who is the team?

- Two Phd engineering candidates
  - Materials science
  - Technology commercialization
- UT-Austin faculty
  - SLS machine technology
  - SLS materials
- Angel investors
  - Financial resources
  - 20 startup companies, private and public
  - Chemical engineering and processing background and industry ties
- Harvest Technologies (SLS manufacturer)
  - SLS production knowledge and process
  - Existing customer base

37

SLS Tech.
Fab. Procs.
SiC
IP
Research
The Idea
Market
Advantages
Development
Expansion

How will you address the barriers?

- Fragmented Industry
  - *Partnerships and associations*
- Tradition and Art
  - *Technology based solution*
- New Molding Procedures and Training
  - *Development of best practices*
- High Capital Cost Machines
  - *Leverage UT R&D facilities, partnerships*

38

SLS Tech.
Fab. Procs.
SiC
IP
Research
The Idea
Market
Advantages
Development
Expansion

Business Operations

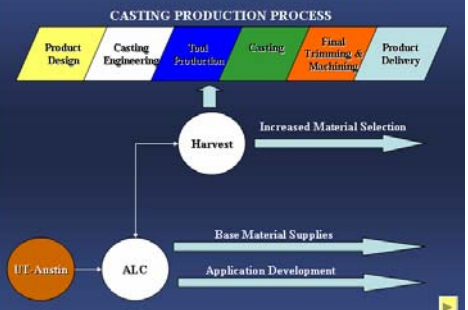

39

Appendix 5 Shirley Murphy Business Plan Comp. - Presentation

The following presentation was prepared for the final round of the Shirley Murphy Business Plan Competition, at the University of North Texas November 13 , 2003. The work was based on work done for the Venture Creation Course during Spring of 2003 and on the Local Idea to Product entry also prepared by Donnie Vanelli and the author. This business plan was selected as one of four entries for the final round. The final round consisted of a presentation in front of Dallas-area business leaders. Donnie Vanelli and the author prepared it based on the business plan submitted, and shown above. Chris Schaefer, an undergraduate mechanical engineering student added some additional research, customer interviews and edits. The three members of the team were all engineering majors and were awarded the first prize (and $25,000) in the competition.

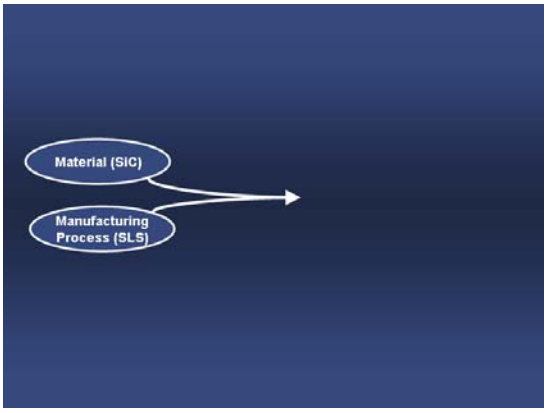

What's special about Silicon Carbide?

Technology
Applications
Market
Vision
Focus
Advantages
Launch Plan
Strategy
Financials
Team
Status
IP
Leadership

- Hardness
- Heat resistance
- Abrasion resistance
- Thermal conductivity
- Corrosion resistance

Very Difficult to Manufacture Products ($400/cubic inch)

But, the powder is cheap ($2/pound), and readily available

Advanced Laser Composites, LLC Better parts for parts™ 3

From Powder to Parts…

Technology
Applications
Market
Vision
Focus
Advantages
Launch Plan
Strategy
Financials
Team
Status
IP
Leadership

- Selective Laser Sintering (SLS)

Advanced Laser Composites, LLC Better parts for parts™ 4

The Technology

Material (SiC)

Manufacturing Process (SLS)

Advanced Laser Composites, LLC

- Materials technology
- MMC manufacturing
- Fully functional parts

Advanced Laser Composites, LLC Better parts for parts™ 5

The Applications

Material (SiC)

Manufacturing Process (SLS)

Machine Seals
Semiconductor Fab.
Metal Casting
Turbines
Military

Advanced Laser Composites, LLC Better parts for parts™ 6

Let's talk about Metal Casting…

"Pressure from offshore sources (is) primarily due to lower tooling costs"

-2002 Quotation Benchmark Study, Feb. 3, 2003

Tooling for metal casting…

"…(Tool making) is one of the few activities connected with modern large-scale industry in which there has not been a general substitution of machinery for basic skills.

These tools are custom-made, one-at-a-time by skilled artisans who patiently and precisely machine, finish, and construct the complicated devices. …."

Arnett, Smith
Tool and Die Making

The Metal Casting Process

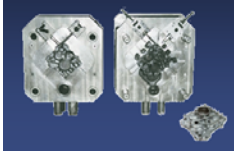

The Vision

We make better metal casting tooling faster and with higher margins.

Our t… …cturing conce… …tooling to the m…

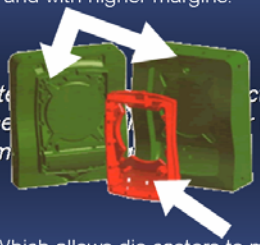

…Which allows die casters to more rapidly and more competitively mass produce their metal parts.

1

The Value Chain

Technology
Applications
Market
Vision
Focus
Advantages
Launch Plan
Strategy
Financials
Team
Status
IP
Leadership

Product Design
Tooling Engineering
Tool Making
Metal Casting (Mass Prod.)
Product Finishing
Delivery

- Market need
- Design – (prototype)
- Design the tooling
- Make the tooling – $5B
- Cast the part – $120B
- Assemble into the final product

Advanced Laser Composites, LLC Better parts for parts™ 12

Market Segmentation

Technology
Applications
Market
Vision
Focus
Advantages
Launch Plan
Strategy
Financials
Team
Status
IP
Leadership

Die Making Market Analysis

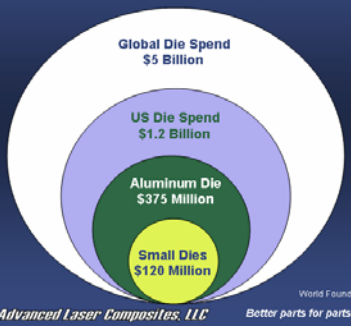

World Foundry Congress, 1999

Advanced Laser Composites, LLC Better parts for parts™ 13

Why Aluminum Casting Tooling?

Technology
Applications
Market
Vision
Focus
Advantages
Launch Plan
Strategy
Financials
Team
Status
IP
Leadership

- Common material
- High growth
- Many small parts
- High complexity castings
- Lowest tool life
- Lowest tool costs ratio to offshore source
  - Aluminum – 57% lower
  - Magnesium – 70% lower
  - Zinc – 81% lower

North American Die Casters Association

Advanced Laser Composites, LLC Better parts for parts™ 14

Technology
Applications
Market
Vision
Focus
Advantages
Launch Plan
Strategy
Financials
Team
Status
IP
Leadership

Competitive Advantage

RAPID PRODUCTION

– Current delivery time = 78 -112 days

– *Our time = 15-20 days*

"We would pay three times as much to get a part twice as fast."

"How fast we can get a die is often the main determining factor in whether we make a new part..."
Rob Arfele
Halliburton

"We offer our customers three levels of speed, at three different prices... 95% of the time they choose the fastest with almost no regard to price difference"
Solidiform
Aluminum Casting

Technology
Applications
Market
Vision
Focus
Advantages
Launch Plan
Strategy
Financials
Team
Status
IP
Leadership

Competitive Advantage

LONGER LIFE

– Current die life 200,000 cycles

– *Our die life – 3-5X*

"Product maximization, in other words, getting the most cast parts per Die is the most important factor in our die purchasing."
Russell Lay
St. Paul Brass and Aluminum

"If you quench the tool steel dies to improve cycle times, you reduce their life by a factor of ten..."
Casting Engineer
LA Aluminum, Inc.

Technology
Applications
Market
Vision
Focus
Advantages
Launch Plan
Strategy
Financials
Team
Status
IP
Leadership

Competitive Advantage

FASTER CASTING

– Cooling represents half of the casting time per part

– *Our cooling time – 1/3*

"If you quench the tool steel dies to improve cycle times, you reduce their life by a factor of ten..."
Casting Engineer
LA Aluminum, Inc.

"50% of our cycle time is spent 'waiting to cool'..."
Arney Tyler
LA Aluminum, Inc.

Launch Timeline

Business Development

Technology
Applications
Market
Vision
Focus
Advantages
Launch Plan
Strategy
Financials
Team
Status
IP
Leadership

Research and Development, Product Qualification

- Research and Development
  - Binder optimization
  - Infiltration refinement
- Product Qualification
  - Stealth Partner
  - Die qualification
  - Commercial acceptance

Technology
Applications
Market
Vision
Focus
Advantages
Launch Plan
Strategy
Financials
Team
Status
IP
Leadership

Process Refinement, Market Capture

- Process Refinement
  - Manufacturing Setup
  - Production Process Optimization
- Market Capture
  - Maximize Tolling Partner
  - Capacity Expansion
  - R&D to new applications

Marketing Strategy

Technology
Applications
Market
Vision
Focus
Advantages
Launch Plan
Strategy
Financials
Team
Status
IP
Leadership

Product Design → Market Entry

Harvest Technologies
- Joint venture partner
- 3,000 customers
- Rapid prototyping, patterns

Tooling Engineering

Tool Making → Market Capture

Advanced Laser Composites
- Tooling engineer expert
- Industry Journal articles
- Trade Associations
  - NADCA
  - AMBA
- Active sales force

Metal Casting (Mass Prod.)

Product Finishing

Delivery

Advanced Laser Composites, LLC Better parts for parts™ 21

Basic Production Model

Technology
Applications
Market
Vision
Focus
Advantages
Launch Plan
Strategy
Financial
Team
Status
IP
Leadership

SLS Machine ~$400K
~$150K High Temp Furnace
~$150K High Temp Furnace
CNC Mill ~$50K
Finished Product

Manpower - 1 operator per production unit

Production Output ~ 90 dies/year per production unit

Average US Small Die Cost ~ $30,000/die

Yearly revenue ~ $2,700,000/production unit

Advanced Laser Composites, LLC Better parts for parts™ 22

Financials

Summary Financials

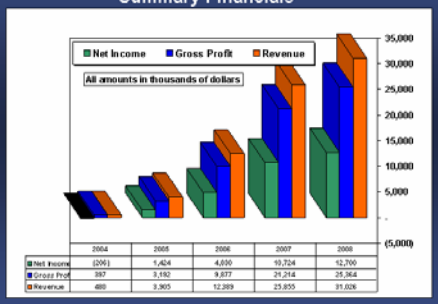

Technology
Applications
Market
Vision
Focus
Advantages
Launch Plan
Strategy
Financial
Team
Status
IP
Leadership

Advanced Laser Composites, LLC Better parts for parts™ 23

ALC is looking for…

Technology
Applications
Market
Vision
Focus
Advantages
Launch Plan
Strategy
Financials
Team
Status
IP
Leadership

- Year 1 Investment of $500,000
  - Product Refinement
  - Qtr 4, 2004 Break Even
  - Contingency Cash Fund
- Product Qualification Partner
  - Product verification
  - Product credibility

Advanced Laser Composites, LLC Better parts for parts™ 24

Exit Strategy

Technology
Applications
Market
Vision
Focus
Advantages
Launch Plan
Strategy
Financials
Team
Status
IP
Leadership

- Acquisition Partners
  - Casting company
  - Assembled products manufacturer
- Public Launch
  - Integrated group of companies
    - SLS Commercial Partner
    - R&D Operation
    - Materials supply

Advanced Laser Composites, LLC Better parts for parts™ 25

Who is the team?

Operating Team

Technology
Applications
Market
Vision
Focus
Advantages
Launch Plan
Strategy
Financials
Team
Status
IP
Leadership

- **Scott Evans**
  - Vice President, Manufacturing and Technology
    - Phd candidate, materials science
    - Manufacturing systems and product design experience
- **Chris Schaefer**
  - Applications Engineer & Technical Sales
    - Mechanical engineer, business minor
    - Halliburton, tooling applications engineer
- **Donnie Vanelli**
  - Vice President, Marketing and Development
    - Phd candidate, technology commercialization
    - Mechanical and electrical engineer

Advanced Laser Composites, LLC Better parts for parts™ 26

Technology
Applications
Market
Vision
Focus
Advantages
Launch Plan
Strategy
Financials
Team
Status
IP
Leadership

Who is the team?

Advisory Team

- **Bruce Thornton**
  - Chairman, ALC Board of Managers
    - President, CMS Technologies
    - UT-Austin entrepreneur in residence
- **Dudley Warner**
  - VP, CMS Technologies
  - Extensive start-up, chemical engineering expertise
- **Bill McMinn**
  - 'Super-angel'
  - Former senior executive, Sterling Chemical Group
- **Matt Miller**
  - President, Hickory Acquisitions Group
  - Former VP Georgia Pacific Chemicals

Venture Status

- Silicon carbide prototype
- Grant funding
- Business formation
- Seed investment
- License agreement
- Research plan
- Austin Technology Incubator member

Proprietary Position

- Patent
  - Filed, 1999
  - Silicon carbide and SLS
- License Agreement
  - Exclusive license
  - All fields of use
- Additional IP
  - Binder material
  - Enables multiple metal matrix composites
  - Trade secret and future patents

Staying ahead…

R&D FOUNDATIONS

- UT-Austin Research Partnership
  - Dr. Joe Beaman, Dr. David Bourell
- Advanced Manufacturing Center
  - SLS materials and process development
- ALC Research Team
  - Visiting scientists at UT-Austin
  - Engineering and process expertise
- Commercial Joint Venture Partner
  - SLS production
  - Market testing

Market Outreach…

Summary

- Innovative technology
- Burning industry need
- Superior product
- Solid launch team
- Strong IP and R&D assets

Our technology and manufacturing concept will provide superior tooling to the metal casting industry.

Advanced Laser Composites, LLC

What's so great about SLS?

- Fast
- Complex Geometry
- Material Variety
- Low Labor
- Not for mass production

How does SLS work?

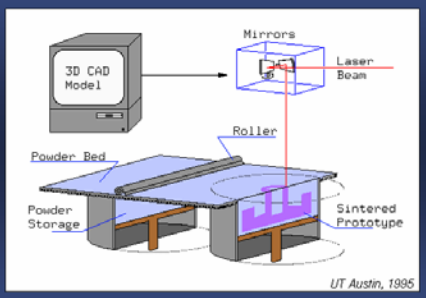

What can you build?

- 1980's - Plastics (*Direct*)
  - Functional prototypes
  - Low volume production (F/A-18)
- 1990's - Metals (*Indirect*)
  - Functional prototypes
  - Mold making for plastic production
- 2000's – Composites (*Reactive*)
  - Fully functional parts
  - Composites from cheap powder
  - Best manufacturing technique

What's the "reactive" process?

SLS Final Part Shape (Green Part)

Turn the Binder to Carbon in a Furnace (Brown Part)

Infiltrate with Liquid Metal to Form MMC

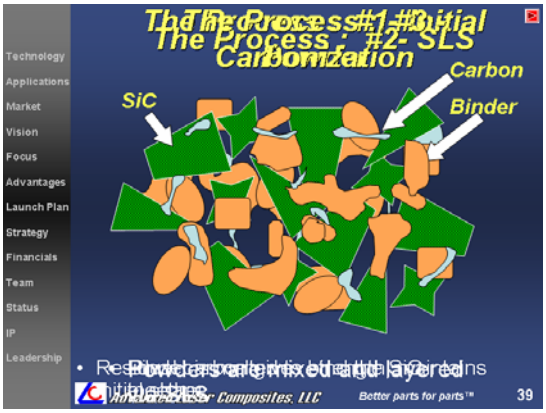
The Process : #2- SLS
Carbonization
Carbon
Binder
SiC
Technology
Applications
Market
Vision
Focus
Advantages
Launch Plan
Strategy
Financials
Team
Status
IP
Leadership
Advanced Laser Composites, LLC
Better parts for parts™
39

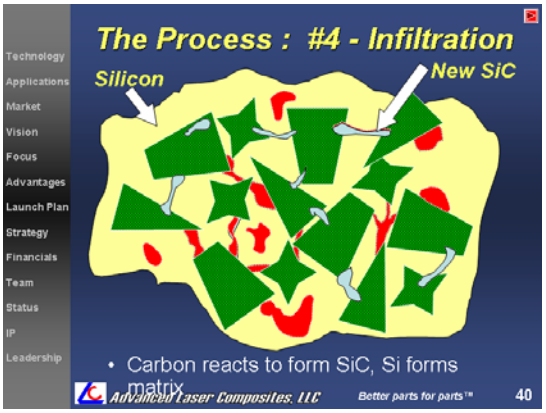
The Process : #4 - Infiltration
Silicon
New SiC
• Carbon reacts to form SiC, Si forms matrix
Technology
Applications
Market
Vision
Focus
Advantages
Launch Plan
Strategy
Financials
Team
Status
IP
Leadership
Advanced Laser Composites, LLC
Better parts for parts™
40

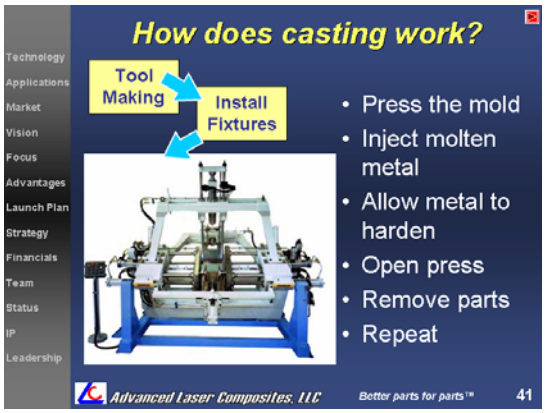
How does casting work?
Tool Making
Install Fixtures
• Press the mold
• Inject molten metal
• Allow metal to harden
• Open press
• Remove parts
• Repeat
Technology
Applications
Market
Vision
Focus
Advantages
Launch Plan
Strategy
Financials
Team
Status
IP
Leadership
Advanced Laser Composites, LLC
Better parts for parts™
41

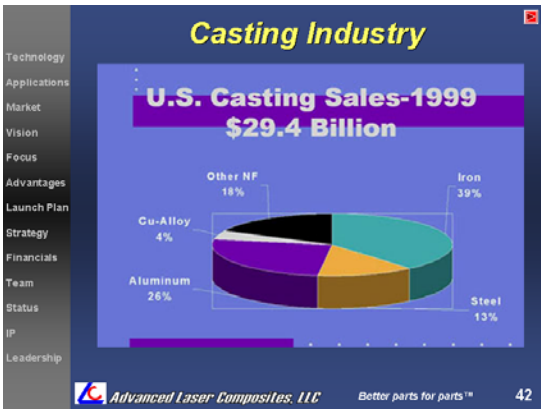
Casting Industry
U.S. Casting Sales-1999
$29.4 Billion
Other NF 18%
Iron 39%
Cu-Alloy 4%
Aluminum 26%
Steel 13%
Technology
Applications
Market
Vision
Focus
Advantages
Launch Plan
Strategy
Financials
Team
Status
IP
Leadership
Advanced Laser Composites, LLC
Better parts for parts™
42

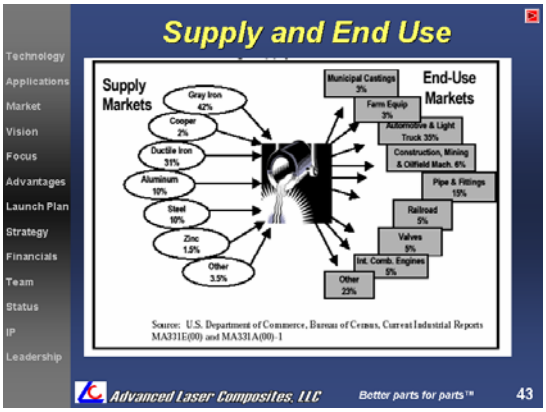
Supply and End Use
Supply Markets
End-Use Markets
Gray Iron 42%
Cooper 2%
Ductile Iron 31%
Aluminum 10%
Steel 10%
Zinc 1.5%
Other 3.5%
Municipal Castings 3%
Farm Equip 3%
Automotive & Light Truck 33%
Construction, Mining & Oilfield Mach. 6%
Pipe & Fittings 15%
Railroad 5%
Valves 5%
Int. Comb. Engines 5%
Other 23%
Source: U.S. Department of Commerce, Bureau of Census, Current Industrial Reports MA331E(00) and MA331A(00)-1
Technology
Applications
Market
Vision
Focus
Advantages
Launch Plan
Strategy
Financials
Team
Status
IP
Leadership
Advanced Laser Composites, LLC
Better parts for parts™
43

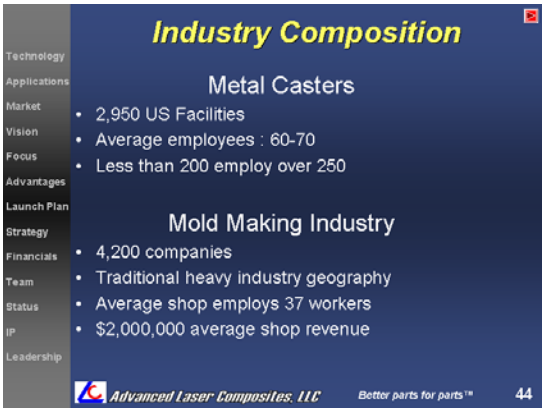
Industry Composition
Metal Casters
• 2,950 US Facilities
• Average employees : 60-70
• Less than 200 employ over 250
Mold Making Industry
• 4,200 companies
• Traditional heavy industry geography
• Average shop employs 37 workers
• $2,000,000 average shop revenue
Technology
Applications
Market
Vision
Focus
Advantages
Launch Plan
Strategy
Financials
Team
Status
IP
Leadership
Advanced Laser Composites, LLC
Better parts for parts™
44

Casting Company Costing Profiles

%Cost breakdown

- Factory Shipping 77%
  - Labor (20%), Materials (22%)
- Sales 3%
- General and Admin 11%
- Other 7%
- Profit 2%

Sapolsky Research Inc.
Confidential Metalcasting Operational Cost Survey

Market Focus – US Tooling Market

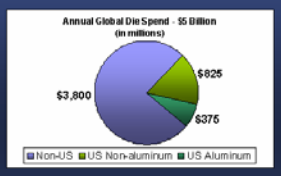

- $5B annual global die spend
- $1.2B die spend in the U.S.
- $375 million on aluminum casting dies

World Foundry Congress, 1999

Market Trends

- Materials with biggest increase in output
  - Aluminum 44%
  - Magnesium 38%
  - Zinc 4%
- Biggest Process Type Increase
  - High Pressure (Die) 16%
- Biggest markets for growth
  - Automotive 56%
  - Applications 10%

NADCA
Die Casting Benchmarking Study

R&D in Casting

R&D Focus in Casting Technologies

- Die Life 18%
- Simulation 12%
- Process Control 12%
- New Casting Tech 8%
- Die Cooling 4%

NADCA
Die Casting Benchmarking Study

Cost Pressures in Aluminum Casting

"SciCast recently bid on a 550,000 piece job, offering to make the tool for $28,000 and the pieces for 42 cents each…The overseas price was $5,000 for the tool, less than 20 cents per part…."

Harold Brubaker
Philadelphia Inquirer, 2/9/03

Aluminum Market Trends

Foundry survey – 44% expect increased demand

Aluminum Dies

- Common causes of rejects for aluminum dies
  - Porosity 31%
  - Short Fill 25%
  - Damage 2%
- Die Life
  - Aluminum 200,000 cycles
  - Magnesium 275,000 cycles
  - Zinc 2,500,000 cycles

NADCA
Die Casting Benchmarking Study

Metal Matrix Composites

- Benefits
  - Superior Performance
    Mechanical, Thermal, Electrical
  - Tailored Properties
- Pains
  - Expensive
  - Many-stage fabrication

SiC versus Tool Steel

Reaction Bonded Silicon Carbide (Si2C)
- Thermal conductivity (145 W/m K)
- Thermal expansion coefficient (4.3 x 10 -6 /C)
- Maximum use temperature (1375 C)
- Hardness (2500 VHN)

Tool Steel (Traditional Aluminum Mold Material)
- Thermal conductivity (20 W/m K)
- Thermal expansion coefficient (12 x 10 -6 /C)
- Maximum use temperature (850 C)
- Hardness (700 VHN)

Cooling time varies with the inverse of HTC.

What about CNC machining?

- On average, lead times were 12 weeks prior to the use of unattended machining. That is now down to an average of 10 weeks with unattended machining.

– AMBA Business Forecast Survey, 2002

Market Flow

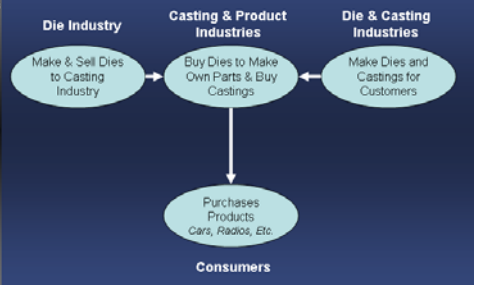

Barriers to Entry

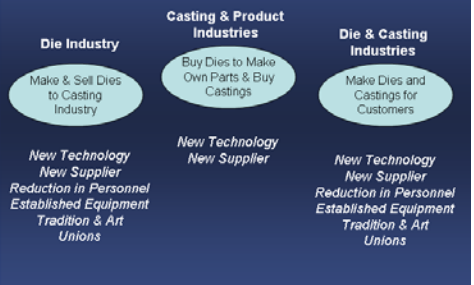

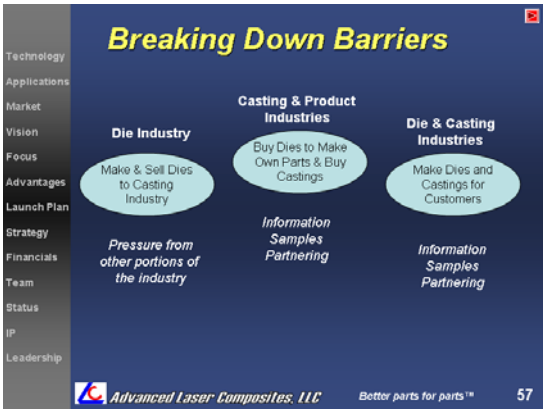
Technology
Applications
Market
Vision
Focus
Advantages
Launch Plan
Strategy
Financials
Team
Status
IP
Leadership
Breaking Down Barriers
Die Industry
Make & Sell Dies to Casting Industry
Pressure from other portions of the industry
Casting & Product Industries
Buy Dies to Make Own Parts & Buy Castings
Information
Samples
Partnering
Die & Casting Industries
Make Dies and Castings for Customers
Information
Samples
Partnering
Advanced Laser Composites, LLC
Better parts for parts™
57

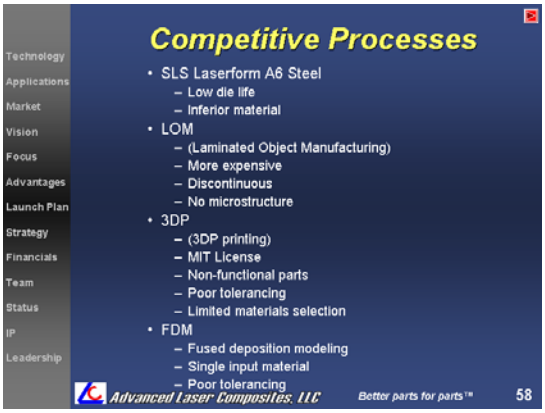
Technology
Applications
Market
Vision
Focus
Advantages
Launch Plan
Strategy
Financials
Team
Status
IP
Leadership
Competitive Processes
• SLS Laserform A6 Steel
– Low die life
– Inferior material
• LOM
– (Laminated Object Manufacturing)
– More expensive
– Discontinuous
– No microstructure
• 3DP
– (3DP printing)
– MIT License
– Non-functional parts
– Poor tolerancing
– Limited materials selection
• FDM
– Fused deposition modeling
– Single input material
– Poor tolerancing
Advanced Laser Composites, LLC
Better parts for parts™
58

Appendix 6 ISLS Platform Product Cost Model

Product	4x4x4" Duraform Block	4x4x4" Phenolic/ Glass/ DCPD	4x4x4" Windform	4x4x4" Phenolic/ Alumina/ DCPD
Margin	21.84%	61.77%	1.75%	25.80%
Profit per Build	$ 4,371.28	$ 12,365.81	$ 351.02	$ 5,164.82
Product Price	$ 1,500.00	$ 1,500.00	$ 1,500.00	$ 1,500.00
Mfg. Cost (/ Part)	$ 1,172.44	$ 573.38	$ 1,473.70	$ 1,112.98
Mfg. Cost ($/ build)	$ 15,646.28	$ 7,651.75	$ 19,666.55	$ 14,852.74
Base Materials ($/build)	$ 9,022.57	$ 132.30	$ 13,042.83	$ 7,333.29
Setup ($/build)	$ 565.00	$ 565.00	$ 565.00	$ 565.00
SLS Procs. ($/build)	$ 5,625.00	$ 5,625.00	$ 5,625.00	$ 5,625.00
Infil. Matl's ($/part)	$ -	$ 7.12	$ -	$ 7.12
Infil./ Curing ($/ part)	$ -	$ 60.00	$ -	$ 60.00
Post Processing ($/part)	$ 32.50	$ 32.50	$ 32.50	$ 32.50
Part Vol.	64	64	64	64
Spacing Envelope Vol.	467	467	467	467
Pwdr./ Part	7.296875	7.296875	7.296875	7.296875
Parts/ Build	13.3450416	13.3450416	13.3450416	13.3450416
Furnace (hours/ part)				
Furnace (parts/ run)				
Furnace (hours/ run)				
DCPD (hours/ part)		0.5		0.5
Oven (hours/ part)		1		1
Hand work (hrs/ part)	0.5	0.5	0.5	0.5
CNC/ mach (hrs/ part)	0.25	0.25	0.25	0.25
Packaging ($/part)	$ 2.50	$ 2.50	$ 2.50	$ 2.50

Base Material Const.									
Cost ($/in^3)	$	1.06	$	0.02	$	1.54	$	0.86	
TOTAL FRACT.		100%		100%		100%		100%	
Phenolic				10%				10%	
SiC (280 Grit)								0%	
Potters Glass (Size ?)				90%					
Alumina (34-54micron)								90%	
TiC (-325 mesh)									
WC (-325 mesh)									
Windform GF						100%			
Windform Pro									
Windform Pro B									
Castex 1.0									
Castex 2.0									
Pebax									
Duraform		100%							
Duraform GF									
Castform									
ST-200									

Infiltrant Const.									
Cost ($/in^3)	$	-	$	0.11	$	-	$	0.11	
TOTAL FRACT.		0%		100%		0%		100%	
DCPD				100%				100%	
Si									
Al-Si									
Ductile Iron									
Bronze									
Red Wax									

SLS Process	DTM 2000	2500	VanguardHS
Build Speed (in/hr)	0.2		
Part Bed Area	530.929158		
Total Depth	16		
Build Area	415.475628		
Build Depth	15		
Build Volume	6232.13443		
Extra Powder Volume	2262.73211		

Infiltrant Cost	Cost/in^3	Density	Part Fill %	Price/lb.
DCPD	$ 0.11	1.6	50%	$ 3.85
Si	$ 0.12	3.2	50%	$ 2.00
Al-Si	$ 0.56	2.8	50%	$ 11.00
Ductile Iron	$ 0.41	7.6	50%	$ 3.00
Bronze	$ 0.33	6	50%	$ 3.00
Red Wax	$ 0.01	1.2	50%	$ 0.25

Processing Fees	
Engineering/ Setup	$ 500.00
Material Processing	$ 65.00
Furnace Setup	$ 100.00
Furnace (/hr)	$ 35.00
SLS (/hr)	$ 75.00
Hand Work (/hr)	$ 35.00
CNC Milling (/hr)	$ 50.00
DCPD Infiltration (/hr)	$ 50.00
Oven Processing (/hr)	$ 35.00
Packaging Costs (/unit)	$ 25.00

Material Calculations	Cost/in^3	Bulk Density	Pwdr. Dens.	Price/lb.
Phenolic	$ 0.03	1.3	40%	$ 1.80
SiC (280 Grit)	$ 0.07	3.2	50%	$ 1.20
Potters Glass (Size ?)	$ 0.01	2.5	60%	$ 0.25
Alumina (34-54micron)	$ 0.96	3.965	50%	$ 13.34
TiC (-325 mesh)	$ 2.57	4.93	50%	$ 28.90
WC (-325 mesh)	$ 11.23	15.63	50%	$ 39.76
Windform GF	$ 1.54	1.7	50%	$ 50.00
Windform Pro	$ -			
Windform Pro B	$ -			
Castex 1.0	$ -			
Castex 2.0	$ -			
Pebax	$ -			
Duraform	$ 1.06	0.98	50%	$ 60.00
Duraform GF	$ 1.82	1.68	50%	$ 60.00
Castform	$ -			
ST-200	$ -			

References and Additional Reading

3D Systems, Inc., http://www.3dsystems.com.

Abhinadan, L., Chari, R., Nath, A.K., Trivedi, M.K. (1999), "Laser Curing of Thermosetting Powder Coatings : A Detailed Investigation", *Journal of Laser Applications*, Vol. 11, No. 6, pp.248-57.

Arpón, R., Molina, J.M., Saravanan, R.A., García-Cordovilla, Louis, E., Narciso (2003), "Thermal Expansion Behavior of Aluminum/ SiC Composites with Bimodal particle Distributions", *Acta Materialia*, Vol. 51, pp.3145-56.

Babula, A. J. (1997), "Silicon Carbide : Its Nonabrasive Electrical Properties and Applications," *IEEE Potentials*, Feb./Mar., 1997, p.27-30.

Basu, H., Godkhindi, M.M., Mukunda, P.G. (1999), "Investigation on the Reaction Sintering of Porous Silicon Carbide", *Journal of Materials Science Letters*, Vol. 18, pp. 389-92.

Bhandari, S. (2004), "Binder Optimization for Manufacturing of Silicon Carbide Preforms", Masters thesis, University of Texas at Austin, TX.

Bibb, R., Taha, Z., Brown, R., Wright, D. (1999), "Development of a Rapid Prototyping Design Advice System", *Journal of Intelligent Manufacturing*, Vol. 10, pp.331-39.

Biron, M. (2004), *Thermosets and Composites : Technical Information for Plastics Users*, Elsevier Advanced Technology, Oxford, UK.

Booth, R. (2004), Materials Development Director, Advanced Laser Materials, L.L.C., Personal Correspondence.

Brown, I.W.M., Owers, W.R. (2004), "Fabrication, Microstructure and Properties of Fe-TiC Ceramic-metal Composites", *Current Applied Physics*, Vol. 4, pp.171-74.

Carrere, N., Maire, J.-F., Kruch, S., Chaboche, J.-L. (2004), "Multiscale Analysis of SiC/ Ti Composites", *Materials Science and Engineering*, A 365, pp.275-81.

Chakrabarti, O., Das, P.K. (2000), "Reactive Infiltration of Si-Mo Alloyed Melt Into Carbonaceous Preforms of Silicon Carbide", *Journal of the American Ceramics Society*, Vol. 83, No. 6, pp.1548-50.

Chatterjee, A.N., Kumar, S., Saha, P., Mishra, P.K., Choudhury, A.R. (2003), "An Experimental Design Approach to Selective Laser Sintering of Low Carbon Steel", *Journal of Materials Processing Technology*, Vol. 136, pp.151-57.

Choe, C.R., Lee, K.H. (1992), "Effect of Processing Parameters on the Mechanical Properties of Carbonized Phenolic Resin", *Carbon*, Vol. 30, No. 2, pp.247-49.

Choi, S.H., Chan, A.M.M. (2003), "A Virtual Prototyping System for Rapid Product Development", *Journal of Computer Aided Design*, June, 25, 2003.

Choi, S.H., Samavedam, S. (2002), "Modelling and Optimization of Rapid Prototyping", *Computers in Industry*, Vol. 47, pp.39-53.

Chong, S.Y., Atkinson, H.V., Jones, H. (1993), "Effect of Ceramic Particle Size, Melt Superheat, Impurities and Alloy Conditions on the Threshold Pressure for Infiltration of SiC Powder Compacts by Aluminum-based Melts", *Materials Science and Engineering*, A 173, pp.233-37.

Clyne, T. W. (2001), "3.7.12. Metal Matrix Composites : Matrices and Processing", from *Encyclopaedia of Materials : Science and Technology*, Mortensen, A. (ed.), Elsevier, London.

Cooper, K. G. (2001), *Rapid Prototyping Technology : Selection and Application*, Marcel Dekker, New York.

Corman, G.S., Einset, E.O., Hillig, W.B. (1997), "Observations on the Processes for the Formation of SiC from Elemental Carbon and Silicon", *GE Research and Development Center, Technical Information Series*, 97CRD033, March 1997.

Cymetech, Inc., http://www.cymetech.com.

Dai, K., Shaw, L. (2004), "Thermal and Mechanical Finite Element Modeling of Laser Forming from Metal and Ceramic Powders", *Acta Materialia*, Vol. 52, pp.69-80.

Deckard, L., Claar, T.D. (1993), "Fabrication of Ceramic and Metal matrix Composites from Selective Laser Sintered Ceramic Preforms", *1993 Solid Freeform Fabrication Symposium Proceedings*, pp.215-22.

Dimla, D. E., Singh, H., Day, M. (2002), "Fabrication of Functional Metal Parts Using Laser Sintering – A Case Study", *Third National Conference on Rapid Prototyping, Tooling, and Manufacturing Proceedings*, 20-21 June 2002, Professional Engineering Publishing, London, p.115-22.

Dyban, Y. (2001), "Structuring of Multiphase Compacts in the SiC-Carbon System. I. Structuring in Green Blanks", *Powder Metallurgy and Metal Ceramics*, Vol. 40, No.1-2.

Dyban, Y. (2001), "Structuring of Multiphase Compacts in the SiC-Carbon System. II. Structuring During Sintering", *Powder Metallurgy and Metal Ceramics*, Vol. 40, No.5-6.

Dyban, Y. (2002), "Structuring of Multiphase Compacts in the SiC-Carbon System. III. Structuring in Green Blanks", *Powder Metallurgy and Metal Ceramics*, Vol. 41, No.3-4.

Dynacer, Inc., http://www.dynacer.com/hot_pressing.htm.

Evans, R.S., Bourell, D.L., Beaman, J.J., Campbell, M.I. (2003), "Reaction Bonded Silicon Carbide: SFF, Process Refinement and Applications", *2003 SFF Symposium Proceedings*, Austin, TX, pp.163-71.

Evans, R.S., Bourell, D.L., Beaman, J.J., Campbell, M.I. (2005), "Rapid Manufacturing of Silicon Carbide Composites," *Rapid Prototyping Journa*l, Vol. 11, No. 1, pp. 37-40.

Farag, M. M. (1989), *Selection of Materials and Manufacturing Processes for Engineering Design*, Prentice Hall, New York.

Favre, A., Fuzellier, H., Suptil, J. (2003), "An Original Way to Investigate the Siliconizing of Carbon Materials", *Ceramics International*, Vol. 29, p.235-43.

Fernandez, J. M., Muñoz, A., Lopez, A.R. D., Feria, F. M. V., Dominguez-Rodriguez, A., Singh M. (2003), "Microstructural-Mechanical Properties Correlation in Siliconized Silicon Carbide Ceramics", *Acta Materialia*, Vol. 51, p.3259-75.

Firestone, K. (2003-04), Solid Concepts, Inc., Personal Correspondence.

German, R. (1989), *Particle Packing Characteristics*, Metal Powder Industries Federation, Princeton, NJ.

Greco, A., Maffezzoli, A. (2003), "Polymer Melting and Polymer Powder Sintering by Thermal Analysis", *Journal of Thermal Analysis and Calorimetry*, Vol. 72, pp.1167-74.

Groover, M. P. (2002), *Fundamentals of Modern Manufacturing : Materials, Processes and Systems*, John Wiley and Sons, New York.

Hague, R., Campbell, I., Dickens, P. (2003), "Implications on Design of Rapid Manufacturing", *Journal of Mechanical Engineering Science*, Vol. 217, pp. 25-30.

Harvest Technologies, Inc., http://www.harvest-tech.com

Hibiya, T., Azami, T., Sumiji, M., Nakamura, S. (2003), "Surface Tension Driven Flow of Molten Silicon : It's Instability and the Effect of Oxygen", *Lecture Notes in Physics*, Vol. 628, p.131-55.

Hopkinson, N., Dickens, P. (2003), "Analysis of Rapid Manufacturing – Using Layer Manufacturing Processes for Production", *Journal of Engineering Science*, Vol. 217, pp.31-9.

Hozer, L., Lee, J.-R., Chiang, Y.-M. (1995), "Reaction-Infiltrated, Net-Shape SiC Composites", *Materials Science and Engineering*, A 195, pp.131-43.

Ion, J.C., Shercliff, H.R., Ashby, M.F. (1992), "Diagrams for Laser Materials Processing", *Acta Metallica Materialia*, Vol. 40, No. 7, pp.1539-51.

Jardinil, A.L., Maceill, R., Scarparol, M.A., Andrade, S.R., Moura, L.F. (2003), "The Development in Infrared Stereolithography Using Thermosensitive Polymers", *Proceedings of the 1st International Conference on Advanced Research in Virtual and Rapid Prototyping*, Leiria, Portugal, pp.273-7.

Ji, Z., Wu, S. (1998), "FEM Simulation of the Temperature Field During the Laser Forming of Sheet Metal", *Journal of Materials Processing Technology*, Vol. 74, pp.89-95.

Jung, Y.S., Kwon, O.J., Oh, S.M. (2002), "Formation of Silica Coated Carbon Powder and Conversion to Spherical β-Silicon Carbide by Carbothermal Reduction", *Journal of the American Ceramics Society*, Vol. 85, No. 8, pp.2134-6.

Kai, C. C., Fai, L. K. (1997), *Rapid Prototyping : Principles & Applications in Manufacturing*, John Wiley & Sons, Singapore.

Kai, K., Shaw, L. (2004), "Thermal and Mechanical Finite Element Modeling of Laser Forming from Metal and Ceramic Powders", *Acta Materialia*, Vol.52, pp.69-80.

King, D., Tansey, T. (2002), "Alternative Materials for Rapid Tooling", *Journal of Materials Processing Technology*, Vol. 121, pp.313-7.

King, D., Tansey, T. (2003), "Rapid Tooling: Selective Laser Sintering Injection Tooling", *Journal of Materials Processing Technology*, Vol. 132, pp.42-8.

Knop, A., Pilato, L.A. (1985), *Phenolic Resins : Chemistry, Applications and Performance, Future Directions*, Springer-Verlag, Berlin.

Ko, T.H., Kuo, W. S., Chang, Y. S. (2001), "Microstructural Changes of Phenolic Resin During Pyrolysis", *Journal of Applied Polymer Science*, Vol. 81, pp.1084-9.

Kolossov, S., Boillat, E., Glardon, R., Fischer, P., Locher, M. (2004), "3D FE Simulation for Temperature Evolution in the Selective Laser Sintering Process", *International Journal of Machine Tools & Manufacture*, Vol. 44, pp.117-23.

Lee, J.A., Mykkanen, D.L. (1987), *Metal and Polymer Matrix Composites*, Noyes Data Corporation, Park Ridge, NJ.

Leigh, D.K. (2004), President, Harvest Technologies, Personal Correspondence

Lessing, P.A., Erickson, A.W., Kunerth, D.C. (2001), "Thermal Cycling of Siliconized-SiC at High Temperatures", *Journal of Materials Science*, Vol. 36, pp.1389-94.

Lindholm, D., Tate, D., Harutunian, V. (1999), "Consequences of Design Decisions in Axiomatic Design", *Transactions of the Society for Design and Process Science*, Vol. 3, No. 4, pp. 1-12.

Luo, Y.M., Li, S.Q., Chen, J., Wang, R.G., Li, J.Q., Pan, W. (2002), "Effect of Composition on Properties of Alumina/ Titanium Silicon Carbide Composites", *Journal of the American Ceramics Society*, Vol. 85, No. 12, pp.3099-101.

Lytle, C.A., Bertsch, W., McKinley, M. (1998), "Determination of Novolac Resin Thermal Decomposition Products by Pyrolysis-Gas Chromatography-Mass Spectrometry", *Journal of Analytical and Applied Pyrolysis*, Vol. 45, pp.121-31.

Mansour, S., Hague, R. (2003), "Impact of Rapid Manufacturing on Design for Manufacture for Injection Moulding", *Proceedings of the Institution of Mechanical Engineers*, Vol. 217, Part B, *Journal of Engineering Manufacture*, pp. 453-61.

McDonald, J. A., Ryall, C. J., Wimpenny, D. I.(editors) (2001), *Rapid Prototyping Casebook*, Professional Engineering Publishing Limited, London.

Meier, S., Heinrich, J.G. (2002), "Processing – Microstructure Properties Relationships of $MoSi_2$-SiC Composites", *Journal of the European Ceramic Society*, Vol. 22, pp.2357-63.

Mills, A.F. (1999), *Heat Transfer*, Prentice Hall, NJ.

Molina, J.M., Saravanan, R.A., Arpón, R., García-Cordovilla, Louis, E., Narciso, J. (2002), "Pressure Infiltration of Liquid Aluminum Into Packed SiC Particulate with a Bimodal Size Distribution", *Acta Materialia*, Vol. 50, pp.247-57.

Moon, J., Caballero, A.C., Hozer, L., Chiang, Y.M., Cima, M.J. (2001), "Fabrication of Functionally Graded Reaction Infiltrated SiC-Si Composite by Three-Dimensional Printing (3DP™) Process", *Materials Science and Engineering*, A 298, pp.110-9.

Morgan Advanced Ceramics, Inc., http://www.morganadvancedceramics.com

Mortensen, A. (2001), "Metal Matrix Composites in Industry : An Overview", *MMC ASSESS Final Presentation, MMC VIII conference*, London, November 26th to 27th 2001.

Nelson, J.C., Vail, N.K., Barlow, J.W., Beaman, J.J., Bourell, D.L., Marcus, H.L. (1995), "Selective Laser Sintering of Polymer-coated Silicon Carbide Powders", *Industrial and Engineering Chemistry Research*, Vol. 34, pp.1641-51.

Nichols, S.P. (2004), "Engineering Professional Responsibility 101", Presentation, The University of Texas at Austin, July 12, 2004.

Paik, U., Park, H. C., Choi, S. C., Ha, C. G., Kim, J. W., Jung, Y. G. (2002), "Effect of Particle Dispersion on Microstructure and Strength of Reaction-bonded Silicon Carbide", *Materials Science and Engineering*, A 334, pp.267-74.

Pech-Canul, M.I., Katz, R.N., Makhlouf, M.M (2000), "The Role of Silicon in Wetting and Pressureless Infiltration of SiC_p Preforms by Aluminum Alloys", *Journal of Materials Science*, Vol. 35, pp.2167-73.

Pech-Canul, M.I., Makhlouf, M.M. (2000), "Processing of Al-SiC_p Metal Matrix Composites by Pressureless Infiltration of SiC_p Preforms", *Journal of Materials Synthesis and Processing*, Vol. 8, No. 1, pp.35-53.

Persson, P., Jarfors, A.E.W., Savage, S. (2002), "Self-propagating High-temperature Synthesis and Liquid-phase Sintering of TiC/Fe Composites", *Journal of Materials Processing Technology*, Vol. 127, pp.131-9.

Pham, D.T., Dimov, S. S. (2003), "Rapid Prototyping and Rapid Tooling – The Key Enablers for Rapid Manufacturing", *Journal of Mechanical Engineering Science*, Vol. 217, pp.1-23.

Pham, D.T., Wang, X. (2000), "Prediction and Reducation of Build Times for the Selective Laser Sintering Process", *Proceedings of the Institution of Mechanical Engineers*, Vol. 214, Part B, pp.425-30.

Poco Graphite, Inc., http://www.poco.com/SiliconCarbide

Pujar, V.V., Jansen, R.P., Padture, N.P. (2000), "Densification of Liquid-Phase-Sintered Silicon Carbide", *Journal of Materials Science Letters*, Vol. 19, pp.1011-4.

Rajesh, G., Bhagat, R. B. (1999), "Infiltration of Liquid Metals in Porous Compacts: Modeling of Permeabilities During Reactive Melt Infiltration", *Transport in Porous Media*, Vol. 36, p. 43-68.

Richardson, F.D. (1974), *Physical Chemistry of Melts in Metallurgy*, Academic Press, London.

Roewer, G., Herzog, U., Trommer, K., Müller, E., Frühauf, S. (2002), "Silicon Carbide – A Survey of Synthetic Approaches, Properties and Applications", *Structure and Bonding*, Vol. 101, pp. 60-127.

Rohm and Haas Company, The, http://www.cvdmaterials.com/silicon.htm

Ryder, G. J., Harrison, D. K., Green, G., Ion, W. J., Wood, B. M. (2002), "Benchmarking the Rapid Design and Manufacture Process", *Third National Conference on Rapid Prototyping, Tooling and Manufacturing*, 20-21 June 2002, High Wycombe, UK, pp.97-104, Professional Engineering Publishing, London.

Saint-Gobain Ceramics Co., http://www.carbo.com

Schulte-Fischedick, J., Zern, A., Mayer, J., Rühle, M., Frieβ, M., Krenkel, W. (2002), "The Morphology of Silicon Carbide in C/C-SiC Composites", *Materials Science and Engineering*, A 332, pp.146-52.

Singh, M. (1998), "Joining of Sintered Silicon Carbide Ceramics for High-temperature Applications", *Journal of Materials Science Letters*, Vol. 17, pp.459-61.

Singh, M. (1998), "Microstructure and Mechanical Properties of Reaction-formed Joints in Reaction-bonded Silicon Carbide Ceramics", *Journal of Materials Science*, Vol. 33, pp.5781-7.

Sirisalee, P., Parks, G.T., Clarkson, P.J., Ashby, M.F. (2003), "A New Approach to Multi-Criteria Material Selection in Engineering Design", *International Conference on Engineering Design*, Stockholm, August 19-21, 2003.

Suyama, S., Kameda, T., Itoh, Y. (2003), "Development of High-strength Reaction-sintered Silicon Carbide" *Diamond and Related Materials*, Vol. 12, p.1201-4.

Taylor, A., Laidler, D. S. (1950), "The Formation and Crystal Structure of Silicon Carbide" *British Journal of Applied Physics*, Vol. 1, No. 7, p.174-81

Thornton, B.C. (2003-04), Chairman, Advanced Laser Materials, L.L.C., Personal Correspondence

US Patent #4,247,508 : "Molding Process"

US Patent #4,863,538 : "Method and Apparatus for Producing parts by Selective Sintering"

US Patent #4,944,817 : "Multiple Material Systems for Selective Beam Sintering"

US Patent #5,076,869 : "Multiple Material Systems for Selective Beam Sintering"

US Patent #5,147,587 : "Method of Producing Parts and Molds Using Composite Ceramic Powders

US Patent #5,156,697 : "Selective Laser Sintering of Parts by Compound Formation of Precursor Powders"

US Patent #5,284,695 : "Method of Producing High-temperature Parts by way of Low-temperature Sintering"

US Patent #5,296,062 : "Multiple Material Systems for Selective Beam Sintering"

US Patent #5,342,919 : "Sinterable Semi-crystalline Powder and Near-fully Dense Article Formed Therewith"

US Patent #5,382,308 : "Multiple Material Systems for Selective Beam Sintering"

US Patent #5,431,967 : "Selective Laser Sintering Using Nanocomposite Materials"

US Patent #5,527,877 : "Sinterable Semi-crystalline Powder and Near-fully Dense Article Formed Therewith"

US Patent #5,648,450 : "Sinterable Semi-crystalline Powder and Near-fully Dense Articles Formed Therewith"

US Patent #5,733,497 : "Selective Laser Sintering with Composite Plastic Material"

US Patent #5,749,041 : "Method of Forming Three-dimensional Articles Using Thermosetting Materials"

US Patent #5,817,206 : " Selective Laser Sintering of Polymer Powder of Controlled Particle Size Distribution"

US Patent #5,990,268 : "Sinterable Semi-crystalline Powder and Near-fully Dense Article Formed Therewith"

US Patent #6,048,954 : "Binder Compositions for Laser Sintering Process"

US Patent #6,136,948 : "Sinterable Semi-crystalline Powder and Near-fully Dense Articles Formed Therewith"

US Patent #6,503,572 : "Silicon Carbide Composites and Methods for Making Same"

US Patent #6,713,125 : "Infiltration of Three-dimensional Objects Formed by Solid Freeform Fabrication"

Vanelli, D.L. (2004), "Student Led Commercialization," Presentation to European Delegation on Technology Business Incubation, Austin, TX, March, 2, 2004.

Vanelli, D.L. (2003-04), President, Advanced Laser Materials, L.L.C., Personal Correspondence

Vaucher, S., Paraschivescu, D., Andre, C., Beffort, O. (2002), "Selective Laser Sintering of Aluminum-Silicon Carbide Metal Matrix Composites", *Materials Week*, October, 2002.

Vergnaud,J.-M., Bouzon, J. (1992), *Cure of Thermosetting Resins : Modeling and Experiments*, Springer-Verlag, London.

Wacker Ceramics, Inc., http://www.wacker.com/internet/noc/Products/P_Materials/P_SiliconCarbide/.

Wang, H.Y. (1999), "Advanced Processing Methods for Microelectronics Industry Silicon Wafer Handling Components," Dissertation, University of Texas at Austin, TX.

Weisstein, E.W. (2004), "Spherical Cap", *MathWorld–A Wolfram Web Resource*, http://mathworld.wolfram.com/SphericalCap.html.

Wohlers, T. (2004), *Wohlers Report 2004 : Rapid Prototyping, Tooling and Manufacturing State of the Industry*, Wohlers Associates Inc., Fort Collins, Colorado.

Wohlert, M., Bourell, D. (1996), "Rapid Prototyping of Mg/ SiC Composites by a Combined SLS and Pressureless Infiltration Process", *1996 SFF Symposium Proceedings*, Austin, TX, pp.79-87.

Wolfenden, A., Burris, C.P., Singh, M. (1998), "Young's Modulus and Vibrational Damping of Sintered Silicon Carbide Ceramics at High Temperatures", *Journal of Materials Science Letters*, Vol. 18, pp.1995-7.

Wouters, M., de Ruiter, B. (2003), "Contact Angle Development of Polymer Melts", *Progress in Organic Coatings*, Vol. 48, pp.207-13.

Yilbas, B.S. (1998), "3-dimensional laser heating Model Including a Moving Heat Source Consideration and Phase Change Process", *Heat and Mass Transfer*, Vol. 33, pp.495-505.

Yilbas, B.S., Sami, M. (1997), "Heat transfer Analysis of a Semi-infinite Solid heated by a Laser Beam", *Heat and Mass Transfer*, Vol. 32, pp.245-53.

Vita

Robert Scott Evans was born on August 9, 1973 in Albuquerque, New Mexico, the son of Robert Clark Evans and Linda Jan Evans. After graduating from Canyon del Oro High School in Tucson, Arizona in 1991, he enrolled in the University of Arizona to pursue his Bachelor of Science in Mechanical Engineering. After graduation he was a product development and manufacturing engineer for two years at Thermax/ CDT, a maquiladora wire and cable manufacturer in Nogales, Sonora, Mexico. After a year as a special project engineer for an aerospace electronics firm, Reynolds Industries, Inc., in Marina Del Rey, California and six days after marrying Kelsey Eugenia Spies, he enrolled in the Georgia Institute of Technology to study Microelectromechanical Systems for his Master of Science degree. He then began his doctoral work at the University of Texas at Austin in August of 2001. After working briefly with optical circuits, after an attempt to create a new project in micro-machine design and after examining the commercial potential for the technology described in this dissertation he began his work on the research.

Permanent address: 508 E. 42nd St.
Austin, TX 78751

This dissertation was typed by the author